Investigations into mechanisms of macrophage clearance via the lymphatic system during acute inflammation

Shaumick Bhattacharjee,
Wolfson college and Weatherall Institute of Molecular Medicine, Oxford



A thesis submitted for the degree of *Doctor of Philosophy*

University of Oxford

Hilary 2016

Word count - 49287

Abstract

The lymphatic system is an important vascular network with many important roles which include maintaining fluid homeostasis and acting as a conduit for immune surveillance as well as to clear leucocytes from inflammatory zones. Macrophages are one such population that require to be removed from sites of inflammation to restore physiological homeostasis; persistent accumulation of macrophages is seen as a hallmark of chronic inflammation which has severe consequences in health. This thesis is concerned with the mechanisms regulating entry of these myeloid cells into the lymphatic capillaries.

In vitro adhesion and transmigration assays revealed macrophages actively adhere and migrate across activated lymphatic endothelial cells (LECs) rapidly although both mechanisms do occur without inflammatory stimulation of the endothelial cells. Unlike neutrophils and dendritic cells, ICAM-1 and VCAM-1 were surprisingly redundant to macrophage transmigration of activated LECs although β2 integrin was significantly involved. A more involved role was found in the LYVE-1-hyaluronan (HA) axis; macrophage derived HA as well as lymphatic hyaluronan receptor LYVE-1 were critical to transmigration but quantitatively minimally involved in adhesion. These findings were consolidated with an *in vivo* sterile peritonitis model which demonstrated the importance of the receptor to trafficking of macrophages to draining lymph nodes. Furthermore, macrophage expressed CD44 was also shown to be significantly associated in both inflammatory trafficking and transmigration. The results described in this thesis provide novel evidence of the CD44-HA-LYVE-1 axis playing an active role in migration of macrophages via the lymphatics.

Acknowledgements

Firstly, I would like to thank Professor David Jackson for his supervision and advice throughout this D.Phil. as well as teaching me how to be a better scientist. Also, my colleagues (past and present) in the Jackson laboratory: Louise, Neale, Will, Tess, Ying-Jie, Daniel, Kayla, and Steven for sharing their knowledge and brightening my days. I sincerely appreciated being mentored by Dr David Rigby from the lab and will be forever grateful for his guidance and friendship in my beginners days as a D.Phil. student.

Finally, I would like to acknowledge the love and support of my parents as well as my girlfriend, Tharini Selvakumar, throughout the good and bad times of this enriching educational experience.

Abbreviations and acronyms

Ab	Antibody
APC	Antigen presenting cell
bp	Base pair
BSA	Bovine serum albumin
CCR	Chemokine receptor
cDNA	Complementary DNA
CD	Cluster of differentiation
CSF	Colony stimulating factor
Ctrl	Control
DC	Dendritic cell
DNA	Deoxyribonucleic acid
dNTP	Deoxynucleoside triphosphate
EGM-2	Endothelial growth media
ECM	Extracellular matrix
EDTA	Ethylenediaminetetra-acetic acid
EGF	Epidermal growth factor
ELISA	Enzyme linked immunosorbant assay
FACS	Fluorescence activated cell sorting
FBS	Foetal bovine serum
Fc	Fragment crystallisable
GAG	Glycosaminoglycan
GM-CSF	Granulocyte monocyte colony stimulating factor
h/hr	Hour
HA	Hyaluronan
HAS	Hyaluronan synthase
HA’ase	Hyaluronidase
HDLEC	Human dermal lymphatic endothelial cell
HUVEC	Human umbilical vein endothelial cell
ICAM	Intercellular adhesion molecule
Ig	Immunoglobulin

JAM	Junctional adhesion molecule
kb	Kilobase
LEC	Lymphatic endothelial cell
LFA	Leucocyte function associated antigen
LPS	Lipopolysaccharide
LYVE-1	Lymphatic vessel endothelial hyaluronan receptor-1
mAb	Monoclonal antibody
MACS	Magnetic associated cell sorting
MHC	Major histocompatibility complex
min	Minute
MMP	Matrix metalloproteinase
mRNA	Messenger RNA
PBS	Phosphate buffered saline
PCR	Polymerase chain reaction
Prox-1	Prospero-related homeobox 1
RNA	Ribonucleic acid
RT-PCR	Reverse transcriptase PCR
TNF	Tumour necrosis factor
TSG-6	Tumour necrosis factor inducible gene-6
V	Volume
v/v	Volume per volume
VCAM-1	Vascular adhesion molecule-1
VEGF	Vascular endothelial growth factor
VLA-4	Very late antigen-4
VE-cadherin	Vacular endothelial cadherin
w/v	Weight per volume

Table of contents

Chapter 1. ----4

General Introduction ----4

1.1 The lymphatic system ----5

1.2 Macrophages ----39

1.3 Aims of the thesis ----59

Chapter 2.----60

Materials and methods ----60

2.1 Materials ----61

2.2 Tissue Culture ----69

2.3 Transmigration and adhesion assays----77

2.4 Animal Experiments ----80

2.5 Immunostaining and microscopy ----83

2.6 Purification of monoclonal antibodies----86

2.7 Molecular biology methods ----88

Chapter 3.----91

Elucidating mechanisms of macrophage adhesion and transmigration of the lymphatic endothelium via an in vitro model ----91

3.1 Introduction ----92

3.2 Aims ----100

3.3 Results ----101

3.4 Discussion ----153

Chapter 4. ----163

The role of LYVE-1 in trafficking of macrophages to draining lymph nodes-163

4.1 Introduction ----164

4.2 Aims ----173

4.3 Results ----174

4.4 Discussion ----215

Chapter 5. ----225

The role of CD44 in trafficking of macrophages to draining lymph nodes and characterisation of hyaluronan production by macrophages----225

5.1 Introduction ----226

5.2 Aims ----233

5.4 Discussion ----260

Chapter 6 ----267

General discussion ----------267

6.1 Identification of key adhesion molecules mediating macrophage transmigration across lymphatic endothelium and trafficking ----------268

6.2 Role for the LYVE-1-hyaluronan axis in macrophage adhesion/ transmigration in vitro and migration via lymphatics in vivo ----------276

6.3 The importance and contribution of CD44 and HA production for macrophage trafficking to lymph nodes ----------284

6.4 Conclusions ----------292

Bibliography ----------294

Chapter 1.

General Introduction

1.1 The lymphatic system

1.1.1 Anatomy and physiology

Blood circulation has evolved in large multicellular organisms as a special mechanism with one essential function - transport. It is used to distribute oxygen, nutrients and hormones throughout all tissues of the body as well as carry metabolic wastes to tissues for exit out of the body. Oxygenated blood is delivered via arteries into tissues while deoxygenated blood is taken via the veins back into the heart. At the terminal arterioles, arterial blood pressure drives fluid loss into the interstitial space as plasma. A majority of water is reabsorbed back into circulation at low pressure venules while the small amount left behind is returned to blood circulation via the lymphatic system.

They lymphatic system, a part of the circulatory system, comprises of vessels and secondary lymphoid organs (Fig 1-1). Lymphatics are present in all tissues and was believed to be absent in the central nervous system (CNS), bone and bone marrow; however recently, lymphatics have been discovered in association with the CNS, found specifically within the dural sinuses and drain into the deep cervical lymph nodes performing classical functions, discussed further below (Swartz 2001, Louveau, Smirnov et al. 2015). Lymphatic vessels are divided into initial capillaries, pre-collectors, collectors or lymphatic trunks. The blind ended initial capillaries serve as the proximal region of the lymphatic vasculature where they drain into the collectors and ultimately into the thoracic duct terminating into venous blood circulation at the level of the subclavian vein

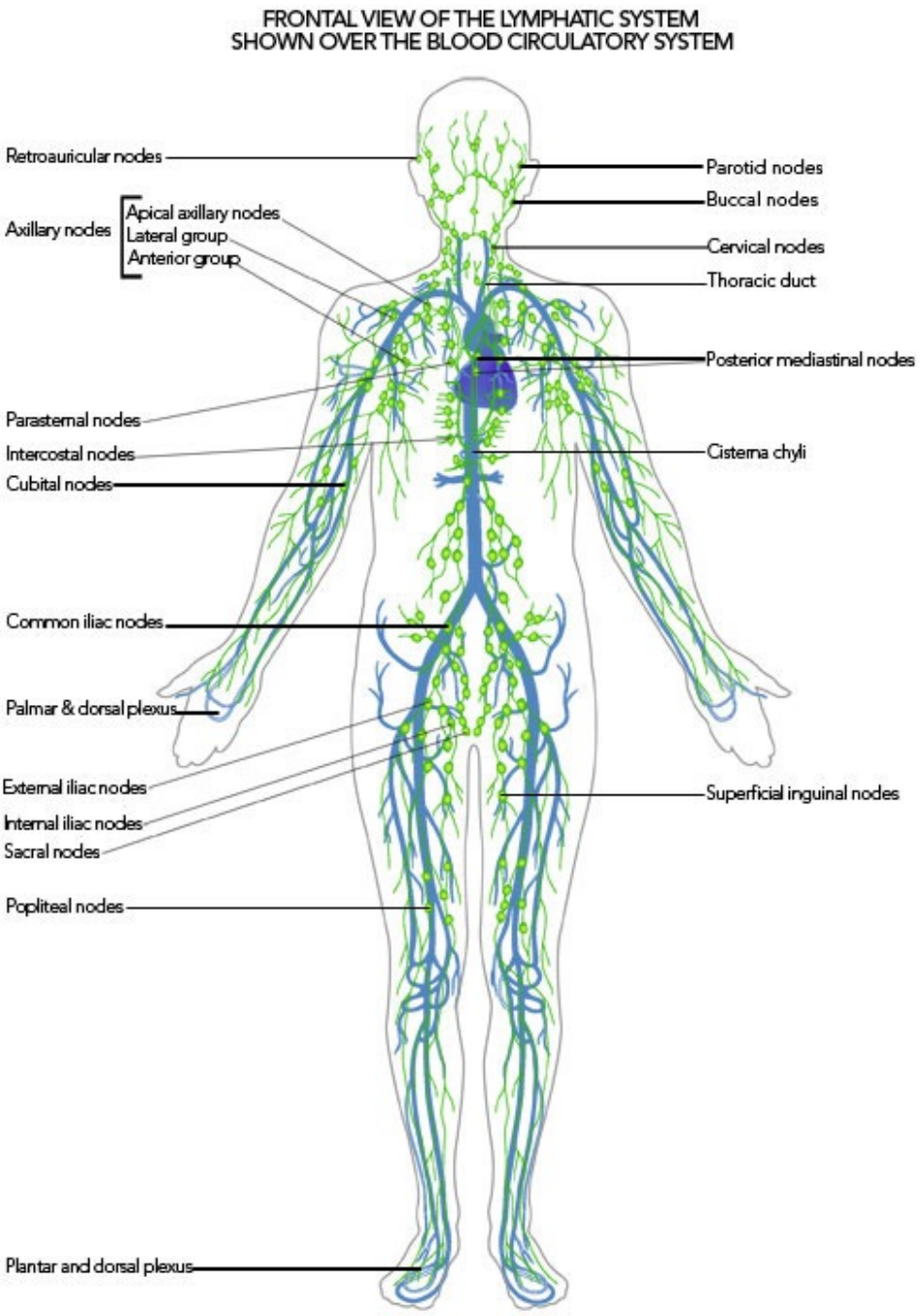


Fig 1-1: Schematic representation of the lymphatic system and lymph nodes overlaid with blood vessels. Image taken from: http://lymphatictherapy.co.za/manual-lymph-drainage/the-lymphatic-system/

(Swartz 2001). The initial capillaries are the main entry points for the plasma along with other macromolecules and leucocyte populations. In healthy homeostasis, the lymphatics are responsible for returning up to 2 litres of interstitial fluid, with 20-30 grams of protein per litre, to the venous circulation each day (Oliver and Alitalo 2005).

The initial lymphatic capillaries are blind-ended with thin constricted walls of loosely overlapping single endothelial cells, which range in size with diameters of 30-80 μm . They have little or no basement membrane and are not surrounded by pericytes or smooth muslce cells, unlike blood vessels (Leak 1976). However, collagen fibres are shown to tether lymphatic vessels to the surrounding matrix. This prevents vessels collapsing when fluid pressure within is less than the surrounding interstitium. Lymphatic vessels often appear collapsed and distended in histological sections, with thin attenuated walls of loosely overlapping endothelial cells and nuclei bulging into lumen. The loose overlapping borders of the endothelial cells creates ‘primary valves’ within the vessels that allows unidirectional fluid movement into the vessels and prevents fluid from leaking back out once the intra-vascular pressure increases (Parson and McMaster 1938, reviewed by (Swartz 2001). The endothelium of these initial capillaries have distinct discontinuous junctions that have been termed as ‘button-junctions’, with the endothelial cells displaying a noticeable oak leaf-shaped morphology . These junctions are composed of various tight junction proteins such as claudin-5, zonula occludens (ZO-1), endothelial cell-selective adhesion molecule (ESAM) and junctional adhesion molecule-A (JAM-A), organised with these is VE-cadherin at the borders. Platelet endothelial cell adhesion molecule (PECAM)/CD31 is found at the tips of these junctions along

with the lymphatic vessel endothelial hyaluronan receptor (LYVE-1) (Fig 1-2) (Baluk, Fuxe et al. 2007, Lynch, Delano et al. 2007).

Once lymph is collected within these initial capillaries, they drain into the pre-collector vessels. They are notably larger than the capillaries and are found deeper within tissues. These pre-collectors connect to even larger collecting vessels (Oliver and Alitalo 2005).

The vessels are marked by a definite basement membrane and covered abundantly by lymphatic smooth muscle cells (SMCs) as they progress towards the terminal draining location (von der Weid and Zawieja 2004). These collectors are also different from the capillaries in their organisation of the inter-endothelial junctions appearing much more similar to those of blood vessels, displaying a continuous 'zipper-like' structure. The tight-junction proteins along with VE-cadherin are also organised at these 'zipper' junctions although LYVE-1 is noticeably less abundant (Baluk, Fuxe et al. 2007). The collectors are primarily responsible for the transit of lymph into draining lymph nodes and eventually into venous circulation. The SMCs surrounding the collectors provide spontaneous and rhythmic contractillity that provides the force for lymph flow at these regions, along with contractility from skeletal muscle cells (von der Weid and Zawieja 2004). These larger vessels also have specialised mature valves to prevent the backflow of lymph. Confocal microscopy has revealed the valves to consist of two sheets of lymphatic endothelial cells (LECs) with a matrix sandwiched in between them. This provides a strong yet elastic connective tissue core. The valve leaflet is defined by an upregulation of integrin-α9 expression throughout development with a deposition of its direct ligand, EIIIA

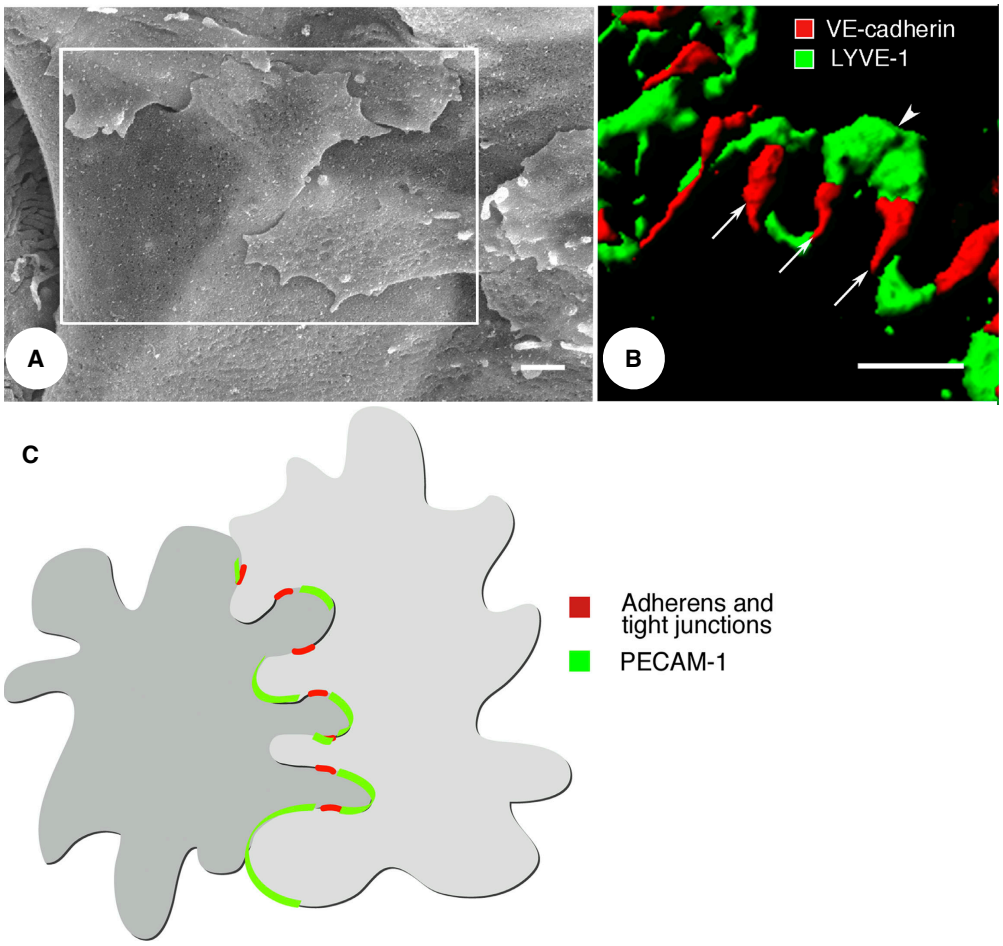


Figure 1-2: Distinct features of lymphatic vessel interendothelial junctions. The lymphatic endothelial cells of initial blind ended capillaries have a distinctive 'oak-leaf' morphology in which the interdigitating borders are shown in (A) electron microscopy, (B) confocal microscopy, and (C) cartoon format. These borders which are lined at the sides by junction adhesion molecules (e.g. VE-cadherin) and at the tips by molecules such as LYVE-1 are thought to be sites for leucocyte entry. All panels are taken from Baluk et al. (2007). Originally published in the Journal of Experimental Medicine, 204: 2349-2362.

splice isoform of fibronectin, in the ECM in between the LECs (Ji 2006, Bazigou, Xie et al. 2009).

During embryonic development, it was identified that activity of Drosophila Prospero-related homeodomain transcription factor PROX-1 was sufficient for venous blood endothelial cells (BECs) to differentiate into LECs; *PROX-1*$^{-/-}$ endothelial cells are not able to differentiate into LECs with no expression of classic lymphatic markers (Wigle and Oliver 1999). Amongst the more important markers are the homeobox gene PROX-1 (Wilting, Papoutsi et al. 2002), the membrane glycoprotein podoplanin (Hirakawa, Hong et al. 2003), vascular endothelial growth factor receptor-3 (VEGFR-3) (Joukov, Pajusola et al. 1996) and lymphatic HA receptor LYVE-1 (Banerji, Ni et al. 1999). LYVE-1 has recently become evident to play an important role in immunity and homeostasis and will be discussed in detail below.

1.1.2 Lymph nodes

Lymph nodes are specialised secondary lymphoid organs distributed widely throughout the body. There are hundreds of lymph nodes throughout the body with lymph delivered into these tissues by lymphatic vessels. Their major function involves filtering lymph to remove cell debris and foreign matter for immune surveillance. In humans, they range from 1-2 mm to 1-2 cm in length and 1-10 mm in diameter (reviewed by (Swartz 2001). They are organised into clusters throughout different regions depending on their drainage pattern. These can be the neck (cervical), armpits (axillary), in between the lungs

(mediastinary), the abdominal cavity (mesenteric) and groin (inguinal), the schematic with lymphatic vessels shown in figure 1-1.

Histological observation of cross sections of lymph nodes reveals two distinct regions - the cortex and the medulla (Fig 1-3). These regions are encapsulated by a collagenous membrane with a sinus separating the capsule from the cortex. This subcapsular sinus is connected to afferent lymphatic vessels allowing lymph to enter into the lymph node. The lymph drains into cortical sinuses that subsequently drain into underlying medullar sinuses. The fluid after filtration passes through to the terminal sinus exiting at the hilum via the efferent lymphatic vessel (reviewed by (von Andrian and Mempel 2003). The cortex is subdivided into the paracortex, rich in T cells; and the superficial B-cell area that consists of primary follicles and germinal centres (after antigen challenge). B cell follicles are the main site of humoural responses and the paracortex is the region where antigen presenting cells interact with T cells. The rest of the cortex contains cortical sinuses and specialised postcapillary venules known as high endothelial venules (HEVs) (Girard, Moussion et al. 2012). In higher animals, the lobular regions of the cortex are separated by fibrous radial bands termed trabeculae. The central medulla is composed of lymph-draining sinuses that are separated by medullary cords. Immune cells found in association with these cords are plasma cells, macrophages and memory T cells (Gretz, Anderson et al. 1997).

The lymph node has been identified as an important site of initiation of adaptive immune responses and its architecture is such that it allows cells to traffic in and out with ease. This migration is a carefully orchestrated process known as

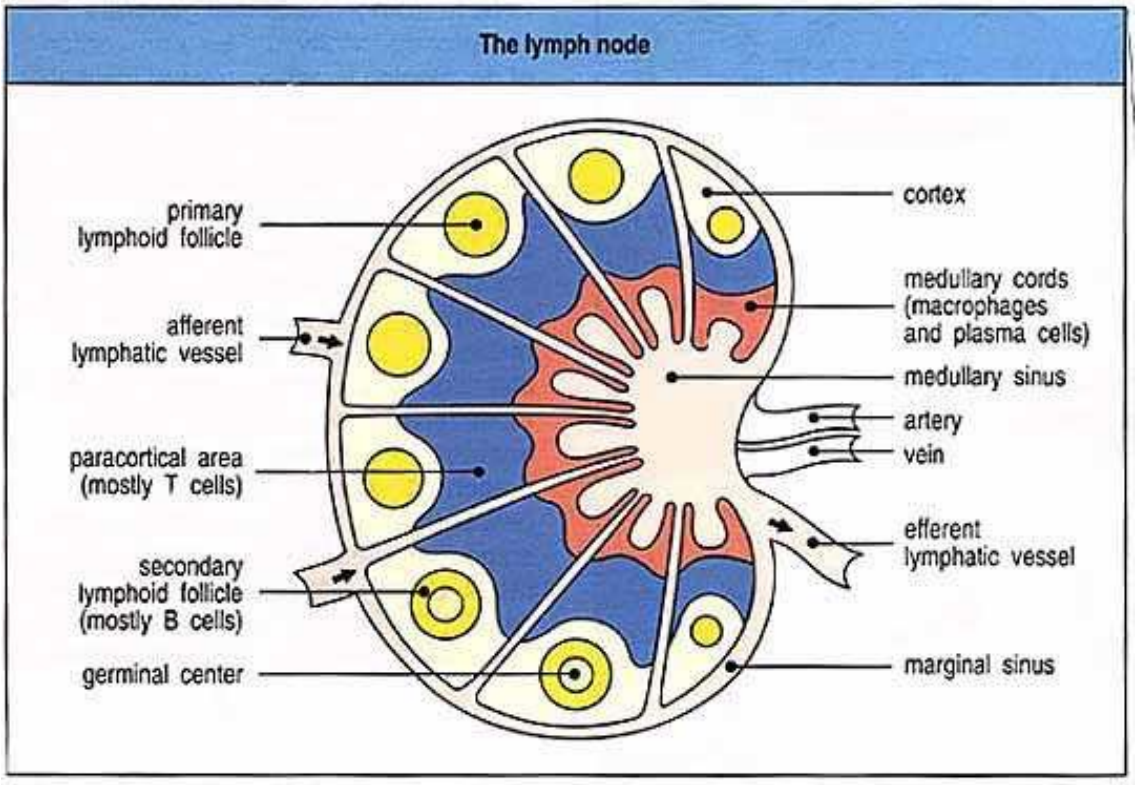


Figure 1-3: Structure of a lymph node. Schematic diagram of a lymph node illustrating the cortex containing the lymphoid follicles, rich in B lymphocytes, and the surrounding parafollicular cortex which contains T lymphocytes. The inner medulla contains large numbers of macrophages and dendritic cells, with some scattered lymphocytes. Lymph fluid enters from afferent lymphatic vessels and enters the subcapsular sinus. After passing through the node, the filtrate exits the through the single efferent lymphatic vessel found at a region called the hilus (unlabelled in the diagram).

ecotaxis and involves key steps involving cellular interactions, chemokine gradients and expression of specific proteins within the lymph node. Lymphocytes that populate the lymph node enter the lymph node directly from the blood stream by extravasation at HEVs and then localise at their respective B- or T-cell regions. Leucocytes such as dendritic cells (DCs) enter the lymph node via the afferent lymphatics through which they transport antigen for lymphocytes and gaining access via lymphatic vessels into the lymph node restricts cells and lymph particles in the sinuses (Gretz, Norbury et al. 2000). A special category of these macrophages, identified as $CD169^+$, reside within the subcapsular sinus where they would encounter the lymph first and assist in the transport of antigen for presentation to closely juxtaposed B-cells (Carrasco and Batista 2007). Recently, the mechanism of T-cell activation in the lymph node was shed light on. Gerner et al. (2015) identified specialised DCs in association with the endothelium lining lymphatic sinuses that were responsible for catching lymph borne antigen in the sinuses and rapidly activating $CD4^+$ and $CD8^+$ T-cells.

1.1.3 Functions of the lymphatics

The lymphatic system plays an essential role in maintaining physiological homeostasis of the body with its functions broadly categorised into three key actions. Firstly, it is responsible for carrying triacylglycerols and cholesterol from the intestines to the tissues (Christensen, Hoy et al. 1995), the function which originally lead to its discovery. As mentioned in intercerpts throughout this General Introduction, the lymphatics are a conduit for APCs to activate adaptive

immunity consequently having an important immunological function (involved mechanisms are discussed in more detail in section 2.4) (von Andrian and Mempel 2003, Johnson, Clasper et al. 2006). The third category is the regulation of body fluid levels, draining excess interstitial fluid, returning macromolecules to the circulation to maintain constant colloid osmotic pressure, transporting extracellular matrix components, eliminating unwanted cellular by-products and removing foreign organic and inorganic material. Each day approximately 50 % of the total circulating protein escapes from the blood vessels and as it cannot be reabsorbed through the same route, it is the responsibility of the lymphatic system to return extravasated fluid and macromolecules to the circulation (Choi, Lee et al. 2012).

1.1.4 Lymphatic vessels in inflammation

As mentioned above, the lymphatic vessels function as a conduit for the transport of antigen presenting cells (APCs) as well as soluble antigen to lymph nodes for the initiation of adaptive immune responses, a key event during inflammation. Lymphatic vasculature under homeostatic and inflammatory conditions represent very different landscapes. A classic hallmark of inflammation is an increased cellularity of the draining lymph node (dLN) due to the large scale immigration of DCs via afferent lymphatics along with other leucocytes such as neutrophils and lymphocytes (von Andrian and Mempel 2003). This rapid increase in the number of cells able to enter into lymphatic vessels is due to numerous changes the endothelial cells undergo upon inflammation, with certain similarities found in events associated with exit from

blood vessels. The trafficking of leucocytes through afferent lymphatics is discussed in detail below.

Despite not being as well characterised as cell trafficking associated with blood vasculature, numerous advancements have been made understanding the mechanisms utilised by leucocytes exiting from tissues via lymphatics, a majority of work focussing on DCs (Johnson, Clasper et al. 2006, Johnson and Jackson 2010, Johnson and Jackson 2013). Previous work in the Jackson laboratory also published on the mechanisms utilised by neutrophils, and their accumulation in draining lymph nodes (Rigby, Ferguson et al. 2015).

The involvement of adhesion molecules ICAM-1 and VCAM-1 were found to be essential during during *in vitro* and *in vivo* transmigration, in inflammation (Johnson, Clasper et al. 2006). For neutrophils, the work identified that although significant contributions are made by the two molecules, β2 integrins expressed by neutrophils are quantitatively more influential (Rigby, Ferguson et al. 2015). The other aspect to migration are chemokines, which attract leucocytes to the vasculature and promote trafficking to draining lymph nodes; the most reported regarding lymphatics being C-C chemokine, CCL21 (Johnson and Jackson 2010, Tal, Lim et al. 2011). Unpublished findings from the Jackson laboratory (Rigby DA, D.Phil. thesis, 2011) also uncovered evidence of IL-8 secreted by activated HDLECs attracting neutrophils. Such mechanisms are also shared by lymphocytes, which use CC -chemokines and ICAM-1 in their migration (Moser and Loetscher 2001, von Andrian and Mempel 2003). Another molecule shared by both DCs and T cells in their migration is sphingosine-1-phosphate (S1P), which as a lipid reorganises the cytoskeletal proteins thus affecting movement of the leucocytes (Czeloth, Bernhardt et al. 2005, Pappu, Schwab et al. 2007).

Extensive microscopy work by the group of Michael Sixt demonstrated the arrangement of the basement membrane of initial lymphatic vessels as a key factor in homeostatic migration of DCs; the membrane being discontinuous with permissive entry sites for transmigration (Pflicke and Sixt 2009). Moreover, the button like structures associated with the junctions of initial lymphatics that form flap valves (as commented above) is hypothesised to allow DC traffic to pass unhindered, although conclusive evidence is yet to be demonstrated (Baluk, Fuxe et al. 2007, Jackson 2009). Pflicke and Sixt (2009) demonstrated that constitutive DC transmigration through these permissive sites was both protease- and MMP-independent. The data exhibited however, was from uninflamed conditions and it is yet to be shown if there are changes within those transmigratory hotspots in inflamed conditions. Both monocytes and neutrophils degrade the basement membrane during extravasation of blood vasculature in inflammation by secretion of proteases and MMPs as an exit strategy and is plausibly involved similarly with the basement membrane of lymphatics (Heck, Blackburn et al. 1990, Voisin, Woodfin et al. 2009). Interestingly, the utilisation of such tissue digesting enzymes was seen with neutrophils adhering to activated LEC monolayers stimulating production of MMP-8 and MMP-9 and causing endothelial cells to retract, forming gaps in the monolayer that allow for neutrophil transmigration (Rigby, Ferguson et al. 2015).

Taken together, the enrichment of adhesion molecules known to mediate monocyte trafficking across blood vasculature and monocyte derived DC transit across lymphatic endothelium raises intriguing possibilities regarding the strategies macrophages could use to traffic to draining lymph nodes via afferent lymphatic vessels. Limited investigations have shown that macrophages indeed use integrins in their transit to draining lymph nodes although detailed

knowledge of the specific mechanisms is yet to be demonstrated robustly. In light of the utilisation by monocytes, the inflammatory macrophage progenitor, of various chemokines, adhesion molecules, lipids and sugars for blood vasculature trafficking, it seems as if exploration of macrophage trafficking via afferent lymphatic vessels is lacking. Ultimately, these findings indicate a possible role for these approaches in macrophage migration to draining lymph nodes.

A frequent occurrence at sites of inflammation is lymphangiogenesis - induced by key lymphangiogenic factors - VEGF-C and VEGF-D, secreted by leucocytes such as macrophages which respond to inflammatory cytokines such as TNF-α (Karkkainen, Saaristo et al. 2001, Kataru, Jung et al. 2009). The signaling pathways associated with inflammation also contribute to induction of lymphangiogenesis. NF-κβ signalling pathway is commonly induced upon inflammation and induction of this pathway in LECs leads to increased expression of PROX-1 and VEGFR-3, thus rendering the cells more responsive to lymphangiogenic factors (Flister, Wilber et al. 2010). NF-κβ is also known to promote expression of key leucocyte chemoattractants such as CCL2, CCL5, and in turn, plausibly, promoting leucocyte trafficking to draining lymph nodes (Rovin, Dickerson et al. 1995).

LECs undergo significant changes physically as well in an inflammatory environment. Infections that produce such environments are responsible for production of lymphatic sprouts along with significant remodelling of the lymphatic vessels with notable increase in vessel area density along with junctional plasticity of the LECs at the initial capillaries. These effects appear to

be mediated by TNF-α although other inflammatory cytokines can induce such effects (Johnson, Clasper et al. 2006, Baluk, Yao et al. 2009).

As noted above, the endothelial cells of the initial capillaries have 'button' junctions under homeostatic conditions. However, upon infection, the inflammatory environment promotes the junctions to change to 'zipper' like junctions that are associated with collecting lymphatics and blood vessels. Reducing inflammation reverts the cells back to having button type junctions highlighting the plasticity of these cells to their environment (Yao, Baluk et al. 2012).

Lymphatic function has been shown to be affected by neuropeptides such as substance P (SP). SP was recently found to modulate inflammatory signalling pathways along with contractility of lymphatic vessels, linking inflammation as a possible inducer of increasing contraction of lymphatic vessels and henceforth lymphatic flow into draining lymph nodes (Amerini, Ziche et al. 2004, Davis, Lane et al. 2008).

Lymph formation by fluids and macromolecules and leaked from blood capillaries is a dynamic process with a constant change driven by delivery to draining lymph nodes. The direction of flow of lymph is believed to be generated by autocrine chemokines and molecules within the lymph. A key macromolecule that has high turnover via the lymphatic system and is influential in inflammation is hyaluronan. Hyaluronan is a key ECM molecule associated with the lymphatic system and is discussed further below in section 1.1.6 (Jackson 2009).

1.1.5 Diseases in association with the lymphatics

The lymphatic system has long been associated with numerous clinical complications and are an important structure in the pathogenesis of diseases. Most prominently, they have been identified since the early 1700s as a course for metastasising tumour cells. Breast, lung, and gastrointestinal tumours frequently metastasise to draining lymph nodes, which present as lumps across the body, an important clinical indicator and red flag in physical examinations (Cao 2005, Swartz and Lund 2012). Mechanisms associated with lymphatic dissemination and growth within lymph nodes is poorly characterised although indicatory correlations have been derived. The pathologies also reflect the lymphatic system as a conduit for immune cells and a compartment for the generation of immune responses as well as its primary role in maintaining homeostasis by returning fluid to circulation.

Prominent human tumours such as those named above, which have a correlation with lymph node metastasis have an increased expression of VEGF-C, a well reported lymphangiogenic factor (Swartz and Lund 2012). Investigations into the role of this cytokine also revealed it to be a selective agonist to VEGFR-3 along with another lymphangiogenic factor, VEGF-D. Mandriota et al. (2001) demonstrated that VEGF-C overexpression in pancreatic β cells of transgenic mice results in extensive lymphatic channel formation around the islets of Langerhans which, do not usually have contact with the lymphatics in wild-type mice thus indicating to *de novo* lymphatic vessel formation. Interestingly, when these transgenic mice were crossed with transgenic mice that develop rapid local only B-cell tumours, 37 % of the crossed mice presented with draining mesenteric lymph node metastases. Apart from the principal molecules named above, further knowledge of this exhaustive

topic will not be covered as an extensive range of reviews have detailed the process comprehensively (Royston and Jackson 2009, Karaman and Detmar 2014, Stacker, Williams et al. 2014).

The primary problem related to a failure of returning interstitial fluid back to circulation is oedema due to a compromise in the lymphatic system termed lymphoedema. Although it can have hereditary aetiology, which is characterised by hypoplastic or aplastic lymphatic vessels which cannot transport lymph back to venous circulation, common clinical complications are seen as a result of traumatic injury, or infection which is termed secondary lymphoedema (Wright and Carty 1994, Szuba and Rockson 1998, Oremus, Dayes et al. 2012). In cases of traumatic injury, the most likely cause is surgery involving lymph node resections, a common management of tumour metastasis. This damages the local lymphatic vessels causing lymphoedema, proximal to the biopsy site (Radhakrishnan and Rockson 2008). Infections with filarial parasites such as *Wuccheria bancrofti*, or *Brugia malayi* which physically obstruct the the lymphatic system and allow fluid retention in the interstitium; the resulting accumulation of lymph in tissues is seen in the limbs and the pathology termed elephantiasis (Fig 1-4) (Sisto and Khachemoune 2008). Treatment of lymphoedema primarily focuses on the symptoms rather than the underlying pathology. Despite this, primary and effective management most frequently consists of complete decongestive therapy (CDT), which involves trained practitioners performing manual lymphatic drainage (MLD) regularly; the technique fundamentally comprising massage of the affected areas, followed by application of a variety of compression bands (Sisto and Khachemoune 2008). Increasing understanding of lymphatic biology as well as lymphatic specific



Figure 1-4: Elephantiasis in both legs of a female patient. Failure of fluid uptake due to lymphatic vessel obstruction by a filarial worm results in accumulation in the interstitium producing lymphoedema. This presents, as shown, by thickening of the skin and subcutaneous tissue that gives rise to enlarged and swollen limbs. (Image taken from news-medical.net).

markers, such as LYVE-1, presents promising opportunities for treatment of such lymphatic system based disorders.

The lymphatics are also a conduit for dissemination of microorganisms, the most common being gram negative bacteria. One of the most deadly of these is *Yersinia pestis*, responsible for several plague pandemics and the deaths of over 200 million people worldwide. The bacteria migrates to lymph nodes directly via lymphatic vessels or upon being taken up by DCs. Once inside lymph nodes, they replicate in resident macrophages that gives rise to distinctly inflamed lymph nodes, termed buboes (Perry and Fetherston 1997). Despite producing a clear lymphatic pathology, such as lymphangitis (inflammation of lymphatic vessels), or lymphadenitis (inflammation of lymph nodes), the attention towards understanding mechanisms of dissemination by extracellular pathogens has been minimal. Lynskey et al. (2015) have however, provided some partial understanding to mechanisms involving pathogen migration; the hyaluronan capsule of group A streptococcus bacterium interacts with the lymphatic receptor LYVE-1 to clear to draining lymph nodes, two molecules which will be discussed further below.

1.1.6 Hyaluronan and its association with the lymphatics

Hyaluronan or hyaluronic acid (HA) is an important sugar molecule and component of the extracellular matrix of all tissues across the body. It is technically described as a nonsulfated glycosaminoglycan (GAG) that has

repeating chains of D-glucuronic acid and N-acetylglucosamine (Fig 1-5) (Jackson 2009).

Hyaluronan is synthesised as a large, extended non-sulphated polysaccharide and as a free chain without attachment to a core protein, catalysed by large single chain enzymes called hyaluronan synthases (HA synthase), unlike other GAGs (such as chondroitin sulphate, heparin sulphate and keratan sulphate) that are bound to a core protein to form a glycosylated protein or proteoglycan. These enzymes are located on the inner leaflet of the plasma membrane, where HA is produced and then released to the cell surface (Toole 2004). This GAG has the capacity to bind to a wide range of HA-binding proteins; the functions of HA thus determined by its association resulting in a wide range of actions such as, regulation of cell motility and proliferation, cell adhesion and activity, matrix stability and water retention. (Day and Prestwich 2002)

Along with association with diverse proteins, HA function is also affected by its chain length. High molecular weight glycosaminoglycans are known to mediate anti-inflammatory functions as well as provide cancer resistance whereas smaller fragments of HA generated by degradation bind to Toll-like receptors (TLRs) to mediate pro-inflammatory and pro-angiogenic actions. HA size can also be a determinant of tissue integrity (McKee, Penno et al. 1996, Termeer, Hennies et al. 2000). Breakdown of HA size in the interstices that occurs from tissue damage or inflammation is thought to function of as danger signal for innate immune cells (Termeer, Hennies et al. 2000).

Beside functions through binding to proteins, HA on its own is an important structural component of extracellular matrix in tissues, where it forms a highly

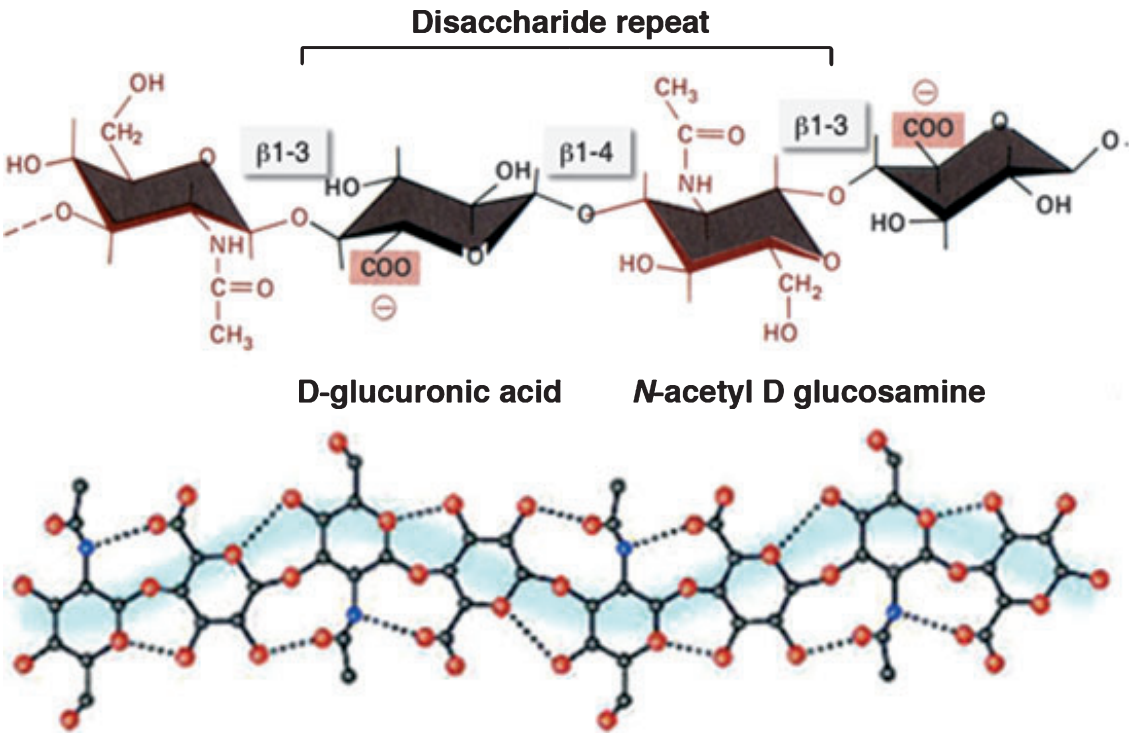


Figure 1-5: Schematic diagram of the structure of hyaluronan. The repeating disaccharide unit consists of alternating units of glucuronic acid and N-acetyl glucosamine (top) and intra-chain hydrogen-bonding within the polymer that 'stiffens' the chain as depicted in 8mer (red, oxygen; blue, nitrogen; black, carbon; bottom). Image taken from Jackson et al. (2009). Originally published in Immunological Reviews, 230: 216-231.

hydrated gel. This is due to the ability of the GAG to attract polar water molecules at physiological pH (HA is an acid at pH 7.4 with a net negative charge, thus attracting positive ions which in turn attract water molecules) (Laurent and Fraser 1992). The gel forms a matrix by binding to proteoglycans (e.g – aggrecan and versican) that either wraps around cells forming a pericellular coat or glycocalyx, or can coalesce into 'cables' spanning several cell lengths (Luft 1966, Selbi, de la Motte et al. 2006, Reitsma, Slaaf et al. 2007). The glycocalyx is an important structural component of cells acting primarily as a barrier and filtering interacting molecules with a cells plasma membrane. Recently identified functions of glycocalyx involve integrin clustering by funnelling active integrins into adhesions, and altering integrin state by applying tension to matrix-bound integrins, independent of actomyosin contractility (Paszek, Boettiger et al. 2009, Paszek, DuFort et al. 2014). Interestingly, the bulkier the glycocalyx, the more pronounced the integrin based effects are which would noticeably have an effect on cell migration. Presence of an HA pericellular coat is critical for migratory cells during development and can indeed hypothetically be extended to other types of migratory cells in adults such as leucocytes (Evanko, Angello et al. 1999, Evanko, Potter-Perigo et al. 2012). The other structural shape, HA cables incorporate components of the inter-alpha-inhibitor (IαI) family of proteins and versican that interestingly, appear upon inflammatory stimulation and is structurally associated with increased HA dependent leucocyte adhesion to cell surface (Selbi, de la Motte et al. 2006, Jokela, Lindgren et al. 2008).

As mentioned above, HA is found in all tissues with its total content to be in the region of 15 g; one third of this amount is replaced daily. HA catabolism is

mediated by a family of enzymes known as hyaluronidases (Hyal 1-3) or reactive oxygen species (ROS) after local uptake by fibroblasts and macrophages. Even though this is how the majority of HA turnover occurs, a significant amount is also removed from tissues in lymph for terminal degradation in lymph nodes (Reed and Laurent 1992, Jackson 2009). This degradation is mediated via HA receptor for endocytosis (HARE) receptor in lymph nodes. Under homeostatic conditions, the rate of turnover of HA was found to be brisk compared to other matrix molecules with it particularly rapid in certain tissues such as skin and synovial fluid (Reed, Lilja et al. 1988, Reed, Laurent et al. 1990). This rapid turnover is accelerated along with flux through lymph where a concentration of approximately 18 μg/ml is observed. Serum concentrations of HA was found to be much lower than in lymph at 0.1 μg/ml, any HA being rapidly transported to either the liver, spleen or kidneys to avoid increasing the viscosity of blood (Laurent, Dahl et al. 1991, Laurent and Fraser 1992, Cowman, Lee et al. 2015).

Along with uptake via lymphatic vessels for degradation in lymph nodes, HA is believed to have other functions relevant to lymphatics.

1.1.7 Two major hyaluronan receptors - CD44 and LYVE-1

CD44

As mentioned above, HA function is determined by the protein it binds to and associates with. The majority of HA-binding proteins within tissues belong to the

Link protein superfamily with major cell surface receptors being CD44, LYVE-1, Stabilin-1 and HARE (Fig 1-6) (Jackson 2009).

CD44 is a major HA receptor that is expressed on most cells found in the body. These cells are usually of epithelial, mesothelial and haematopoietic in origin. The few tissues that have been consistently reported as CD44-negative are cardiac muscle, renal tubular epithelium, testis and portions of the skin (Ponta, Sherman et al. 2003). As a complex polymorphic molecule, many years were spent since its first identification to its characterisation. The CD44 proteins are all encoded by a single, highly conserved gene. Confusions arose in its characterisation due the protein having numerous post-translational modifications that differ depending on cell type and growth conditions. Structural studies categorised CD44 as a type I transmembrane protein that is 314 amino acid residues in length. The extracellular domain is 248 amino acids in length and contains the Link module at the N-terminus, with three disulphide bridges. 23 hydrophobic residues and a cysteine residue constitute the transmembrane domain. A 72 residue cytoplasmic tail precedes the carboxy terminus. The extracellular domain also consists of six putative N-linked and O-linked glycosylation sites.

HA binding occurs in a specific region located in the extracellular domain. This domain, known as the Link domain/module, consists of a stretch of 90 amino acids (residues 32-123) shows considerable homology with both the cartilage Link protein and with the proteoglycan core protein. The structure of the Link module has a compact α/β fold comprised two antiparallel β sheets made from a total of six β strands and two α helices stablised a pair of conserved

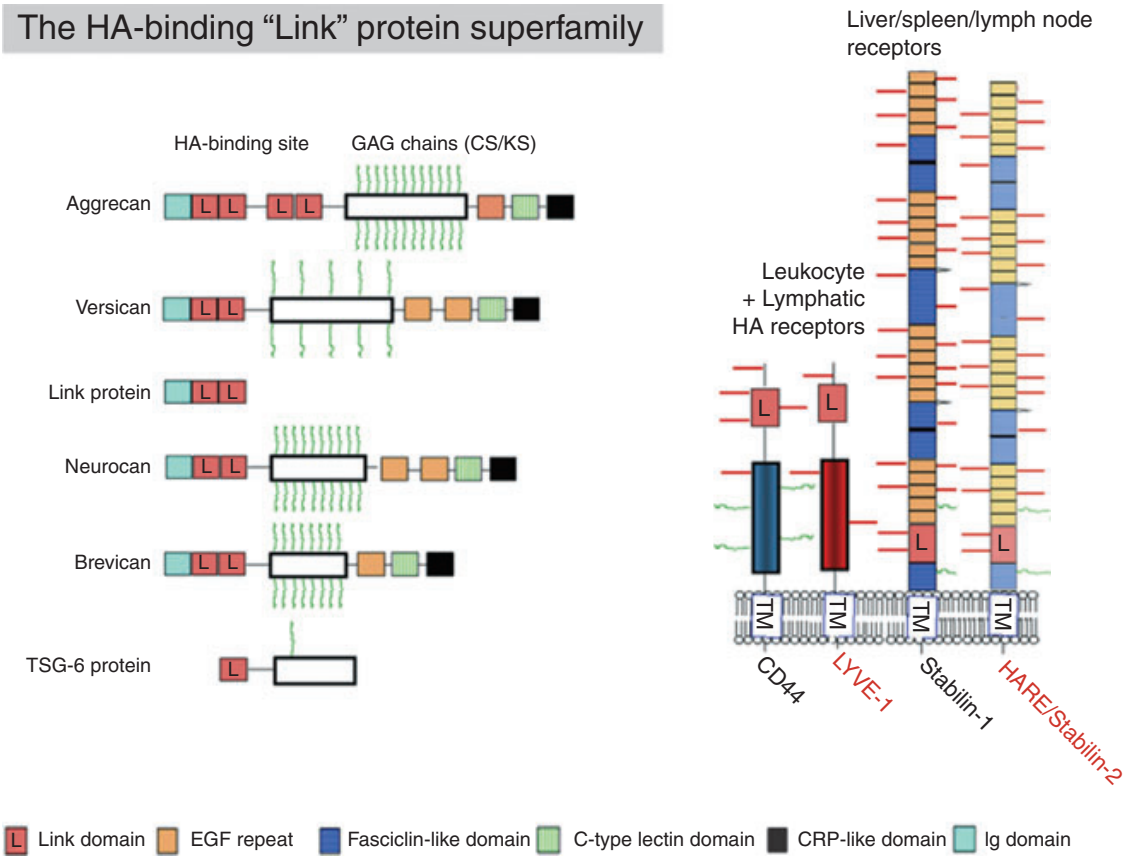


Figure 1-6: Schematic diagram of the Link superfamily of hyaluronan-binding proteins. Members include extracellular matrix proteoglycans and small soluble binding molecules (shown on left) as well as a small group of transmembrane receptors (shown on right). Carbohydrate chains are denoted as either red lines (N-glycans) or green lines (O-glycans). Image taken from Jackson et al. (2009). Originally published in Immunological Reviews, 230: 216-231.

disulphide bridges (Kohda, Morton et al. 1996). X-ray crystallography and NMR spectroscopy helped determine that the HA binding domain (HABD) of human CD44 is extended at the N- and C- termini by further β strands and a third disulphide bridge. However, further structural studies of murine CD44 revealed that the Link extension does not contribute directly to HA binding. Rather it allows a conformational change in the molecule reverting it between high and low binding states (Teriete, Banerji et al. 2004, Banerji, Wright et al. 2007).

CD44 has a wide variety of functions that have mostly been identified with experiments using specific monoclonal antibodies that are directed against either all or subsets of variant proteins. *CD44*$^{-/-}$ mice have not proved helpful in determining functions as the mice exhibit a normal phenotype (albeit with impaired homing of lymphocytes to the thymus and lymph nodes), most likely due to compensatory mechanisms such as upregulation of other similar HA receptors named above (Protin, Schweighoffer et al. 1999). Some functions that have been identified due to such studies are adhesion and migration, mediating cytokine signalling and mediating cell growth and differentiation (Protin, Schweighoffer et al. 1999, Jackson 2009).

The binding of CD44 with HA is affinity mediated and this is influenced by mitogenic stimuli, glycosylation of extracellular domains or exposure to inflammatory cytokines (Siegelman, DeGrendele et al. 1999, Pure and Cuff 2001). The modulation of binding affinity is believed to be important for cellular migration as CD44 has been shown to localise to lamellipodia and leading edges of several cell types *in vitro* (Zohar, Suzuki et al. 2000). HA is believed to act as an adhesive bridging molecule between cells expressing CD44 thus allowing cell-cell communication. CD44-HA interactions are important in the

rolling phase of leucocyte extravasation and the migration of T cells to sites of inflammation was critically dependent on such interactions (DeGrendele, Estess et al. 1997). The earlier stage of rolling was demonstrated by (Clark, Alon et al. 1996) using CD44 positive lymphocytes within a flow chamber coated with hyaluronan or tonsillar stromal cells. These findings were further validated with demonstrations that showed CD44-HA interactions are of critical importance in migration of T cells to sites of inflammation. With such a wide range of functions, it is logical to believe that other Link proteins interacting with HA might similar important roles in maintaining physiology and homeostasis.

LYVE-1

LYVE-1 was discovered during the search for a homolog of CD44, initiated by the largely normal phenotype of *CD44*$^{-/-}$ mice. This was achieved using a human expressed sequence tag (EST) database search that revealed a receptor with a primary sequence 51 % similar to CD44 (Banerji, Ni et al. 1999, Prevo, Banerji et al. 2001). The amino acid sequence encodes a 322-residue polypeptide, with typical characteristics of a type I integral membrane glycoprotein. 26 largely hydrophobic residues are found at the amino terminus of the protein and most likely constitute the leader peptide. These are followed by hydrophilic sequences of 212 amino acids which encode the extracellular domain. 21 hydrophobic residues correspond to the transmembrane anchor, followed by the dibasic motif KR and a highly charged stretch forming the 63 residue cytoplasmic tail. A heavily O-glycosylated serine/threonine-rich region, comprising 71 residues lies within the extracellular domain, as do two motifs for N-linked glycosylation , centred on residues 54 and 131, respectively. The HA-

binding Link domain is composed of two β sheets flanked by two short α helices encapsulating a hydrophobic core. The domain is stabilised by four central cysteine residues (C2-C5) with a flanking pair (C1 and C6). A cysteine residue is also found within the transmembrane domain which is believed to be involved in covalent dimerisation of the receptor, similarly to CD44. The cytoplasmic tail of LYVE-1 is a well conserved region, based upon comparison of sequence alignment of five different species, and suggests that downstream signalling and other functions might form an integral part of its role within physiology, along with HA binding. Interestingly, the expression of the receptor was initially discovered to be restricted mainly to lymphatic vessels and lymph node sinus endothelia, although this has been challenged with expression shown in other cell types such as alveolar epithelial cells, cortical neurons and renal epithelium (Royston, unpublished findings from Jackson laboratory (Mouta Carreira, Nasser et al. 2001). This is distinct from the expression of CD44, which is absent from LECs but expressed widely on other cell types, including leucocytes (Kennel, Lankford et al. 1993). Its abundant expression on lymphatics raises interesting questions of the function of lymphatics in maintaining homeostasis. Binding of hyaluronan to recombinant LYVE-1 showed specificity that was not competitively inhibited by other glycosaminoglycans. However, a rather perplexing result arose along with the identification of LYVE-1 - LECs expressing endogenous LYVE-1 failed to bind HA. Banerji et al, (1999) attempted to colocalise LYVE-1 from tissues to either endogenously or exogenously added HA using fluorescent HA binding probe (bHABP), with unsuccessful results. However, this result led to further identification of similarity with CD44, its closest homolog. CD44 is usually expressed on circulating leucocytes in a low affinity state, as is LYVE-1 (Kd 10^{-4}

- 10^{-5} M), and is only able to bind HA after appropriate activation following exposure to inflammatory cytokines, engagement of the antigen receptor on T or B cells, or receptor clustering (Ponta, Sherman et al. 2003). With this hypothesis in place, (Nightingale, Frayne et al. 2009) demonstrated that the functional status of LYVE-1 is regulated by cell specific changes in receptor sialylation. The autoinhibitory sialic acid moieties were concluded to reside on the O-glycans rather than N-glycans. However, the conditions under which HA binding is uninhibited have remained a mystery until recently. Prior experiments involved stimulation of LECs with a wide range of pro-inflammatory cytokines in a manner similar to CD44. This however, proved unsuccessful in activation and unmasking of endogenous LYVE-1. Another mystery that remains is the structure of the LYVE-1-HABD as the crystal structure has not been yet been determined. However, with LYVE-1 sharing sequence similarity with CD44, it can be presumed that the HABDs of the two receptors are similar as well. Initial models generated using the crystal coordinates of the CD44 apoprotein structure suggested some but not all elements of the CD44 Link extension were present. However, updated models using optimised LYVE-1/CD44 sequence alignment indicated a very similar extended HABD structure as that of CD44 with the same long 10-stranded β-spiral stablised by three conserved disulphide linkages forming an analogous supplementary lobe to that of CD44. Following on from this, site directed mutagenesis studies revealed that the HA binding site is a shallow cleft that is smaller in size to the HA binding site of CD44, albeit in a similar location and orientation i.e. below the characterisitic hook-like region contributed by the β4/β5 loop (Fig 1-7) (Banerji, Wright et al. 2007).

With the structure modelled, studies identified the nature of HA binding to LYVE-1 as a charge dominated interaction, unlike the H-bonding and hydrophobic interactions of CD44-HA (due to the aliphatic arrangement of the

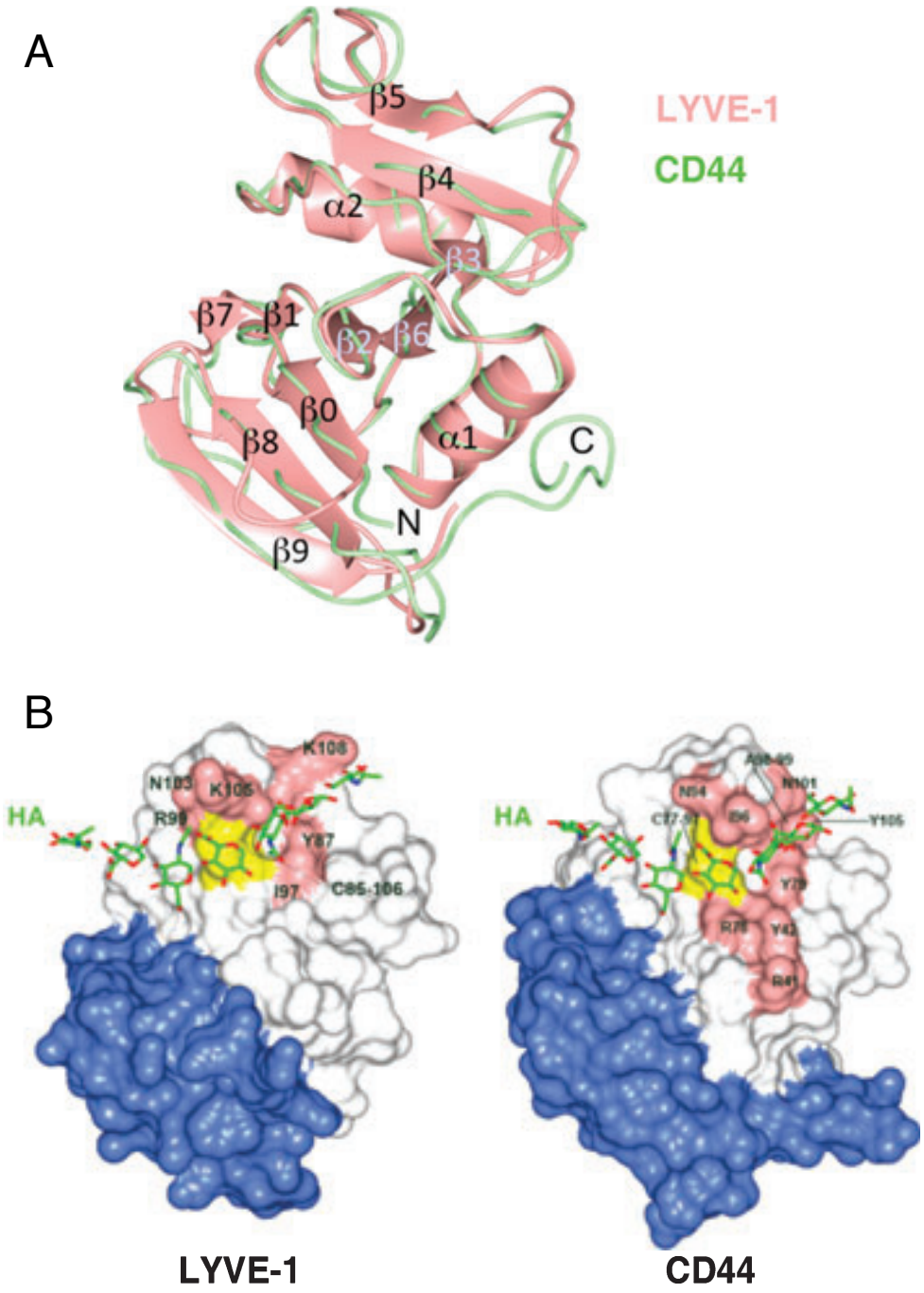


Figure 1-7: Structure of extended hyaluronan binding domain (HABD) in LYVE-1 and CD44. Modeling of the hyaluronan-binding domain of LYVE-1 based on the crystal coordinates of the murine CD44 structure predicts a Link module with similar N- and C-terminal β-stranded exten- sions (A). Projection of known hyaluronan-binding residues (pink) onto a space-filling representation of the LYVE-1 domain indicates the hyaluronan-binding surface is smaller than that of CD44 albeit in a similar location and orientation (hyaluonan 8mer colored green; conserved cysteine residues colored yellow; Link extension colored blue). Image taken from Jackson et al. (2009). Originally published in Immunological Reviews, 230: 216-231.

HA binding site of CD44). Such charge based interactions are also observed amongst selectins binding to prototypic fucosylated tetrasaccharide sialyl LewisX. These occur between the carboxylate group of NeuNAc and primarily lysine and arginine residues (Torgersen, Mullin et al. 1998, Bouyain, Rushton et al. 2001). Recently, it has been discovered that LYVE-1 is a low-affinity and avidity receptor that requires either receptor clustering or appropriate HA presentation (tentative unpublished evidence from the Jackson laboratory show that this requires engagement with suitable HA binding partners such as TSG-6) (Lawrance et al. 2015; manuscript submitted). The finding of cross-linked HA complexes being able to bind to LYVE-1 presents interesting notions to the physiological role of such binding and their roles in homeostasis. Example of such proteins linking to HA and forming in biological fluids include serum derived HA-associated protein (SHAP) and Link superfamily binding proteins TSG-6 and versican in HA cables (Huang, Yoneda et al. 1993, Selbi, de la Motte et al. 2006).

SHAP was discovered as the heavy chain (HC) of the serum inter-α trypsin inhibitor (IαI), a complex of HCs in ester linkage with the chondroitin sulphate chains of the proteoglycan bikunin, that is generated by enzymatic transesterification. SHAP complexes exert matrix stablising effects in both normal physiological processes as well as pathological conditions such as inflammation and malignancy.

Tumour necrosis factor (TNF)-stimulated gene 6 (TSG-6) is a ~35 kDa secreted protein composed mainly of Link and CUB modules. Its expression appears to be highly regulated not being found in healthy adult tissues but rather in tissues in association with inflammatory mediators. This upregulation with inflammation appears to be at sites of ECM remodelling highlighting its association with HA.

While directly acting as an important component of HA cross-linking, TSG-6 appears to indirectly influence the interaction of HA with IαI by catalysing the transfer of IαI heavy chains to HA (Milner and Day 2003).

Such complexes have been shown to bind to CD44 in its low affinity state, most likely by inducing receptor clustering, owing to the multivalency of their cross-linked structure. (de la Motte, Hascall et al. 2003) showed that HA cables expressed by polyinosinic-polycytidylic acid (polyI:C) treated mucosal smooth muscle cells were able to bind to low affinity CD44 more readily than non-complexed HA present adjacently. The unpublished finding of TSG-6-HA complex being able to bind to LYVE-1, a low affinity binder of HA, sheds light to a possible mechanism for binding of analogous fashion to that of CD44. Such binding also indicates to a role for the receptor in organising the HA matrix or in the recruitment of inflammatory cells. However, whether such mechanisms occur *in vivo* on lymphatic vessels is yet to be identified.

Detection of binding to HA in 293T transfectants revealed the ligand receptor complex to undergo internalisation through receptor mediated endocytosis suggesting an involvement of LYVE-1 in the transport of HA across lymphatic endothelium. However, the uptake of HA by LYVE-1 is considerably slower than that by the professional scavenger receptor, HARE, possibly suggesting that LYVE-1 is involved in a regulated role with downstream effects rather than mediating rapid uptake and degradation of lymphatic HA (Johnson, Prevo et al. 2007, Jackson 2009).

Although HA has been identified as the primary ligand for LYVE-1, other ligands to the receptor have been identified. These are fibroblast growth factor-2

(FGF-2) and platelet derived growth factor (PDGF). FGF-2 has been shown to bind to LYVE-1 with a higher affinity than HA and this interaction was dependent on the glycosylation of LYVE-1. From a physiological point of view, this interaction acted as mechanism of sequestering FGF-2, to prevent it from exerting known effects such as lymphangiogenesis (Platonova, Miquel et al. 2013). The interaction of PDGF to LYVE-1 was identified as an interaction between CRSBP-1 with PDGF. However, further characterisation of the molecule led to it being identical to LYVE-1 (Boensch, Huang et al. 1999, Huang, Tang et al. 2003). With LYVE-1 binding to PDGF, the junctions between LECs were found disrupted with VE-cadherin (notably present on LECs) internalised.

These preceding descriptions into LYVE-1 give the impression of an important molecule, with the likelihood to play a significant function in inflammatory pathologies. Surprisingly, a broad investigation into *LYVE-1*$^{-/-}$ mice failed to showcase defects in the overall architecture of lymphatics, either during development or in adulthood, with normal fluid drainage throughout. There also appeared to be no alteration in lymphoid tissue structure or in leucocyte populations in blood or lymphoid organs. Such a phenotype points towards the function of LYVE-1 possibly being partially redundant. Despite the normal findings with *LYVE-1*$^{-/-}$ mice under homeostatic conditions, unpublished findings from Professor Jackson's laboratory do however, suggest a significant role in resolution of inflammation in the lungs of these mice following bleomycin induced inflammation that was related to increased mortality (Royston D, D.Phil. Thesis, 2011). Also, as the similarity with CD44 stretches, it is worth noting that numerous functions of CD44 were discovered with function blocking monoclonal

antibodies (mAbs) rather than with commercially available *CD44*$^{-/-}$ mice (although functions related to inflammation have also been uncovered with the mice) and progressive work in Professor Jackson's laboratory has led to development of LYVE-1-HA interaction blocking mAbs (by Dr R Prevo and Dr L Johnson) as well as human antibodies which crosslink the receptor (clones 6A, 7C, and 8C), the three clones recognise overlapping epitopes in the human LYVE-1 extracellular domain, and promote HA binding to a low affinity receptor (Ponta, Sherman et al. 2003, Jackson 2009). The availability of these resources will enable us to understand the mechanism of LYVE-1 action in leucocyte clearance *in vitro* as well as the physiological action of the receptor *in vivo*.

1.2 Macrophages

1.2.1 Brief history into identification of macrophages

Inflammatory responses are initiated upon invasion of a tissue in the body by a foreign pathogen. Research into the cellular components associated with an inflammatory response was discovered steadily in the 19th and early 20th centuries. In 1841, William Addison published one of the first reports to provide insight into the role of leucocytes at the inflammatory site. In this report, he proposed the important step of leucocytes utilising diapedesis to get to tissues by comparing the colourless corpuscles in blood of inflamed tissues (Addison 1842). This proposal got evidence in 1873, when Julius Connheim reported the very event of transmigration. He observed leucocytes lining up along vessel walls and protruding and extravasating into tissues (Jarcho 1972). The identification of cells associated with inflammation was facilitated with staining techniques developed by Paul Ehrlich in 1880. With improvements in the microscopic study of individual leucocytes, Elie Metchnikoff reported in 1884 the observation of cells engulfing solid particles, an event first observed in ameboid cells of the marine sponge and later in higher species. He termed this event as phagocytosis and the engulfing cells as phagocytes. Metchnikoff identified in 1892 two distinct phagocytic populations associated with human blood which he coined macrophage (large eater) and microphage (small eater). He observed that the microphages were polymorphonuclear leucocytes whereas the macrophages were mononuclear ones (reviewed by (Gordon 2008). In this work he also recognised the relationship between mononuclear phagocytes found in lymph nodes, bone marrow, the spleen and these phagocytes in other organs.

These findings led him to establish this as the 'macrophage system'. These findings have subsequently been expanded throughout the years to provide a rich literature shaping our understanding of macrophage biology.

1.2.2 Monocyte/macrophage biology

Macrophages are described as terminally differentiated leucocytes that function primarily as phagocytes. They are responsible for clearing up debris and foreign bodies at sites of inflammation (Ginhoux and Jung 2014). However, macrophages are much more than just cells as part of the immune system. They are critically important in aspects of embryonic development, homeostasis and wound repair (Wynn, Chawla et al. 2013). Their importance is underlined by their presence in virtually every tissue of the body. These tissue resident macrophages are nonetheless very different from each other as they have become adapted to certain functionality at the location of their tissue (Ginhoux and Jung 2014). Ralph van Furth established, in 1968, his paradigm - the mononuclear phagocyte system (MPS) which explained the homeostasis of tissue-resident macrophages was reliant on the constant recruitment of blood monocytes (van Furth and Cohn 1968). Although they are progenitors to macrophages, especially in an inflammatory setting, this general model of monocytes arriving and replenishing tissue macrophage populations, has undergone revision (Ginhoux and Jung 2014).

Inflammatory macrophages, along with dendritic cells can be thought of as the final step in the development and differentiation of monocytes. These

leucocytes are produced in primary lymphoid organs (such as the bone marrow) as part of haematopoiesis, with production induced in inflammatory conditions and represent 10 % of all nucleated cells in blood circulation of humans, which have a short half-life of 20 hours (reviewed by (Geissmann, Manz et al. 2010). They exist in different subsets in blood, with two major groups identified in human blood - one of them is defined as $CD14^{+}$ and the other as $CD14^{low}CD16^{+}$. These subsets are correlated in mice as $Ly6C^{hi}$ and $Ly6C^{low}$, respectively. The $CD14^{+}/Ly6c^{hi}$ population of monocytes typify the characteristics associated with 'classical monocytes'; they are recruited to sites of inflammation and act as precursors of macrophages and dendritic cells (DCs) (Shi and Pamer 2011). The recruitment of this subset of monocytes to sites of infection/inflammation is dependent on two key chemokines - CCL2 and CCL7 (Fuentes, Durham et al. 1995, Gunn, Nelken et al. 1997, Tsou, Peters et al. 2007). Although the importance of these chemokines to recruitment is now well established, the exact mechanism of action is still not determined.

The next step following attracting monocytes to sites of inflammation, is the exit of them from blood circulation into the tissue. They are believed to follow the same paradigm of exit as all other leucocytes as explained in the review by (Ley, Laudanna et al. 2007). The 'classical monocytes' described above express a wide array of key adhesion molecules such as L-selectin, lymphocyte function associated antigen 1 (LFA-1), macrophage receptor 1 (Mac1), platelet endothelial cell adhesion molecule 1 (PECAM-1). All these molecules have been reported to play a role in leucocyte transmigration via blood vessels. For classical monocytes, L-selectin is critical in their arrival to a site of inflammation, such as in the popular inflammation studying model of thioglycollate induced peritonitis and further involvement of Mac-1 and ICAM-1 has been shown via

antibody blockade studies .(Rosen and Gordon 1987, Tedder, Steeber et al. 1995, Shi, Velazquez et al. 2010). The involvement of adhesion molecules is covered in detail further down the chapter.

Upon arrival at sites of inflammation, monocytes differentiate into either macrophages or dendritic cells, depending on the cues they receive from the inflammatory environment, macrophages arising from signals from cytokines such as, M-CSF and GM-CSF (Pollard, Bartocci et al. 1987).

As mentioned above, the previously established idea that only monocytes give rise to macrophages at various tissues under steady-state conditions no longer holds certain credibility, with the majority of tissue resident macrophages shown to be derived from yolk-sac progenitors (Ginhoux, Greter et al. 2010, Hashimoto, Chow et al. 2013, Gomez Perdiguero, Klapproth et al. 2015). It is interesting to note that within mice, all tissue-resident macrophages are defined as pan-macrophage marker high ($F4/80^{high}$) whereas those derived from bone-marrow progenitors such as monocytes are defined as $F4/80^{med/low}$ (Zhang, Goncalves et al. 2008). The molecule, F4/80, corresponds to a G-protein coupled adhesion receptor that was identified on macrophages from peritoneal cavity and other sources, blood monocytes, and bone marrow derived macrophages and not on polymorphonuclear leucocytes, lymphocytes or fibroblasts (Austyn and Gordon 1981). The differing levels of expression of this molecule on the surface of other granulocytic white blood cells such as, eosinophils and basophils, is now known to complicate the identification of macrophages from thioglycollate induced peritonitis and has prompted re-thought into the use of appropriate inflammatory stimuli in studying macrophage biology (Personal communication with Iqbal AJ and Greaves DR). Interestingly, the human homologue of F4/80, EMR1, is not found on macrophages or

basophils, but specifically on the surface of eosinophils (Hamann, Koning et al. 2007).

Macrophages play an important role in the clearance of pathogens as professional phagocytes and are responsible for the rapid uptake of foreign bodies. They possess much more membrane movement compared to other cells, which makes them very efficient at uptake of particles. Once engulfed, the pathogen is transported to a lysosome where they are rapidly destroyed due to and acidic environment and presence of reactive oxygen species (ROS), an important mechanism in the resolution of inflammation (Hart and Young 1975, Knapp and Swanson 1990, Aits and Jaattela 2013). Upon differentiation, they also clear apoptotic bodies of neutrophils and pathogens by phagocytosis. The mechanism of recognition of apoptotic bodies is yet to be completely determined and the currently established hypothesis explains apoptotic bodies exposing molecules associated with recognition and healthy cells expressing molecules providing inhibitory signals to prevent phagocytosis (Savill, Fadok et al. 1993). Two major candidate molecules associated with pro-recognition function are phosphatidylserine (PS) and calreticulin (Callahan, Williamson et al. 2000, Gardai, McPhillips et al. 2005). PS is usually found in the inner surface of the plasma membrane and calreticulin is within the endoplasmic reticulum (Michalak, Corbett et al. 1999, Elmore 2007). It is believed that upon apoptosis, these molecules become exposed which can be recognised by receptors on the macrophages. The other hypothesis is based around the observation that healthy cells are able to detach from the phagocytes. PECAM-1 (also known as CD31) on healthy cells is able to bind to CD31 on phagocytes, this homotypic association causing the detachment that prevents binding and engulfment (Brown, Heinisch et al. 2002).

Another important phenotype of inflammatory macrophages are that they express cell surface major histocompatibility complex-II (MHC-II), an important molecule in the presentation of antigen to initiate adaptive immune responses. They are abundantly expressed on classical dendritic cells (cDCs) which are professional antigen presenting cells (APCs). Thus, macrophages can facilitate the function of adaptive immune initiation along with dendritic cells (Baumgart, Moos et al. 1998).

Macrophages at the site of inflammation are able to play two distinct roles - they can respond in both a pro- and anti-inflammatory manner. This is dependent on the cues they receive that polarise them to either phenotypes and this division of phenotype on such function has been labelled as M1 (pro-inflammatory) and M2 (anti-inflammatory), a mimic of T helper cell nomenclature (reviewed by (Martinez, Sica et al. 2008). M1 polarisation is stimulated by TLR ligands (e.g. lipopolysaccharide) and IFN-γ, whereas M2 polarisation is stimulated by IL-4/ IL-13 (Nau, Richmond et al. 2002, Mantovani, Sica et al. 2004, Martinez, Helming et al. 2009). Plasticity is a key feature of the activated states of macrophages. The ability to revert from an M1 to an M2 phenotype, and vice versa, is influential in orchestrating remodelling and repair during inflammation. M1 macrophages secrete inflammatory cytokines and mediates tissue damage, removing present foreign bodies. Although initially believed to be two distinct phenotypes, there has been a growing body of evidence which suggests such simple polarisation is not the case (Sica and Mantovani 2012). *In vitro*, it has been possible to label macrophages as either only M1 or M2 but *in vivo*, cells have been found to display characteristics of both M1 and M2. So, macrophages are labelled either more M1 or M2. Indeed, in a peritoneal model of inflammation induced by zymosan, the macrophages in the resolution phase,

expressed a distinct phenotype. They had elevated levels of M1 markers yet presented an M2 phenotype along with weaker bactericidal properties (Bystrom, Evans et al. 2008).

The fate of macrophages after the resolution of inflammation is a question that is yet to be answered efficiently and our current understanding from the literature is discussed below.

1.2.3 Fate of macrophages

Unresolved inflammation can have devastating consequences and to allow homeostatic physiology to return following injury, clearance of accumulated macrophages is paramount. Until recently, the exact fate of these macrophages was unclear and the two major hypotheses appear prominent from published works suggest macrophages undergoing either local apoptosis similar to neutrophils, or clearing to draining lymph nodes (LNs).

The emigration of macrophages to draining LNs has been a very popular concept with Bellingan's (1996) work demonstrating in a sterile model of peritonitis that macrophages adoptively transferred to another inflamed peritoneum drain to the mediastinal/parathymic lymph nodes. Further elaboration on this work determined that this emigration is dependent upon α4β1 and α5β1 integrins but not on β2 integrins. Interestingly, the findings of this study are contested by the demonstration that Mac-$1^{-/-}$ mice have decreased macrophage efflux to draining lymph nodes (Bellingan, Xu et al. 2002, Cao, Lawrence et al. 2005).

With both hypotheses holding credibility in published works, it is interesting to note that a majority of the data under both concepts is showcased through qualitative studies. However, with this shortcoming in site, (Gautier, Ivanov et al. 2013) published a comprehensive quantitative study to determine the true fate of inflammatory macrophages. Using the same thioglycollate peritonitis model as described by previous papers demonstrating the phenomenon, Gautier et al. presented through their findings with extensive flow cytometry that although a population of macrophages do arrive at draining lymph nodes, this was quantitatively minor and would not account for the extent of retraction during the resolution of inflammation. However, blocking apoptosis prevented the homeostatic reduction observed, thus implying that this was the major mechanism of clearance.

Although this study seems to settle the debate of the fate of the recruited macrophages, it does leave us with an important question - how are the apoptotic bodies of these macrophages cleared? It would seem impractical for sites of inflammation to have high amounts of apoptotic bodies not cleared. Are further macrophages recruited? Or do tissue macrophages engulf them? They explain that the surrounding endothelial cells engage in efferocytosis although it seems unlikely that retraction of such numbers would be by non-phagocytic cells. It is also worth noting as well that indeed a significant number of cells do indeed migrate to the draining lymph node. What is the role of these macrophages at the LN? Another shortcoming of the studies above is that none have demonstrated a direct interaction of the macrophages with the lymphatics. Even though it would be assumed that cells arriving at draining lymph nodes would be through lymphatic vessels, there is the possibility that they have arrived via blood circulation and enter via high endothelial venules (HEVs).

Much remains to be elucidated on the mechanisms by which macrophages migrate to draining lymph nodes.

1.2.4 Complexities and association of macrophages in disease

Macrophages have a causal association with numerous diseases. This association is through continuous insults where their homeostatic functions are corrupted to become harmful with most commonly observed clinical issues branched from chronic inflammatory disease pathologies (Allison, Ferluga et al. 1978). The progression into disease is impacted by the plasticity and conversion from M1 to M2 phenotype and vice versa. Some common inflammatory pathologies where macrophages play a harmful role are atherosclerosis, multiple sclerosis, Crohn's disease and arthritis (Kinne, Brauer et al. 2000, Mahida 2000, Heymann, Trautwein et al. 2009). In such diseases, macrophages secrete inflammatory cytokines that are now known to drive autoimmune inflammation. For example, a subset of macrophages ($TLR2^{+}CCR2^{+}Ly6c^{hi}GR1^{+}$) have been identified that secrete TNF-α and exacerbate colonic inflammation in mice (Platt, Bain et al. 2010). Other subsets have been identified in Crohn's disease patients that give a clue to their origin (as discussed above in section 1.2.2). $CD14^{+}$ macrophages that produce IL-23 and TNF-α, have been discovered that further aggravate the inflammation at hand (Kamada, Hisamatsu et al. 2008).

A consequence of the ongoing chronic inflammation is that macrophages respond to the environment with further secretion of factors that promote fibrosis (scarring) and maintain the inflammatory cascade. Increased fibrosis is

associated with a loss of function in tissues, seen in the pathology of multiple chronic inflammatory diseases condition such as cirrhosis (Grivennikov, Greten et al. 2010). Two such secreted molecules, transforming growth factor (TGF)-β1 and platelet derived growth factor (PDGF), are known to directly activate fibroblasts promoting their proliferation. TGF-β1 promotes myofibroblast production which in turn results in the production of tissue inhibitor of metalloproteinases (TIMPs) and interstitial fibrillar collagens (Pierce, Vande Berg et al. 1991, Desmouliere, Geinoz et al. 1993). Activated macrophages at such sites are known to produce chemokine (C-C motif) ligand 2 (CCL2), a strong chemoattractant for inflammatory monocytes, promoting their infiltration in greater numbers. Arrival of such monocytes is believed to promote worsening inflammation and fibrosis (Yoshimura, Robinson et al. 1989). It has been shown that in a $CCR2^{-/-}$ mice, there is less fibrosis and macrophage accumulation after bleomycin induction of pulmonary fibrosis (Gharaee-Kermani, McCullumsmith et al. 2003).

A major disease that macrophages are affiliated with is cancer. They are found abundantly within the tumour microenvironment. A major risk factor for cancer is persistent injury and inflammation and since macrophages play a role towards promoting chronic inflammation, it has been assumed that they play a causal role in tumour initiation and progression. However, once a tumour establishes, it converts macrophages to have an immunosuppressive role. With such a phenotype they are labelled as tumour associating macrophages (TAMs) and are responsible for further tumour progression, malignancy and growth (reviewed by (Pollard 2004). A specific role is in its ability to remodel the tumour microenvironment through the secretion of key matrix degrading enzymes called matrix metalloproteinases (MMPs) such as MMP-2, MMP-7 and MMP-9.

Such activity provides accessible routes for tumour cells to invade out of the primary tumour site and metastasise (Kessenbrock, Plaks et al. 2010). Another family of proteases that function similarly to MMPs are cathepsins. Macrophage derived cathepsin B has been shown to promote the metastasis of mammary tumour cells to the lung (Vasiljeva, Papazoglou et al. 2006).

1.2.5 Monocyte/macrophage trafficking

Henri Dutrochet, a renowned nineteenth century pathologist, made the very first accounted observation of leucocytes attaching to blood vessel endothelium. His findings were subsequently backed by similar independent findings of other physicians (Nezelof 2003). Of note were the findings by Waller and Wagner, who demonstrated not only adhesion of leucocytes to blood vessel walls but also emigration out of such blood vessels (Wagner and Frenette 2008). Most of our understanding of leucocyte trafficking have come from the events studied with use of neutrophils, monocytes, DCs and T cells. The process involves three major phases before transmigration, which is summarised in figure 1-8. The cell first arrives to the endothelium and has to roll across the endothelium while resisting the shear flow of blood. This process is mediated by a group of glycoprotein receptors known as selectins. Afterwards, the cell needs to firmly adhere to the blood vessel. Integrins on the surface of leucocytes interact with selectins or chemokines to activate themselves, allowing to bind to its primary ligands such as ICAM-1 and VCAM-1. The steps are discussed in detail in this subsection (also reviewed by (Ley, Laudanna et al. 2007). There are similarities in the steps and mechanisms used for blood vessel extravasation as there are

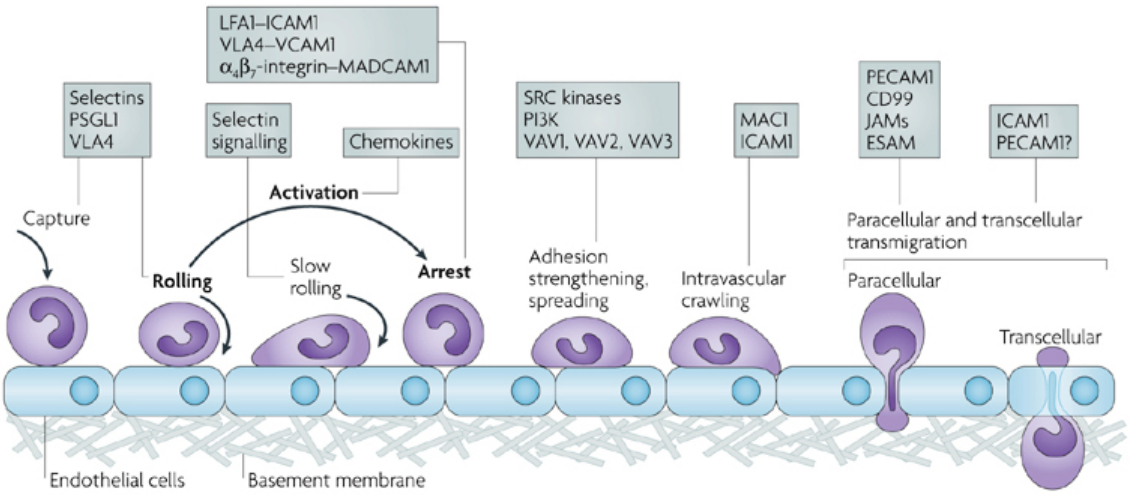


Figure 1-8: The leucocyte adhesion cascade. The three major steps to the process are (i) rolling, (ii) activation, and (iii) activation. However, further levels of regulation to the process have been uncovered and are present in the image: capture (or tethering), slow rolling, adhesion strenghtening and spreading, intravascular crawling and para- or trans-cellular migration. The various molecules involved are labelled in the boxes above each step. Image taken from Ley et al. (2007). Originally published in Nature Reviews Immunology, 7: 678-689

for lymphatic vessel intravasation and these parallels are highlighted throughout this section.

Role of chemokines

Arrival of leucocytes towards vessels is a complex process reliant upon chemokine gradients. Chemokines come in four groups - C, CC, CXC and CX_3C. The nomenclature is as such because they contain two, or four conserved cysteines that are classified according to the N-terminus of the peptide. For example, CXC chemokine have an amino acid spaced between the two cysteine residues where as they are adjacent to each other in CC chemokines. CX_3C chemokine have three amino acids spaced between the residues. C chemokines lack the first and third cysteine residues (Graves and Jiang 1995). Macrophages are known producers of a wide variety of chemokines that is responsible for recruiting other leucocytes whereas there are limited examples of macrophages responding to a chemokine gradient (Mantovani, Sica et al. 2004). M1 macrophages have been identified to express CCR7, the chemokine receptor for CCL19 and CCL21, commonly associated with trafficking to lymph nodes (Yoshida, Nagira et al. 1998, Badylak, Valentin et al. 2008, Johnson and Jackson 2010). Despite a lack of evidence on part of macrophages, there is a good body of evidence detailing inflammatory monocyte responses to chemokines. Two prominent chemokines for monocytes are CCL2 and CCL5 which upon binding to their cognate receptors, CCR2 and CCR5, respectively, can induce signalling pathways which promote expression and activation of integrins for attachment to blood endothelium (Fuentes,

Durham et al. 1995, Szabo, Butcher et al. 1997, Zhang, Yoshimura et al. 1997, Mack, Cihak et al. 2001). The interactions of adhesion are discussed below.

Role of adhesion molecules

Adhesion is a fundamentally important step to either exit from blood vessels or entry into lymphatic vessels (Johnson, Clasper et al. 2006, Rigby, Ferguson et al. 2015). As with studies with chemokines, there is currently limited understanding of adhesion molecules and if they mediate macrophage adhesion to lymphatic endothelium. In their clearance from the peritoneum (in models of thioglycollate stimulated peritonitis) to draining lymph nodes, macrophages have been determined to be reliant on both β1 and β2 integrins (Bellingan, Xu et al. 2002, Cao, Lawrence et al. 2005). In different contexts there are examples of macrophages being able to bind to adhesion molecules. They have been shown to express P-selectin and bind to PSGL-1 (also expressed by the macrophage) and assemble into 'strings' under flow conditions, a similar scenario to exit of monocytes from circulation (Tchernychev, Furie et al. 2003). Selectins are a family of three cell adhesion molecules - E-, L-, and P-selectin. These molecules do not have one typical ligand although a common feature of the ligands is the presence of complex sialylated carbohydrate groups (Ley 2003). E-selectin is most commonly associated with expression on endothelial cells. It was first discovered to be induced under conditions of inflammation on blood endothelium (Bevilacqua, Pober et al. 1987). Monocytes are one of the category of cells able to induce expression of E-selectin upon attachment to blood endothelium (Noble, Panayiotidis et al. 1996). E-selectin also appears to play a role in monocyte

recruitment to inflammatory sites but is not critical. Its expression has now been shown to be induced on the surface of human dermal lymphatic endothelial cells, although a role in LEC transmigration is yet to be identified (Rigby DA, D.Phil. Thesis, 2011). P-selectin is also expressed on the surface of monocytes and is critical to their adhesion to VCAM-1 on blood endothelium, a critical step before extravasation (Yago, Tsukuda et al. 1999).

Firm adhesion to endothelium, as mentioned at numerous points above, is mediated by ICAM-1 and VCAM-1 (expressed on the endothelium) binding to their counter receptors on leucocytes - αLβ2 (also known as LFA-1), αMβ2 (also known as Mac-1), or α4β1 and α4β7 integrins, respectively (Barczyk, Carracedo et al. 2010). In the extravasation from blood vessels, monocytes bind to both ICAM-1 and VCAM-1 (Shi and Pamer 2011). Integrins on the surface of monocytes are also able to guide the cells to preferential sites for transmigration, a process termed intravascular crawling that is discussed below.

Intravascular crawling

Monocytes have been demonstrated to move across the surface of blood endothelium against the direction of shear flow in a process called intravascular crawling that is dependent on the expression of Mac-1 on the surface of monocytes (Sumagin, Prizant et al. 2010). Although the molecular mechanisms behind the process are yet to be properly elucidated, it has been revealed in neutrophils to be dependent upon Rho family guanine exchange factor, Vav1 (Phillipson, Heit et al. 2009). Interestingly, a similar process of crawling also

occurs within lymphatic vessels. DCs, upon transmigrating into initial lymphatic capillaries, are able to crawl across on the endothelium in the direction of lymph flow. This crawling was labelled an active process in the initial lymphatic capillaries, migration independent of lymph flow (Tal, Lim et al. 2011). This becomes passive in the collecting lymphatics and migration becomes dependent on lymph flow. The mechanisms behind intra-lymphatic crawling are yet to be extensively uncovered but is believed to involve integrins as well. A subsequent distinctive step that follows from crawling in exit from blood vessels is trans-endothelial migration. Logically, such a step would precede intra-lymphatic crawling. The mechanisms underlying the process are discussed below

Routes of trans-endothelial migration (TEM)

Transmigration involves taking two routes - i) paracellular route, or ii) transcellular route. The paracellular route involves migrating through cell-cell junctions whereas the transcellular route occurs through the body of the endothelial cell itself (Ley, Laudanna et al. 2007). Paracellular diapedesis is believed to be the primary route for transmigration utilised by monocytes although there is a growing body of evidence of utilisation of the transcellular route (Carman and Springer 2004, Mamdouh, Mikhailov et al. 2009).

Paracellular migration occurs with a relaxation of the inter-endothelial contacts which allows gaps to form for monocytes to move towards (Winger, Koblinski et al. 2014). The numerous proteins present at junctions have an important role in the process. VE-cadherin is believed to act as an obstructing molecule and is translocated away from junctions which allows monocytes to transmigrate

(Esser, Lampugnani et al. 1998). Schenkel et al. (2002) identified that blockade of CD99 with mAbs blocked *in vitro* diapedesis at a point where monocytes were partially entering the junctions. CD99 was present on endothelium at inter-cellular junctions and functioned distally of CD31, whose blockade arrested cells on the apical surface of the endothelium. Indeed these two molecules appear to be important to DCs transmigrating across lymphatic endothelium, affecting diapedesis (Torzicky, Viznerova et al. 2012). CD31 at the junctions functions by entering a novel membrane compartment connected to the cell membrane at the borders, called the lateral border recycling compartment (LBRC). The membrane surrounding the LBRC envelops a transmigrating leucocyte at the junctions and shuttles them for TEM (Mamdouh, Kreitzer et al. 2008, Mamdouh, Mikhailov et al. 2009).

The initial evidence for transcellular migration came through single transmission electron micrographs which showed leucocytes indenting the body of endothelial cells (Marchesi and Gowans 1964). ICAM-1 projections which take the form of a cup are critical to this route of migration for monocytes (Carman and Springer 2004). The LBRC is also functional for transcellular migration as it envelops monocytes not on the junctions (Mamdouh, Mikhailov et al. 2009). The LBRC not only constituted CD31, but also CD99 and JAM-A. Cytokines, such as IL-1β influence the levels of transcellular-to-paracellular migration by rearranging the distribution of junctional proteins (Ferreira, McNeil et al. 2005).

Transmigratory cups

Leucocytes interacting with endothelial cells are surrounded by protrusion based structures called transmigratory cups (also known as docking structures or endothelial adhesive platforms). These cups, induced by leucocyte adhesion, are enriched with ICAM-1 and VCAM-1 (Carman and Springer 2004). Similar docking structures such as these cups have been previously identified by (Barreiro, Yanez-Mo et al. 2002) that are linked with the cytoskeletal ERM (ezrin, radixin, moesin) complex and mediate leucocyte adhesion to activated endothelial monolayers. Comprehensive studies have found that these cups are important to both paracellular and transcellular routes of migration (Carman and Springer 2004). Initially thought to be the same structures, endothelial adhesive platforms (EAPs), were distinguished from cups as structures independent of leucocyte adhesion and on inflamed endothelium. It is believed these EAP structures promote adhesiveness before diapedesis towards TEM (Barreiro, Zamai et al. 2008).

Proteins of inter-endothelial junctions

Along with ICAM-1 and VCAM-1, numerous other adhesion molecules found in junctions between endothelial cells mediate transmigration across the endothelium. Prominently amongst those are junctional adhesion molecules (JAMs) which are ligands for β2 integrins as well (Weber, Fraemohs et al. 2007). JAM-C has been shown to regulate monocyte transmigration across inflamed BECs promoting retention at inflamed tissues, and real time imaging experiments have shown that JAM-C (as well as JAM-A) mediates sequential steps in the transmigration cascade (Bradfield, Scheiermann et al. 2007). Baluk et al. (2007) located the expression of JAM-A on borders of lymphatic

endothelial cells button junctions co-localising with VE-cadherin and it would be logical to speculate the involvement of this family of receptors in lymphatic trafficking of macrophages.

Negotiating the basement membrane

A key part of the mechanism to transmigration involves penetrating the basement membrane, a fibrous extracellular matrix sheath that surrounds the endothelium. Blood basement membrane is a well organised and closed structure unlike the discontinuous architecture in association with lymphatic vessels (Kalluri 2003, Pflicke and Sixt 2009). Within the basement membrane are sites that exhibit a 60 % reduction in expression levels of significant matrix proteins; laminin-10, collagen IV and nidogen-2 that correlate as leucocyte entry points (Wang, Voisin et al. 2006). These areas, called low expression regions (LERs) under inflammatory conditions, was believed to be specific to neutrophil transmigration until Voisin et al. (2009) found that monocytes could also penetrate the vascular endothelium through these sites. Despite such similarity, distinct mechanisms suggested differences, such as, neutrophils could increase the size of LERs whereas monocytes could deform to a greater extent i.e. 'squeeze' in migrating through these spots. The ability to increase the size of the LER has been related to a difference in the ability to secrete degrading enzymes, for example, with neutrophils secreting more serine proteases than monocytes. Despite not possessing these LERs, the discontinuities within lymphatic basement membrane have been identified as hotspots for DC entry into initial lymphatic capillaries and although the knowledge behind macrophage

migration in the literature is scant, such investigations provide some insight into mechanisms they could utilise as well.

Overall, careful consideration of the literature has identified a lack of understanding in the migration of macrophages to draining lymph nodes and although there is partial identification of molecules involved in the procedure, much remains to be elucidated.

1.3 Aims of the thesis

Since the initial report of macrophages arriving from an inflamed peritoneum to draining lymph nodes in 1996 by Bellingan et al. indicating a lymphatic route for exit of these myeloid cells, there have been limited explorations into understanding specific mechanisms that mediate this process as well as clarifying the involvement of the lymphatic system in this clearance. This D.Phil. has sought to characterise the involvement of lymphatics in the clearance of macrophages from sites of acute inflammation and address the relatively unknown strategies of macrophage interactions with lymphatic endothelia.

- *In vitro* transmigration and adhesion assays were prepared and characterised, as described in chapter 3, to permit investigations into factors regulating the process of transendothelial migration (TEM) by macrophages of primary human dermal lymphatic endothelial cells (HDLECs).
- The impact of LYVE-1 and hyaluronan (HA) on transmigration, identified in Chapter 3, were pursued in Chapter 4 to study the involvement of the lymphatic receptor on trafficking of macrophages from the peritoneum, under both homeostatic and inflamed conditions, through an *in vivo* murine peritonitis model.
- Further studies into the role of the primary leucocyte HA receptor, CD44, in macrophage transmigration and trafficking via lymphatics were explored in Chapter 5 using both *in vitro* and *in vivo* models as in the previous two chapters. Furthermore, the work in the chapter pursued the levels of HA production by macrophages and the impact of changing polarity on production and retention on the cell surface.

Chapter 2.

Materials and methods

2.1 Materials

2.1.1 General reagents

2.1.1.1 Chemical reagents

- Acetone was purchased from Merck, Germany
- Disodium ethylenediaminetetraacetate (EDTA) dehydrate was purchased from Sigma, United Kingdom. A 0.5 M stock solution was prepared in distilled water (dH_2O) and adjusted pH 8.0 using sodium hydroxide (NaOH)
- Paraformaldehyde (PFA) was purchased from Sigma, United Kingdom. A 2 % (w/v) stock solution was prepared in dH_2O with stirring at 55 ºC. NaOH (1M) was added dropwise until all PFA was dissolved and a 1 % solution was prepared by dilution into 2X phosphate buffered saline (PBS)
- PBS tablets were purchased from Sigma, United Kingdom. One tablet was dissolved per 100 ml dH_2O to give a 1X solution
- Saponin (from quillaja bark) was purchased from Sigma, United Kingdom. A 0.1 % (w/v) solution was prepared in 1X PBS
- Sodium azide (NaN3) was purchased from Sigma, United Kingdom. It was usually applied at 0.05 % (w/v) for solutions (e.g. FACS buffer) requiring the reagent
- Evans blue dye was purchased from Sigma, United Kingdom. A stock solution of 1 % (w/v) was prepared in 1X PBS
- Hyaluronidase from Streptomyces hyaluroticus was purchased from Sigma, United Kingdom. A stock solution of 100 U/ml was prepared in 1X PBS

- Biotinylated hyaluronan binding protein from bovine nasal cartilage was purchased from Merck, Germany
- Bio-Gel® P-100 polyacyrlamide beads were purchased from Bio-Rad Laboratories, United Kingdom. A 2 % stock solution was prepared in 1X PBS
- PKH26-PCL kit was purchased from Sigma, United Kingdom
- CellVue® NIR-815 and Lavender cell labelling kits were purchased from eBioscience, United Kingdom
- CellTracker™ Green CMFDA Dye was purchased from Life Technologies, United Kingdom
- Triton® X-100 was purchased from Sigma, United Kingdom

All other chemicals were purchased from Sigma, or eBioscience (United Kingdom), unless otherwise stated.

2.1.1.2 Cell culture reagents

- Accutase was purchased from Sigma, United Kingdom. A 2 M solution was prepared in dH2O and adjusted to pH 8.0 with NaOH
- Dulbecco's modified eagle medium (DMEM) was purchased from Sigma, United Kingdom
- Roswell park memorial institute (RPMI) 1640 medium was purchased from Sigma, United Kingdom
- Microvascular endothelial growth medium-2 (EGM-2MV) consisted of basal media plus SingleQuot ampoules. SingleQuot ampoules provided 5 % (v/v) foetal calf serum (FCS) and undisclosed final concentrations of : hydrocortisone, epidermal growth factor (EGF), vascular endothelial growth

factor (VEGF), fibroblast growth factor (FGF), basic insulin growth factor (IGF), ascorbic acid, gentamicin and amphotericin B

- Foetal bovine serum was purchased from Sigma, United Kingdom. A 0.1 % (v/v) solution was prepared in 1X PBS from the 2 % (v/v) stock
- Goat and rabbit serum were purchased from Sigma, United Kingdom
- L-gluamine was purchased from Sigma, United Kingdom and used from a prepared 200 mM stock solution and typically used at a final concentration of 2 mM in cell culture media
- Penicillin and Streptamycin were purchased from Sigma, United Kingdom as 100 U/ml and 10 mg/ml stock solution, respectively. It was typically used at 10U/ml and 1 mg/ml, respectively in cell culture media preparations
- Trypsin/EDTA was purchased from Sigma, United Kingdom
- Hypoxanthine and thymidine (HT) were purchased from Life Technologies, United Kingdom as 10 mM and 1.6 mM stock solutions, respectively. Final concentrations of HT used in hybridoma cell culture media were 100 µM and 16 µM, respectively

All other cell culture reagents were purchased from Sigma, unless otherwise stated.

2.1.1.3 MACS® reagents

MACS® cell separation reagents were purchased from Miltenyi Biotec, United Kingdom. Cell separation was carried out according to the manufacturer's instructions and cell specific methodologies are detailed further down in this Chapter. Reagents used included MACS® LS, or MS columns, a MACS® stand,

appropriate magnets for either the MACS LS or MS columns, 30 µM MACS® pre-separation filters, goat anti-mouse MACS® bead conjugates, goat anti-rat MACS® bead conjugates and MACS® CD14 human microbeads.

2.1.1.4 Tissue cultureware

Tissue culture flasks and multiwell dishes were purchased from Corning, Europe and used for routine cell culture. Non tissue culture treated 12 well plates for basal macrophage culture were purchased from Becton Dickinson (BD) Falcon, Europe. FluorBlock® tissue culture inserts with a pore size of 3 µm and 24 well companion plates, used for transmigration assays, were also purchased from Becton Dickinson (BD) Falcon, Europe. 8 chamber slides were also purchased from Becton Dickinson (BD) Falcon, Europe. Nunc™ UpCell™ 12 well culture plates for M1 macrophage culture were purchased from Thermo Scientific, United Kingdom

2.1.1.5 Molecular biology reagents

- MyTaq™ Red mix was purchased from Bioline, United Kingdom
- RNeasy Mini kit was purchased from Qiagen, United Kingdom and used per manufacturer's instructions
- MMLV Reverse transcriptase 1st-Strand cDNA synthesis kit was purchased from Epicentre Biotechnologies, United States of America
- 100bp DNA ladders were purchased from New England Biolabs, United Kingdom and diluted in glycero-bromophenol blue loading buffer to 50 ng/ml

- SYBR® Sae DNA gel stain was purchased from ThermoFisher Scientific, United Kingdom
- dNTPs were purchased from Bioline, United Kingdom
- PCR primers were were purchased from EuroFins MWG Scientific, United Kingdom
- Agarose was purchased from Life Technologies, United Kingdom

2.1.1.6 HA detection reagents

Hyaluronan was detected and measured using a competitive hyaluronan enzyme-linked immunosorbent assay (HA-ELISA) that was purchased from Echelon® Biosciences, United States of America. Detection by microscopy and flow cytometry was with biotinylated HA binding protein listed above in the 2.1.1.1.

2.1.2 Antibodies

Antibodies directed against murine and human cell surface receptors, intracellular proteins are listed in tables 2.1 and 2.2 below, along with their specificity, host, isotype and source.

Table 2.1 Primary anti-mouse antibodies

Specificity	Antibody	Host	Isotype	Source/supplier
CD31	MEC13-3	Rat	IgG	BD Pharmingen
LYVE-1	C1/8	Rat	IgG_{2a}	Dr L Johnson from Professor DG Jackson's laboratory
LYVE-1	mAb2125	Rat	IgG_{2a}	R&D Systems
LYVE-1	-	Goat	Polyclonal	R&D Systems
Podoplanin	8.1.1	Hamster	IgG	DHSB, Iowa
F4/80	BM8	Rat	IgG_{2a}	eBioscience
F4/80	CI:A3-1	Rat	IgG_{2b}	Abcam
CD11b	M1/70	Rat	IgG_{2b}	eBioscience
MHC-II	M5/114.15.2	Rat	IgG_{2b}	eBioscience
CD68	FA-11	Rat	IgG_{2a}	AbDserotec

Table 2.2 Primary anti-human antibodies

Specificity	Antibody	Host	Isotype	Source/supplier
LYVE-1	3A	Mouse	IgG_1	Dr R Prevo from Prof DG Jackson's laboratory
LYVE-1	8C	Mouse	IgG_1	Dr R Prevo from Prof DG Jackson's laboratory
LYVE-1	MAB20891	Mouse	IgG_{2b}	R&D Systems
LYVE-1	MAB20893	Mouse	IgG_1	R&D Systems
CD31	JC70A	Mouse	IgG_1	Dako
Podoplanin	NZ-1	Rat	IgG_{2a}	Acris
VE-cadherin				
ICAM-1	P2A4	Mouse	IgG_1	Dr L Johnson from Professor DG Jackson's laboratory
VCAM-1	1G11	Mouse	IgG_1	Dr L Johnson from Professor DG Jackson's laboratory
ALCAM	MAB656	Mouse	IgG_1	R&D Systems
PROX-1	-	Rabbit	Polyclonal	Fitzgerald
CD14	ME52	Mouse	IgG_{2a}	BD Pharmingen
CD11b	ICRF44	Mouse	IgG_1	BD Pharmingen
CD68	Y1/82A	Mouse	IgG_{2b}	BD Pharmingen
CD44	BRIC235	Mouse	IgG_{2b}	Dr S Banerji from Prof DG Jackson's laboratory

Table 2.3 Secondary antibodies and conjugates

Specificity	Conjugate	Host	Source/supplier	Notes
Goat IgG	Alexa 568	Donkey	Molecular probes	red fluorescent
Hamster IgG	Alexa 568	Goat	Molecular probes	red fluorescent
Mouse IgG	Alexa 488	Goat	Molecular probes	green fluorescent
Mouse IgG	Alexa 568	Rabbit	Molecular probes	red fluorescent
Mouse IgG	Alexa 647	Donkey	Molecular probes	far red fluorescent
Rat IgG	Alexa 488	Donkey	Molecular probes	green fluorescent
Streptavdidin	Pacific blue	-	Molecular probes	violet fluorescent

2.2 Tissue Culture

2.2.1 Cell lines and transfectants

2.2.1.1 Primary cell lines

Primary human dermal lymphatic endothelial cells, HDLECs, were prepared as described in section 2.2.7 of this chapter.

Human umbilical vein endothelial cells were purchased from Totem Biologicals.

Primary human monocyte derived macrophages were prepared as described in section 2.2.8 of this chapter.

Primary mouse bone marrow derived macrophages, BMDMs were prepared as described in section 2.2.9 of this chapter.

Primary mouse peritoneal macrophages were prepared as described in section 2.2.10 of this chapter.

2.2.1.2 Transformed cell lines

L929 cells : Mouse fibroblast cell line were obtained from American Type Culture Collection (ATCC) cell bank

RAW 264.7 mouse monocyte macrophage cells were kindly donated by Dr. Amanda Stranks, MRC Human Immunology Unit, Oxford

2.2.2 Culture conditions

All mammalian cells were grown at 37ºc in humidified conditions with 5% CO_2.

RA264.7 were cultured in RPMI 1640 supplemented with 10% FCS (heat inactivated at 55ºc for 20min), 2mM L-glutamine, IU/ml penicillin and 50 µg/ml streptomycin, hereafter referred as RPMI 10% FCS.

Primary monocyte derived macrophages were cultured in identical medium supplemented with 50 ng/ml of GM-CSF

L929 cells were grown in Dulbecco's modified eagle medium (DMEM) supplemented with 10% FCS (heat inactivated at 55ºc for 20min), 2mM L-glutamine, IU/ml penicillin and 50 µg/ml of streptomycin, hereafter referred as DMEM 10% FCS. The supernatant obtained from this culture is referred to as L929 conditioned medium.

Primary mouse BMDMs were cultured in DMEM 10% FCS that is supplemented with 20% L929 conditioned medium.

Endothelial cells were cultured in in EGM-2 MV media supplemented with supplied SingleQuots (Hydrocortisone, EGF, FBS, VEGF, FGF-B, R^3 -IGF-1, Ascorbic acid, GA-1000). All primary endothelial cells (both human and mouse) were cultured on gelatin-coated plasticware.

2.2.3 Gelatin-coating of tissue culture dishes for primary endothelial cells

Sufficient gelatin, 0.1% in PBS was applied to the culture dish or flask to cover the bottom and incubated at 37ºc for 2 hours before removing the solution and using the tissue culture ware for plating the cells.

2.2.4 Passaging of cells

2.2.4.1 L929 cells

Adherent cells were grown to confluence, washed with PBS and incubated in pre-warmed Trypsin/EDTA for 5 min at 37ºc . Lifted cells were resuspended in 3 x the original volume of culture medium by gentle pipetting and divided over fresh culture flasks.

2.2.4.2 RAW264.7 cells

Adherent cells were grown to confluence, washed with PBS and incubated in pre-warmed Trypsin/EDTA for 5min at 37ºc. Lifted cells were resuspended in 5 x the original volume of culture medium by gentle pipetting and divided over fresh culture flasks.

2.2.4.3 Endothelial cells

Endothelial cells obtained from the dermis of the skin of humans and mice were cultured in EGM-2 MV. All endothelial cells were cultured in gelatin-coated flasks.

2.2.5 Frozen storage of cells

Confluent cultures of cells were detached with Trypin/EDTA and 1 x volume of fresh medium added. Endothelial cells were detached with Accutase and 1 x volume of fresh EGM-2 MV. Cells were centrifuged in a bench top centrifuge. The pellet was then resuspended in freezing medium (90% FCS, 10% DMSO) and transferred to cryovials (1 ml per vial) for storage at -80ºc or transferred to liquid nitrogen after 1-2 days at -80ºc.

2.2.6 Recovery of frozen cells

The cryo-vial was warmed rapidly to 37ºc and thawed cells were immediately transferred to culture medium. Endothelial cells were centrifuged at 300 X G for 4 min. The pellet is resuspended in fresh pre-warmed EGM-2 MV and placed in flasks at a minimum density of 10000 cells/cm^2 and cultured overnight before applying fresh pre-warmed medium. All other cell types were suspended in medium and centrifuged at 300 X G for 5 min before resuspending in fresh culture medium and transferring to a culture dish or flask.

2.2.7 Preparation of HDLEC from skin

LECs were isolated from the skin of human patients undergoing elective surgery at the Plastic Surgery Department of the John Radcliffe Hospital, Oxford. This was kindly donated by said department in guidance with appropriate ethical

approval and consent obtained from patient and the surgery department. Guiding principles were the Human Tissue Act (2004) and the MRC Ethics Series (last updated in 2014). The skin has the subcutaneous fat removed and is transferred to Dispase (Gibco), 2 mg/ml in PBS in a 50 ml Falcon tube.

The following day, skin was rinsed in PBS and the epidermis removed. With the dermis exposed, the skin is placed into a 15 cm tissue culture dish with 15 ml of EGM-2 MV. Using a pair of tweezers, the dermal cells are physically forced out of the skin into the medium. The cell suspension is then run through a 70 μm filter (BD Falcon) and is centrifuged at 300 X G for 4 min. The pellet is resuspended in medium and plated out in a gelatin-coated tissue culture (T-75) flask. The following day, the cells are washed with PBS before adding fresh EGM-2 MV.

For selection of LECs, cells were detached by incubation with Accutase, pre-warmed to 37ºc. Cells were washed in MACS buffer (0.5% BSA, 2mM EDTA in PBS, maintained on ice throughout the procedure), centrifuging at 1300 RPM for 4 min. Cells were washed once again in the same conditions after resuspending the pellet with 10 ml of MACS buffer. Cells were then resuspended in 2 ml of MACS buffer. Mouse anti human LYVE-1 monoclonal antibody, 8C, was added to a final concentration of 10 μg/ml and the cells were incubated on ice for 20 min. Cells were then washed 2 times in 10 ml of MACS buffer, then resuspended in 200 μl MACS buffer and 40 μl goat anti-rat MACS beads, incubating for 15 min on ice. Cells were then washed with MACS buffer twice and resuspended in 1 ml MACS buffer. A Miltenyi MS MACS column on a magnetic stand were pre-equilibrated with 500 μl MACS buffer and the cells

were loaded onto the column. Further washing steps of the column were followed according to manufacturer's instructions. Cells bound to the column were eluted by removing the column from the magnetic stand, adding 2 ml MACS buffer and forcing it through using the plunger. Eluted cells were then made to go through another round of selection on another MS column to obtain a purer population of selected cells. Cells were pelleted by centrifugation and resuspended in 13 ml EGM-2 MV, plating out in a medium-sized (T-75) gelatin-coated flask.

2.2.8 Culture of primary human macrophages from peripheral blood

Macrophages were differentiated in culture from $CD14^+$ monocytes isolated from Leuko-cones (NHS Blood and Transplant). Leuko-cones were transferred to 50 ml Falcon tubes and it's volume made up to 50 ml using 1 X D-PBS, without cations (Gibco). The tube is inverted 3 times to allow a sufficient homogenous mixture to form. This mixture is then layered over a stock Lymphoprep™ (Stemcell Technologies) density gradient solution and centrifuged at 400 x G, for 20 min, without brakes. The mononuclear cell band was identified post centrifugation and aspirated off. The isolated peripheral blood mononuclear cells (PBMCs) were washed 3 times in PBS, without cations. Cells were re-suspended in MACS buffer and washed an additional 2 times. PBMCs were then immunoselected in MACS buffer with human CD14 MACS microbeads (Miltenyi Biotec), followed by magnetic recovery according to Miltenyi Biotec's instructions. Recovered CD14+ cells are washed in MACS

buffer an additional 2 times and resuspended in RPMI-1640 supplemented with 10 % FCS (Sigma), 100 IU/ml penicillin & 100 µg/ml Streptomycin (Sigma), 2 mM L-Glutamine (Sigma) and 50 ng/ml of GM-CSF (R&D Systems, Bio-Techne). Cells are plated on non tissue culture treated 12-well plates at 1 x 10^6 cells/ml and allowed to differentiate into macrophages for 6 days at 37 ºC, 5 % CO_2 in a humidified atmosphere. To polarise macrophages into an M1 phenotype, differentiated cells were stimulated with 1 µg/ml of LPS from *E.Coli* O55:B55 (Sigma) and 20 ng/ml IFN-ɣ (PeproTech) for 24 hours.

2.2.9 Culture of primary murine bone-marrow derived macrophages

Female C57BL/6 mice, aged 8-12 weeks were killed by rising CO_2 and death was confirmed by cervical dislocation. Four mice were used per preparation. The hind limbs from the mice were removed and the major bones (i.e. femur, tibia and fibula) stripped of soft tissue. Both the proximal and distal tips of the femur and tibia were cut off and 5 ml PBS with 5 mM EDTA was flushed through the cavity using a 25 gauge needle to extract the bone-marrow derived cell populations. This cell suspension was filtered through a 70 µm cell strainer (BD Falcon™) and washed in PBS three times at 300 x G for 5 min. Cells were suspended in Dulbecco's Modified Eagle Medium supplemented with 10 % FCS, 100 IU/ml penicillin & 100 µg/ml Streptomycin, 2 mM L-Glutamine and 20 % L929-conditioned medium. Cells are plated on non tissue culture treated 12-well plates at 1 x 10^6 cells/ml and allowed to differentiate into macrophages for 7 days at 37 ºC, 5 % CO_2 in a humidified atmosphere.

2.2.10 Isolation of murine macrophages from peritoneum

Female C57BL/6 mice, aged 8-12 weeks were injected intraperitoneally with Bio - Gel P - 100 Gel polyacrylamide beads (Bio-Rad, UK), using a 26 gauge needle. Inflammatory reaction was allowed to carry on for five days. On the fifth day post injection, mice were killed by rising CO_2 and death was confirmed by cervical dislocation. An incision was made to the skin in the gut region and tweezed apart. The peritoneum was injected with cold 5mM EDTA in PBS and massaged gently. The lavage containing peritoneal exudate cells (PECs) is then retrieved using a 21 gauge needle and collected in 15 ml centrifugation tubes on ice. Cells were spun down and washed in ice cold PBS two times. PECs were suspended in RPMI-1640 supplemented with 10 % FCS, 100 IU/ml penicillin & 100 µg/ml Streptomycin, 2 mM L-Glutamine for further usage.

2.3 Transmigration and adhesion assays

2.3.1 CMFDA labelling of macrophages

Macrophages were typically labelled with 2.5 µM chloromethylfluorlscein dictate (CMFDA, Invitrogen, United Kingdom) in EGM-2 MV, at 37 ºC in a humidified atmosphere, with 5 % CO2 for 40 min. Macrophages were then resuspended in fresh EGM-2 MV and rested for 20 min prior to use in macrophage transmigration and adhesion assays (see Section 2.3.2 and 2.3.3).

2.3.2 Adhesion assays

Primary HDLECs were seeded in 24 well dishes coated with 0.1 % (v/v) gelatin and cultured to confluence. As appropriate, macrophages, or primary HDLECs (both unstimulated and TNF-α-stimulated) were pre incubated with monoclonal antibodies, or enzymes for 30 min. CMFDA-labelled macrophages (5 x 10^5) were then applied to primary HDLEC monolayers and incubated for between 0 - 6 hours, after which time the media was removed and wells were washed 4 x with PBS to remove non-adherent cells. Numbers of adherent macrophages were measured using a fluorescent plate reader (Synergy™ HT; BioTek®, United States) at 37 ºC running Gen5™ software (BioTek®, United States) and the fluorescence was calibrated against a standard curve of CMFDA-labelled macrophages.

2.3.3 Transmigration assays

Primary HDLECs (1 x 10^5) were seeded onto the lower surface of FluroBlock cell culture inserts with a pore size of 3 µm (BD™ Falcon, Europe), coated with 0.1 % (v/v) gelatin. Briefly, cell culture inserts coated with primary HDLECs were incubated for 2 h at 37 ºC to allow efficient adhesion of majority of cells plated on to the inserts. Following this incubation time, individual inserts were removed and immersed into a companion plate containing EGM-2 MV. Typically, primary HDLECs were cultured for 4 days to allow junctional stability and cell confluence to be achieved. As appropriate, macrophages or HDLECs (both unstimulated and TNF-α stimulated) were pre-incubated with monoclonal antibodies, or enzymes for 30 min. CMFDA-labelled macrophages (5 x 10^5) were then co-incubated into the inserts cultured with HDLEC monolayers. The number of fluorescent macrophages that were able to transmigrate from above the monolayer to below it was typically quantified at 20 min intervals. Quantification was done using a fluorescent plate reader (Synergy™ HT; BioTek®, United States) at 37 ºC running Gen5 software (BioTek®, United States). The number of transmigrating cells was calculated from a series of known CMFDA-labelled macrophages added to the lower chamber of cell culture inserts to produce a standard curve.

2.3.4 Statistical analyses of macrophage transmigration across primary HDLEC monolayers

Two-tailed, unpaired Student's t-tests were carried out as stated in the figure legends, using Excel software (Microsoft Corporation, United States). The level of significance was set at $p < 0.05$. The tests were carried out on the assumption of the data producing a normal distribution. However, if such an assumption does not hold then non parametric tests would have to be done.

Of such tests, include one way and two way analysis of variance (ANOVA) and Mann-Whitney U-test. One way ANOVA is used to compare samples of an F distribution and is suitable for experiments with a difference in a single factor with all subjects completely randomised. However, such an ANOVA works on the presumption that responses within a given group are independent and identically distributed normal random variables, which doesn't hold true for complex interactions observed in the experimental settings performed in this thesis as many internal factors may contribute to variability which may not be consistent across all subjects/technical replicates of an experiment. Because of such a limitation, a two way ANOVA can be considered where the assumptions consider that errors in an experiment are independent of each randomised replicate. It also takes into account any interactions between independent variables which may influence the dependent variable thus providing more robust calculation of significance from analysis of experimental data. Finally, the Mann-Whitney U-test is another test of significance that does not assume normality within randomised subjects being tested and is reported to be as efficient as t-tests on normal distributions. The test also presumes that observations from both groups are independent of each other and prevents type I errors. The U-test however, pertains to assessing the median rather than the mean and for such an assessment a larger sample population is required which was beyond the scope of the work produced in this thesis.

2.4 Animal Experiments

2.4.1 Animals

Animal experiments were conducted in line with the principal of the 3Rs - replace, reduce and refine. *In vitro* experiments with human cells were conducted to facilitate minimal usage of animals to determine answers to research questions. To use the minimal necessary animals for statistically significant results, the statistical power was set to 80 % and so, 4/5 animals per treatment group was decided for significance level of 5 % (information was based from http://www.3rs-reduction.co.uk/html/6__power_and_sample_size.html). In terms of refinement, techniques were previously mastered before attempts on live animals. Also, animals were maintained in the Biomedical Services (BMS) facility at the John Radcliffe Hospital, Oxford. C57BL/6 mice aged between 8 - 12 weeks were purchased from Harlan Laboratories, United Kingdom and housed in the BMS in individually ventilated cages (IVCs). All animal procedures were carried out in accordance with Home Office licences and local ethical committee guidelines.

2.4.2 Elicitation of inflammatory peritonitis using Bio - Gel® polyacrylamide beads

Mice were sensitised with intra - peritoneal injection of 1 ml of 2 % Bio - Gel P - 100 polyacrylamide beads. Five days after the first injection, mice are ready for

extraction of peritoneal lavage or for further injection with fluorescently labelled cells.

2.4.3 Macrophage trafficking experiments

Mice were either unsensitised or sensitised as described above in section 2.4.2. After cells were collected from the peritoneum by lavage (which would consist of mostly macrophages), they were labelled with a lipophilic dye specific for uptake by phagocytic cells, PKH26 (Sigma, United Kingdom) and CellVue® NIR - 815 (eBioscience, United Kingdom). Peritoneal exudate cells (PECs) were labelled with these dyes as per manufacturer's instructions. Cells were resuspended in 1 x PBS at 1 - 2 x 10^6 cells / ml and injected into the peritoneum of pre - sensitised mice. Between 12 - 36 h post adoptive transfer, mice were killed and their mediastinal lymph nodes (MdLNs) were removed using scissors and forceps. MdLNS were crushed and passed through a 70 µm cell strainer and cells were collected for flow cytometry staining.

2.4.4 Blockade of macrophage trafficking

To observe blockade of macrophage trafficking from the peritoneum, an intra - peritoneal injection of 0.5 mg of either mAb2125, C1/8 or B1/10, LYVE - 1 blocking antibodies, or isotope control IgG was administered 24 hours before adoptively transferring dye labelled peritoneal macrophages. Following injection of macrophages, mice were killed 12 hours later and mdLNs were removed and

collected as previously described (see Section 2.4.3). Lymph nodes were then processed for flow cytometry staining (see Section 2.5.1).

2.4.5 Tissue explant preparation

Mice had undergone experimental preparation as previously described (see Section 2.4.3) and killed 12 h later. Peritoneal lining was removed and processed as fresh - frozen sections (see Section 2.4.2) or whole - mount for analysis by confocal (see section 2.5.5).

2.5 Immunostaining and microscopy

2.5.1 Flow cytometry

Cells were detached from tissue culture ware with either Accutase® (for HDLECs) or 5 mM EDTA (for macrophages) and suspended in flow cytometry blocking buffer (PBS containing 10 % FCS (v/v, 0.1 % BSA (w/v), 0.05 % (w/v) NaN_3). Human macrophages were suspended in a specifically formulated flow cytometry buffer (PBS containing 10 % (v/v) FCS and human type AB serum, 0.1 % (w/v) BSA, 0.05 % (w/v) NaN_3). Murine macrophages and lymph nodes were suspended and processed in a specifically formulated flow cytometry buffer (PBS containing 10 % (v/v) rabbit and goat serum, 0.1 % (w/v) BSA, 0.05 % (w/v) NaN_3). Approximately 1 x 10^6 cells ml^{-1} were incubated for 30 min at 4 ^oC with primary antibody, prior to incubation with the appropriate fluorescent conjugate for a further 30 min (where required). Cells were then washed 3 times prior to fixation in formaldehyde (PBS containing 1 % (v/v) formaldehyde, 0.1 % (w/v) NaN_3). Samples were run on a flow cytometer (CyAn™ ADP Analyser; Beckman Coulter, United Kingdom) and analysed with FlowJo software (TreeStar, United States). Typically, ≧ 400,000 events were acquired for analysis.

2.5.2 Frozen mouse tissue explants

Mouse peritoneal lining and lymph nodes were obtained from 8 - 12 week old, female C57BL/6 mice, killed by rising CO2 (death was confirmed by cervical dislocation). Tissues were embedded in ornithine carbamoyl - transferase (OCT™) compound and stored at -80 ºC. Tissue explants were cut into 5 - 10 µm [sections] by cryostat and adsorbed onto SuperFrost® slides (VWR®, United Kingdom) for sub - sequent antibody staining.

2.5.3 Immunofluorescent staining of cells and tissues

Dual immunofluorescent staining of cells was carried out in chamber slides and cells were fixed in 1 % (v/v) PFA prior to staining. Dual immunofluorescent staining of fresh frozen tissue sections (see section 2.4.2) was carried out after cold acetone fixation. Appropriate primary antibodies diluted in immunofluorescence blocking buffer (PBS containing 10 % (v/v) FCS, 1 % (w/v) BSA) were applied to cells for 30 min at room temperature, followed by incubation with appropriate fluorescent conjugates for a further 30 min (where necessary). Preparations were mounted with Vectorshield® and viewed under a fluorescence microscope (Axiovert S 100; Carl Zeiss, United Kingdom). Images were captured using Zen imaging software (Carl Zeiss, United Kingdom).

2.5.4 Intracellular antigen staining

Adherent cells were permeabilised by incubation in 0.1 % (v/v) Triton® X-100 (Sigma, United Kingdom) for 10 min in the cases of PAL-E and Prox1 staining.

IN the case of Prox1 cell staining proceeded in immunofluorescence blocking buffer (see section 2.4.3) supplemented with 0.1 % (w/v) saponin from quillaja bark (Sigma, United Kingdom). Otherwise, cell staining proceded as described previously (as in section 2.4.3).

2.5.5 Wholemount staining

Wholemount staining of mouse tissue preparations was carried out after fixation in PFA (1 % (w/v) in PBS) for 2 h at 4 ºC. Sections were incubated with appropriate primary antibodies in whole mount blocking buffer (PBS containing 0.3 % (v/v) Triton® X-100, 3 % (w/v) milk powder) at 4 ºC overnight before appropriate fluorescent conjugates were applied for 2 h at 25 ºC. Stained tissues were then mounted with Vectashield® (Vector Laboratories, United Kingdom) to be viewed on a confocal microscope (LSM 510 and LSM 780; Carl Zeiss, United Kingdom). Images were captured using Zen imaging software (Carl Zeiss, United Kingdom).

2.6 Purification of monoclonal antibodies

2.6.1 Hybridoma culture

Hybridomas for various adhesion and transmigration blocking antibodies were obtained in-house. Cryopreserved stocks were thawed as previously described (see Secion 2.1.6) and cultured in RPMI - 1640 media containing 100 µM hypoxanthine and 16 µM thymidine. Cells were maintained at between 1 x 10^5 cells ml^{-1} and 1 x 10^6 cells ml^{-1} in 10 % (v/v) FCS, gradually reducing to 1 % (v/v). Supernatants were harvested and spun at 4000 x G and passed through a 0.22 µm vacuum driven filter (Millipore™, United Kingdom) to remove residual debris. The supernatant pH was adjusted to pH 7.5 with 2mM Tris, pH 8.0 and was loaded onto Poly-prep® chromatography columns containing 1 ml Protein G or Protein A Sepharose® (Sigma, United Kingdom). Chromatography columns were attached to a peristaltic pump (Pump P-1; Pharmacia Biotech, United Kingdom) and washed with PBS prior to the elution of antibody in 1 ml fractions using 0.1 M glycine, pH 3.0. Antibody fractions were neutralised by the addition of 5 % (v/v) 2 M Tris, pH 8.0 and were stored in aliquots at -20 ºC for future usage.

2.6.2 Quantifying IgG yield of hybridomas

IgG concentration was assessed using a spectrophotometer (Ultraspec 2000; Pharmacia Biotech, United Kingdom) at OD_{280nm}. Samples were blanked using

a solution of 0.1 M Glycine, pH 3.0 containing 5 % (v/v) 2 M Tris pH 8.0. Unknown sample absorbance was divided by 1.4 to yield the approximate IgG concentration in mg ml^{-1}.

2.7 Molecular biology methods

2.7.1 RNA isolation and cDNA preparation

Cultured cell monolayers had RNA isolated using RNeasy® Mini Kit (Qiagen, Netherlands) as per manufacturer's guidelines. All reagents used were maintained in RNAase- free conditions.

Buffers included as part of kit were - Buffer RLT, RNA-ase free water, RNA-ase free 70 % ethanol, Buffer RW1 and Buffer RPE.

Briefly, cell culture monolayers were disrupted with 350 µl of Buffer RLT after which the lysate were homogenised by passing through a blunt 20-gauge needle fitted to an RNA-ase free syringe. Homogenised lysate is then mixed with 350 µl of 70 % ethanol and then transferred to an RNeasy spin column that was centrifuged for 15 s at 30000 x G. Flow-through was discarded and 700 µl of Buffer RW1 was added to the spin column and spun at 30000 X G for 15 s. Flow-through is again discarded and column is washed with 700 µl of Buffer RPE at 30000 X G for 15 s and then again repeated with freshly added Buffer RPE for 2 min. RNeasy spin column was placed in a fresh RNA-ase free collection tube and had 30 µl of RNA-ase free water added and spun at 14000 RPM for 1 min.

RNA concentration was measured with a spectrophotometer (Ultraspec 2000; Pharmacia Biotech, United Kingdom) at OD280nm. Samples were blanked with RNA-ase free water.

Subsequent cDNA preparation involved use of an MMLV reverse transcriptase 1st-strand cDNA synthesis kit (Epicentre, Illumina, United States of America) under the manufacturer's guidelines.

2.7.2 PCR

PCR was performed using a Hybaid PCR express. Amplification was carried out with MyTaq™ Red mix PCR system and carried out according to manufacturer's instructions. Briefly, reaction mixes were prepared as such - 12.5 µl of MyTaq™ Red mix, forward and reverse primers at 0.2 µM each, 8.5 µl of water and 1 µl of prepared cDNA, added last, thus performing the reaction in a total volume of 25 µl. The melting temperatures (T_m)for the primers were calculated according to their GC content : each A or T = 2 ºC, each G or C = 4 ºC. Annealing temperatures were set at 5 ºC below the calculated T_m. The cycling parameters used were denaturing at 94 ºC for 30 seconds, followed by annealing at T_m-5 ºC for 40 seconds, then extension at 72 ºC for another 40 seconds/kb of DNA. 39 cycles were carried out of the above parameters.

2.7.3 Agarose gel electrophoresis

Agarose gels (1 % w/v) were prepared in TBE buffer (0.09 M Tris borate, 0.0002 M EDTA, pH 8.0, stored at room temperature) supplemented with 0.15 µg/ml SYBR® Safe DNA gel stain. DNA samples from PCR with MyTaq™ Red mix were added to gels and run under constant voltage (80 V). Gels were visualised under ultra-violet (UV) illumination with BioRad® Gel Doc™ XR+ system and images taken with BioRad® Image Lab™ software.

Chapter 3.

Elucidating mechanisms of macrophage adhesion and transmigration of the lymphatic endothelium via an *in vitro* model

3.1 Introduction

Macrophages accumulate at sites of tissue inflammation following the recruitment of circulating monocytes and their subsequent differentiation *in situ* (Ginhoux and Jung 2014). The mechanisms underlying the exit of monocytes from blood vasculature have been well documented, yet there is still little understanding of how recruited macrophages exit the tissues after inflammation has subsided. It is now accepted that clearance of macrophages to draining lymph nodes via the afferent lymphatics is one potential route along with local apoptosis, although the itinerary for the latter is again unclear (Bellingan, Caldwell et al. 1996, Gautier, Ivanov et al. 2013). Furthermore, the roles played by macrophages in draining lymph nodes and the processes by which they gain entry to the proximal lymphatics are uncertain. In particular, the mechanisms by which macrophages interact with lymphatic endothelial cells and transmigrate have yet to be determined.

Recent studies of macrophage differentiation have led to the notion of two distinct populations with separate developmental origins, those that originate in the yolk sac (otherwise known as tissue resident macrophages) and those that derive from circulating monocytes, whose development occurs in the bone marrow (Ginhoux, Greter et al. 2010, Hashimoto, Chow et al. 2013, Gomez Perdiguero, Klapproth et al. 2015). The functional aspects of both are discussed in detail in the General Introduction to this thesis.

A further level of differentiation has been defined at the level of macrophage activation. Pioneering contributions from the groups of Siamon Gordon and

David Mosser classified activation of macrophages into two types - M1 activation (also known as classical activation) and M2 activation (also known as alternative activation) (Stein, Keshav et al. 1992, Anderson and Mosser 2002, Mosser and Edwards 2008). The activation of macrophages depends on the environment they occupy; inflammatory environments (i.e. those in which macrophages differentiate from recruited monocytes) generally produce M1 macrophages. However, it is worth noting that the categorisation of M1 and M2 is a based almost entirely on findings from *in vitro* culture experiments. It is now accepted that the macrophages in inflammatory sites *in vivo* correspond mostly to the M1 phenotype but can also express markers characteristic of M2 cells (Bystrom, Evans et al. 2008). M1 macrophages broadly fit into the pro-inflammatory category on account of their secretion of molecules such as IL-12, TNF-α and reactive oxygen species (ROS), and hence must be cleared out of inflamed tissues to return to normal physiological homeostasis. The key factor for classical activation of macrophages is stimulation with IFN-γ in concert with a microbial component, such as lipopolysaccharide (LPS), or a pro-inflammatory cytokine, such as TNF-α (Mills, Kincaid et al. 2000).

The *in vitro* differentiation of human monocytes into macrophages also has components of M1 and M2 activation depending upon the cytokines present in the culture media. Monocytes differentiated in the presence of GM-CSF produce macrophages with M1 characteristics, whereas monocytes cultured in M-CSF differentiate into macrophages with M2 characteristics (Verreck, de Boer et al. 2004, Verreck, de Boer et al. 2006). For the purposes of the work presented in this chapter, macrophages were in most cases derived from human peripheral blood monocytes differentiated in GM-CSF in order to mimic

the M1 phenotype found *in vivo* in inflammatory tissue. However, in some experiments macrophages representing different stages of activation were generated in order to allow comparison of their clearance rates *in vivo*.

As outlined in the General Introduction, the concept of macrophage clearance via draining lymphatics is broadly accepted (Bellingan, Caldwell et al. 1996). However the molecular mechanisms underlying the process have yet to be identified. Numerous *in vivo* studies have demonstrated a dependence on integrins, such as VLA-4, VLA-5 and β2 integrin, during clearance from inflamed tissues and Gautier et al. (2013) provided evidence that the process is dependent on Gαi proteins, most likely indicating a chemokine driven process. Adhesion has been established as a key step in leucocyte transmigration across blood vessel endothelium and whether this was also the case for macrophage transit across lymphatic endothelium was one of the key issues to be addressed in this chapter.

The ability to study molecules involved in adhesion and transmigration has come from pioneering development of methods for the isolation and propagation of primary lymphatic endothelial cells (LECs). This has been a relatively recent breakthrough in comparison to the study of blood endothelial cells (BECS) because of newly discovered lymphatic endothelial specific markers that have aided in the isolation process. Specifically these are the membrane mucoprotein podoplanin (Hirakawa, Hong et al. 2003), the lymphatic lineage transcription factor PROX-1 (Wilting, Papoutsi et al. 2002) and the lymphatic hyaluronan receptor LYVE-1 (Banerji, Ni et al. 1999). *In vitro* studies of leucocyte adhesion to and transmigration across adherent LEC monolayers

involved *in vitro* static adhesion and transmigration assays with fluorescent labelled leucocytes and confluent human dermal lymphatic endothelial cell (HDLEC) monolayers. The preparation of both assays have been described in detail by Johnson et al. (2006) and a simplified diagram of the latter in Figure 3-1 illustrates the setup by which the physiologically relevant basolateral to luminal transit can be monitored continuously using HDLEC monolayers cultured on the underside of transwell inserts. These assays permit initial identification of molecules involved in lymphatic adhesion and transmigration, prior to validation through whole animal experiments *in vivo*. However, it must be remembered that they are limited artificial systems that can only partly model the conditions within intact tissues. Firstly, LECs cultured as monolayers cannot accurately reproduce the architecture of authentic lymphatic capillaries or collectors, as they do not form the characteristic button and zipper-like endothelial junctions that have been identified as critical for leucocyte transit (Johnson, Clasper et al. 2006, Kakei, Akashi et al. 2014). Also, these monolayers lack the basement membrane, and extracellular matrix that surrounds lymphatic capillaries in tissues and which present at least a partial barrier to leucocyte transit *in vivo*. Nonetheless, they provide a useful starting point in identifying the main components involved in macrophage adhesion and transmigration before performing more physiologically oriented trafficking studies in mice.

Since this D.Phil. is focussed on learning the mechanisms macrophages use to clear from inflammatory environments, particular attention is given to performing said assays with activated HDLECs (i.e. those stimulated with TNF-α). Morphologically, LECs transform from a rounded and cobble-stone like shape to become elongated with intercellular junctions relaxed, upon stimulation with

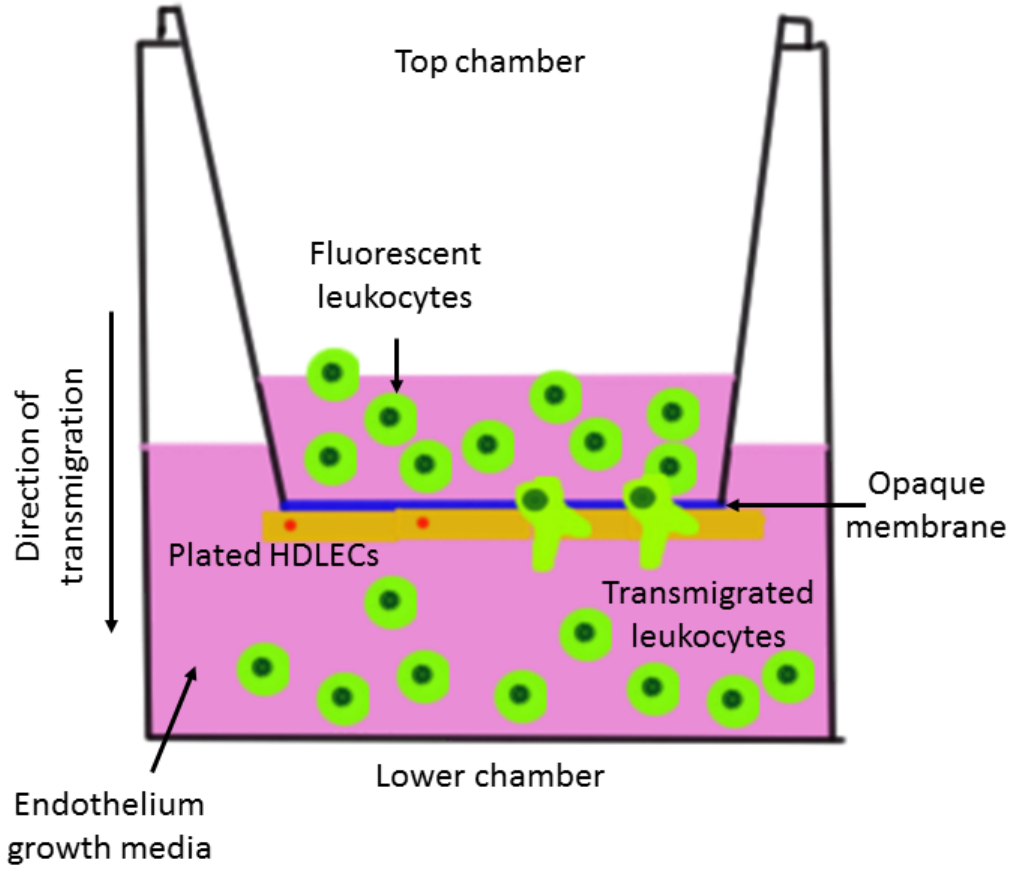


Figure 3-1: Schematic representation of *in vitro* transmigration assay. Primary HDLECs are plated on the underside of UV opaque 3μm pore FluoroBlok inserts to mimic basolateral-luminal polarity for transmigration and cultured in EGM-2 for four days to promote stable adhesion and inter-endothelial junctional integrity. Fluorescent leukocytes added to the top chamber transmigrate towards the bottom chamber and measured by a fluorescence plate reader.

TNF-α. These physical changes would allow for a passive increase in cells transmigrating as there is less trans-endothelial resistance (TER) and an increase in permeability (Johnson, Clasper et al. 2006). Along with a change in morphology, activated HDLECs have been reported to up-regulate the expression of key adhesion molecules ICAM-1 and VCAM-1, which play an active role in transmigration of leucocytes across blood endothelium and of dendritic cells across lymphatic endothelium. Both ICAM-1 and VCAM-1 mediate firm adhesion to the endothelial surface by interacting with their receptors on the surface of leucocytes, β2 integrin and β1 integrin, respectively (Johnson, Clasper et al. 2006, Rigby, Ferguson et al. 2015). Since monocyte derived macrophages (Mϕ's) have been reported to express the two integrins at high levels on their surface it is conceivable that both molecules would play a role in mediating adhesion to LECs, although this mechanism has yet to be investigated (McNally and Anderson 2002).

ALCAM is another molecule with reported increase in expression on the surface of inflamed LECs. A member of the immunoglobulin superfamily (IgSF) as ICAM-1 and VCAM-1, its functional relevance came to light upon demonstration that it mediated transmigration of monocytes and lymphocytes across inflamed blood brain barrier endothelium (Cayrol, Wosik et al. 2008). Afterwards, a functional role in lymphatic trafficking was demonstrated when reduced numbers of dendritic cells (DCs) arrived to draining lymph nodes in ALCAM$^{-/-}$ mice compared to WT counterparts (Iolyeva, Karaman et al. 2013). A demonstration of its role in adhesion and transmigration of macrophages has yet to be shown, in both blood and lymphatic endothelium. However, due to similarity of macrophages with DCs and origin from monocytes, it seems likely

that ALCAM would have a contributory role in macrophage interaction with LECs.

A notable point to be made throughout this chapter will be comparing aspects of macrophage transmigration with that of DCs and neutrophils, and if there are similarities in the mechanisms employed.

Another class of molecules that have been shown to contribute to transmigration of leucocytes across blood endothelium are glycosaminoglycans of which the most direct role has been noted with hyaluronan (HA) (Jackson 2009). Hyaluronan is a major component of the endothelial glycocalyx on blood endothelium, first shown by Luft in 1966. The glycocalyx separates the endothelium from the bloodstream and functions in aiding transmigration by trapping chemokines to attract leucocytes and sensing shear flow and promoting expression of adhesion molecules (Reitsma, Slaaf et al. 2007). Hyaluronan is involved in these functions as well as mediating rolling interactions with the endothelium by binding to CD44 on leucocytes (Clark, Alon et al. 1996, DeGrendele, Estess et al. 1997). Although such a glycocalyx is yet to be found associated with lymphatic endothelium, the possibility is promising. LECs express mRNA for hyaluronan synthases (HAS 1-3) and express the hyaluronan receptor LYVE-1 (Banerji, Ni et al. 1999). HA binding to LEC expressed LYVE-1 has been difficult to demonstrate with extensive understanding into the process uncovered by the Jackson laboratory. LYVE-1 binding to HA is dominated by charge, similar to selectin binding to fucosylated tetrasaccharide sialyl LewisX, and is quantitatively much weaker than CD44 (regarded as the main receptor to HA) (Torgersen, Mullin et al. 1998, Bouyain, Rushton et al. 2001, Jackson 2009). However, clustering the receptor with

monoclonal antibodies significantly increases its ability to bind to HA, analogous to findings where dimers of the receptor form to bind to HA (Lawrance et al. 2015, manuscript submitted). Constitutive dimer formation is believed to be blocked by the sialylation of the molecule (described in the General Introduction) causing charge repulsion between monomers (Jackson 2009). A physiological correlate to promoting clustering is yet to be determined but current hypothesis states the availability of cross-linked HA complexes (such as TSG-6-HA complexes) that enhance binding to HA, as seen with CD44, might be relevant to observing HA binding to endogenous LYVE-1. With abundant expression on the surface of LECs, it is likely that LYVE-1 would play a role in transmigration across lymphatic endothelium and identifying an interaction between LYVE-1 and macrophages forms a key component of the findings of this chapter.

3.2 Aims

The main aim of the work presented in this chapter was to optimize *in vitro* assays to measure the adhesion and transmigration of human macrophages across monolayers of primary lymphatic endothelium and to identify key endothelial receptors involved in these processes. In particular the following questions were addressed:

- Do macrophages adhere and transmigrate LEC monolayers efficiently, and how are these parameters influenced by macrophage activation or by stimulation of lymphatic endothelium by inflammatory cytokines?
- Does adhesion or transmigration of macrophages involve interactions with adhesion molecules known to mediate similar events in vascular endothelial such as ICAM-1 and VCAM-1, or lymphatic endothelial specific molecules such as the lymphatic hyaluronan receptor, LYVE-1?

3.3 Results

3.3.1 Isolation and characterisation of human dermal lymphatic endothelial cells

A key factor in the study of macrophage adhesion and transmigration in lymphatics is the availability of cultured primary lymphatic endothelial cells that retain as far as possible the authentic phenotype of vessel endothelium in intact tissue. In this regard, the techniques and resources for isolating human dermal LEC are well established within the Jackson laboratory (Johnson, Clasper et al. 2006). Nevertheless, because they were critical for the initial parts of my project, the isolation and phenotypic characterisation of these cells will be described in some detail.

LECs were isolated from human skin tissue that was kindly donated by patients undergoing elective surgery at the John Radcliffe Hospital, Oxford. The skin was treated with Dispase overnight to remove the epidermis, followed by physical disruption to detach endothelium and associated stromal cells from the lymphatic network. These cells (a mixture of LECs, BECs and fibroblasts) were cultured in Endothelial Growth Media (EGM-2) till confluence. An enriched LEC population was then derived through selection with mouse anti-human LYVE-1 mAb and anti-mouse magnetic cell sorting (MACS). The population of cells were then allowed to expand up to a maximum of eight passages after which de-differentiation and loss of normal lymphatic phenotype including LYVE-1 surface expression has been observed to occur. Phenotypic confirmation of the identity of cells as HDLECs and assessment of purity was determined by flow cytometry. Prior to staining, cells were lifted with Accutase™, a natural enzyme

mixture with proteolytic activity used as a substitute to Trypsin to lift cells from culture, because it preserved integrity of LYVE-1 on the surface. Primary antibodies specific for the lymphatic endothelial markers LYVE-1, podoplanin, along with the pan-endothelial marker CD31 were used in the staining procedure (Fig 3-2). In parallel, permeabilised cells that had been cultured to confluence in 8 chamber slides were stained with the antibodies used above along with antibodies against the lymphatic endothelial lineage transcription factor PROX-1, and the blood endothelial marker PAL-E which recognises extracellular vimentin secreted by a population of these cells (Xu, deWaal et al. 2004), for imaging by immunofluorescence microscopy (Fig 3-3). Analysis of expression of these markers indicated that the selected cells were HDLECs and of high purity. Indeed from analysis by flow cytometry, more than 80% of cells were of endothelial origin (determined by CD31 staining); more than 80 % of the cells also staining positive for LYVE-1 and podoplanin expression. The lymphatic phenotype was also confirmed by immunofluorescence microscopy which indicated the cells were uniformly positive for CD31, contained PROX-1^{+} nuclei and were negative for PAL-E. The enriched HDLEC populations were to be used for subsequent transmigration and adhesion assays, studying these processes in an inflammatory setting. The ubiquitous inflammatory cytokine TNF-α has been shown to up-regulate key adhesion molecules ICAM-1 and VCAM-1 along with ALCAM (Johnson, Clasper et al. 2006, Iolyeva, Karaman et al. 2013). All three molecules play a significant role in adhesion of dendritic cells to lymphatic endothelia and subsequent transmigration. To further validate the authentic phenotype of the isolated HDLEC, the induced surface expression of these molecules in response to TNFα was assessed by flow cytometry. Following overnight incubation with TNFα or media alone, cells were lifted and

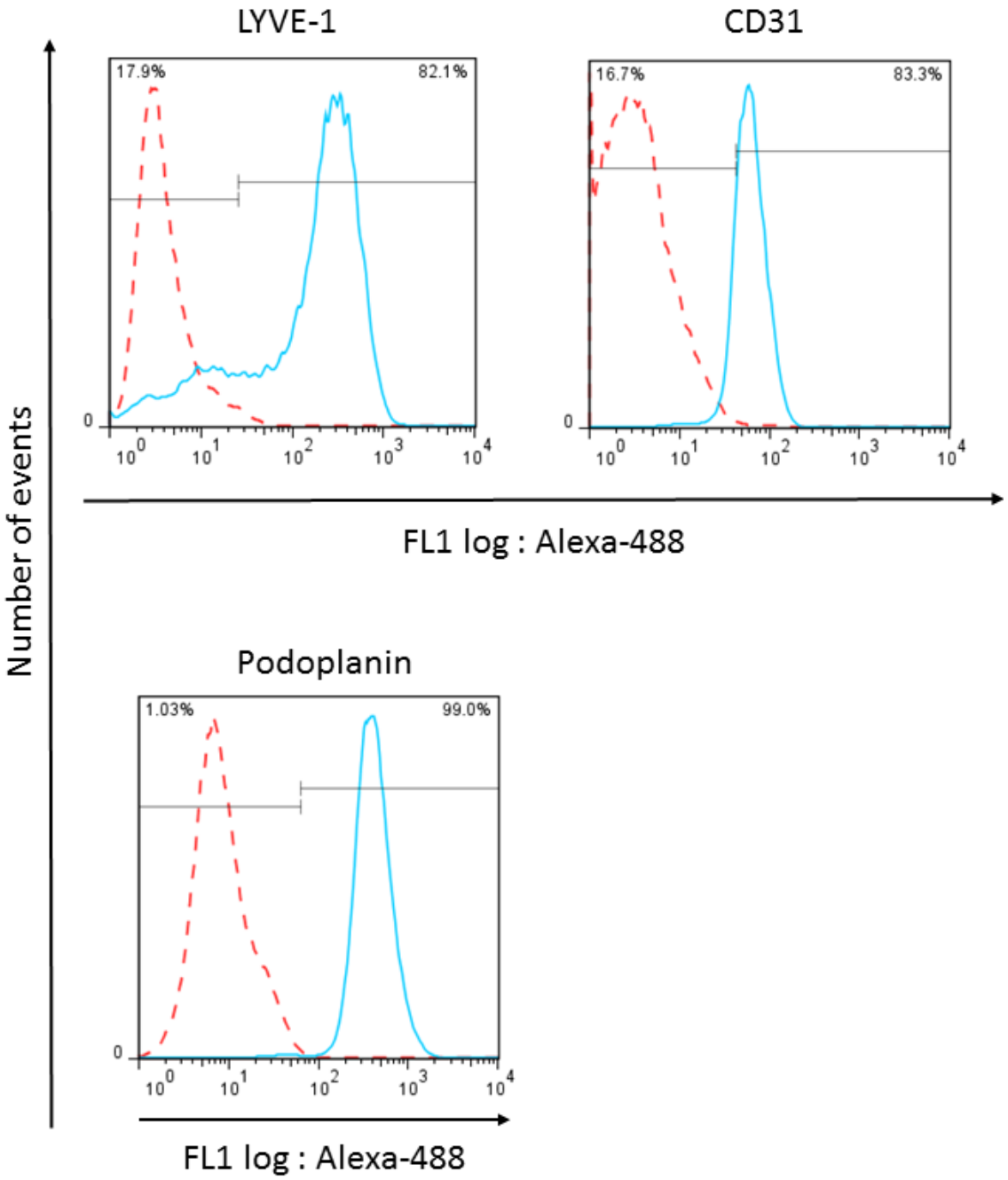


Figure 3-2: Flow cytometric analysis of primary HDLECs isolated by LYVE-1 immunoselection. HDLECs isolated from dermis by MACS selecting LYVE-1, were stained with primary antibodies for a series of cell surface markers such as the pan endothelial marker, CD31 using antibody clone JC70A, or the lymphatic endothelial markers podoplanin using antibody clone NZ-1 and LYVE-1 using polyclonal antibody raised against LYVE-1 (blue histograms). Isotype controls are also shown (red histograms). Expression levels were quantified by flow cytometry and representative histograms are shown of an experiment repeated > 3 times.

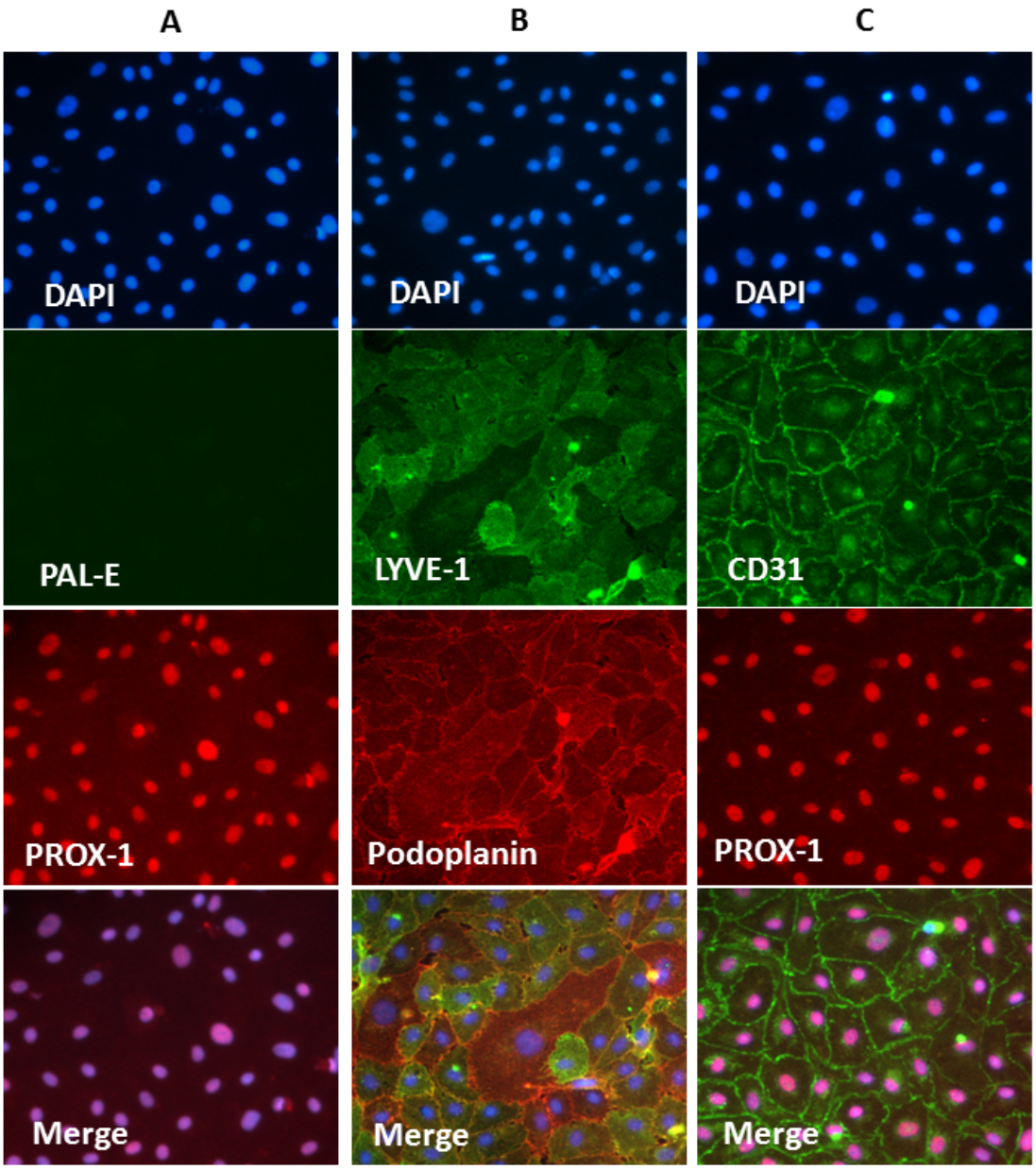


Figure 3-3: Characterisation of primary HDLECs isolated by LYVE-1 immunoselection. Primary HDLECs isolated from human dermis by MACS selecting LYVE-1 were stained with primary antibodies to cell surface markers as shown in (A) intra-cellular blood vascular endothelial marker PAL-E antigen using monoclonal antibody PAL-E and lymphatic specific transcription factor PROX-1 using polyclonal antibody raised against PROX-1, (B) lymphatic endothelial markers LYVE-1 using polyclonal antibody raised against LYVE-1 and podoplanin using antibody clone NZ-1, and (C) pan-endothelial marker, CD31 using antibody clone JC70A and PROX-1. Slides were mounted in VectaShield™ containing DAPI evident on all panels. Representative microscopy images are shown of an experiment repeated > 3 times.

stained with primary antibodies specific to ICAM-1, VCAM-1 and ALCAM (Fig 3-4). Analysis of the cell surface levels revealed an increase in expression of ICAM-1 and VCAM-1 on the surface of HDLECs treated with TNF-α compared to unstimulated HDLECs. However, there appeared to be no similar increase in the levels of ALCAM, unlike ICAM-1 and VCAM-1, basal LECs had a high level of expression of ALCAM on the cell surface. Adherent and confluent HDLECs on 8 chamber slides were assessed for expression of ALCAM by immunofluorescence microscopy (Fig 3-5). Analysis of the images reveal a junctional expression of ALCAM with these ALCAM junctions being disrupted on LECs treated with TNF-α.

3.3.2 Isolation and characterisation of human monocyte-derived macrophages

In addition to isolating lymphatic endothelial cells, my studies into adhesion and transmigration were dependent on generating purified populations of human peripheral blood monocytes for *in vitro* differentiation to macrophages – the relevant population associated with sites of tissue inflammation.

Accordingly, monocytes were separated from peripheral blood mononuclear cells (PBMCs) that were isolated from commercially available Leuko cones, white blood cells obtained from roughly 300 ml of whole blood by leukoreduction and concentrated in a small volume. It was a more preferable source than obtaining such large volumes of fresh blood from volunteers. Enriched monocyte populations were derived from PBMCs through immunoselection with human CD14 microbeads and MACS separation. Monocytes were cultured with

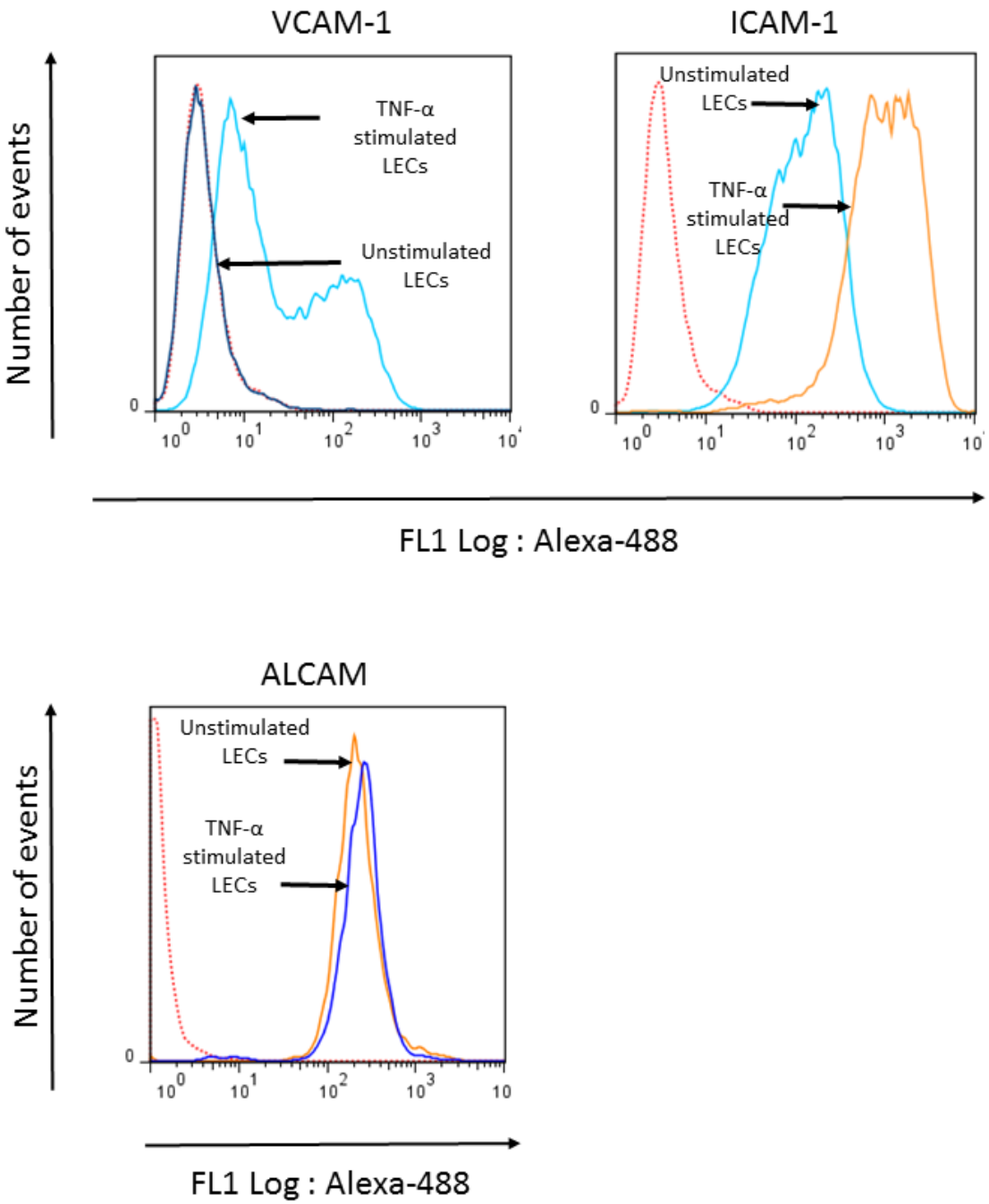


Figure 3-4: Flow cytometric analysis of expression of ICAM-1, VCAM-1 and ALCAM on the cell surface of TNF-α induced primary HDLECs. Primary HDLECs were incubated in media alone, or media containing TNF-α for between 0 – 24h. The HDLECs were then stained with primary antibodies to cell surface proteins ICAM-1 using monoclonal antibody P2A4, VCAM-1 using monoclonal antibody 1G11 and ALCAM using monoclonal antibody MAB656, for analysis by flow cytometry. Arrows indicate to HDLECs either in media only, or stimulation with TNF-α. Isotype controls are shown as red dots. Expression levels were quantified by flow cytometry and representative histograms are shown of an experiment repeated > 3 times.

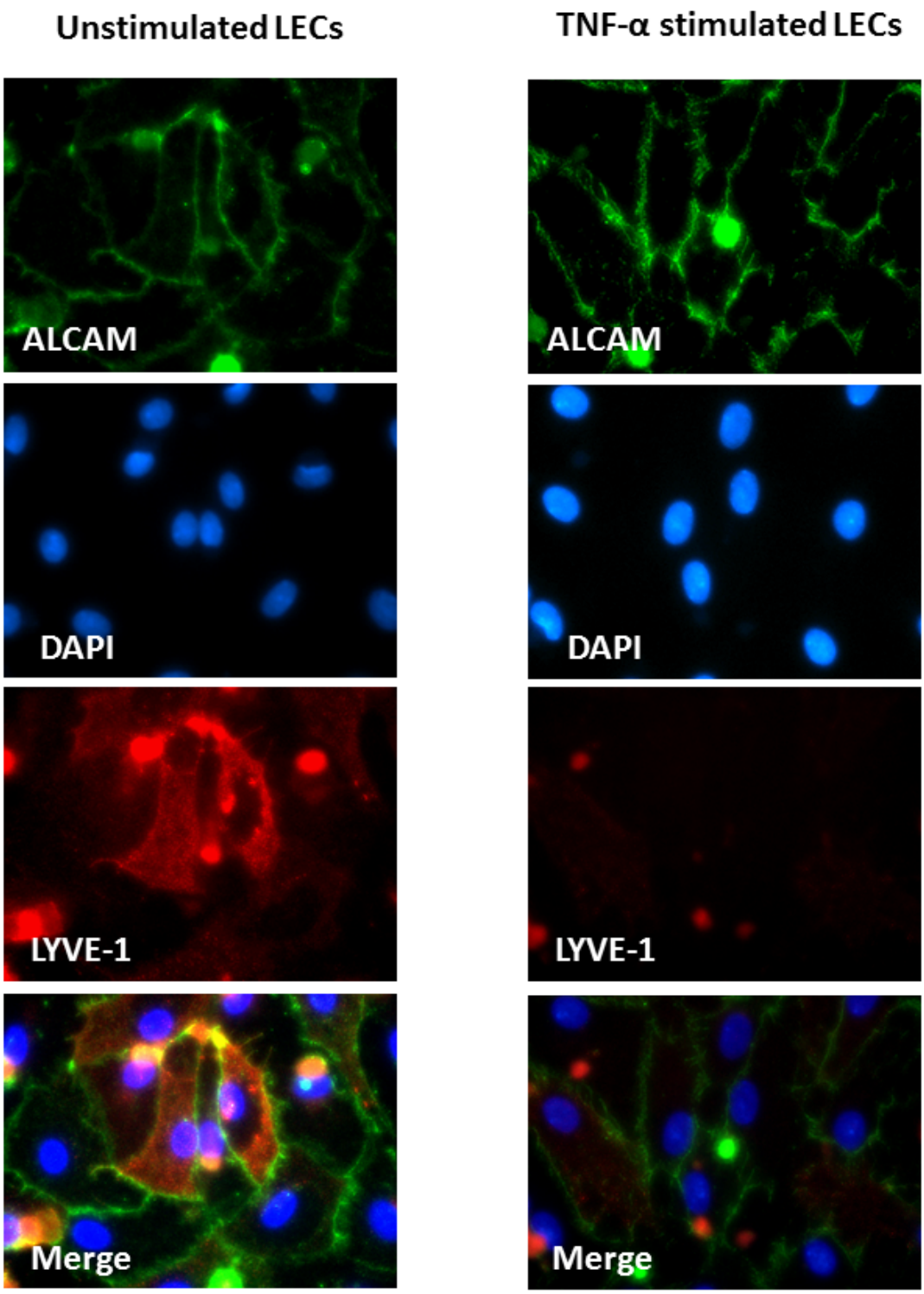


Figure 3-5: Characterisation of ALCAM expression on lymphatic endothelium. Primary HDLEC monolayers on 8 chamber slides were incubated with either media alone, or media containing TNF-α for 0-24 h. HDLECs were then stained with primary antibodies to cell surface markers LYVE-1, using a rabbit polyclonal antibody raised against LYVE-1 and ALCAM, using monoclonal antibody MAB656, for analysis by immunofluorescence microscopy. Slides were mounted in VectaShield™ containing DAPI. Representative images are shown of an experiment repeated > 3 times.

granulocyte-macrophage colony stimulating factor (GM-CSF) to promote differentiation of monocytes into macrophages, henceforth termed M0. A set of differentiated M0 macrophages was further treated with bacterial LPS and IFN-γ to promote polarisation to an activated inflammatory phenotype, henceforth termed M1. The polarisation could be observed as a change to the physical appearance of the macrophages by microscopy (Fig 3-6a). M0 macrophages have the characteristic 'fried egg' morphology associated with cultured macrophages. Activation to M1 caused macrophages to adhere less firmly to the culture plate and had a clumped appearance.

Phenotypic confirmation of the identity of the cells was determined by flow cytometry. Cells were lifted with cold 5 mM EDTA in PBS rather than using proteolytic enzymes such as Trypsin in order to maintain the expression of cell surface markers used for subsequent phenotyping. These comprised the myeloid markers CD14 and CD11b (Shi and Pamer 2011) along with scavenger receptor CD68 (Holness and Simmons 1993), which is expressed intracellularly in other myeloid cells (monocyte, neutrophils) but has also been reported to be present on the surface of macrophages. Primary antibodies specific to these markers were used to stain the lifted macrophages (Fig 3-6b). Positive expression of all markers in combination, confirmed the M0 macrophage phenotype.

Activation of monocytes to an M1 phenotype is associated with up-regulation of numerous molecules including cytokines, membrane receptors and effector molecules. Amongst those up-regulated surface molecules are CD80, the co-stimulatory protein for activating T cells (Young, Koulova et al. 1992), and CCR7, the chemokine receptor for ligands CCL19 and CCL21 associated with

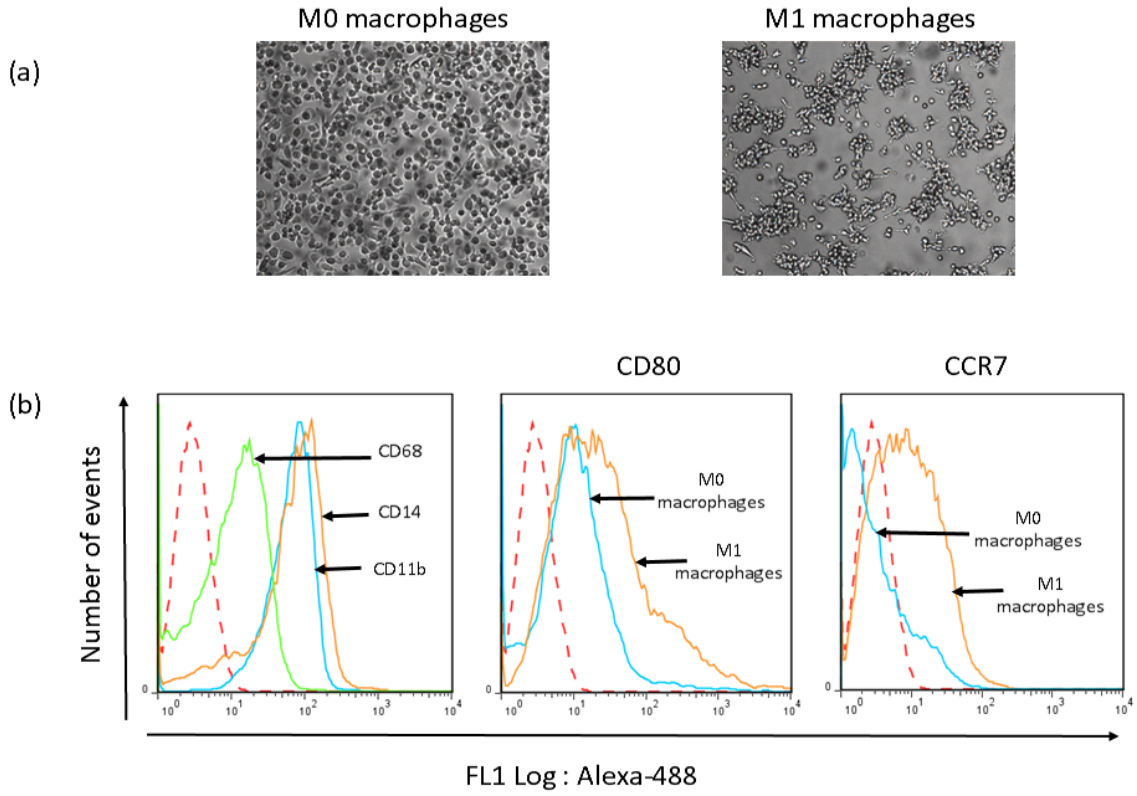


Figure 3-6: Characterisation of macrophages differentiated from peripheral blood monocytes isolated by CD14 immunoselection. Monocytes isolated from peripheral blood mononunclear cells with MACS selecting CD14 were cultured for 7 days in media supplemented with GM-CSF to differentiate into M0 macrophages. M0 macrophages were further stimulated, with LPS and IFN-γ for 24 hours, to M1 macrophages evidenced by (a) phase contrast microscopy showing effect of activation, and (b) flow cytometric analysis demonstrating expression of macrophage surface markers CD14, CD11b and CD68 as indicated by arrows, with effect of activation shown by increases in expression of CD80 and CCR7. Isotype controls are also shown (red dashed histograms). Representative images and histograms are shown of an experiment that was repeated > 3 times.

lymphatic trafficking. Both M0 and M1 macrophages (derived from the same population of M0s) were stained with primary antibodies to CD80 and CCR7 for comparative analysis by flow cytometry (Fig 3-6b). A greater level of both molecules on the surface of M1 cells compared to M0s illustrated that the above stimulation yielded the M1 subset.

3.3.3 Adhesion and transmigration of macrophages across LECs

Despite compelling evidence in previously published reports that macrophages emigrating from inflamed tissues can be recovered in draining lymph nodes, implying their migration via afferent lymphatics, there have been no reports addressing the process of lymphatic entry or its molecular mechanisms. One of the main aims in this chapter was to investigate possible interactions of macrophages with lymphatic endothelial cells and their involvement in macrophage transmigration.

Adhesion is one of the key steps preceding the actual process of trans-endothelial migration. As discussed in the introduction, LECs have been reported to express adhesion molecules that contribute both to adhesion and transmigration of dendritic cells and neutrophils. In addition, both processes are known to be dramatically upregulated after exposure of lymphatic endothelium to inflammatory cytokines. To identify if macrophages could adhere in a similar manner as DCs and neutrophils, an *in vitro* adhesion assay was performed with the set up as described in the introduction to this chapter. Detached single cell suspensions of M0 macrophages were labelled with CellTracker™ green

CMFDA (5-chloromethylfluorescein diacetate), a stable fluorescent dye that is retained in the cytoplasm as the free acid derivative after cleavage by cellular esterases. These labelled macrophages were added to confluent HDLEC monolayers that were either left untreated, or treated with TNF-α overnight, and incubated for set time points of 2 and 4 hours. At each time point, the numbers of adherent cells were quantitated using a fluorescence ELISA plate reader (Fig 3-7). Approximately 20% of added cells adhered to unstimulated LECs. However, there was a fivefold increase in numbers of macrophages adhering to TNF-α treated (activated) LECs. Adhesion was maximal at two hours of incubation with little to no change at later time points.

Having established the capacity of macrophages to adhere to both resting and activated lymphatic endothelium, the impact of the interaction on transmigration across LECs was explored with the *in vitro* transmigration assay as described in the introduction. The objectives of these assays were to determine (1) if macrophages (both M0 and M1) could transmigrate across LECs and, (2) the effect of TNF-α stimulation of the LECs on the process. Lifted macrophages were labelled with CMFDA and added to inserts with confluent HDLEC monolayers that were either left untreated, or treated with TNF-α overnight, prior to measurement of transmigration with a fluorescence plate reader (Fig 3-8). The resulting time-courses reveal 8 % of introduced M0 and M1 macrophage subsets transmigrate efficiently across unstimulated HDLEC monolayers, reaching a maximum after approximately 6 hours. The numbers of transmigrating macrophages increased almost 3-fold when the HDLECs had been treated with TNF-α overnight, reaching a plateau, similarly to transmigration across unstimulated LECs, 6-8 hours of transmigration. Despite an increase in transmigration upon activation of LECs, the fact that only more

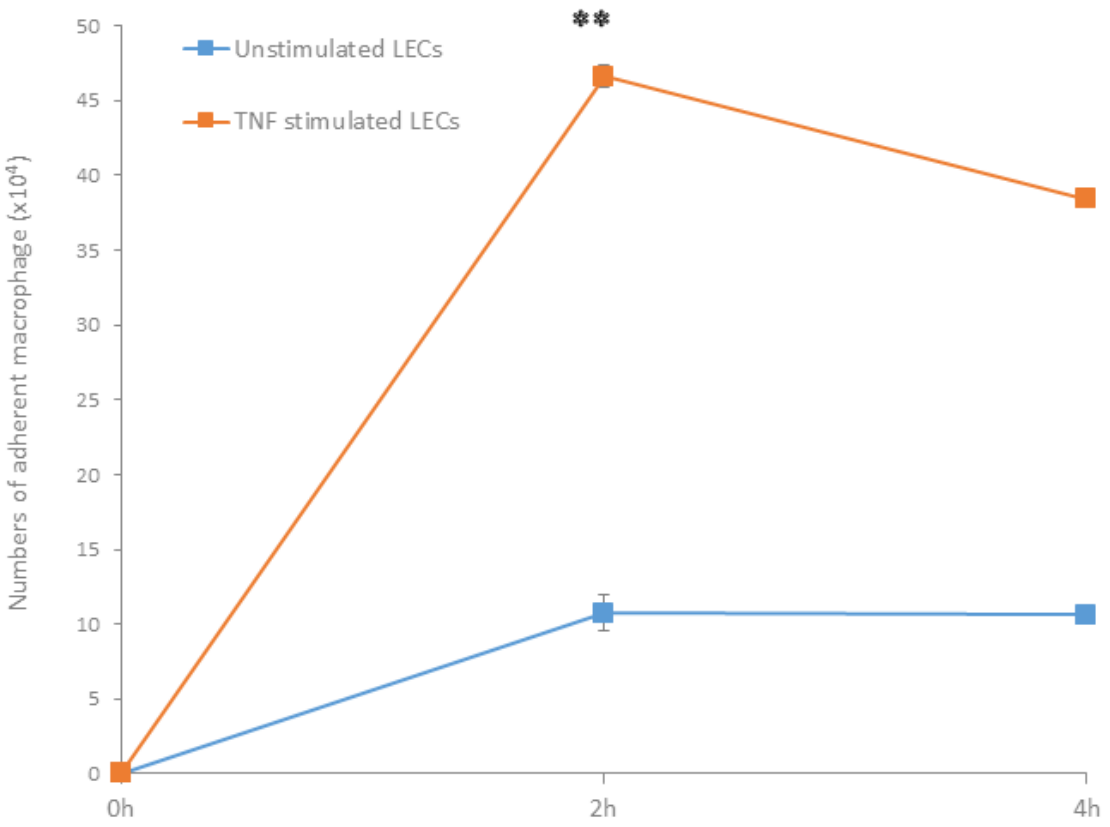


Figure 3-7: Effect of TNF-α stimulation on macrophage adhesion to primary HDLECs. Primary HDLEC monolayers were stimulated with TNF-α for between 0-24 h. CMFDA labelled macrophages (5 x 10^5) were applied to the monolayers which were then incubated with media alone (blue), or media containing TNF-α (orange) in 24 well dishes. Numbers of adherent macrophages were measured using a fluorescent plate reader at 2h and 4h. Data are the mean ± SD of quadruplicate technical replicates. The graph shown is representative of 3 independent experiments and the appropriate statistical test to analyse this data would be a two way analysis of variance (ANOVA).

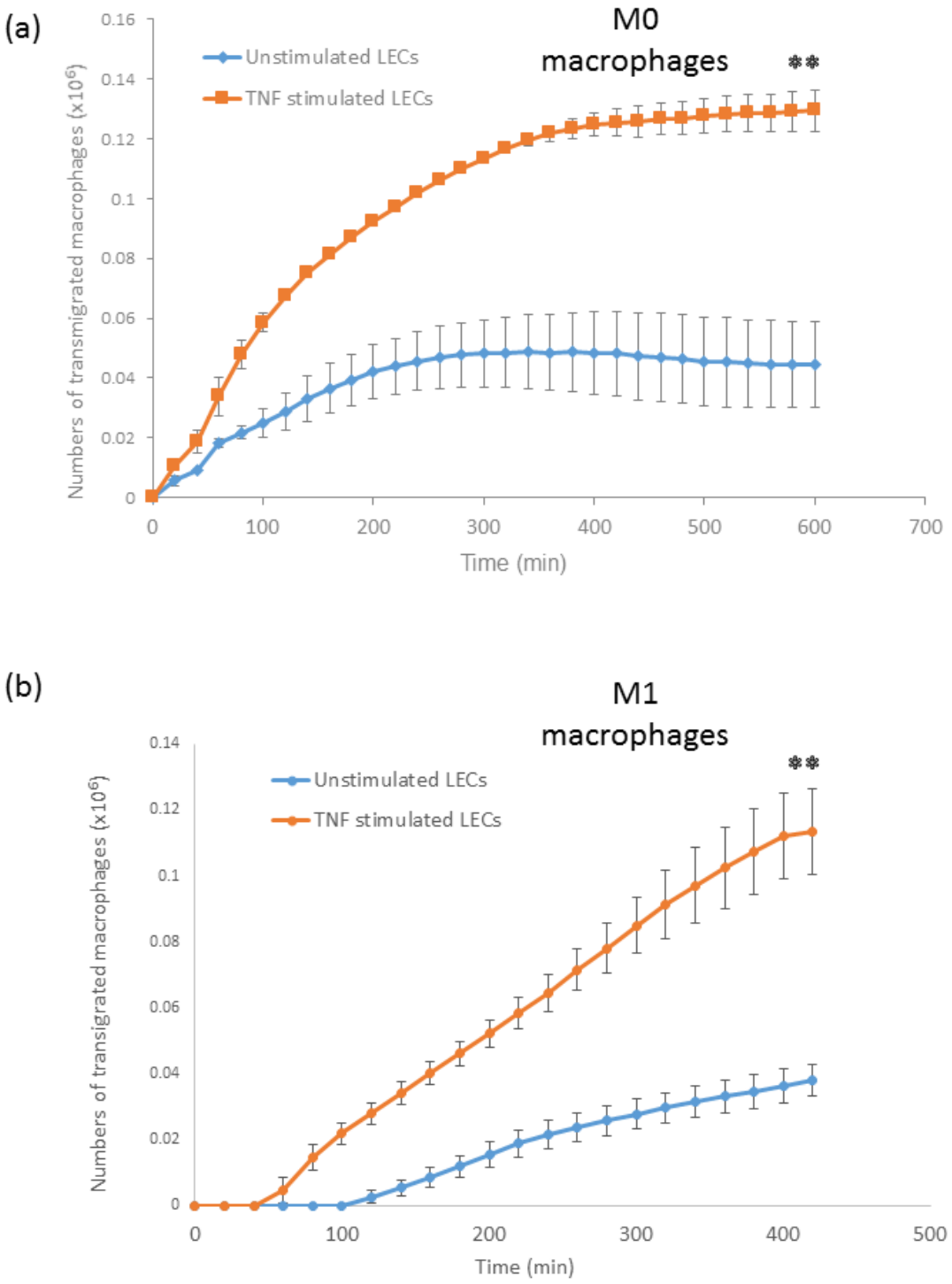


Figure 3-8: Effect of TNF-α stimulation on macrophage transmigration across primary HDLECs. Primary HDLEC monolayers plated on the lower surface of cell culture inserts were stimulated with TNF-α for between 0-24 h. CMFDA labelled (a) M0 macrophages, and (b) M1 macrophages (5 x 10^5) were applied to primary HDLECs incubated with media alone (blue), or media containing TNF-α (orange) in 24 well dishes. Numbers of transmigrating macrophages were measured using a fluorescent plate reader at 20 minute intervals for 10 hours. Data are the mean ± SD of quadruplicate technical replicates. The graph shown is representative of 3 independent experiments and the appropriate statistical test to analyse this data would be a two way analysis of variance (ANOVA).

than 25 % of added cells crossed over to the luminal side suggested that migration across the lymphatics might not be a major manner of clearance during the resolution, a conclusion reached by Gautier et al. (2013). It is also conceivable that a subset within the cultured macrophages is only able to cross lymphatics; these possibilities are considered in the discussion to this chapter.

3.3.4 Roles of key cell adhesion molecules (CAMs) in transmigration of macrophages

Having shown the capacity of macrophages to adhere and transmigrate HDLEC monolayers, and the dramatic increase in both processes following endothelial activation, it was appropriate to explore what endothelial cell adhesion molecules were involved. In particular, I investigated the involvement of the key adhesion molecules, ICAM-1 and VCAM-1. Prior to adding CMFDA labelled macrophages, transwell inserts with activated HDLEC monolayers were treated with adhesion blocking antibodies to ICAM-1 or VCAM-1, or their respective IgG isotype controls. After adding labelled macrophages to these treated transwell inserts, transmigration was then measured with a fluorescence plate reader. Surprisingly, as shown in both figures 3-9 and 3-10, neither blocking antibodies had any significant effect on macrophage transmigration, despite the fact that both have been reported to impair transmigration of DCs, and more recently neutrophils.

As a control to validate the functional integrity of the antibodies used, CMFDA labelled neutrophils were added to transwell inserts with activated HDLEC monolayers that had been treated with either ICAM-1 or VCAM-1 mAbs, or their

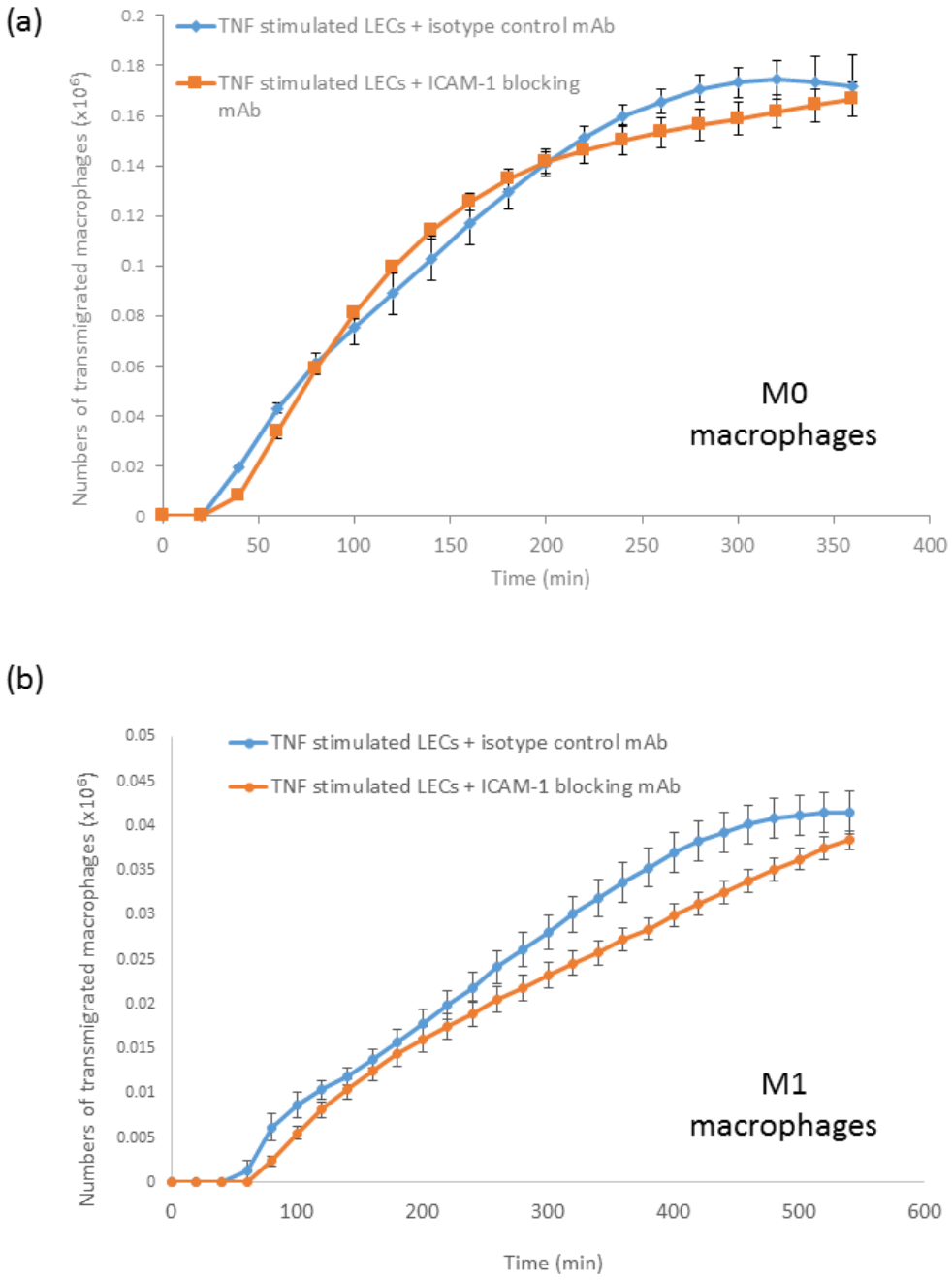


Figure 3-9: Effect of ICAM-1 antibody blockade on macrophage transmigration across TNF-α stimulated primary HDLECs. Primary HDLEC monolayers plated on the lower surface of cell culture inserts were stimulated with TNF-α for between 0-24 h. Stimulated cells were then incubated in media containing TNF-α and either 50 μg/ml isotype control IgG (blue), or P2A4, an ICAM-1 blocking antibody (orange). CMFDA labelled (a) M0 macrophages, and (b) M1 macrophages (5 x 10^5) were applied to treated HDLEC monolayers, as appropriate. Numbers of transmigrating macrophages were measured using a fluorescent plate reader at 20 minute intervals for 10 hours. Data are the mean ± SD of quadruplicate technical replicates. The graph shown is representative of 3 independent experiments and the appropriate statistical test to analyse this data would be a two way analysis of variance (ANOVA).

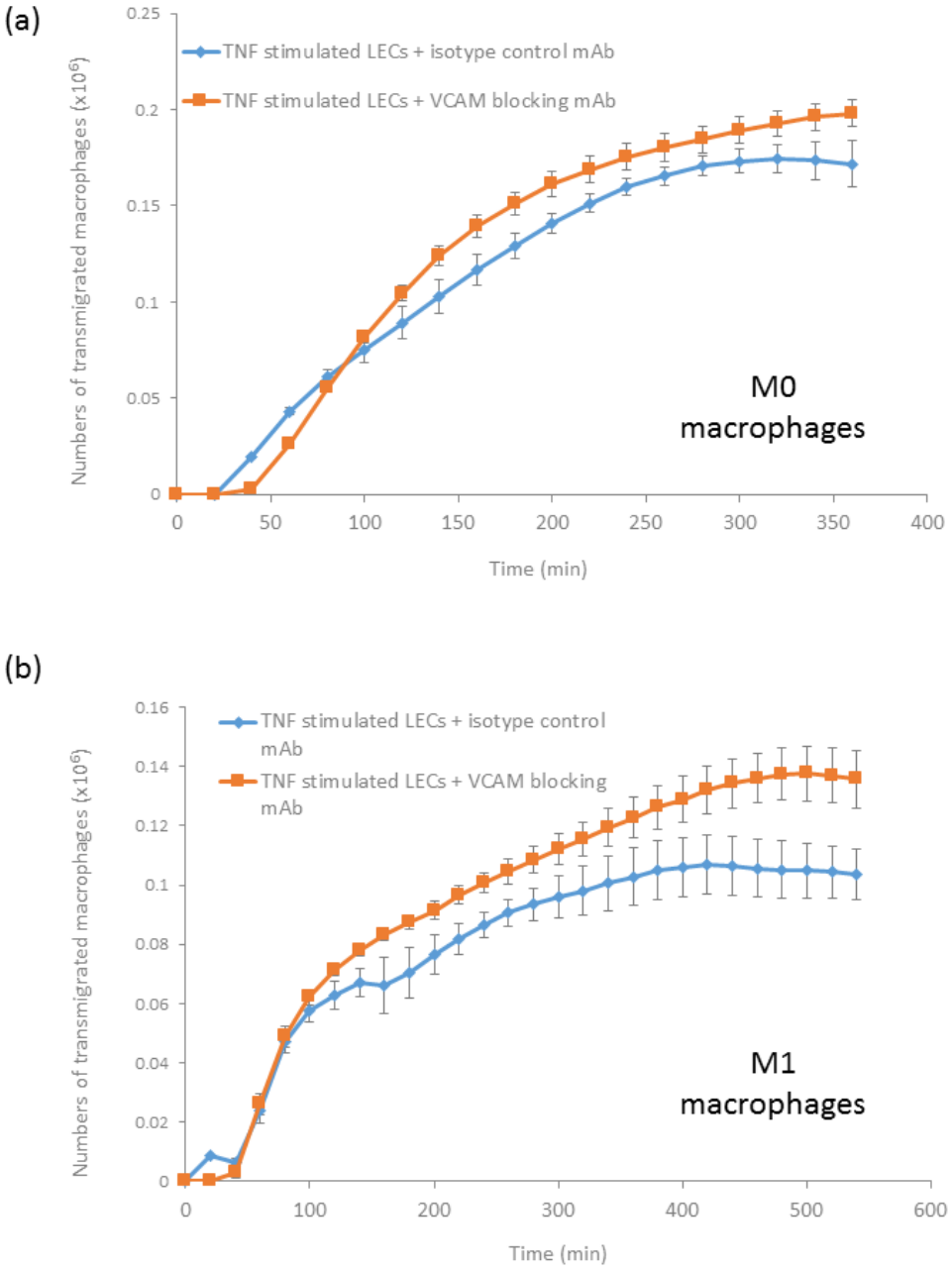


Figure 3-10: Effect of VCAM-1 antibody blockade on macrophage transmigration across TNF-α stimulated primary HDLECs. Primary HDLEC monolayers plated on the lower surface of cell culture inserts were stimulated with TNF-α for between 0-24 h. Stimulated cells were then incubated in media containing TNF-α and either 50 μg/ml isotype control IgG (blue), or 1G11, a VCAM-1 blocking antibody (orange). CMFDA labelled (a) M0 macrophages, and (b) M1 macrophages (5 x 10^5) were applied to treated HDLEC monolayers, as appropriate. Numbers of transmigrating macrophages were measured using a fluorescent plate reader at 20 minute intervals for 10 hours. Data are the mean ± SD of quadruplicate technical replicates. The graph shown is representative of 3 independent experiments and the appropriate statistical test to analyse this data would be a two way analysis of variance (ANOVA).

respective isotype IgG controls. Quantitative analysis of transmigration measured on the fluorescence plate reader showed that ICAM-1 and VCAM-1 blockade reduced levels of transmigrating neutrophils (by an extent similar to that reported previously by Rigby et al. (2015))(Fig 3-11). ICAM-1 blockade was more effective than VCAM-1 (a similar result shown by Rigby et al. (2015), demonstrating approximately 50 % reduction in transmigrating neutrophils. These findings confirm retention of adhesion blocking properties for both antibodies and suggest instead that their failure to impair macrophage transmigration reflects involvement of other adhesion receptors distinct from those that mediate the process in neutrophils and DCs.

In considering which additional adhesion receptors might be involved, I next evaluated ALCAM, which is expressed abundantly in HDLEC (see Fig 3-4 and 3-5) and has recently been reported to play a significant contributory role in DC trafficking to draining lymph nodes. Accordingly, I analysed the impact of adhesion blocking antibodies to ALCAM on the *in vitro* transmigration of CMFDA labelled M0 macrophages across activated HDLEC monolayers (Fig 3-12). However, in common with the ICAM-1 and VCAM-1 blocking mAbs, ALCAM blocking antibodies also failed to demonstrate any significant effect on macrophage transmigration.

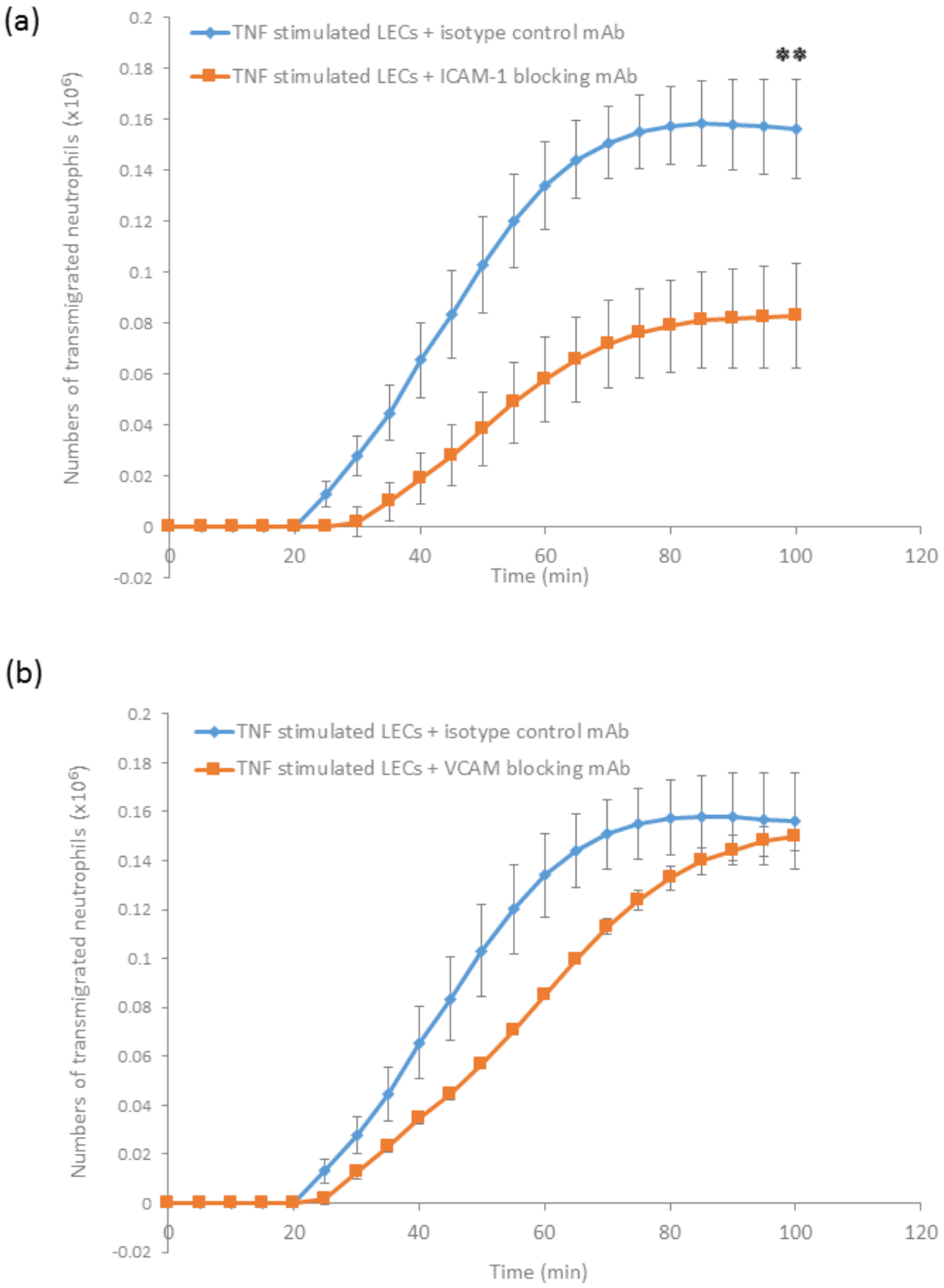


Figure 3-11: Effect of ICAM-1 and VCAM-1 antibody blockade on neutrophil transmigration across TNF-α stimulated primary HDLECs. Primary HDLEC monolayers plated on the lower surface of cell culture inserts were stimulated with TNF-α for between 0-24 h. Stimulated cells were then incubated in media containing TNF-α and either 50 μg/ml isotype control IgG (blue), or (a) P2A4, an ICAM-1 blocking antibody (orange), or (b) 1G11, a VCAM-1 blocking antibody (orange). CMFDA labelled neutrophils (5 x 10^5) were applied to treated HDLEC monolayers, as appropriate. Numbers of transmigrating macrophages were measured using a fluorescent plate reader at 20 minute intervals for 10 hours. The graphs shown are representative of an experiment that was repeated 2 times.

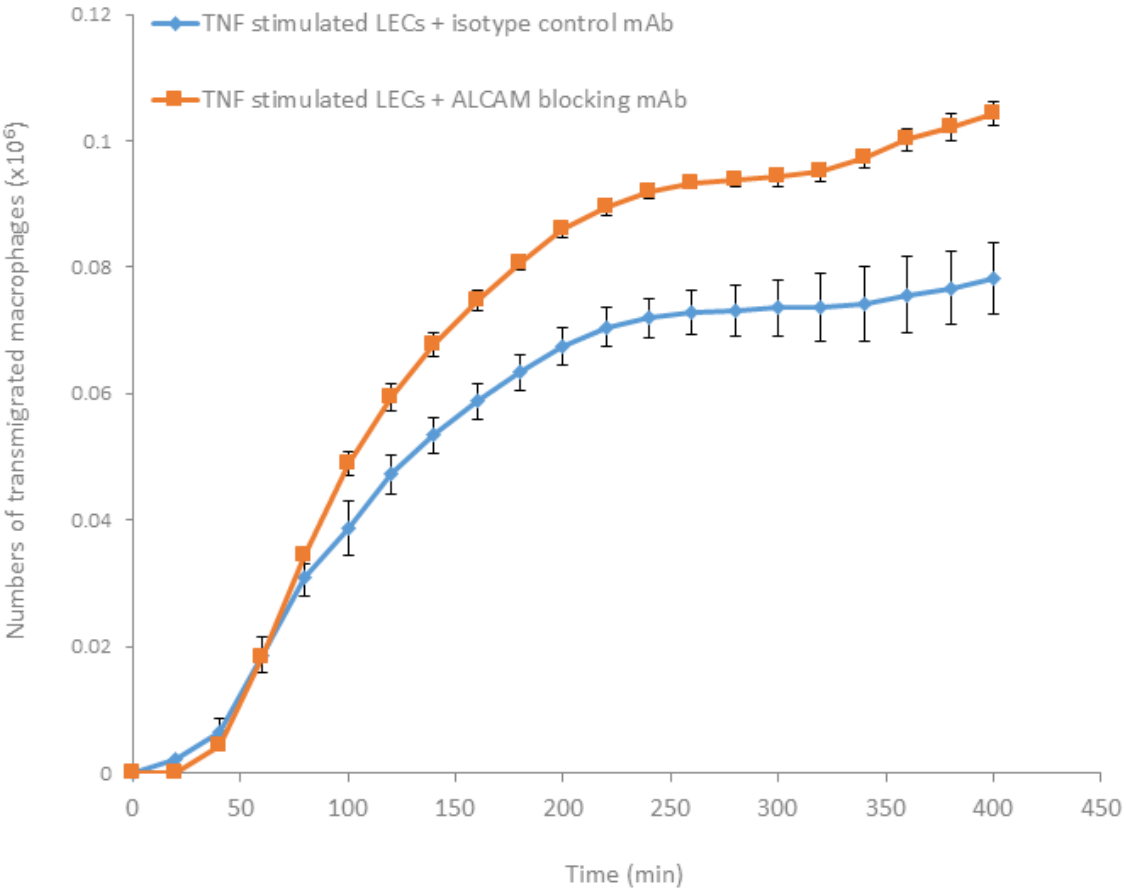


Figure 3-12: Effect of ALCAM antibody blockade on macrophage transmigration across TNF-α stimulated primary HDLECs. Primary HDLEC monolayers plated on the lower surface of cell culture inserts were stimulated with TNF-α for between 0-24 h. Stimulated cells were then incubated in media containing TNF-α and either 50 μg/ml isotype control IgG (blue), or MAB656, an ALCAM blocking antibody (orange). CMFDA labelled M0 macrophages (5 x 10^5) were applied to treated HDLEC monolayers, as appropriate. Numbers of transmigrating macrophages were measured using a fluorescent plate reader at 20 minute intervals for 7 hours. Data are the mean ± SD of quadruplicate technical replicates. The graph shown is representative of 3 independent experiments and the appropriate statistical test to analyse this data would be a two way analysis of variance (ANOVA).

3.3.9 The role of β2 integrins in macrophage transmigration

Among the main counter-receptors on macrophages for endothelial CAMs are the integrins. Hence as a corollary to the antibody blocking studies performed with ICAM-1 and VCAM-1, and to further validate the findings that appear to indicate their exclusion, I next investigated the effects of imposing blockade of macrophage β2 integrins, In particular macrophages express both Mac-1 and LFA-1 which share the same beta subunit (CD18). Hence, after labelling M1 macrophages with CMFDA, the cells were treated with either blocking antibodies to β2 integrin, or with the respective isotype control. Subsequently, the treated cells were added to transwell inserts with activated HDLEC monolayers and measured on a fluorescence plate reader (Fig 3-13). Interestingly, functional blockade of β2 integrins caused an approximately 20 % reduction in the numbers of transmigrating macrophages. This result demonstrated that a yet unidentified ligand to β2 integrin on activated HDLECs is significantly involved in mediating adhesion dependent transmigration of macrophages. With ICAM-1 redundant to the process, likely other candidate molecules expressed on LECs would be the JAMs or even ICAM-2. The involvement of β1 integrins were also considered as they have similarly high expression on the surface of macrophages as β2 integrins. Unfortunately, due to time constraints these ideas were left unexplored but such possibilities are discussed later on.

Overall, the result shows that β2 integrins partially mediate transmigration of macrophages across HDLEC monolayers.

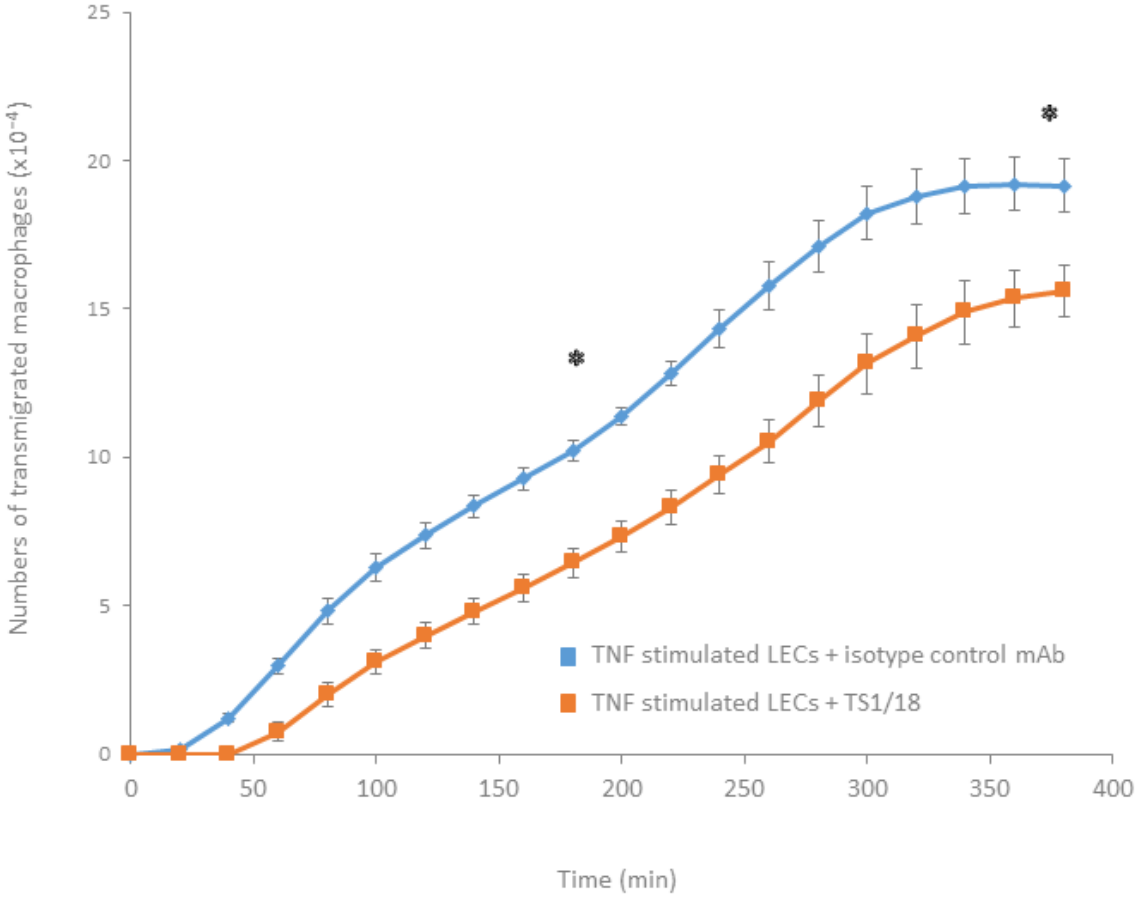


Figure 3-13: Effect of β2 integrin antibody blockade on macrophage transmigration across TNF-α stimulated primary HDLECs. Primary HDLEC monolayers plated on the lower surface of cell culture inserts were stimulated with TNF-α for between 0-24 h. Stimulated cells were then incubated in media containing TNF-α and either 50 μg/ml isotype control IgG (blue), or TS1/18, a β2 integrin blocking antibody (orange). CMFDA labelled M1 macrophages (5 x 10^5) were prepared in media containing the same pre-incubation supplements and applied to treated HDLEC monolayers, as appropriate. Numbers of transmigrating macrophages were measured using a fluorescent plate reader at 20 minute intervals for 7 hours. Data are the mean ± SD of quadruplicate technical replicates. The graph shown is representative of 2 independent experiments and the appropriate statistical test to analyse this data would be a two way analysis of variance (ANOVA).

3.3.5 Investigation into the role of LYVE-1 in macrophage transmigration across unstimulated lymphatic endothelium

While the preceding studies addressed the possible involvement of adhesion molecules common to both blood and lymphatic endothelium, it was also considered likely that molecules more specific to lymphatic endothelium might mediate macrophage adhesion and transmigration. One of the most abundant of these is the major lymphatic endothelial hyaluronan receptor LYVE-1, for which a group of function blocking mAbs has already been generated, one (mAb 3A) in the Jackson laboratory and two by commercial sources (R&D Systems) termed 891 and 893. All three of these mAbs have been shown to disrupt the interaction of recombinant human LYVE-1 with high molecular weight HA.

The initial investigations involved measuring adhesion of CMFDA labelled macrophages to unstimulated HDLEC monolayers that were treated with 3A, or its respective isotype over a period of 6 hours (Fig 3-14). Unexpectedly, functional blockade with mAb 3A led to an apparent 2-fold increase in macrophage adhesion to HDLEC monolayers compared to isotype IgG treated controls.

Next, to assess the effects on macrophage transmigration, unstimulated HDLEC monolayers were treated with 3A, or its respective isotype control, prior to measuring transit of CMFDA labelled macrophages. As shown in (Fig 3-15), such blockade led to an approximately two-fold increase in the number of transmigrating macrophages compared to isotype IgG treated controls, consistent with the stimulatory effect already observed for macrophage adhesion. These initially paradoxical findings suggested that the interaction

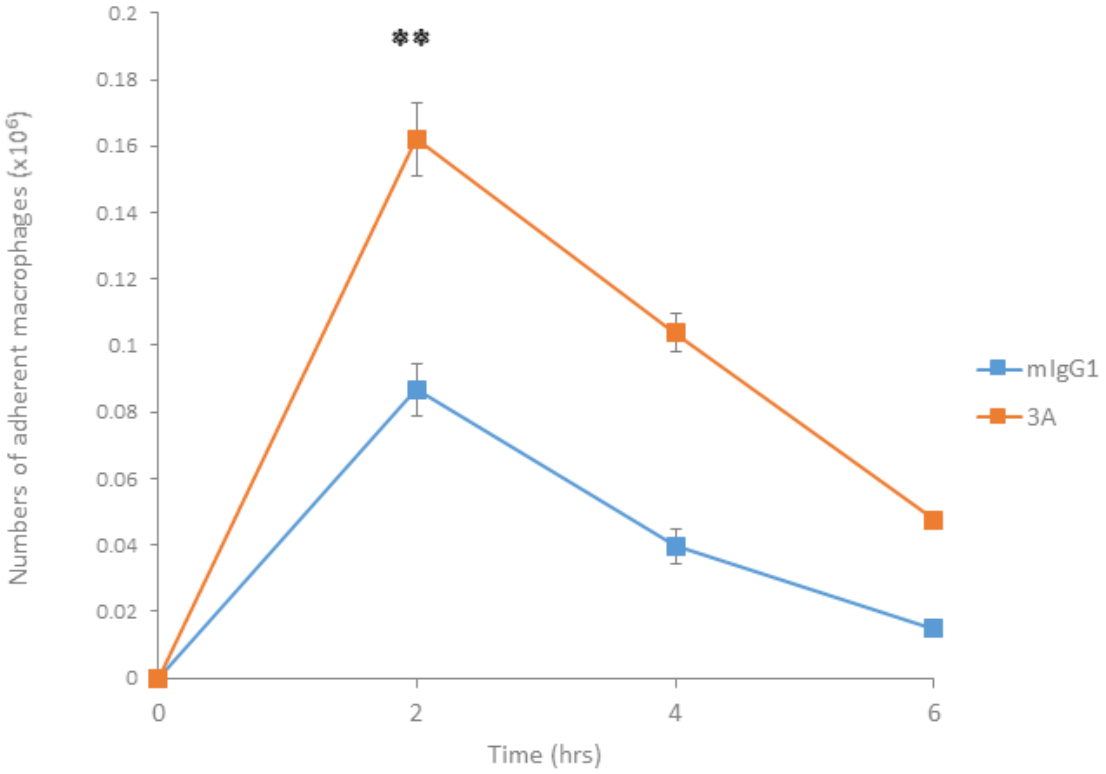


Figure 3-14: Effect of LYVE-1 antibody blockade on macrophage adhesion to unstimulated primary HDLECs. Primary HDLEC monolayers were cultured in media without any stimulation. Monolayers were then pre-incubated for 30 min in media containing either 50 μg/ml isotype control IgG (blue), or 3A, a LYVE-1 function blocking antibody (orange). CMFDA labelled macrophages (5 x 10^5) were applied to the treated primary HDLECs in 24 well dishes, as appropriate. Numbers of adherent macrophages were measured using a fluorescent plate reader at 2 and 4 hour. Data are the mean ± SD of quadruplicate technical replicates. The graph shown is representative of 3 independent experiments and a two-tailed, unpaired Student's t-test was performed on this figure and p values below 0.05 were considered statistically significant (** $p < 0.01$; isotype control IgG vs 3A at 2 hours). The appropriate statistical test to analyse this data would be a two way analysis of variance (ANOVA).

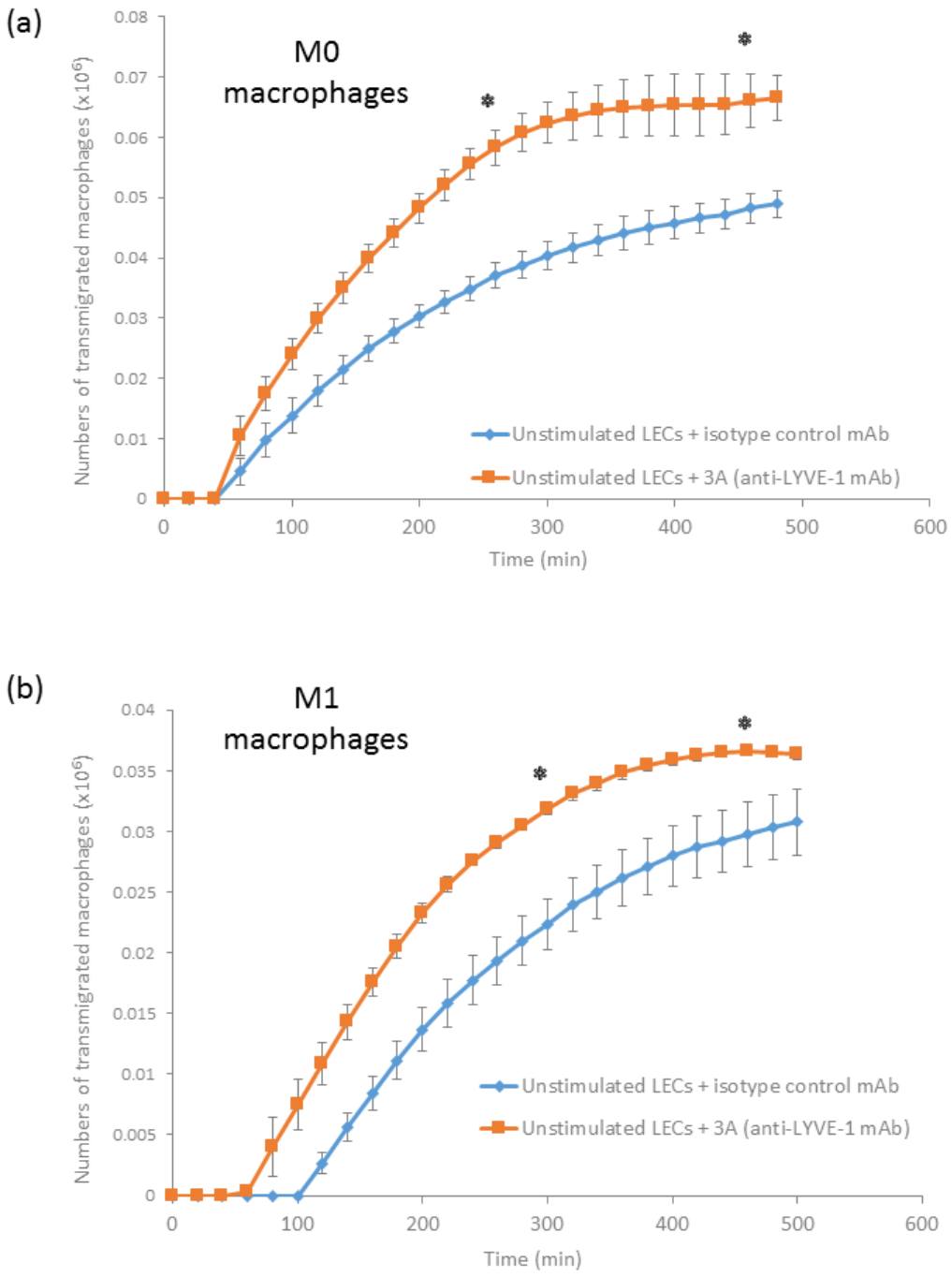


Figure 3-15: Effect of LYVE-1 antibody blockade on macrophage transmigration across unstimulated primary HDLECs. Primary HDLEC monolayers plated on the lower surface of cell culture inserts were incubated in media containing either 50 μg/ml isotype control IgG (blue), or 3A, a LYVE-1 function blocking antibody (orange). CMFDA labelled (a) M0 macrophages, or (b) M1 macrophages (5 x 10^5) were applied to treated HDLEC monolayers, as appropriate. Numbers of transmigrating macrophages were measured using a fluorescent plate reader at 20 minute intervals for 8 hours. Data are the mean ± SD of quadruplicate technical replicates. The graph shown is representative of 3 independent experiments and a two-tailed, unpaired Student's t-test was performed on this figure and p values below 0.05 were considered statistically significant (* $p < 0.05$; isotype control IgG vs 3A at 300 and 460 minutes). The appropriate statistical test to analyse this data would be a two way analysis of variance (ANOVA).

between LYVE-1 and HA suppressed macrophage adhesion/transmigration, since both processes appeared to be enhanced after LYVE-1 functional disruption.

To further explore this anomaly and its general validity, I next assessed whether the apparent enhancement in macrophage adhesion/transmigration could be recapitulated with the LYVE-1 HA blocking mAbs 891 and 893, or if it was an effect peculiar to 3A. Comparative analyses of the HA blocking capacity the three HA blocking mAbs revealed that 3A had a much lower potency, with an estimated IC50 of approximately 25-30 μg/ml, some 30-fold higher than mAbs 891 or 893 (Fig 3-16). With this in mind, I decided to further explore the role of LYVE-1 by assessing the effects of function blocking with mAb981 and mAb893. It is also worth stating that certain elements of the 3A epitopes are known whereas such information for the more potent antibodies are not yet known, complicating the effects of mAbs 891 and 893.

When the effects of mAbs 891 and 893 on M0 macrophage transmigration were assessed in transwell assays with unstimulated HDLEC monolayers neither was found to have any significant impact (Fig 3-17). Hence the anomalous stimulatory effect on macrophage behaviour is a property restricted to mAb 3A.

Clearly there may be many possible explanations for the unexpected effects of mAb 3A. Although, the possibility could be of the mAb promoting adhesion by crosslinking macrophage expressed FcRs while bound to LYVE-1 on LECs, it would seem unlikely since serum Ig is added to block FcRs. Also, if such is the artifact, a similar effect would be noticed with mAb893 which shares the same isotype as 3A. However, one formal possibility is that treatment with mAb 3A

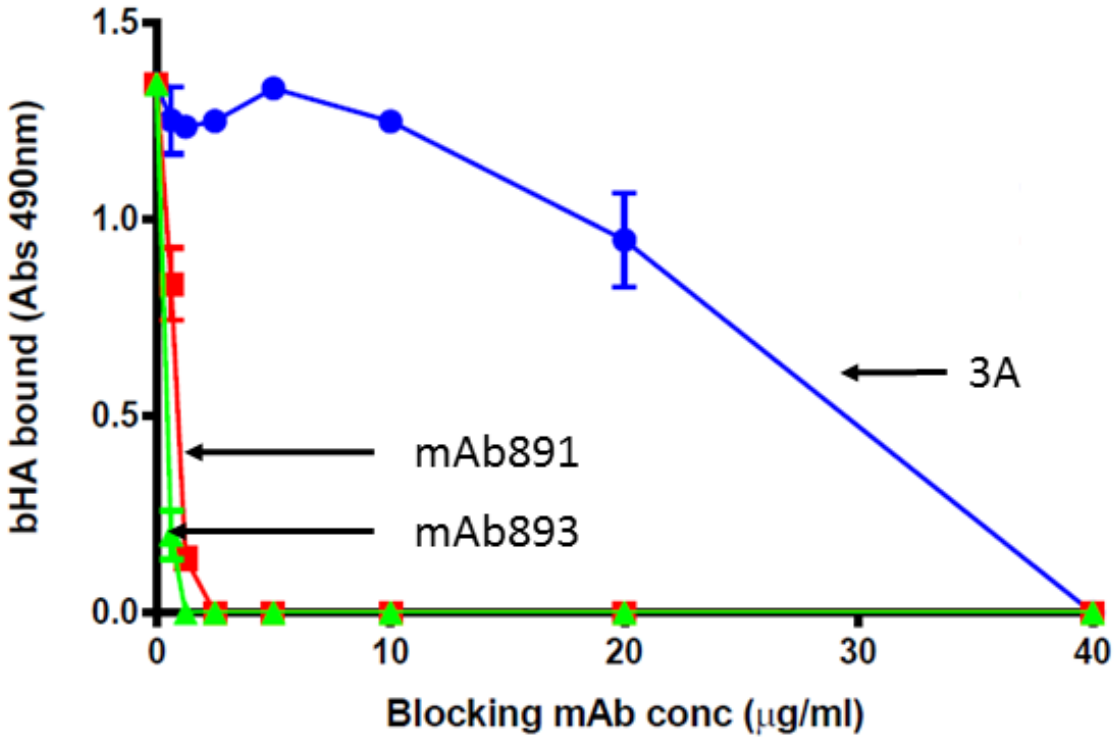


Figure 3-16: Comparison of human LYVE-1 mAbs for HA blocking capacity LYVE-1 extracellular domain (ECD) dimer with a 10X his tag at the C-terminus was coated on wells of a Nunc Maxisorb plate at 10 μg/ml in PBS at room temperature (RT) overnight. Coated wells were blocked in PBS containing 0.05 % Tween 20 for 2h at RT. LYVE-1 blocking antibodies were added for 30 min at concentrations shown prior to the addition of biotinylated HMW HA (bHA) at a final concentration of 5 μg/ml. After washing, bound bHA was detected with streptavidin HRP (1 μg/ml) and visualised using OPD substrate (Sigma). Colour was allowed to develop before quenching with H_2SO_4. The plate was read using a Bio-Rad I-mark plate reader at 490 nm. Plotted values are from triplicated determinations and error bars represent the standard error of the mean. Data produced by Suneale Banerji, Jackson group

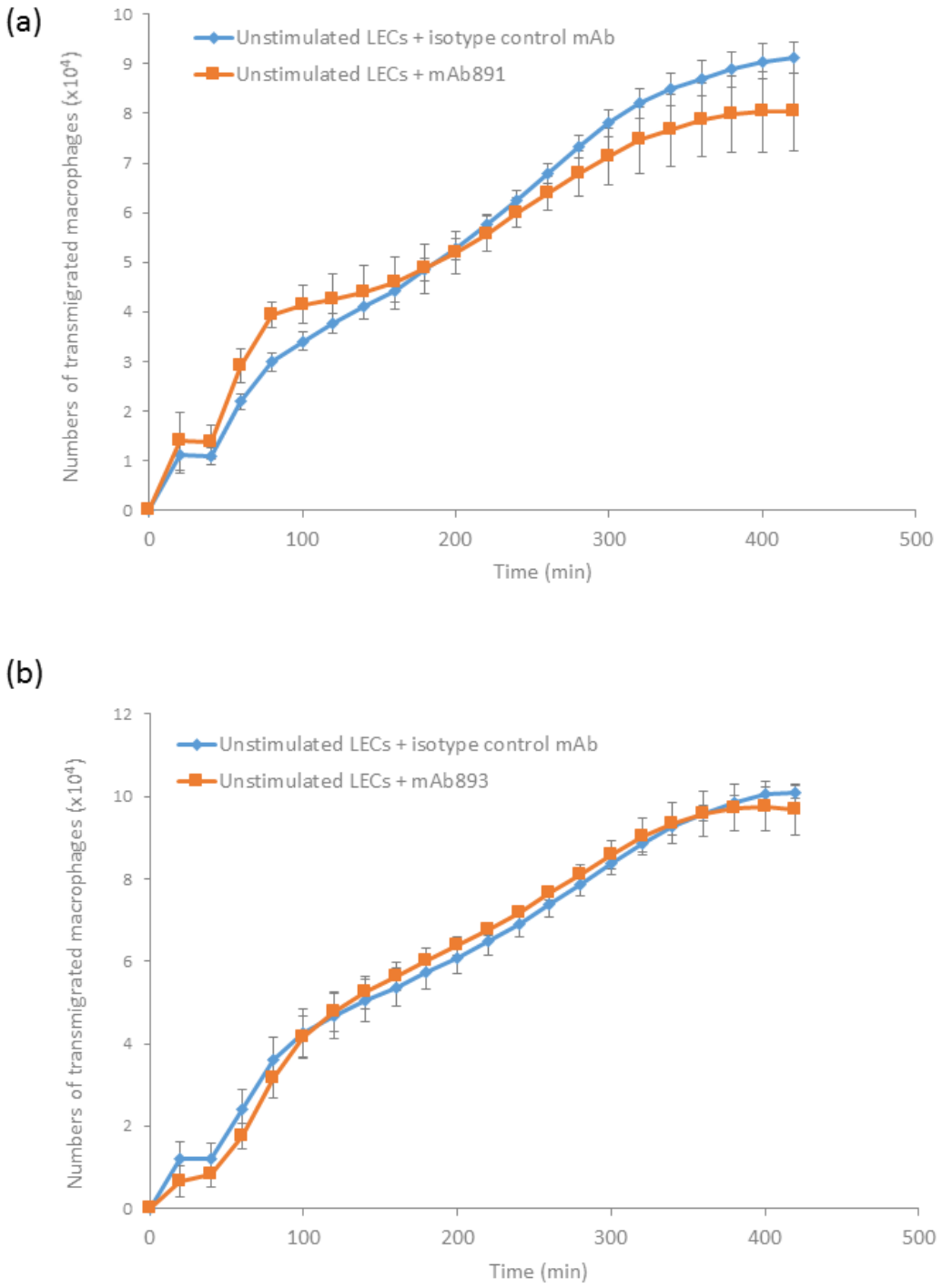


Figure 3-17: Effect of LYVE-1 antibody blockade on macrophage transmigration across unstimulated primary HDLECs. Primary HDLEC monolayers plated on the lower surface of cell culture inserts were incubated in media containing either 50 μg/ml isotype control IgG (blue), or (a) mAb891, or (b) mAb893, LYVE-1 function blocking antibodies (orange). CMFDA labelled M0 macrophages (5 x 10^5) were applied to treated HDLEC monolayers, as appropriate. Numbers of transmigrating macrophages were measured using a fluorescent plate reader at 20 minute intervals for 7 hours. Data are the mean ± SD of quadruplicate technical replicates. The graph shown is representative of 3 independent experiments and a two-tailed, unpaired Student's t-test was performed on this figure and p values below 0.05 were considered statistically significant. The appropriate statistical test to analyse this data would be a two way analysis of variance (ANOVA).

leads to a block in macrophage detachment from the endothelial monolayer rather than a block in initial attachment. Since the transwell assay registers all cells on the undersurface of the filter membrane as having transmigrated, it cannot discriminate between those that fully transit the endothelial layer and any that remain attached to its luminal surface To further evaluate this possibility, the transmigration assay was repeated in the presence of either mAb 3A, or isotype control mAb, but in this case the numbers of fluorescent macrophages attached to the underside of inserts and those present in the lower chamber media were measured separately (Fig 3-18). There was no difference in fluorescent macrophage numbers between the lower chamber media from transwells treated with 3A or, mIgG$_1$. Significantly however, there was a 2-fold greater number of macrophages associated with the inserts from mAb 3A treated LECs.

Although not fully conclusive, these data suggested that mAb 3A had indeed prevented detachment of macrophages from the luminal side of the endothelial monolayer. To further validate the findings, the inserts were removed from a parallel transwell assay set at 6h, and the LEC monolayers and associated macrophages imaged by confocal microscopy after staining with an antibody to the endothelial junctional marker VE-cadherin . As shown by the images in Figure 3-19, there were considerably more macrophages adherent to endothelial monolayers that were treated with 3A, compared to mIgG1. Also, there was the observation that the macrophages were transmigrating in association with junctions.

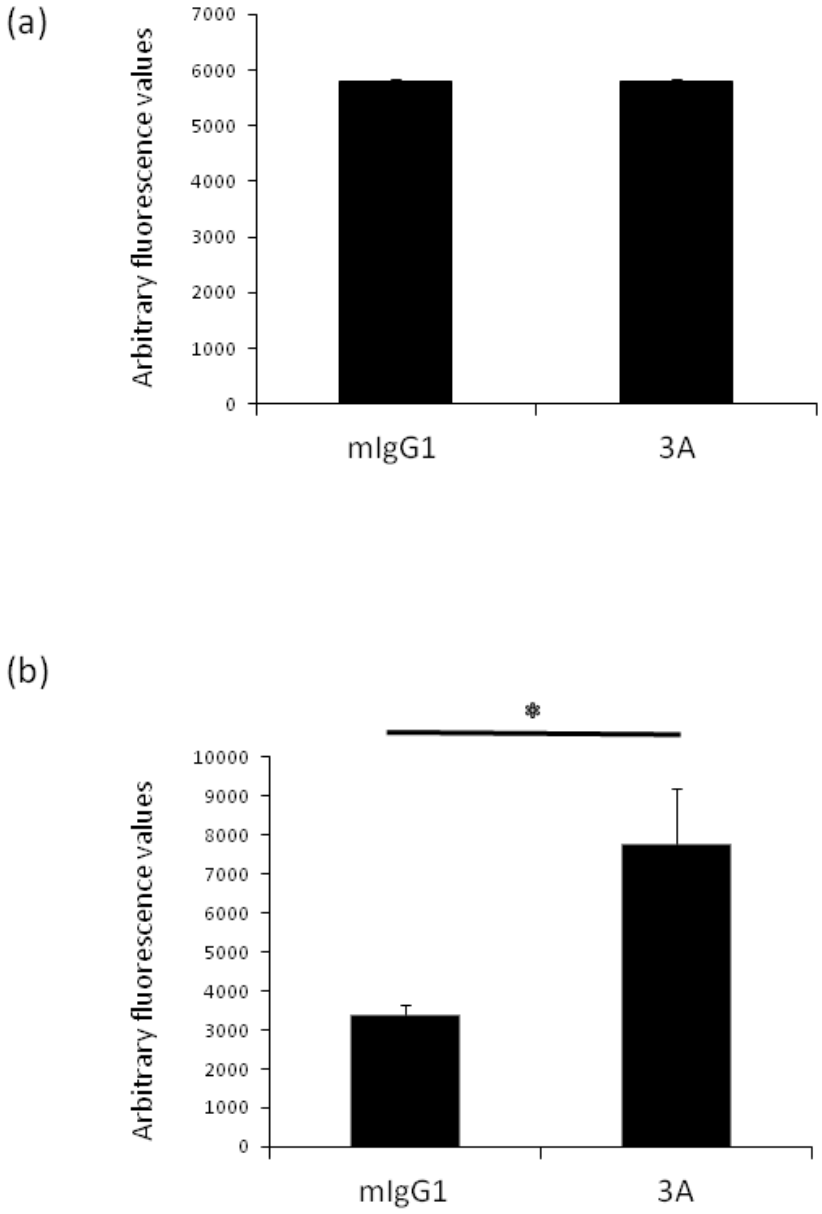


Figure 3-18: Effect of LYVE-1 antibody, 3A, blockade on macrophage detachment from endothelium after transmigration across unstimulated primary HDLECs. Primary HDLEC monolayers plated on the lower surface of cell culture inserts were incubated in media containing either 50 μg/ml isotype control IgG, or 3A, a LYVE-1 function blocking antibody. CMFDA labelled M0 macrophages (5×10^5) were applied to treated HDLEC monolayers, as appropriate. After 6 hours of transmigration, individual components of the assay i.e. (a) lower chamber media, and (b) inserts were assessed for fluorescence using a Biotek Synergy HT fluorescence plate reader as described in Chapter 2 Methods. Data are the mean ± SD of triplicate technical replicates. The graph shown is representative of 3 independent experiments and a two-tailed, unpaired Student's t-test was performed on this figure and p values below 0.05 were considered statistically significant (*$p < 0.05$; isotype control IgG vs 3A). The appropriate statistical test to analyse this data would be a two way analysis of variance (ANOVA).

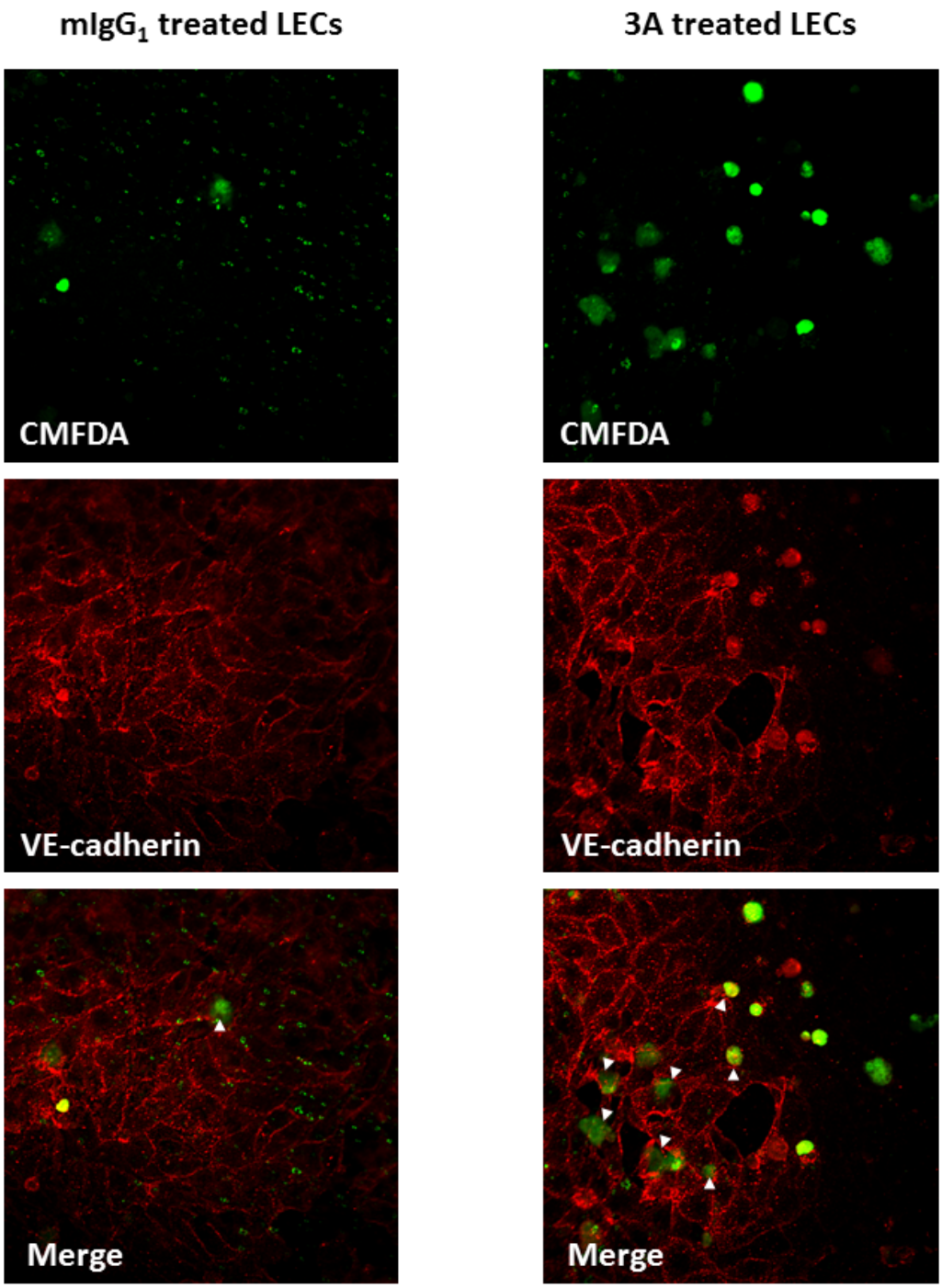


Figure 3-19: Effect of LYVE-1 antibody, 3A, blockade on macrophage detachment from endothelium after transmigration across unstimulated primary HDLECs. Primary HDLEC monolayers plated on the lower surface of cell culture inserts were incubated in media containing either 50 μg/ml isotype control IgG, or 3A, a LYVE-1 function blocking antibody. CMFDA labelled M0 macrophages (5 x 10^5) were applied to treated HDLEC monolayers, as appropriate. After 6 hours of transmigration, membranes of the inserts were stained with primary antibodies to VE-cadherin and faced luminal side up on slides for imaging for localisation of macrophages (green) and VE-cadherin (red). White arrow heads denote transmigrating macrophage in association with junctions.

3.3.6 The role of LYVE-1 in transmigration of macrophages across TNF-α activated HDLEC monolayers

Most of the experiments in the preceding section have focused on macrophage transit across resting unstimulated lymphatic endothelium, modelling events that might occur in lymphatic vessels under normal homeostatic conditions. However, the migration of dendritic cells and neutrophils via lymph is known to increase greatly under conditions of inflammation. Likewise, clearance of macrophages from inflamed sites would involve transit across an inflamed lymphatic endothelium and as shown above, in greater numbers. It is likely that blockade effects of LYVE-1 would be more observable with a greater number of transmigrating macrophages. Interestingly, previous studies in the Jackson laboratory have shown that activation of lymphatic endothelium by inflammatory cytokines leads to considerable alteration in adhesion molecule and chemokine expression, and in particular a partial downregulation of LYVE-1. These results suggest that LYVE-1-HA interactions inhibit leucocyte transit and the greater numbers transmigrating under such conditions is due to this downmodulation. Johnson et al. (2007) further uncovered that the receptor was transported to the lysosome for terminal degradation and this internalisation could contribute to transcellular migration.

Hence, before investigating the potential involvement of LYVE-1 in macrophage adhesion/transmigration, I considered it important to re-assess the extent of LYVE-1 downregulation in isolated HDLECs in response to cytokine exposure, using flow cytometry. Accordingly, HDLECs were either stimulated with TNF-α overnight or left untreated, prior to staining with with primary antibodies to LYVE-1. As shown by the data in Fig 3-20a, there was a greater than 70 %

reduction in the level of LYVE-1 surface expression on activated HDLECs compared to untreated controls. In addition, HDLEC monolayers cultured on 8 chamber slides were treated as above and stained with primary antibodies specific to LYVE-1 prior to imaging by immunofluorescence microscopy (Fig 3-20b). Consistent with the flow cytometry data, LYVE-1 appeared to have been lost from the surface of most LEC.These results confirmed the previously published findings by Johnson et al. (2007) and posed the conceptual problem of how under such circumstances LYVE-1 might support a significant interaction with macrophages for adhesion or transit.

The possibility remained that these residual levels of LYVE-1 might nevertheless function to mediate adhesion and transmigration, and that the process of LYVE-1 downmodulation might even be part of a mechanism for leukocyte translocation. Examination of such interactions was achieved by immunofluorescence microscopy. CMFDA labelled M1 macrophages were incubated for 2 hours with confluent HDLEC monolayers on 8 chamber slides that were either cultured in media alone, or with TNF-α overnight. This incubation period was selected as the optimum to allow maximum numbers of cells to adhere, as established from previous adhesion assays (Fig 3-7). Afterwards, slides were stained with primary antibodies to LYVE-1 for imaging (Fig 3-21). On inspection, there was clearly a greater number of adherent macrophages on activated HDLEC monolayers compared to unstimulated controls. Interestingly, the adherent macrophages on both conditions were surrounded at their perimeter by a circular arrangement of LYVE-1 on the endothelial surface and these LYVE-1 ring-like structures were particularly noticeable on activated HDLECs. On closer observation of unstimulated

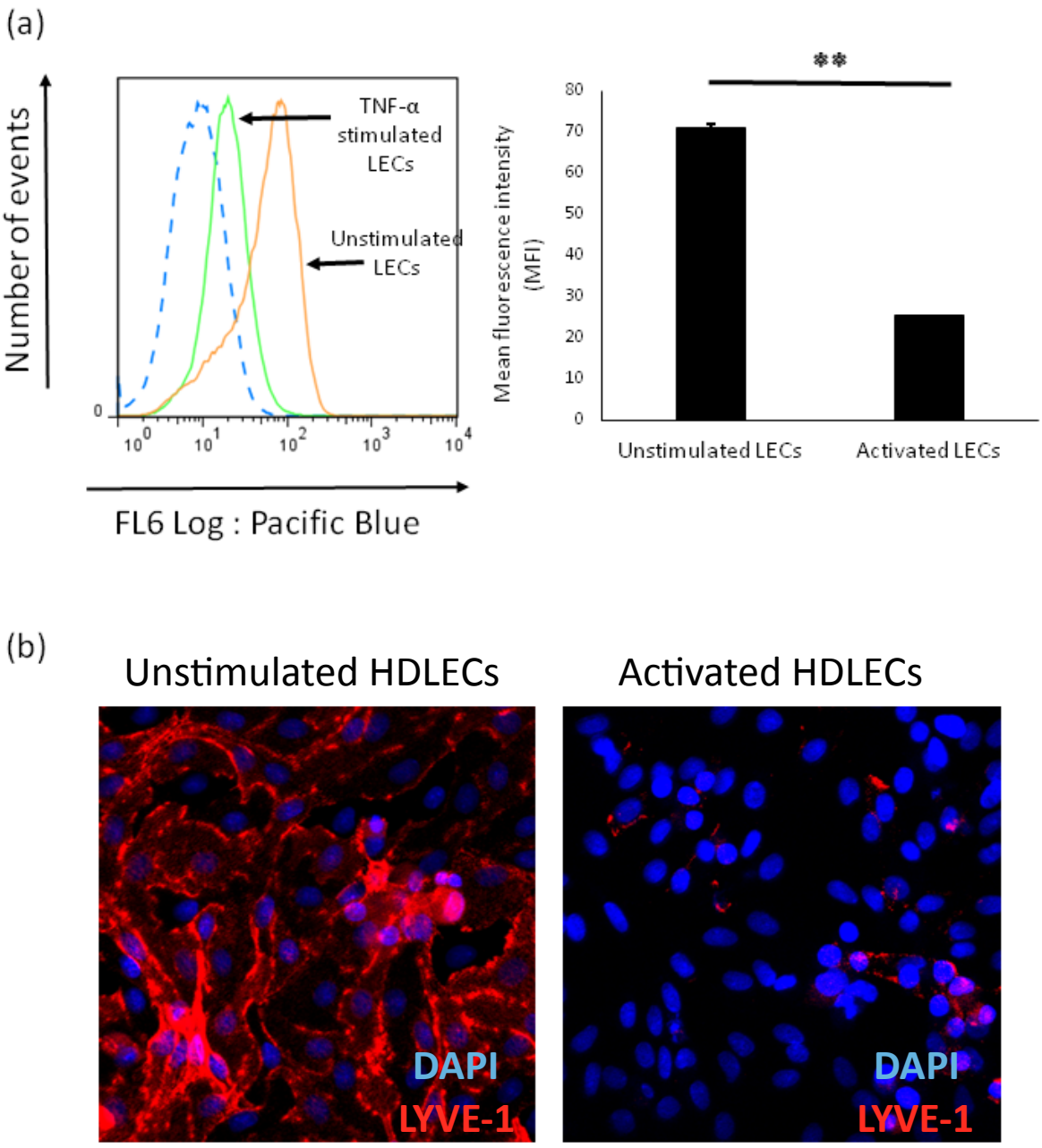


Figure 3-20: Effect of TNF-α on LYVE-1 expression on surface of primary HDLECs. Primary HDLEC monolayers were incubated either in media alone, or media containing 5 ng/ml of TNF-α for 0-24 h. Afterwards, cells were stained with primary antibodies to lymphatic endothelial marker LYVE-1 using a rabbit polyclonal antibody raised against LYVE-1. Stained cells were analysed by (a) flow cytometry, and (b) immunofluorescence microscopy. Isotype controls are shown by dashed histogram. Expression levels were quantified by flow cytometry and histograms are representative of an experiment repeated > 3 times. Data are the mean ± SD of quadruplicate technical replicates. A two-tailed, unpaired Student's t-test was performed on this figure and p values below 0.05 were considered statistically significant (**$p < 0.01$; unstimulated vs TNF stimulated LECs). The appropriate statistical test to analyse this data would be a two way analysis of variance (ANOVA).

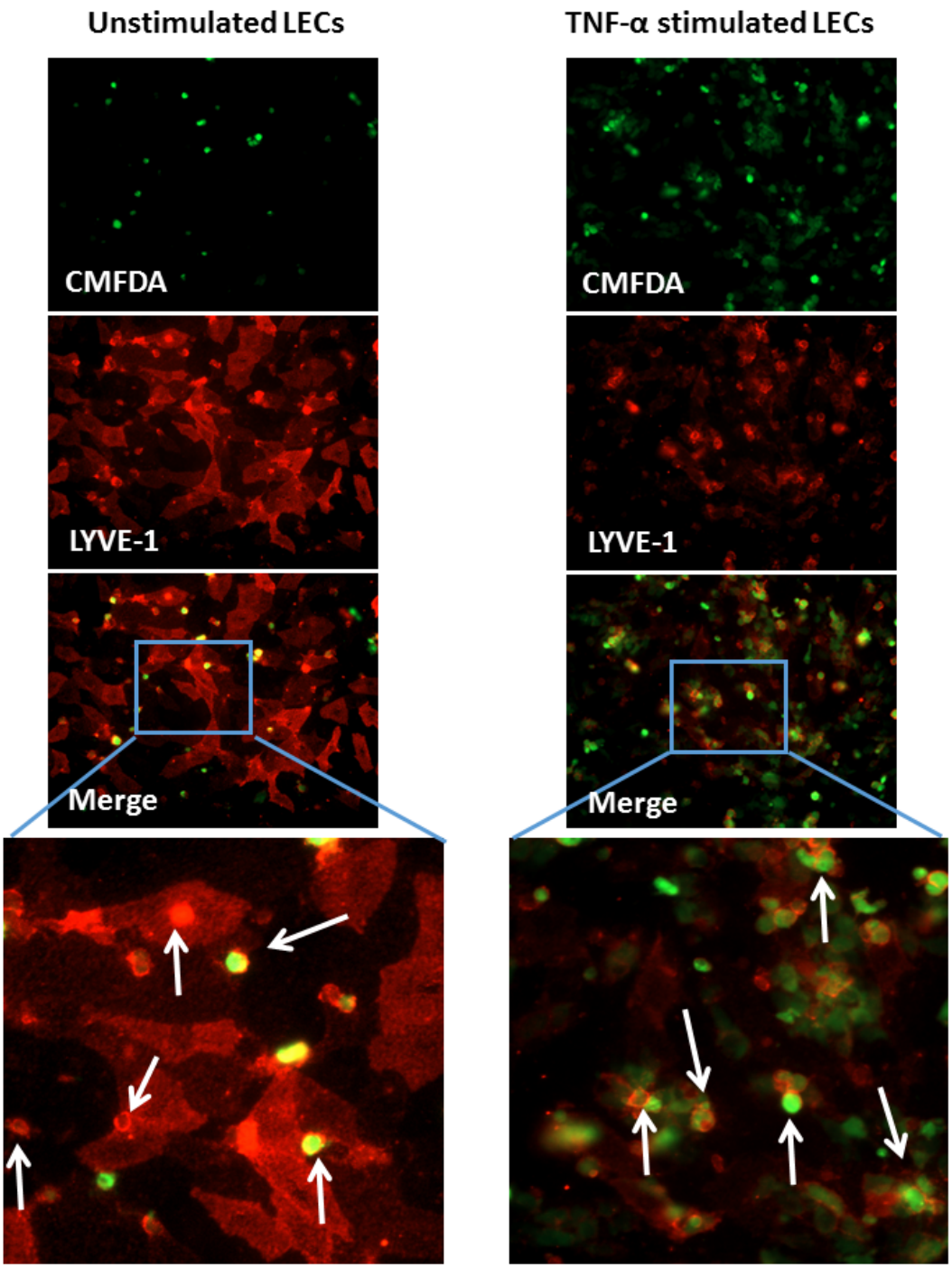


Figure 3-21: Characterisation of LYVE-1 expression in relation to macrophage adhesion. Primary HDLEC monolayers cultured on 8 chamber slides were incubated either in media alone, or media containing 5 ng/ml of TNF-α for 0-24 h. CMFDA labelled M1 macrophages were prepared in media with same respective pre-treatments and incubated to monolayers appropriately for 2 hours. Subsequently slides were washed and to removed non-adherent cells and stained with primary antibodies to lymphatic endothelial marker LYVE-1 using a rabbit polyclonal antibody raised against LYVE-1. Stained cells were analysed by immunofluorescence microscopy. Images are representative of an experiment repeated > 3 times. White arrows show macrophages (green) co-localising with LYVE-1 (red).

HDLECs, the rings of LYVE-1 were also present on cells that lacked adherent macrophages.

The data above not only revealed an interaction between macrophages and LYVE-1 but also suggested that macrophages may be able to re-express or redistribute the receptor on the surface of activated HDLECs after its initial downmodulation. To explore this further, activated lymphatic endothelial monolayers incubated with or without M1 macrophages for 2 hours were lifted and stained with primary antibodies to LYVE-1, and the level of surface receptor assessed by flow cytometry (Fig 3-22). Interestingly, the activated HDLEC monolayers that had been incubated with macrophages displayed 5 % less surface LYVE-1 than those incubated alone. Furthermore, flow cytometric analysis of the macrophages revealed those that had adhered and spontaneously detached from the monolayer, now appeared to have acquired LYVE-1 expression - supposedly by “biting” the receptor from the LECs. The expression of the receptor on macrophages is believed to come from the LEC monolayers since phenotyping of these myeloid cells, when not adhered to LECs, revealed no LYVE-1 expression (data not shown).

Next, to determine whether the interaction of macrophages with LYVE-1 involves hyaluronan and mediates adhesion, CMFDA labelled M1 macrophages were incubated with activated HDLEC monolayers in the presence or absence of the LYVE-1-HA blocking antibody mAb893 for set time points of 2 and 4 hours. As shown in figure 3-23a, blockade of LYVE-1-HA binding with mAb893 caused a significant 20 % reduction in numbers of adherent macrophages at 2

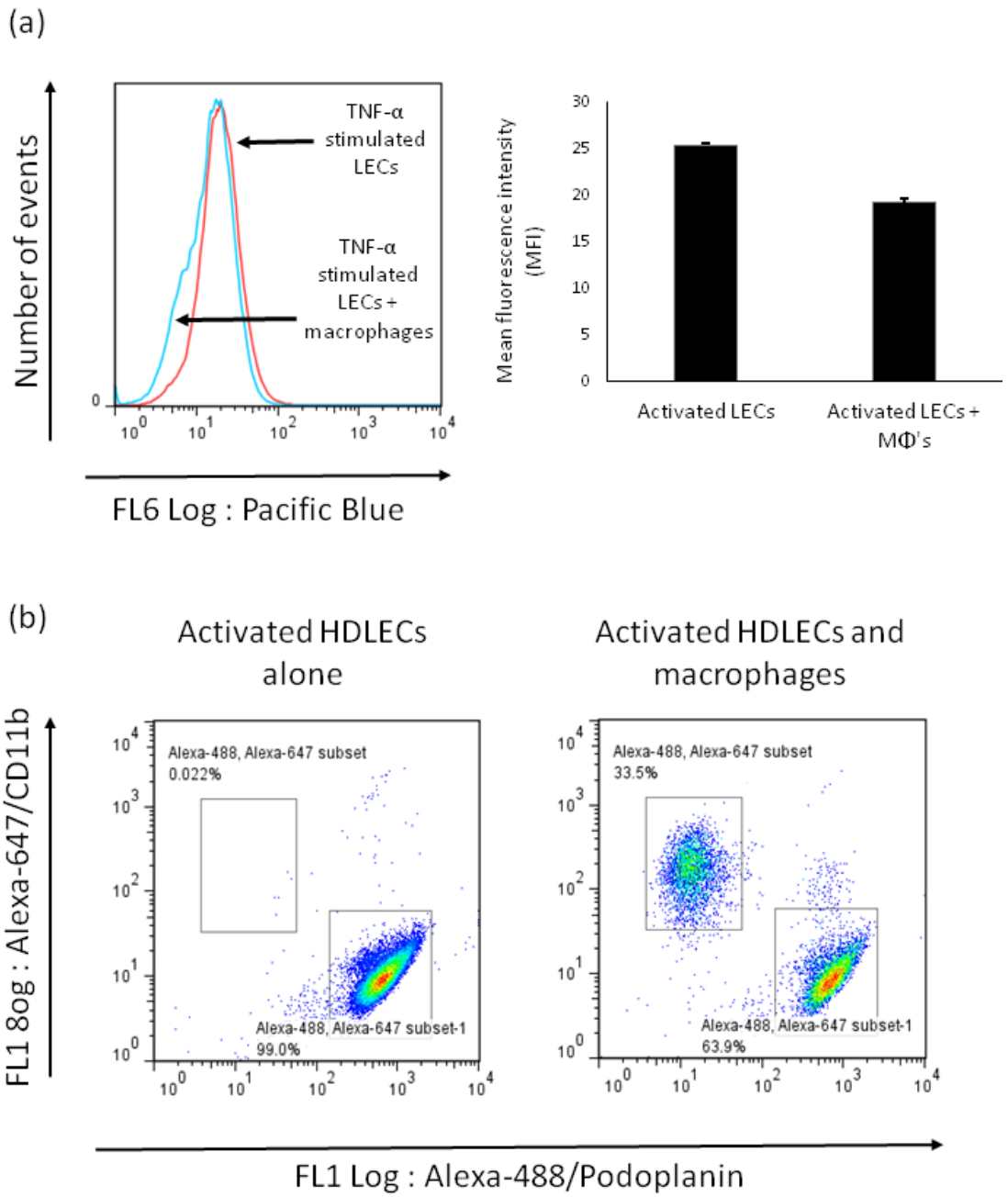


Figure 3-22: Characterisation of LYVE-1 expression in relation to macrophage adhesion. Primary HDLEC monolayers were incubated in media containing 5 ng/ml of TNF-α for 0-24 h. After initial stimulation, monolayers were either left in stimulant media alone, or with stimulant and M1 macrophages for 2 hours. Subsequently, cells were lifted and stained with primary antibodies to lymphatic endothelial marker LYVE-1 using a rabbit polyclonal antibody raised against LYVE-1, podoplanin using monoclonal antibody NZ-1 and myeloid integrin CD11b using monoclonal antibody ICRF44. Stained cells were analysed by flow cytometry. (a) LYVE-1 expression of monolayers incubated with TNF-α alone, or with TNF-α and M1 macrophages. (b) Expression of CD11b and podoplanin on all LYVE-1$^+$ cells. Expression levels were quantified by flow cytometry and histograms and dot plots are representative of one experiment.

hours compared to isotype Ig treated controls. However, there was no significant difference in adherent cell numbers at 4h.

Given the preliminary finding that LYVE-1 and HA contributed significantly to macrophage-LEC adhesion, I next explored the impact of LYVE-1 blockade with mAb893 on macrophage–LEC transmigration. Accordingly, CMFDA labelled M1 macrophages were layered on transwell inserts with activated HDLEC monolayers that were pre-treated for 30 minutes and subsequently co-incubated with either mAb893, or $mIgG_1$, and transmigration was measured on a fluorescence plate reader (Fig 3-23b). Quantitative analysis of the assay revealed a significant reduction in the number of transmigrating macrophages across HDLEC monolayers treated with mAb893 compared to those treated with $mIgG_1$ at the early time points, with a reduction of approximately 75 % at one point. However, with time, the effect of the blockade appears to diminish with equal numbers of transmigrating cells in the two treatments by 6 hours.

The data above indicate that the events up to 2 hours after introduction of macrophages into the *in vitro* systems are where the actions of LYVE-1 are critical. Also, the identification of the rings of LYVE-1 surrounding macrophages suggest the LYVE-1 ring-like structures observed during the macrophage-LEC adhesion assays (see Fig 3-21) are important also in mediating transmigration, CMFDA labelled macrophages were incubated for 2 hours with activated HDLEC monolayers that had been treated with mAb893, or $mIgG_1$ on 8 chamber slides. After the incubation period, slides were stained with primary antibodies to LYVE-1 for imaging by confocal microscopy. As shown by the images in Fig 3-24, treatment with the LYVE-1 HA blocking mAb893 disrupted formation of the ring structures.

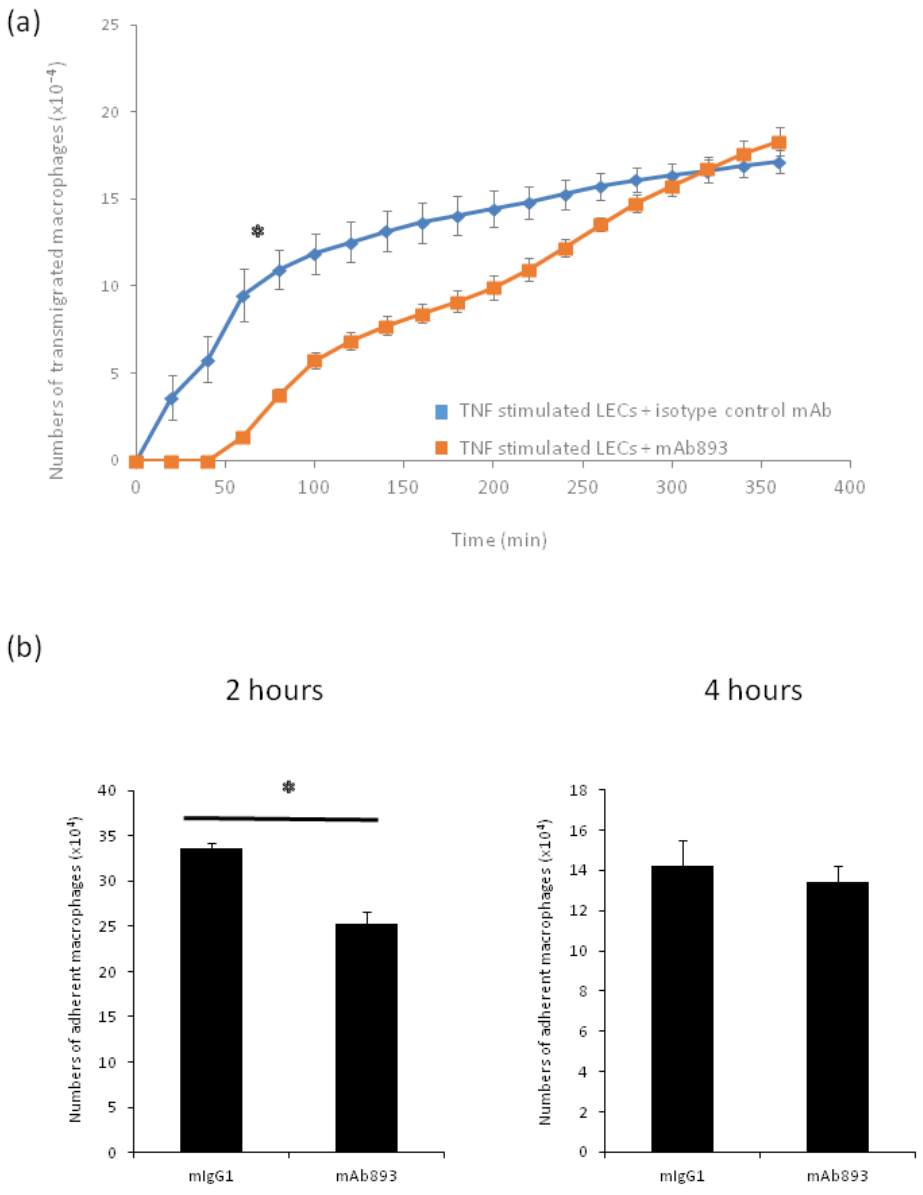


Figure 3-23: Effect of LYVE-1 antibody blockade on macrophage transmigration across stimulated primary HDLECs. Primary HDLEC monolayers plated on the lower surface of cell culture inserts or 24 well plates were stimulated with TNF-α for 0-24 h. Activated monolayers were subsequently incubated in media containing TNF-α and either 50 μg/ml isotype control IgG (blue), or mAb893, LYVE-1 function blocking antibodies (orange). CMFDA labelled M1 macrophages (5 x 10^5) were applied to treated HDLEC monolayers, as appropriate. (a) Numbers of transmigrating macrophages were measured using a fluorescent plate reader at 20 minute intervals for 7 hours while (b) numbers of adherent macrophages were measured at 2 and 4 hours. The graph shown is representative of 3 independent experiments. Data are the mean ± SD of quadruplicate technical replicates. A two-tailed, unpaired Student's t-test was performed on this figure and p values below 0.05 were considered statistically significant (*$p < 0.01$; mIgG1 vs mAb893). The appropriate statistical test to analyse this data would be a two way analysis of variance (ANOVA).

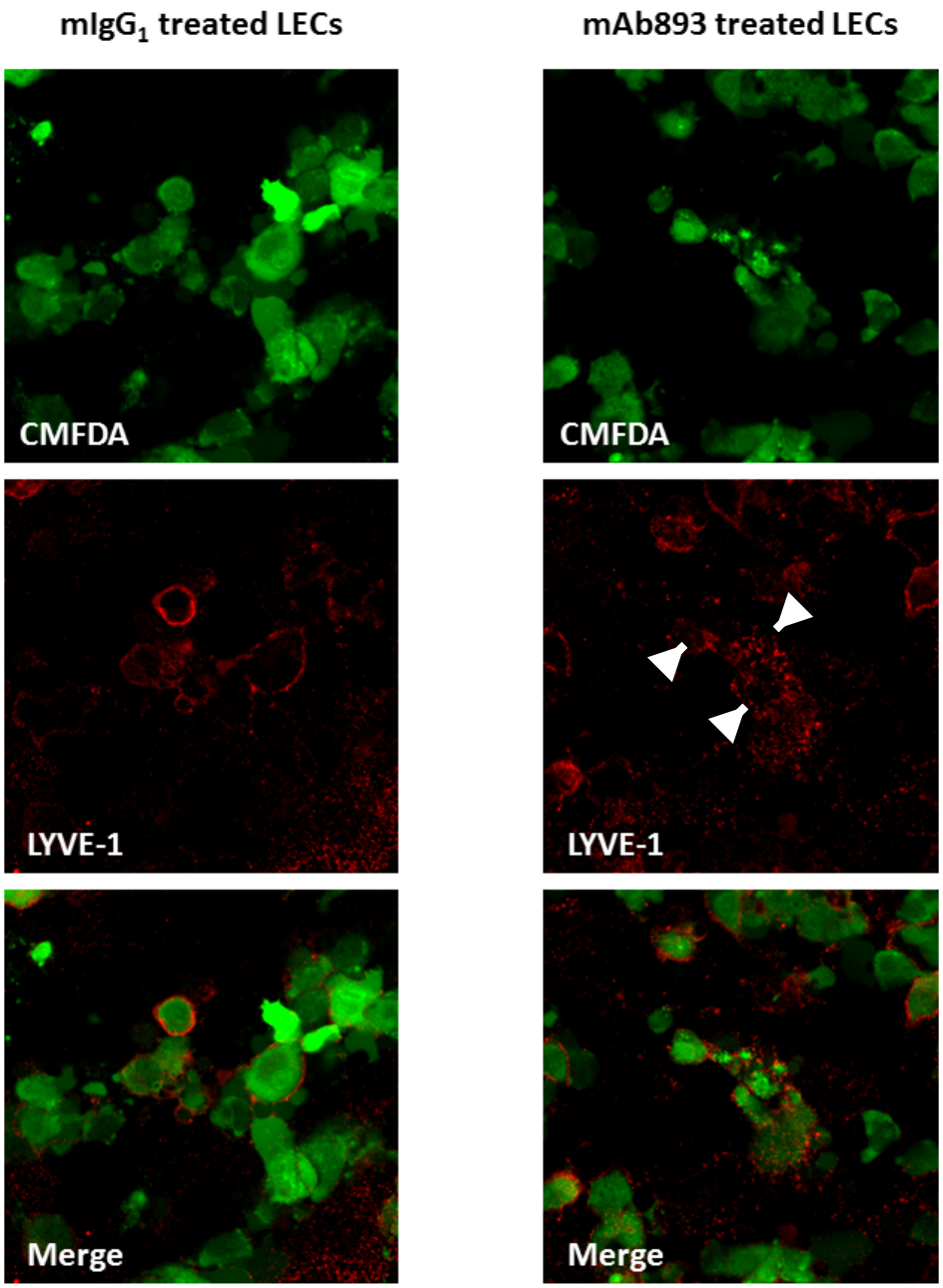


Figure 3-24: Effect of LYVE-1 antibody blockade on localisation of LYVE-1 and adherent macrophages on stimulated HDLECs. Primary HDLEC monolayers plated on 8 chamber slides were stimulated with TNF-α for 0-24 h. Activated monolayers were subsequently incubated in media containing TNF-α and either 50 μg/ml isotype control IgG (blue), or mAb893, LYVE-1 function blocking antibodies (orange). CMFDA labelled M1 macrophages (5 x 10^5) were incubated with treated HDLEC monolayers for 2 hours. Slides were subsequently washed to remove non-adherent cells and stained for LYVE-1 using polyclonal antibodies raised against LYVE-1. Afterwards, slides were imaged by confocal microscopy showing macrophages (green) and LYVE-1 (red). Disrupted LYVE-1 rings are shown by white arrow heads. The images shown are representative of experiments that were repeated 3 times.

Overall, the findings from these experiments suggest that a specific LYVE-1-HA mediated interaction can support macrophage transmigration across TNFα stimulated LECs, despite considerable activation-induced downmodulation of the receptor.

3.3.7 Effect of hyaluronan on macrophage transmigration across activated LECs

The preceding studies provide preliminary evidence for the involvement of a LYVE-1-HA axis in macrophage transmigration of lymphatic endothelium. However this is based almost exclusively on experiments with LYVE-1 HA blocking mAbs. To further substantiate these findings, I performed studies directly addressing the role of hyaluronan itself.

In the first instance, both CMFDA labelled M0 macrophages and TNF-α stimulated HDLEC monolayers were treated with hyaluronidase derived from *Streptomyces hyaluroticus*, to enzymatically cleave surface associated glycosaminoglycan, and the impact of HA depletion from both cell types assessed in transwell assays. To ensure maximal depletion, the two populations were not only pre-treated with hyaluronidase, but the enzyme was also present throughout the assay period. As before, transmigration was quantified by measuring fluorescence of the bottom chamber of the system. The results (Fig 3-25) revealed that hyaluronidase digestion reduced macrophage transmigration by more than 2-fold compared to control untreated cells.

Next, to identify whether HA on the surface of macrophages, lymphatic endothelial cells, or both contributed to transmigration, the transwell assays

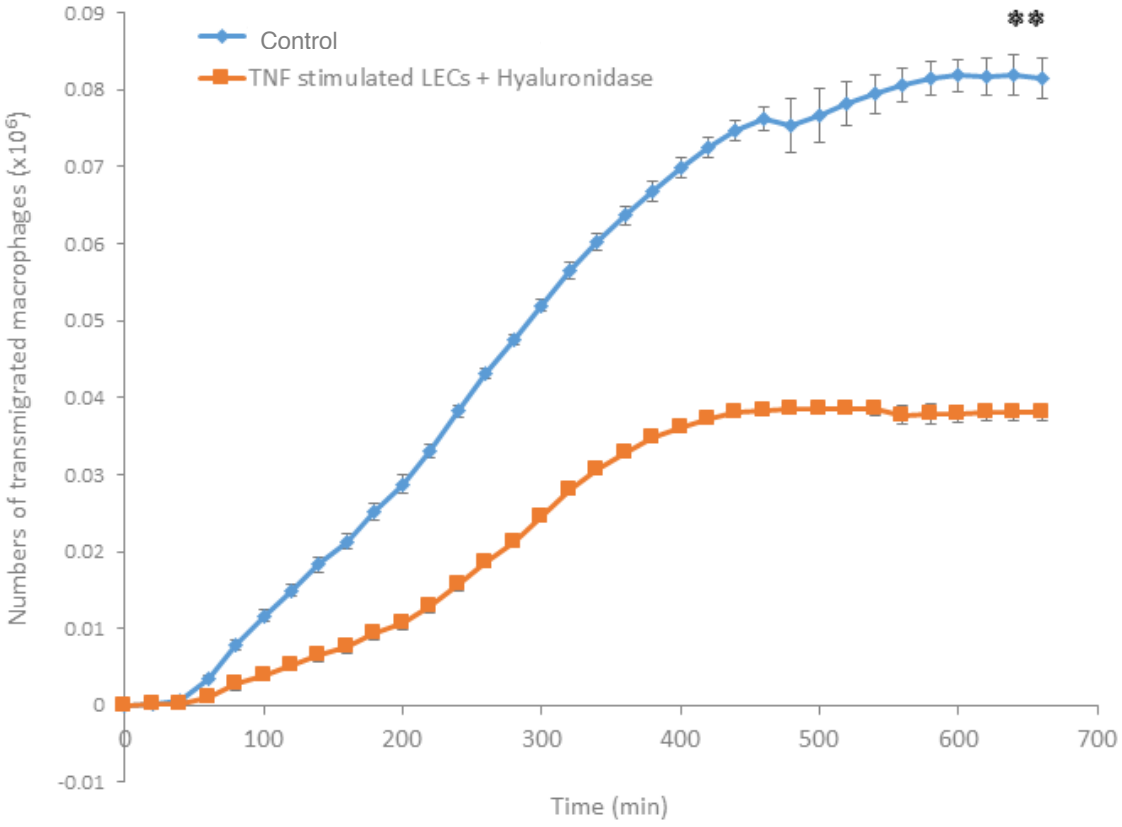


Figure 3-25: Effect of hyaluronidase treatment of both macrophages and LECs on macrophage transmigration across stimulated primary HDLECs. Primary HDLEC monolayers plated on the lower surface of cell culture inserts were stimulated with TNF-α for 0-24 h. Activated HDLECs were then incubated in media containing TNF-α and either 10 U/ml control BSA (blue), or hyaluronidase, hyaluronan specific digestion enzyme (orange). CMFDA labelled M0 macrophages (5 x 10^5) were prepared in media containing the same pre-incubation supplements and applied to treated HDLEC monolayers, as appropriate. Numbers of transmigrating macrophages were measured using a fluorescent plate reader at 20 minute intervals for > 10 hours. The graph shown is representative of 3 independent experiments. Data are the mean ± SD of quadruplicate technical replicates. A two-tailed, unpaired Student's t-test was performed on this figure and p values below 0.05 were considered statistically significant (** $p < 0.01$; Control vs Hyaluronidase at 600 mins). The appropriate statistical test to analyse this data would be a two way analysis of variance (ANOVA).

were performed once again, this time subjecting either the macrophages or the HDLEC monolayers individually to hyaluronidase treatment. Firstly, individual treatment of HDLECs with hyaluronidase had no significant impact on macrophage transmigration. In marked contrast, hyaluronidase digestion of M0 macrophages yielded the same > 2-fold reduction in transmigration compared to untreated controls as that observed when both cell populations were treated with the enzyme (Fig 3-26, see also with Fig 3-25). Moreover, a similar reduction in transmigration was seen when M1 macrophages were treated with hyaluronidase, (Fig 3-27) indicating that the HA glycocalyx of both resting and activated macrophages can contribute to transit across lymphatic endothelium.

Next, to ascertain whether macrophage derived hyaluronan mediated this transmigration via adhesion, CMFDA labelled macrophages treated with or without hyaluronidase were incubated with activated HDLEC monolayers for set time periods of 2 or 4 hours after which time the numbers of adherent macrophages were enumerated using a fluorescence plate reader. As shown in Fig 3-28, depletion of HA from the surface of macrophages reduced adhesion to the activated HDLEC monolayers to a significant extent (approximately 20 %).

Taken together, these results establish that macrophage surface hyaluronan plays an important role in transmigration across activated HDLECs, despite making only an apparently minor contribution to initial adhesion. Clearly, these experiments could not unambiguously identify LYVE-1 as the receptor supporting HA-mediated macrophage transmigration. However, the fact that both LYVE-1 HA blocking mAbs and hyaluronidase treatment independently yielded a similar reduction in transmigration, together with the fact that LYVE-1

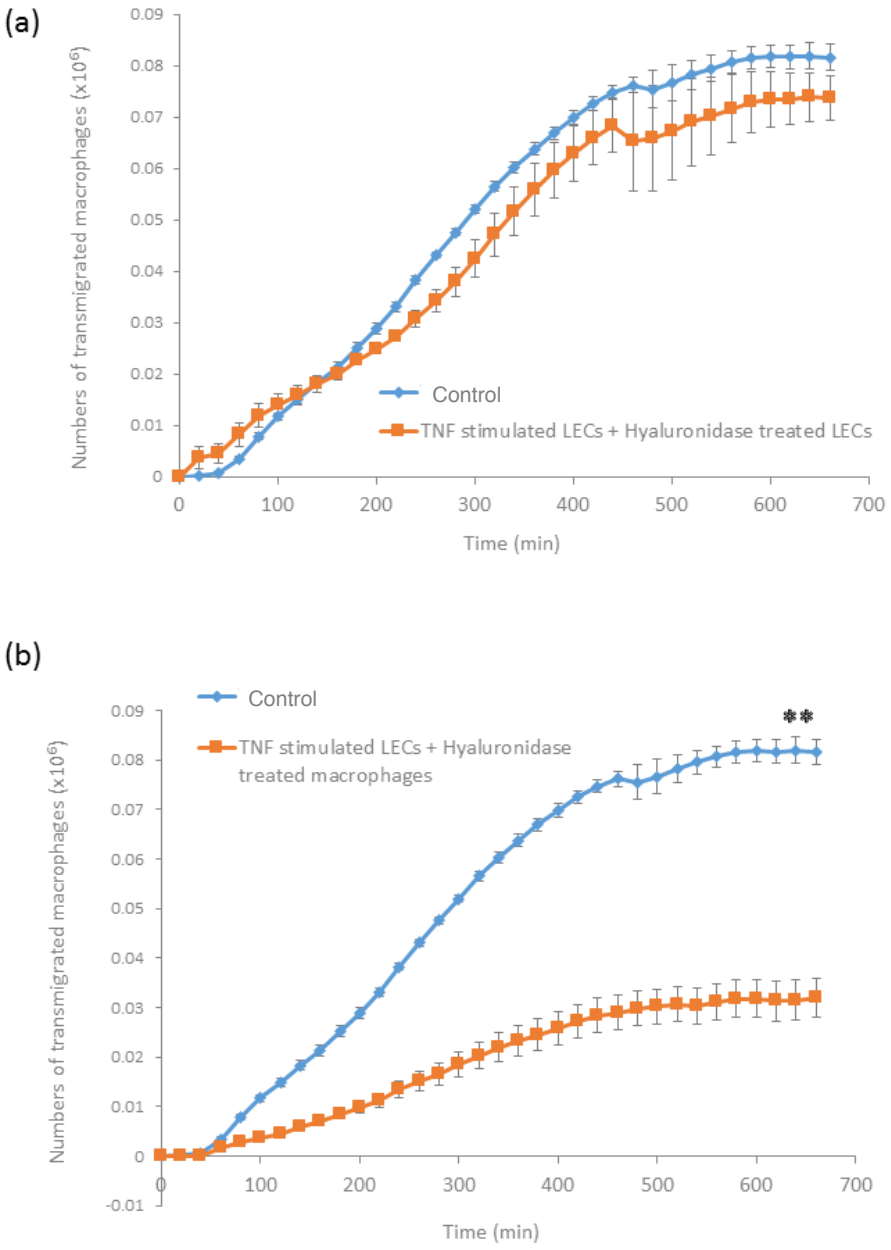


Figure 3-26: Effect of hyaluonidase treatment of macrophages or LECs on macrophage transmigration across stimulated primary HDLECs. Primary HDLEC monolayers plated on the lower surface of cell culture inserts were stimulated with TNF-α for 0-24 h. (a) Activated HDLECs were incubated in media containing TNF-α and either 10 U/ml bovine testicular ? hyaluronidase, (orange) or an equivalent concentration of BSA as a control (blue). CMFDA labelled M0 macrophages (5 x 10^5) were applied to treated HDLEC monolayers, as appropriate. (b) In parallel, CMFDA labelled macrophages (5x10^5) were incubated in media containing 10 U/ml control BSA (blue), or hyaluronidase, (orange) and applied to only TNF-α treated HDLECs. Numbers of transmigrating macrophages were measured using a fluorescent plate reader at 20 minute intervals for > 10 hours. The graph shown is representative of 3 independent experiments. Data are the mean ± SD of quadruplicate technical replicates. A two-tailed, unpaired Student's t-test was performed on this figure and p values below 0.05 were considered statistically significant (** $p < 0.01$; Control vs Hyaluronidase at 600 mins). The appropriate statistical test to analyse this data would be a two way analysis of variance (ANOVA).

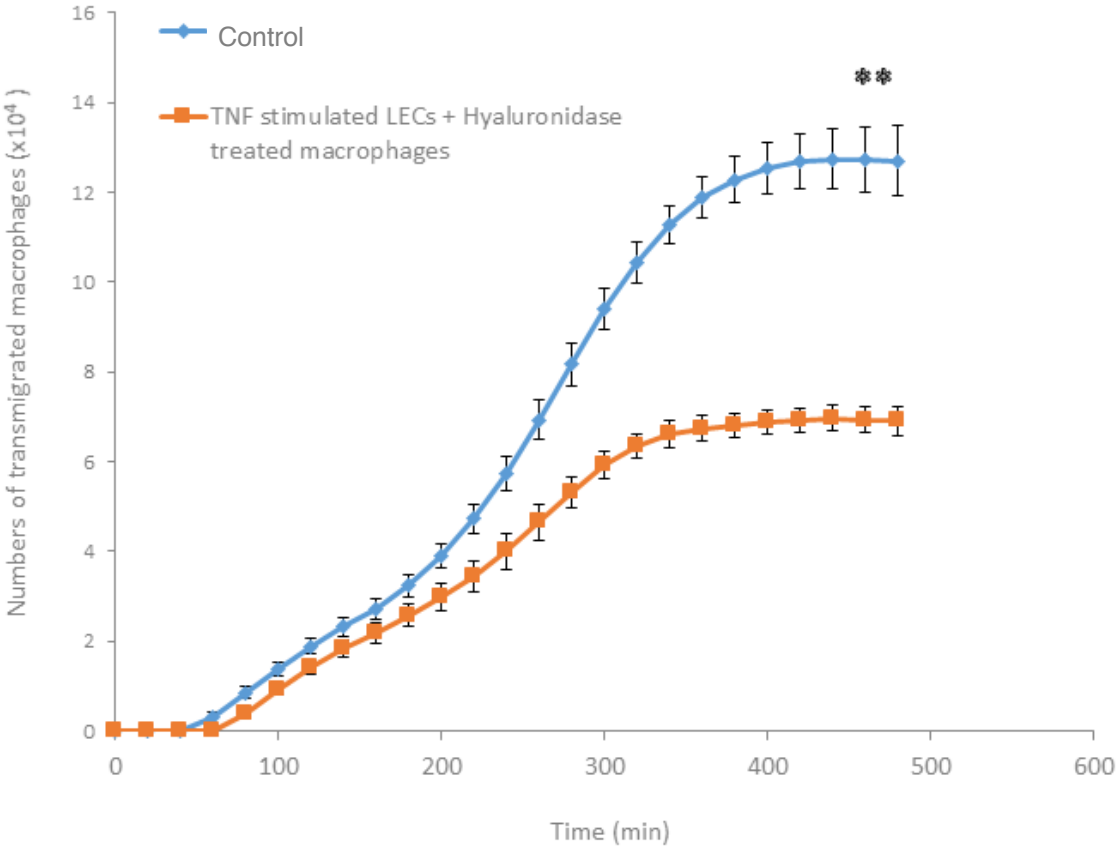


Figure 3-27: Effect of hyaluonidase treatment of macrophages on M1 macrophage transmigration across stimulated primary HDLECs. Primary HDLEC monolayers plated on the lower surface of cell culture inserts were stimulated with TNF-α for 0-24 h. CMFDA labelled M1 macrophages ($5x10^5$) were incubated in media containing 10 U/ml control BSA (blue), or hyaluronidase, (orange) and applied to only TNF-α treated HDLECs. Numbers of transmigrating macrophages were measured using a fluorescent plate reader at 20 minute intervals for > 10 hours. The graph shown is representative of 3 independent experiments. Data are the mean ± SD of quadruplicate technical replicates. A two-tailed, unpaired Student's t-test was performed on this figure and p values below 0.05 were considered statistically significant (** $p < 0.01$; Control vs Hyaluronidase at 480 mins). The appropriate statistical test to analyse this data would be a two way analysis of variance (ANOVA).

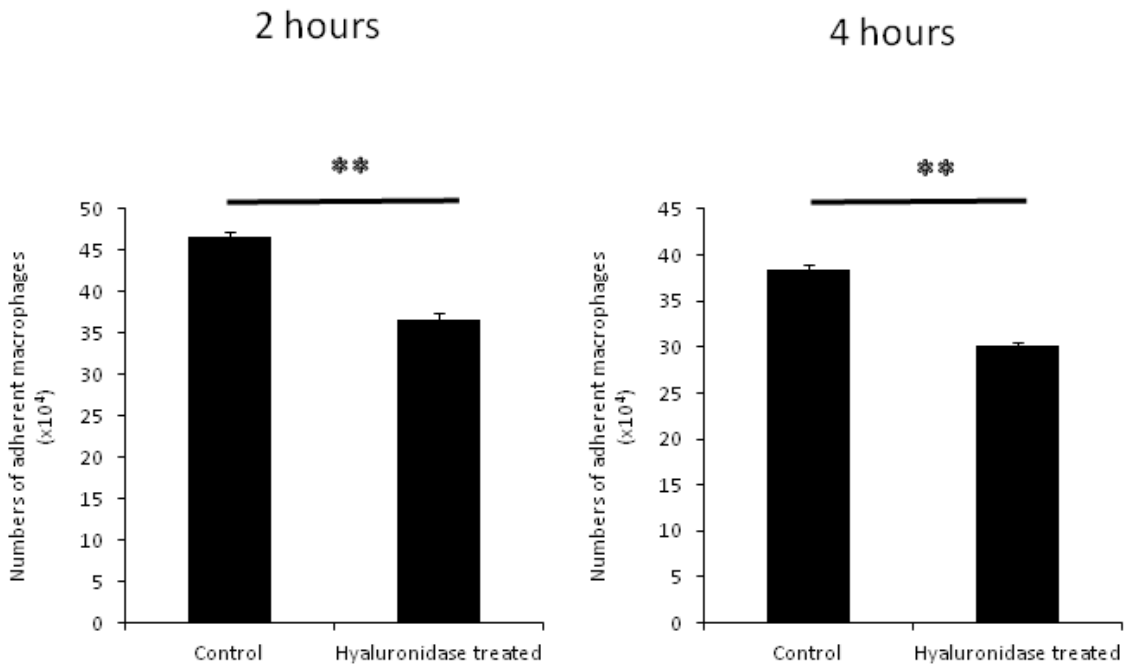


Figure 3-28: Effect of hyaluonidase treatment of macrophages on macrophage adhesion to stimulated primary HDLECs. Primary HDLEC monolayers plated on the lower surface of cell culture inserts were stimulated with TNF-α for 0-24 h. CMFDA labelled macrophages ($5x10^5$) were incubated in media containing 10 U/ml control BSA (blue), or hyaluronidase, (orange) and applied to TNF-α treated HDLECs. Numbers of adherent macrophages were measured using a fluorescent plate reader at 2 and 4 hours. The graph shown is representative of 3 independent experiments. Data are the mean ± SD of quadruplicate technical replicates. A two-tailed, unpaired Student's t-test was performed on this figure and p values below 0.05 were considered statistically significant (** $p < 0.01$; Control vs Hyaluronidase at 2 and 4 hours). The appropriate statistical test to analyse this data would be a two way analysis of variance (ANOVA).

is the only known receptor for HA on these cells strongly implies that this was the case.

3.3.8 Effect of potentiating HA binding to LYVE-1 on macrophage transmigration

To establish the involvement of LYVE-1 in supporting HA-mediated macrophage transmigration more directly, I explored the consequences on transmigration of manipulating its HA-binding capacity through antibody crosslinking. As outlined in the General Introduction to this thesis, the results of recent work in the Jackson laboratory has established that LYVE-1 is a low affinity HA receptor (Kd 125μM) and likely requires prior clustering of the receptor on the cell surface to enable stable multivalent interactions with the glycosaminoglycan. One convenient way in which this can be achieved *in vitro* is by crosslinking with bivalent non HA-blocking LYVE-1 monoclonal antibodies such as mAbs 6A, 7C, or 8C that were previously generated against human LYVE-1 Fc in-house (Remko Prevo, 2002, D.Phil. thesis University of Oxford; Banerji et al. 2010). These have been shown to recognize an epitope within the Link domain remote from the HA-binding surface and potentiate binding of high molecular weight HA by almost two orders of magnitude (Lawrance et al., manuscript submitted). These unpublished findings from the group have indicated that these mAbs are also able to induce both surface clustering of LYVE-1 as well as HA binding, this dependant on antibody bivalency.

Accordingly, CMFDA labelled macrophages were incubated with confluent unstimulated HDLEC monolayers that were treated with 8C, or the respective

isotype control for 2 and 4 hours. To ensure maximal clustering of LYVE-1, the antibody presence was maintained throughout the assay time period even after pre-treatment of LECs. Fluorescence measurement of the plates at the time points (Fig 3-29) reveals an approximately 20% increase in adherent macrophages to HDLECs treated with 8C, compared to those treated with isotype control.

To assess the consequences of mAb induced LYVE-1 crosslinking on *in vitro* transmigration, CMFDA labelled macrophages were layered over transwell inserts with unstimulated HDLEC monolayers that were treated with mAb 8C, or its respective isotype control, and transit measured by fluorescence. As shown in Figure 3-30, ligation of LYVE-1 with mAb 8C significantly increased the numbers of transmigrating macrophages compared to isotype controls, consistent with a capacity for LYVE-1 to support adhesion/transmigration through binding macrophage derived surface hyaluronan when appropriately clustered.

As a final control to substantiate this conclusion, I performed the 8C antibody pretreatment of HDLEC in the presence of exogenous high molecular-weight hyaluronan (HMW-HA), reasoning that this would pre-saturate LYVE-1 with the glycosaminoglycan, preventing engagement with HA presented from the macrophage cell surface and subsequent HA-mediated transmigration. As expected (Fig 3-31a), such treatment, despite potentiating the binding of HA to LYVE-1, prevented to increase the level of macrophage transmigration as seen with 8C alone. In addition, pre-saturation with HA also resulted in a modest reduction in macrophage adhesion (Fig 3-31b).

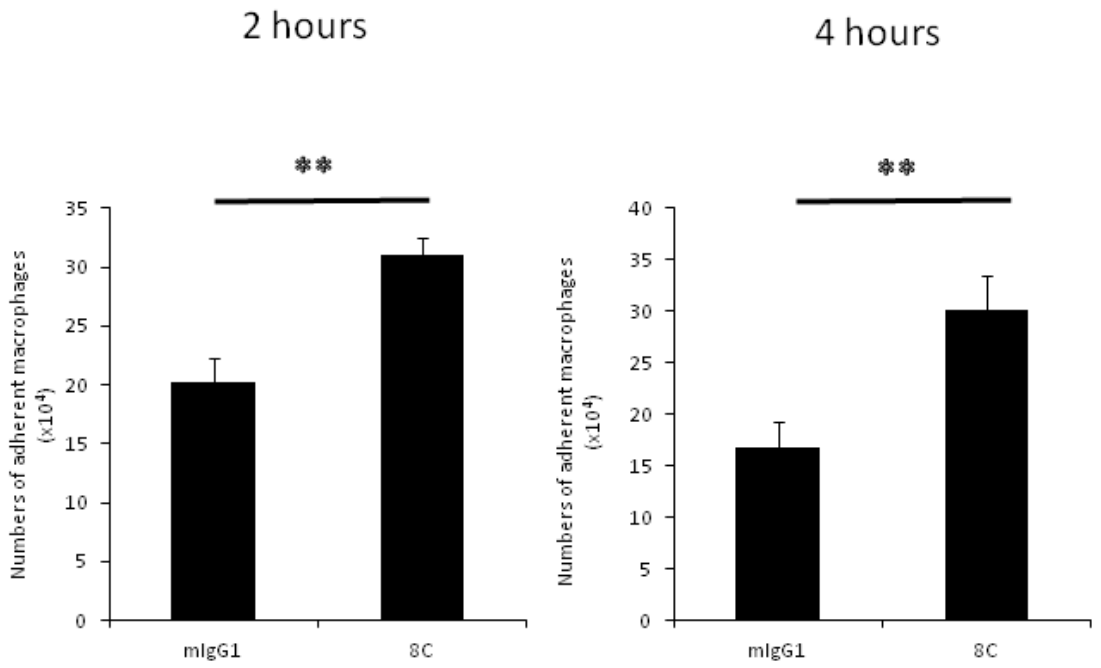


Figure 3-29: Effect of LYVE-1 receptor clustering by antibody 8C on macrophage adhesion to unstimulated primary HDLECs. Primary HDLEC monolayers plated on the lower surface of cell culture inserts were incubated in media containing either 20 μg/ml isotype control IgG (blue), or 8C, a LYVE-1 clustering antibody (orange). CMFDA labelled M0 macrophages (5 x 10^5) were applied to treated HDLEC monolayers, as appropriate. Numbers of adherent macrophages were measured after washing wells to remove non-adherent cells using a fluorescent plate reader at 2 and 4 hours. The graph shown is representative of 3 independent experiments. Data are the mean ± SD of quadruplicate technical replicates. A two-tailed, unpaired Student's t-test was performed on this figure and p values below 0.05 were considered statistically significant (** $p < 0.01$; mIgG1 vs 8C at 2 and 4 hours). The appropriate statistical test to analyse this data would be a two way analysis of variance (ANOVA).

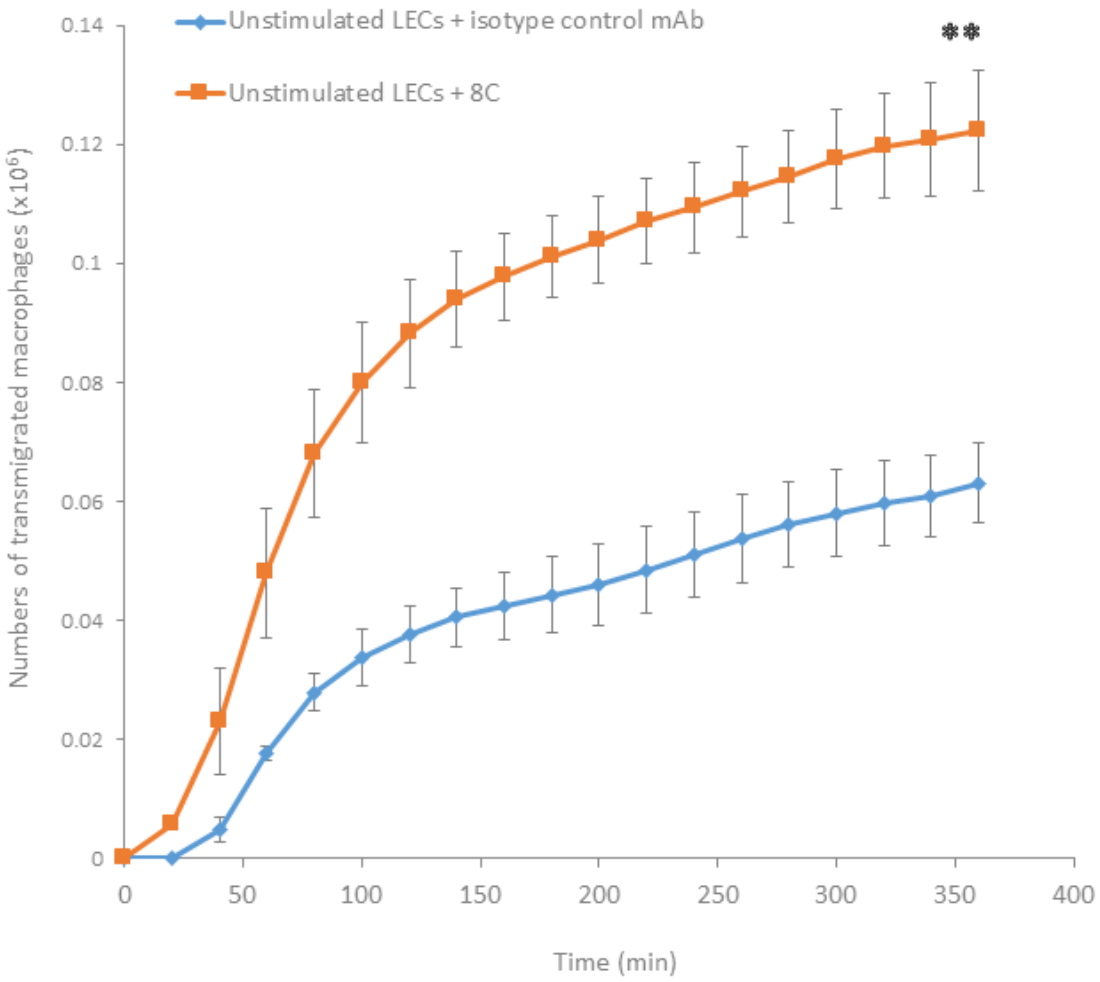


Figure 3-30: Effect of LYVE-1 receptor clustering by antibody 8C on macrophage transmigration across unstimulated primary HDLECs. Primary HDLEC monolayers plated on the lower surface of cell culture inserts were incubated in media containing either 20 μg/ml isotype control IgG (blue), or 8C, a LYVE-1 clustering antibody (orange). CMFDA labelled M0 macrophages (5 x 10^5) were applied to treated HDLEC monolayers, as appropriate. Numbers of transmigrating macrophages were measured using a fluorescent plate reader at 20 minute intervals for >10 hours. The graph shown is representative of 3 independent experiments. Data are the mean ± SD of quadruplicate technical replicates. A two-tailed, unpaired Student's t-test was performed on this figure and p values below 0.05 were considered statistically significant (* $p < 0.05$; isotype control IgG vs 8C at 360 minutes). The appropriate statistical test to analyse this data would be a two way analysis of variance (ANOVA).

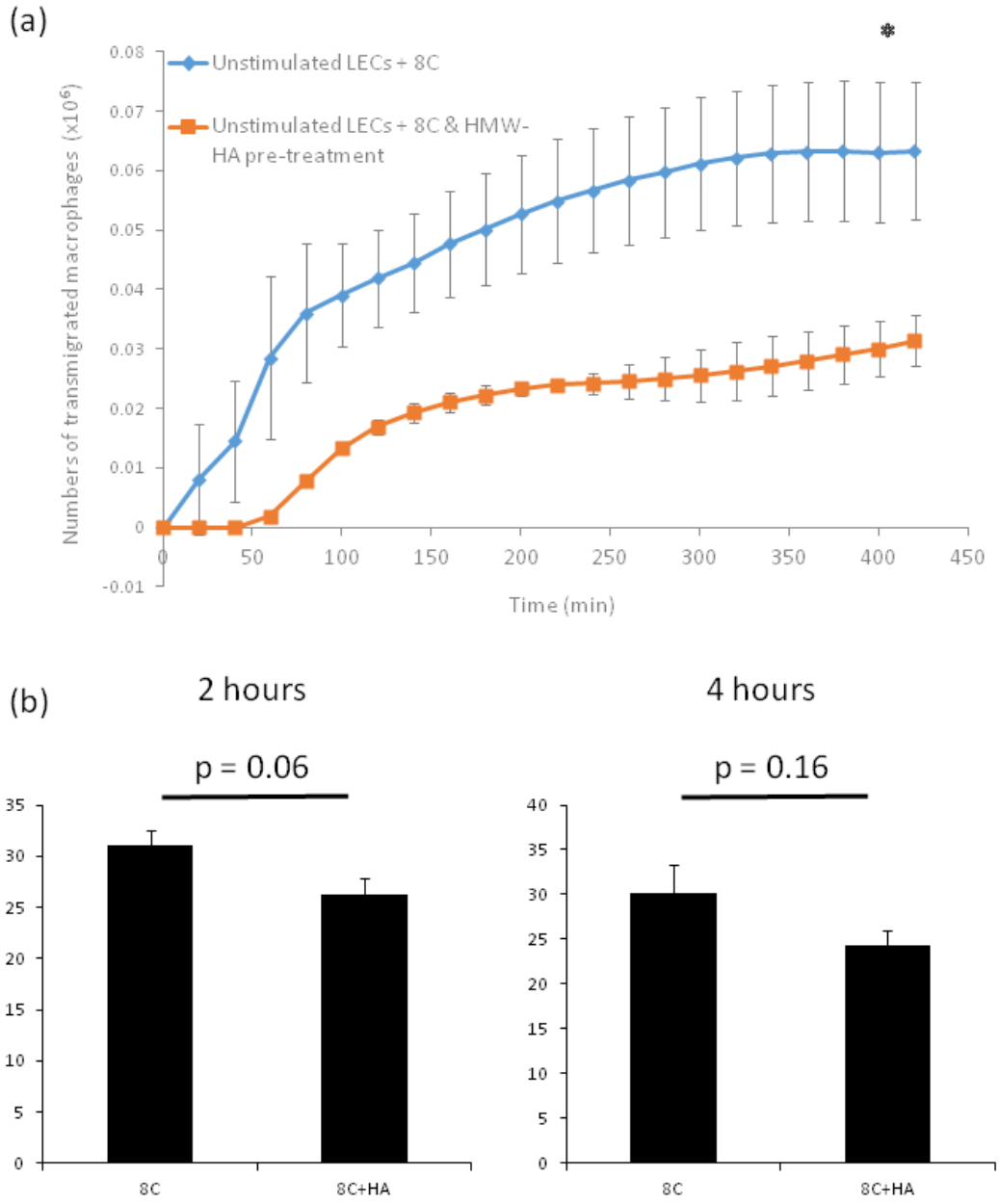


Figure 3-31: Effect of promoting pre-saturation of LYVE-1 with HMW-HA by means of incubation with mAb 8C on macrophage transmigration across and adhesion to unstimulated primary HDLECs. Primary HDLEC monolayers plated on the lower surface of cell culture inserts and wells of 24 well plates were incubated in media containing either 20 μg/ml of 8C (blue), or 8C and HMW-HA (orange). CMFDA labelled M0 macrophages (5 x 10^5) were applied to treated HDLEC monolayers, as appropriate. (a) Numbers of transmigrating macrophages were measured using a fluorescent plate reader at 20 minute intervals for >10 hours. (b) Numbers of adherent macrophages were measured with the plate reader at 2 and 4 hours. The graph shown is representative of 3 independent experiments. Data are the mean ± SD of quadruplicate technical replicates. A two-tailed, unpaired Student's t-test was performed on this figure and p values below 0.05 were considered statistically significant (* $p < 0.05$; 8C vs 8C & HMW-HA pre-treatment at 400 minutes). The appropriate statistical test to analyse this data would be a two way analysis of variance (ANOVA).

These results illustrate that LYVE-1 in native lymphatic endothelium can in principle act as a receptor for HA presented by macrophages is appropriately clustered, a circumstance that may well be encountered during exit across lymphatic vessel endothelium *in vivo*, a circumstance that is further explored in the next chapter.

3.4 Discussion

This results chapter has made the novel observation that macrophages both adhere to and transmigrate lymphatic endothelium on the basis of newly established static *in vitro* assays using primary human lymphatic endothelial monolayers. Additionally, the mechanisms involved were partially uncovered with a combination of specific HA-adhesion blocking studies with monoclonal antibodies and purified hyaluronidase to determine the roles and involvement of individual adhesion molecules.

One of the key findings of was that macrophages can adhere and transmigrate HDLECs under normal resting conditions and that both processes are enhanced after stimulation of the endothelium with TNF-α. This illustrates a distinct similarity with dendritic cells and neutrophils, two major leukocyte populations whose adhesion and transmigration are greatly increased by LEC activation. Such increases are due to morphological changes endothelium undergoes upon activation which result in inter-cell junctional relaxation, as well as changes in expression of molecules which engage with the transmigrating cells (Johnson, Clasper et al. 2006, Rigby, Ferguson et al. 2015).

Adhesion is a fundamental step that precedes transmigration across endothelium. The increase in adhesion of macrophages on TNF-α activated LECs compared to unstimulated endothelium implied that the process was an active one. Stimulation of lymphatic vessel endothelium, in common with that of blood vessel endothelium is known to alter the expression of a wide variety of molecules associated with leucocyte recruitment and endothelial junctional permeability (Deanfield, Halcox et al. 2007, Johnson and Jackson 2014). Such

molecules include cell adhesion molecules (e.g - E-selectin) (Rigby DA, 2010, D.Phil. Thesis), chemokines (e.g - CCL21) (Johnson and Jackson 2010) and enzymes (e.g - cathepsin S) (Helske, Syvaranta et al. 2006), with these group of proteins involved in transmigration of other leukocytes across endothelium.

The inflammation induced leucocyte adhesion molecules ICAM-1 and VCAM-1 have been shown to be involved in the transmigration of DCs and neutrophils across lymphatic endothelium both *in vitro* and *in vivo*. Surprisingly, however as indicated in this chapter ICAM-1 and VCAM-1 were found to be redundant for adhesion and transmigration of macrophages. This was somewhat unexpected, since it is well documented that monocytes, the progenitor cells to macrophages, employ ICAM-1 and VCAM-1 for exit across inflamed blood endothelium. Closer assessment of the literature however, yields possible explanations for these findings. For example, in a model of Wallerian degeneration of peripheral nerves, functional blockade of up-regulated ICAM-1 on blood endothelium failed to reduce recruitment of monocytes/macrophages to the site of injury, a finding also demonstrated with *ICAM-1*$^{-/-}$ mice (Avellino, Dailey et al. 2004). Furthermore, in the case of neutrophil trafficking via lymph, the migration of adoptively transferred cells from skin to draining lymph nodes was reported to be unaffected by ICAM-1 mAb blockade in mice, despite clear evidence for involvement of its β2 integrin counter-receptor on neutrophils (Hampton, Bailey et al. 2015). Despite a lack of contribution of these two CAMs, the involvement of adhesion molecules was highlighted by my demonstration that blockade of β2 integrin/CD18 with antibodies partially reduced macrophage transmigration, a similar result to that demonstrated with DCs and neutrophils. It is possible that in both macrophages and neutrophils alternative β2 integrin ligands (the complementary receptor) mediate interactions with lymphatic

endothelium. Among such candidates are the junctional adhesion molecules (JAMs), a protein family which includes JAM-1 (also known as JAM-A), JAM-2 and JAM-3, members of which have been reported to be expressed within the endothelial junctions of lymphatic capillaries, with the integrin ligands for the following JAMs reported to be expressed on the surface of macrophages - αLβ2, αmβ2 and α4β1 (Ammon, Meyer et al. 2000, Weber, Fraemohs et al. 2007). Indeed, mice with targeted deletion of the *JAM-1* gene have functional abnormalities in the trafficking of dendritic cells to lymph nodes (Cera, Del Prete et al. 2004). However, it is worth noting that the reduction in macrophage transmigration due to blockade of β2 integrin was not as great as the effect of blockade seen with the other leukocytes. This suggests that there are other adhesion molecule based receptors on the surface of macrophages apart from β2 integrin to yet be identified with an involvement in transmigration across inflamed LECs. Despite both cells having the same integrins, they do not necessarily function similarly as shown by the difference in CD11b function in DCs and macrophages in endocytosing LPS after ligation of LPS to TLR4 (Ling, Bennett et al. 2014).

ALCAM was another adhesion molecule investigated that had been reported to be involved in DC trafficking to draining lymph nodes. The major receptor for ALCAM is CD6, a member of the scavenger receptor family and although CD6 expression has not been reported on macrophages, I considered the possibility that other scavenger receptors such as CD36 might bind ALCAM (Huh, Pearce et al. 1996, Cayrol, Wosik et al. 2008). Indeed, macrophages migrating via lymph to mediastinal nodes draining the peritoneum express CD36 (Gautier et al. 2013) in the studies reported in the present chapter macrophage. Nevertheless, one caveat is that the blocking antibody (mAb656) used in the

present studies has been shown to disrupt ALCAM homophilic and ALCAM:CD6 heterophilic interactions, and it is not known whether it can also block interactions with CD36 or other putative ligands. Clearly, further experiments using soluble ALCAM as a competitor would be needed before one can rule out the involvement of ALCAM in macrophage adhesion/transmigration.

Besides the role of integrins, the findings of this chapter provide persuasive evidence of a role for the glycosaminoglycan, hyaluronan, and its cognate receptor on lymphatic endothelium, LYVE-1 in macrophage adhesion and transmigration.

Hyaluronan is a fundamental component of the extracellular matrix, whose numerous functions are dependent on the size of the polymer along with the proteins to which it binds. The results of my experiments indicate that presentation of endogenous hyaluronan on the surface of macrophages is a critical requirement to the transmigration of macrophages across TNF-α stimulated LECs. Such a requirement of a glycosaminoglycan for transmigration across lymphatic vasculature has previously not been reported. It is well established that hyaluronan interactions with its cognate leucocyte receptor, CD44, are responsible for lymphocyte recruitment from the capillary blood circulation into sites of chronic inflammation, most likely by supporting rolling interactions within the vessel lumen during the initial stages of extravasation . Examples include the binding of T-cells to hyaluronan on the endothelium surface (DeGrendele, Estess et al. 1997), and neutrophils to hyaluronan on the surface of inflamed liver sinusoids (McDonald, McAvoy et al. 2008). Importantly, the results obtained in this chapter illustrate the converse may apply in the

lymphatics, where engagement of hyaluronan on the leucocyte surface by LYVE-1 on the endothelium appeared to mediate migration across activated HDLEC monolayers.

My initial investigations focused on resting unstimulated LECs where the receptor is expressed at high levels on the cell surface. Here, my findings with LYVE-1 blocking mAbs yielded unexpected and contrasting results. Intriguingly, mAb 3A was found to promote both adhesion and transmigration whereas mAbs 891 and 893 had no significant effect on either of these parameters. Further exploration revealed that the apparent increase in macrophage transmigration observed with mAb 3A was due to an accumulation of the cells on the lower (luminal) surface of the HDLEC monolayer where the antibody had impaired their final detachment. As the transmigration assay measures the recovery of all fluorescent cells present in the lower chamber of the transwell (i.e. beneath the UV opaque transwell filter), it does not discriminate between cells that have transmigrated fully and those that may be trapped within the LEC monolayer. Currently, an in-depth explanation for why mAb 3A should differ from mAbs 891 and 893 in this respect is not readily apparent, however, it is worth noting that the epitope for 3A appears to lie to one side of the epitopes for these other antibodies, based on site-directed mutagenesis studies carried out by William Lawrance, a former D.Phil. student in the Jackson laboratory. Curiously, mAb 3A is also a weaker blocker of LYVE-1 HA binding than mAbs 891 and 893 and hence it is possible that this antibody affects the interaction between LYVE-1 and some other additional ligand required for macrophage transmigration. One might even speculate that the epitope for mAb 3A partially overlaps with the putative binding site for PDGFR, a tyrosine kinase linked growth factor receptor

reported to interact with LYVE-1 in LECs, or that mAb 3A affects interaction with growth factors such as FGF-2 and PDGF-BB that have been reported to bind LYVE-1 via N-linked glycan chains (Hou, Liu et al. 2011, Platonova, Miquel et al. 2013). Clearly, further experiments will be needed in the future to investigate these possibilities.

Despite these anomalous findings with regard to blockade of HA binding, the results obtained in my experiments using LYVE-1 mAbs that enhanced HA binding were more clear. As discussed at the beginning of the chapter, LYVE-1 monomers have a low affinity to bind to high molecular weigh HA (Kd 125 mM) as determined by BiaCore analysis (Banerji et al. 2015, manuscript submitted) and hence requires engagement with multiple LYVE-1 molecules along the polymer chain for stability. As demonstrated by William Lawrance (Lawrance W, D.Phil. thesis 2013, University of Oxford), one way that this may be achieved *in vitro* is through artificial cross-linking of the receptor with bivalent (non-HA blocking) LYVE-1 mAbs that induce its clustering at the LEC surface. In my experiments, inclusion of either one of the non-HA blocking antibodies (clone 8C) led to a 20 % increase in macrophage binding and a 2-fold increase in transmigration over resting unstimulated LEC monolayers. These findings indicate that native LYVE-1 when appropriately cross-linked on lymphatic endothelium can engage with hyaluronan on the macrophage surface to promote adhesion and subsequent transit. The fact that such cross-linking is necessary for HA mediated binding in resting lymphatic endothelium, suggests that under conditions of normal homeostasis LYVE-1 does not spontaneously form such clusters – a notion that is borne out by confocal microscopy of resting LECs, which reveals a relatively homogeneous LYVE-1 distribution.

The final experiments in this chapter addressed the role of the LYVE-1-HA axis in macrophage adhesion and transmigration over activated lymphatic endothelium. A factor that had to be taken into consideration in these studies was that LYVE-1 undergoes considerable downregulation in LEC over a period of 6-12 hours in response to inflammatory cytokines such as TNF-α and IL-1, a process that was further confirmed in my own experiments (see Fig 3-20). Yet the images taken of macrophages adhering to TNF-α treated LECs that had undergone partial LYVE-1 downregulation revealed that the remaining LYVE-1 molecules appeared to support macrophage adhesion and could be seen to form ring like structures around the macrophage cell bodies. Analogous structures in endothelial cells associated with leukocyte adhesion and transmigration have been reported, ICAM-1 being the most prominent within so called transmigratory cups identified in vascular endothelium (HUVECs) during *in vitro* adhesion/transmigration experiments with T cells (Carman and Springer 2004). Recent unpublished findings by Dr Louise Johnson from the Jackson laboratory have uncovered similar LYVE-1 containing transmigratory cups in lymphatic endothelium associated with the adhesion and transmigration of DCs. Preliminary confocal images of the LYVE-1 positive ring structures in my studies here resemble flattened rather than cup-like structures (data not shown). However, this may be a consequence of timing with the macrophages attaining endothelial LYVE-1 on their surface, after plausibly cleaving the receptor off the surface of LECs within that incubation period thus preventing observation of a cup structure; the ability of the myeloid cell to attain LYVE-1 from endothelium is discussed below. It will be appropriate to observe the kinetics of the formation of these LYVE-1 structures around macrophages at earlier time points. Imaging over the full time-course will have to be undertaken before firmer conclusions

can be made about these structures. The experiments with macrophages expressing LYVE-1 after 2 hours of adhesion will also require further controls, most notably, combining macrophages and LECs without allowing the leukocytes to adhere on to the endothelium for analysis by flow cytometry.

The demonstration that the LYVE-1 HA blocking mAb 893 could impair macrophage transmigration over activated LECs further attested to the specificity of the interaction. Interestingly, the blocking effects of the antibody were apparent over the first 2 hours of the assay, after which there was a gradual recovery in numbers of transmigrating cells. This suggests that LYVE-1 expression on the surface may be dynamically reduced during the assay and the antibody is therefore no longer effective after the initial blockade. It is feasible that while interacting with macrophages, LYVE-1 undergoes further internalisation leading to their basolateral to luminal translocation. Further investigations into the blockade revealed the rings to be a crucial structure to transmigration as mAb893 treatment dispersed the arrangement of the receptor.

A surprising finding in these studies was that neither LYVE-1 nor HA appeared to play a major role in adhesion of the macrophages to activated HDLECs, despite their significant involvement in transmigration. Both hyaluronidase treatment of macrophages and mAb893 blockade of LECs caused only a small decrease in adherent leukocytes on endothelium. One likely explanation for this phenomenon is that many additional adhesion molecules such as integrins also contribute to macrophage adhesion, and their contributions may be quantitatively greater than that of LYVE-1 and HA. Speculatively, this could also be due to the character of charge based HA binding in LYVE-1. Such an interaction makes it susceptible to environment based changes in pH and an

increase in acidity found at inflammatory loci would make LYVE-1-HA binding weak and not suitable for firm adhesion based purposes (Punnia-Moorthy 1987, Jackson 2009). Some similarities have been reported for neutrophil extravasation from blood vasculature a process that is dependent on CD44-HA interactions. Khan et al. (2004) reported that although CD44-HA mediated binding of neutrophils to vascular endothelium was critical to extravasation in vivo, blockade of the interaction did not significantly alter adhesion. The similarity of LYVE-1-HA connections with selectins is also discernible where binding with sialyl LewisX antigen is weak with regular bond formation and breaking thus being suitable for slowing leukocytes under blood flow (Torgersen, Mullin et al. 1998, Bouyain, Rushton et al. 2001). However, since lymph flow is slower than blood flow, it begs to ask the question of why does LYVE-1-HA binding result in such weak adhesion interactions. It may hypothetically be involved in guiding the leucocytes to permissive sites of entry.

With adhesion not being the major process towards promoting transmigration, other possibilities arose of how macrophage HA binding to lymphatic LYVE-1 promoted transmigration. One possibility is by playing a role in changing junctional integrity of the LECs. Unpublished work from the Jackson group attests to this theory. Exogenously added low-molecular weight hyaluronan at a range of concentrations appears to promote junctional relaxation and changing the morphology of LECs from round to elongate, similar to the ones observed by addition of TNF-α to LECs. Hyaluronan binding to its receptors such as CD44 or RHAMM have been shown to promote downstream signalling effects (Matou-Nasri, Gaffney et al. 2009). High-molecular weight HA (HMW-HA) induces smooth cell migration through the actions downstream of the interaction in the form of PI3K and Rac (Goueffic, Guilluy et al. 2006). One such other

downstream target is moesin, which is known to play a role in altering the shape of cells. It is possible that inducing such changes to cell morphology may help make the lymphatics more permissive for not only leukocytes but for increased lymph during inflammation.

Currently, there is limited understanding of signalling pathways downstream of LYVE-1. Work in the Jackson laboratory has begun to uncover aspects of signalling downstream of LYVE-1 after ligation to hyaluronan. A prominent mechanism appears to be by phosphorylation of VE-cadherin (present on the borders of junctions of LECs). This in turn prevents them from binding to adjacent VE-cadherin on the borders of neighbouring cells, thus, relaxing the tight junctions, a similar mechanism seen by VEGF downstream signalling in HUVECs (Esser, Lampugnani et al. 1998). It is likely that signalling pathways will be dependent on the functions usually attributed by the ligand. Through it's interaction with FGF-2, LYVE-1 is able to inhibit phosphorylation of ERK thus allowing it to promote endothelial cell migration and proliferation (Platonova, Miquel et al. 2013).

Overall, the data in this chapter establish a significant role for LYVE-1-HA interactions as well as β2 integrins in facilitating transmigration of macrophages across inflamed lymphatic endothelium *in vitro*. The following chapter will address the importance of these findings in the context of *in vivo* studies using a mouse model of inflammation.

Chapter 4.

The role of LYVE-1 in trafficking of macrophages to draining lymph nodes

4.1 Introduction

The capacity of macrophages to enter lymphatics and traffic to draining lymph nodes is not widely accepted, even though the phenomenon was reported nearly two decades ago, and has since been validated by several laboratories (Bellingan, Caldwell et al. 1996, Gautier, Ivanov et al. 2013). This interesting and potentially important process will therefore be outlined in the following Introduction to the present chapter. The previous chapter explored the premise that macrophages interact with and transmigrate human dermal lymphatic endothelial cells (HDLECs) *in vitro* and uncovered different molecules and mechanisms contributing to the process. The current chapter addresses whether some of these molecules, in particular LYVE-1 and its ligand hyaluronan, are utilised for trafficking *in vivo*.

One of the best established animal models for studying macrophage exit from inflamed tissue and migration to lymph nodes is that of thioglycollate stimulated sterile peritonitis, first described by Bellingan et al. (1996). To date, there have been limited studies exploring macrophages arriving at lymph nodes using models of active infection but Cao et al. (2005) demonstrated enhanced trafficking of macrophages to lymph nodes in thioglycollate induced peritoneum upon further stimulation with bacterial lipopolysaccharide (LPS). In this present Chapter, I employed sterile peritonitis models to track the lymph borne migration of adoptively transferred macrophages that had been labeled with the fluorescent dyes such as, PKH26PCL and CMFDA (5-chloromethylfluorescein diacetate). A scheme of this is shown in figure 4-1. A complicating factor in performing experiments using peritonitis models is that the migrating population

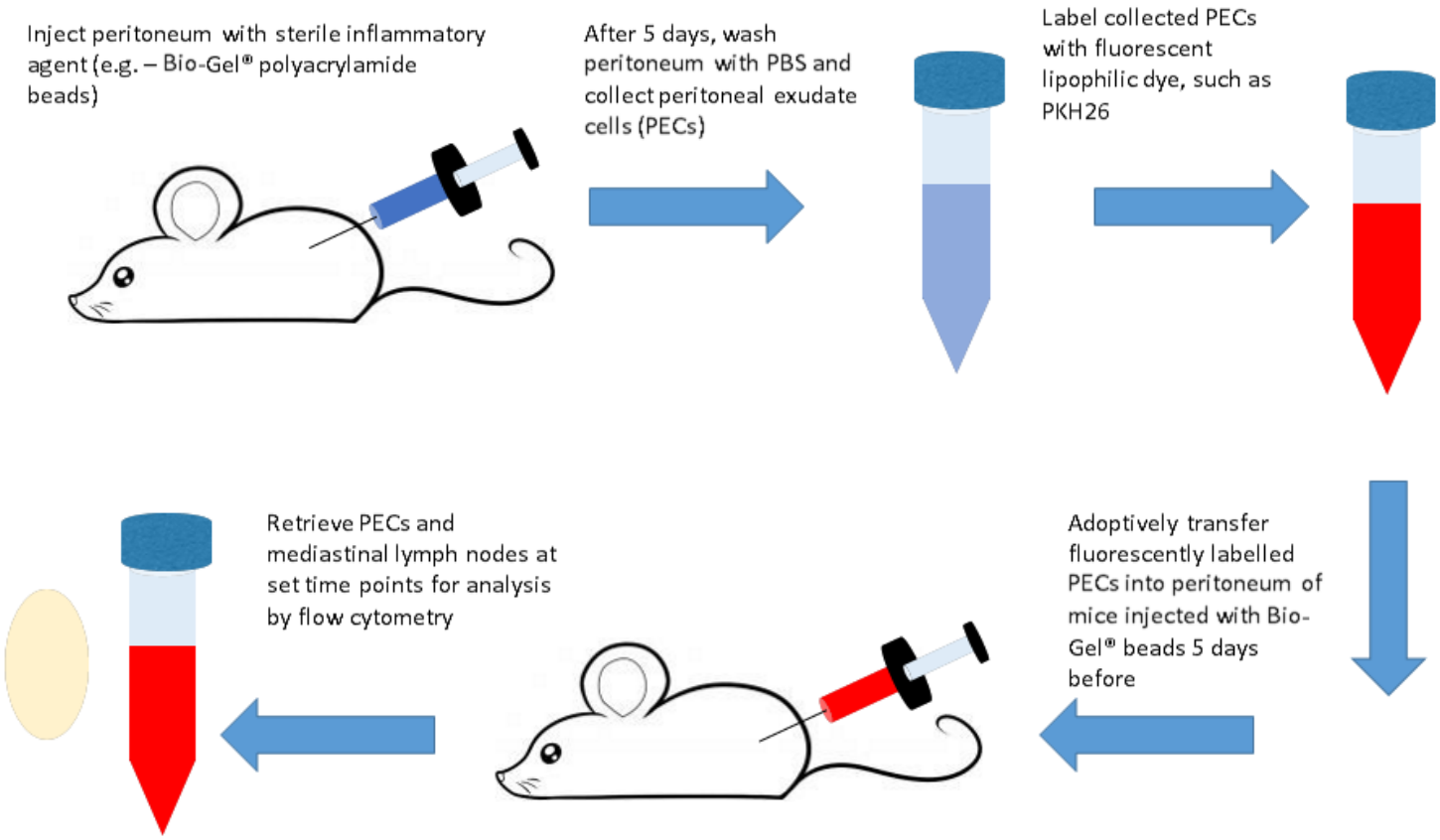


Figure 4-1: Schematic of *in vivo* model to study macrophage trafficking via lymphatics. Macrophages obtained either from inflamed peritoneum or from culturing bone marrow progenitor cells were labelled with a fluorescent dye and adoptively transferred into peritoneum of recipient mice. Draining mediastinal lymph nodes and peritoneal exudate cells (PECs) were retrieved at set time points for analysis by flow cytometry or microscopy.

is heterogeneous, and consists not only of resident and recruited macrophages but also neutrophils, each of which may have different migratory properties and influence trafficking behaviour. To overcome this, I used bone marrow derived macrophages (BMDMs), which share the same myeloid origin as the macrophages which populate the peritoneum during sterile inflammation and represent a more defined, homogenous population for quantitative study (Ginhoux, Greter et al. 2010). On the other hand, when using BMDMs, the contributions associated with the endogenous mixed cell population may potentially be lost and and hence may only provide initial clues that would eventually have to be related back to the full inflammatory peritonitis model.

Despite evidence that macrophages can exit peritoneum to draining lymph nodes via the lymphatics, no studies have yet characterised the mechanisms involved in lymphatic entry, and have been limited largely to demonstrations that macrophages interact with the murine peritoneal membrane (Bellingan, Xu et al. 2002, Cao, Lawrence et al. 2005). In addition, there have only been limited studies in the literature describing the structure of, and expression of molecules on lymphatics involved in drainage from the peritoneal space, with the result that our present understanding is based on the architecture of vessels in the dermis and airways (Baluk, Fuxe et al. 2007, Yao, Baluk et al. 2012).

The peritoneum is a large serous membrane that lines some of the major visceral organs of the abdominal cavity (known as visceral peritoneum) as well as the abdominal and pelvic walls thus creating a potential space encapsulating these two, known as the intraperitoneal cavity. The membrane is composed of the mesothelium supported by connective tissue and contains blood vessels, lymphatic vessels as well as nerves that are part of the peripheral nervous

system. Drainage of the peritoneal space involves initially the mesenteric and periportal lymph node groups. The efferent lymph from these nodes in turn drains into the mediastinal nodes (Abu-Hijleh, Habbal et al. 1995, Melichar and Freedman 2002). The passage of substances from the peritoneal space is through distinct openings within the peritoneal membrane, which have been visualised by electron microscopy and termed stomata (Fig 4-2) (Baradi and Rao 1976, Wang, Li et al. 2010). The location of these stomata is confined to sites with subserous lymph spaces or lacunae, and they are not found in other parts of the peritoneum. The peritoneal membrane is believed to be continuous on to the diaphragm and as such the lymphatic drainage from the peritoneal space follows on to the lymphatics found in the diaphragm. After leaving the diaphragm, lymph enters the collecting ducts/vessels before reaching the mediastinal lymph nodes. The lymphatic vessels of the diaphragm are arranged into two distinct networks - one on the peritoneal surface and one on the pleural surface with both networks of vessels intercommunicating. The distribution of these vessels varies between different animals (Li and Li 2003).

The stomata have been identified as key locations for clearance of particles from the peritoneal space that are located between the lateral borders of the mesothelial cells which overlie the lacunae. The lymphatic lacuna, a specialised drainage unit associated with the peritoneal membrane of the diaphragm, is composed of mesothelial cells and lymphatic endothelial cells (LECs), with a layer of connective tissue. These two cell categories are joined to one another to form a channel (i.e. the stomata) leading from the peritoneal cavity to the lumen of the lacunae. These stomata are composed of lymphatic capillaries with the constituent LECs extending into tubules under the peritoneum, which act as valves allowing entry into the stomata and subsequent lymphatics

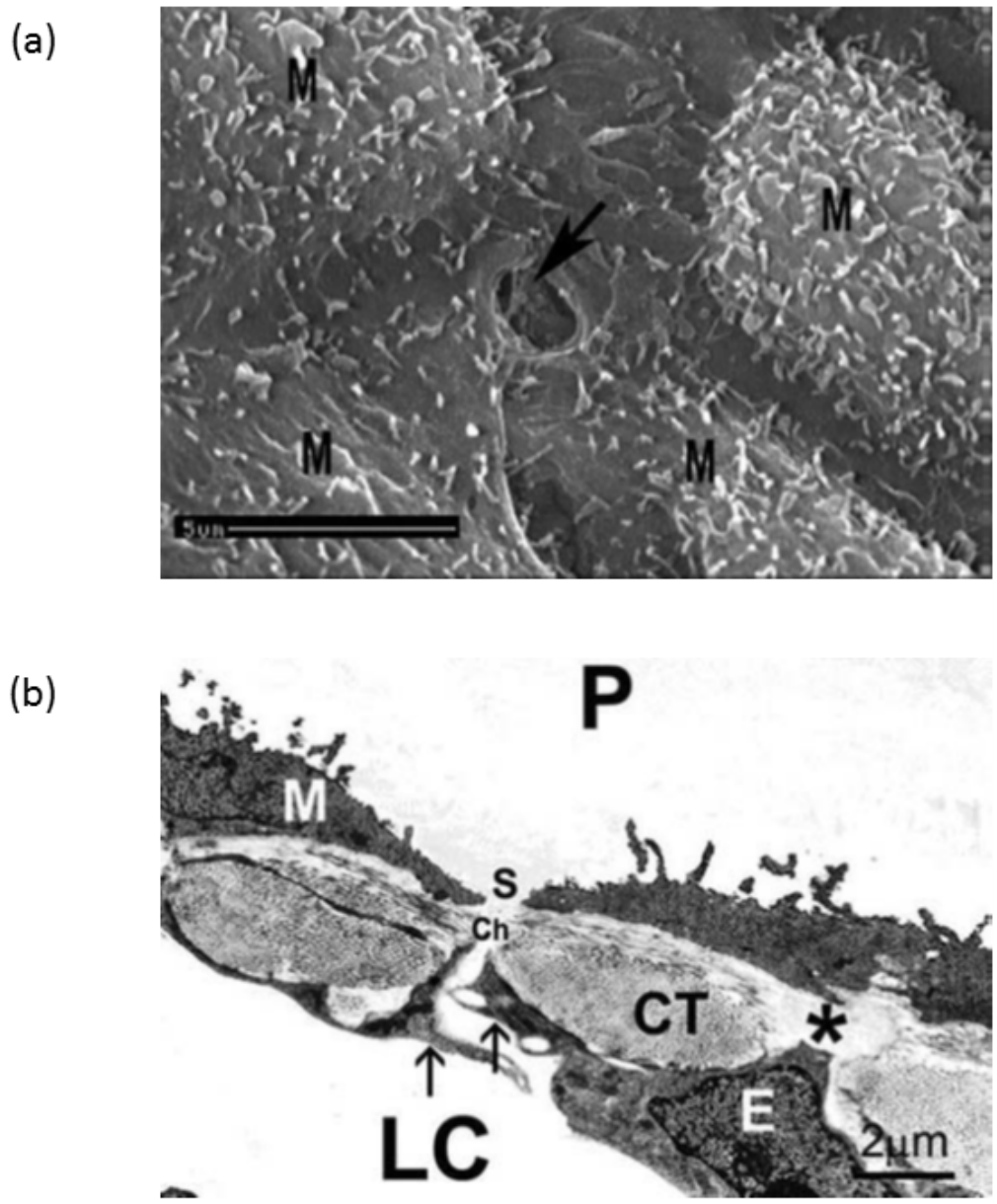


Figure 4-2: Electron microscope views of lymphatic structures on murine peritoneal membrane. (a) Scanning electron microscope image showing the lymphatic stomata (arrow) at the junction of four mesothelial cells (M). **(b)** Transmission electron microscope image of the membrane showing access to or out of the lymphatic capillary (LC) is through the stomata (S), the gap indicated by the arrows. Mesothelial cells (M) and connective tissue (CT) is also shown. **Adapted from:** Wang et al. (2010)

associated with lacunae (Fig 4-3). The major function attributed to these stomata and lacunae is fluid drainage (Mactier, Khanna et al. 1987, Abu-Hijleh, Habbal et al. 1995). However, no published reports have demonstrated the transit of leucocytes across these anatomical structures. Assessing the possible involvement of stomata and their association with the peritoneal lymphatics during clearance of macrophages forms an important component of this Chapter.

Advances in lymphatic biology and study of the vasculature have been bolstered by the identification of the hyaluronan (HA) receptor, LYVE-1. Discovered in the laboratory of my D.Phil. supervisor, Professor David Jackson, it was identified through a search of the human expressed sequence tag (EST) database for homologs of the leucocyte HA receptor, CD44. The resulting cDNA encoded a receptor (now known as LYVE-1) with a primary (ectodomain) sequence 51% similar to CD44. LYVE-1 was initially shown to have a mutually exclusive pattern of tissue expression to that of CD44, being restricted mainly to lymphatic vessels and lymph node sinus endothelia (Banerji, Ni et al. 1999). Although a small numbers of additional cell types (including, alveolar epithelial cells and hepatic blood sinusoidal endothelia) are known to express LYVE-1, the receptor remains a powerful tool for identifying lymphatic vessels (Royston D, Unpublished findings, (Mouta Carreira, Nasser et al. 2001). An extensive study into the structure of initial capillaries by Baluk et al. (2007) demonstrated LYVE-1 to be particulalrly concentrated at the tips of the button junctions between individual oakleaf shaped lymphatic endothelial cells (LECs) within initial lymphatic capillaries. In addition however, LYVE-1 is expressed in lymph node subcapsular and cortical sinuses. Such a specific localisation of the

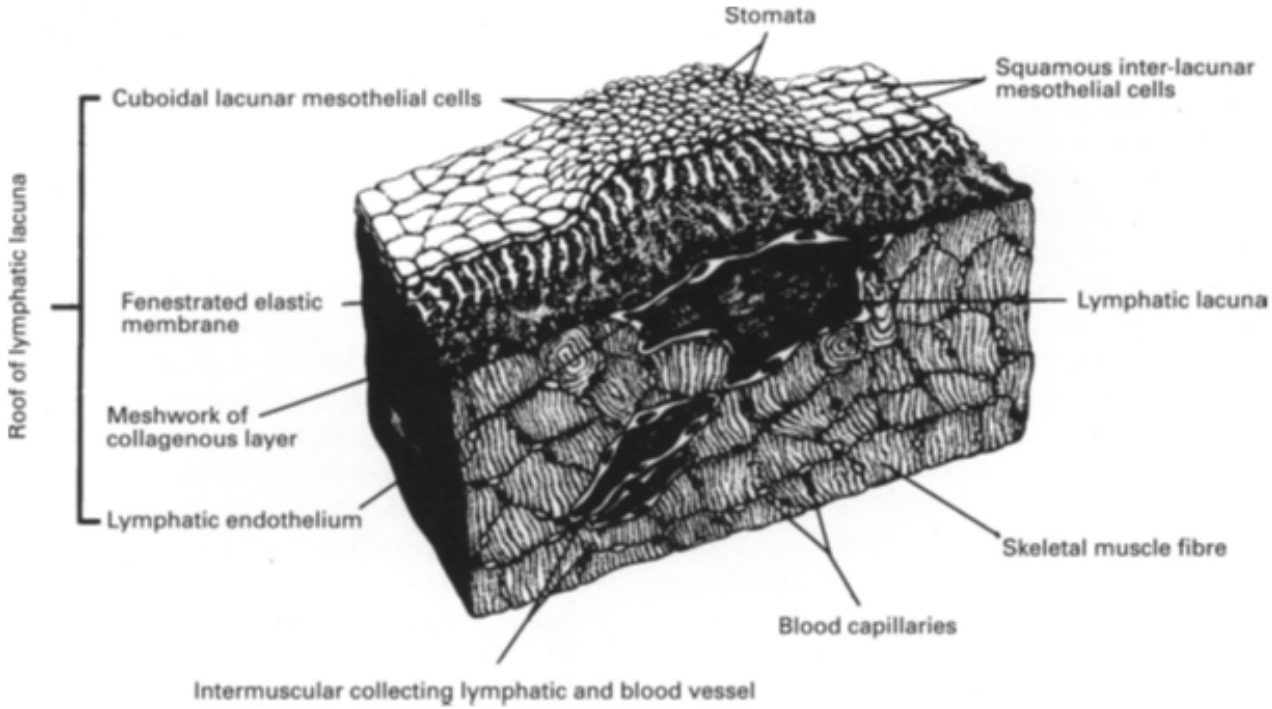


Figure 4-3: Composite three dimensional diagram of peritoneal membrane. Illustrations of the different components associated with the membrane with stomata, surrounded by mesothelial cells, located towards the peritoneal cavity and opening into lymphatic lacunae which eventually drain into capillaries draining towards the pleural surface. **Adapted from:** Abu-Hijleh et al. (1995).

receptor suggested an important role in mediating leucocyte entry and/or exit. Indeed, the data from the *in vitro* transmigration assays in Chapter 3 are suggestive of LYVE-1 playing an influential role in mediating the process. However, there are no examples in the literature that detail whether LYVE-1 can guide entry of cells into the lumen of vessels *in vivo*, a question tackled throughout the course of this Chapter. The modulation of LYVE-1 expression on the lymphatic vessels in inflamed tissues also provides another potential complication. Johnson et al. (2007) demonstrated that exposure of mouse dermal tissue explants to high levels of TNF-α induced partial downregulation of LYVE-1 on lymphatic capillaries. As yet it is unclear if such downregulation specifically targets LYVE-1 in button junctions and hence whether LYVE-1 is retained in this location and mediates leucocyte transit during inflammation. Also, the plasticity of the junctions in transforming from buttons to zippers during persistent inflammation poses further problems to understanding if the localisation of LYVE-1 is key to mediating cell entry to lymphatics, since in the zippers, the expression of the receptor is not localised to a specific location on the cell (Yao, Baluk et al. 2012). Addressing the influence of the HA receptor on trafficking to lymph nodes was therefore undertaken to further validate the *in vitro* findings from Chapter 3.

Macrophages at sites of inflammation have been characterised as innate immune cells derived from monocytes with a host of functions from removal of foreign bodies and debris to wound healing and restoring homeostasis. The reason underlying their transit to lymph nodes is yet to be fully understood although previous studies with bone marrow derived macrophages suggest participation in priming lymphocytes; however, this priming appears to be an

extension of replacing CD169+ subcapsular sinus macrophages (which were depleted in radiation chimeras) and whether such function is present without depletion of the subcapsular sinus macrophages is unknown (Phan, Green et al. 2009). Interestingly, macrophage interactions within lymph nodes have usually been observed with B cells and have generally not been seen with T cells (Carrasco and Batista 2007). Also, it should be noted that lymph nodes might not to be the final destinations of the macrophages, as Cao et al. (2005) detected adoptively transferred macrophages within blood circulation as early as 4 hours after injection into the inflamed peritoneal space. This lack of retention complicates the possibilities of the overall fate of the macrophage after trafficking to draining lymph nodes. Nonetheless, identifying adoptively transferred macrophages in relationship to location of other cells within the lymph node forms part of a relevant section of the Chapter, thus helping to refine views of the function of macrophages in LNs.

4.2 Aims

As outlined in the introduction above, there is currently insufficient knowledge of the route taken by macrophages during clearance from both the normal and inflamed peritoneum. The previous chapter demonstrated that macrophages can migrate across lymphatic endothelial cell monolayers *in vitro* and that LYVE-1 plays an important role in the process. However, there was no published evidence to support such a role for LYVE-1 in macrophage clearance from sites of inflammation *in vivo*. The aim of the work presented here was to establish that macrophages travelled to lymph nodes via lymphatic vessels with further investigation into the mechanism. The model of trafficking utilised was a well-established model of peritonitis, outlined in previous publications. In particular the following questions were addressed:

- Do macrophages migrate *via* lymph from the peritoneum to draining lymph nodes, and how is this traffic influenced by inflammation?
- Does entry and migration of macrophages via lymph depend on LYVE-1?
- What is the functional significance of macrophage migration to lymph nodes?

4.3 Results

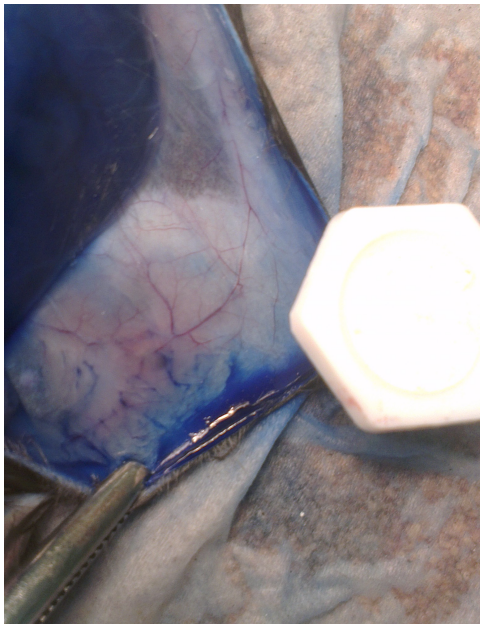
4.3.1 Mapping of lymphatic drainage from the peritoneal cavity

The study of trafficking to draining lymph nodes from the peritoneum required identification of mediastinal lymph nodes as well as verification of injection into the peritoneum.

To achieve this, adult mice (aged 8-12 weeks) were injected with 1 % (w/v) tracer dye Evans blue solution in PBS intra-peritoneally (i.p). Evans blue binds to the albumin in lymph and hence allows visualization of the lymphatics that drain the peritoneal cavity. After four hours, gross evaluation of the blue staining of the body was analysed with photographic images taken (Fig 4-4). By dissecting through the skin and exposing the peritoneal parietal membrane, the dye was concentrated at the site of injection while the whole membrane was stained and progressing upwards towards the thoracic region of the mouse. Analysis of the thoracic cavity reveals staining of the trachea, and more importantly the mediastinal lymph node, affirming this as one of the main nodes draining the peritoneum. Examination of the inguinal region revealed no blue stain while the inguinal lymph node had also failed to acquire the Evans blue dye, serving as a good control to highlight that drainage from the peritoneal cavity does not go via that region.

Overall, these initial experiments established competence in i.p injections and in the identification of mediastinal lymph nodes for subsequent experiments.

Non draining groin/lower abdomen region



Draining thoracic cavity



Non draining inguinal lymph node



Draining mediastinal lymph node

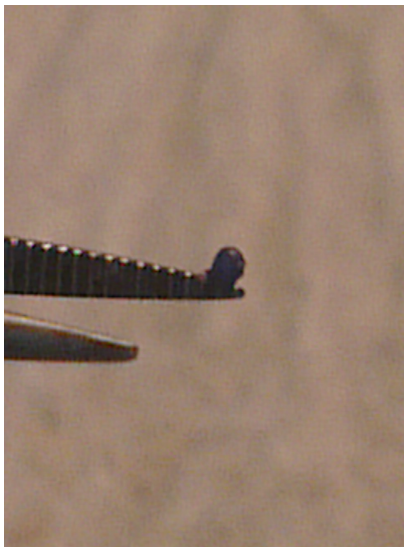


Figure 4-4: Drainage of Evans blue dye solution from the peritoneal cavity of mice. Adult mice (aged 8-12 weeks) were injected with 1 % Evans blue dye solution into the peritoneal cavity. After 3 hours, mice were culled and the abdominal and thoracic cavity was exposed to assess blue colouring, which would represent the drainage route and distinct comparisons were made between the non draining groin region and draining thoracic cavity of which photographs were taken. Representative images are shown above. Three mice were used per injection experiment.

4.3.2 Isolation and characterisation of murine bone-marrow derived macrophages (BMDMs)

As outlined in the Introduction, BMDMs are a convenient model population for studying the trafficking of macrophages to draining lymph nodes and provide good preliminary understandings of the capacity of macrophages to migrate via lymphatic vessels.

Bone marrow progenitor cells were isolated from the limbs of adult mice (aged 8-12 weeks) and cultured for 6 days in media supplemented with supernatant derived from L929 fibroblasts, a cell line which releases macrophage differentiation cytokines such as, M-CSF and GM-CSF. After the differentiation period, the phenotype of the cells was confirmed by flow cytometry. As with the previous Chapter, adherent cells on culture plates were lifted with EDTA rather than proteases in order to maintain the expression of cell surface specific markers for myeloid cells. Primary antibodies to these proteins - scavenger receptor CD68, integrin CD11b and adhesion G-protein coupled receptor F4/80, were used to stain the lifted cells. Positive expression of all markers in combination on the homogenous cell population confirmed macrophage phenotype thus being suitable for use in subsequent trafficking experiments (Fig 4-5).

4.3.3 Trafficking of BMDMs to draining lymph nodes via interactions with peritoneal lymphatic structures

Despite convincing evidence in previously published reports that macrophages migrate out of an inflamed peritoneum to draining lymph nodes there appears to

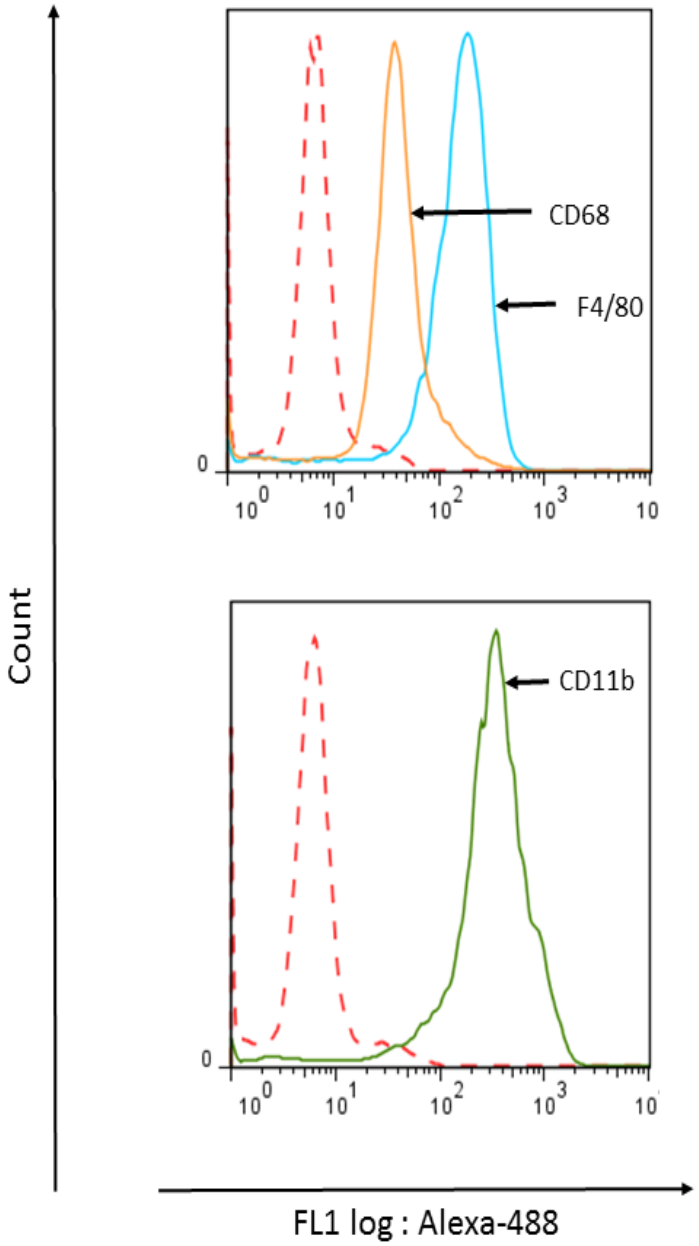


Figure 4-5: Flow cytometric analysis of bone-marrow derived macrophages (BMDMs). Macrophages differentiated from bone marrow progenitor cells isolated from adult female mice (aged 8-12 weeks) in media supplemented with L929 fibroblast culture supernatant were stained with primary antibodies directed against the macrophage markers, macrosialin CD68 (antibody clone FA-11), or myeloid integrin CD11b (antibody clone M1/70), or F4/80 (clone BM8) as indicated by arrows. Isotype controls are also shown (red histograms). Expression levels were quantified by flow cytometry and representative histograms are shown of an experiment repeated > 3 times.

be a conflict between individual workers as to what the optimum time of arrival at mediastinal lymph nodes is, ranging from as early as 4 hours to close to 72 hours, after adoptive transfer into peritoneum (Cao, Lawrence et al. 2005, Gautier, Ivanov et al. 2013).

In vitro experiments from the previous chapter established that macrophages can transmigrate unstimulated HDLECs and furthermore that the process is greatly enhanced in an activated endothelium. Before assessing the kinetics of trafficking from an inflamed environment and the impact of this inflammation on exit, I first explored the process in the peritoneum of normal unstimulated mice.

Differentiated BMDMs were lifted and stained with the red fluorescent dye PKH26PCL (hereafter termed PKH26), a stable lipophilic compound selectively internalised by phagocytic cells and retained in lysosomes. These labelled macrophages were injected into the peritoneum of untreated adult mice after which mediastinal lymph nodes were retrieved from the mice at 12, 24 and 36 hours after injection. Isolated cells from LNs were stained with primary antibodies for macrophage markers F4/80 and MHC-II and analysed by flow cytometry (Fig 4-6). Adoptively transferred macrophages, identified as all fluorescent cells stained $F4/80^{+}MHC\text{-}II^{+}$, made up approximately > 85 % of all PKH26+ cells, and appeared in the mediastinal nodes as early as 12 hours after injection i.p, peaking at 24 hours before slightly decreasing at 36 hours.

To assess if the macrophages had accessed the lymph nodes via afferent lymph, PKH26 labelled BMDMs were injected i.p into untreated mice, and mediastinal (draining) and inguinal (non-draining) lymph nodes retrieved, 24 hours later for quantitation by flow cytometry. Single cell suspensions of the LNs were stained with primary antibodies for F4/80 and MHC-II and evaluated by

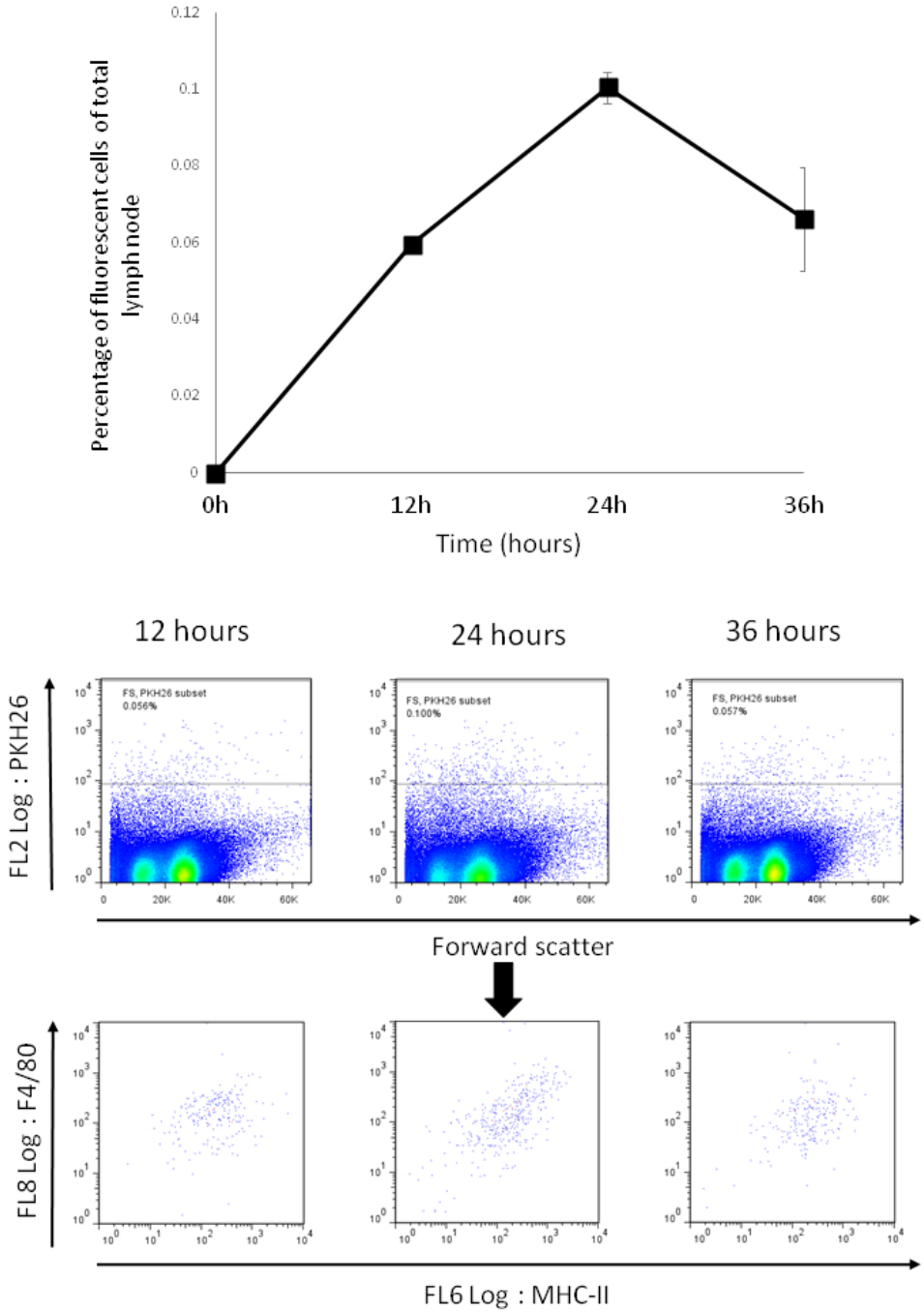


Figure 4-6: Time course of BMDM recovery in draining mediastinal lymph nodes from an uninflamed peritoneum. Differentiated BMDMs were injected into the peritoneum of untreated adult female wild type mice (aged 8-12 weeks). Mediastinal lymph nodes (mdLNs) were collected at time points of 12, 24 and 36 hours after injection, mechanically disrupted and sieved to yield single cell suspensions and cells were immunostained for the macrophage surface markers, F4/80 using clone CI:A3-1, and MHC-II using clone M5/114.15.2 to identify macrophages by flow cytometry. The graph above shows quantitative assessment of cells arriving at mdLNs in WT mice with representative dot plots below the graph. Fluorescent PKH26^{+} cells are gated on for analysis of F4/80 and MHC-II. Four mice were used per treatment group and the data shown are representative of an experiment that was repeated 3 times. Data are mean ± SD.

flow cytometry (Fig 4-7). Mediastinal lymph nodes retain 7 times more adoptively transferred BMDMs compared to inguinal LNs; the result thus establishing macrophages migrating via lymphatics.

Lymphatic drainage of the peritoneal cavity is believed to involve exit of fluids via stomata present on the peritoneal membranes leading into lymphatic lacunae subsequently draining into collecting lymphatics. Most independent studies have identified these structures using electron microscopy providing in-depth insight of the architecture of the peritoneal membrane. However, there is a lack of understanding into the arrangement of proteins/molecules on these structures. With subsequent studies focussing on LYVE-1 and it being a powerful marker of lymphatics, parietal peritoneal membranes from untreated mice were retrieved and stained with primary antibodies to LYVE-1 to make a preliminary exploration of the arrangement of the molecule on lymphatic structures of the peritoneum by confocal microscopy (Fig 4-8). Whole-mount images of the membrane revealed LYVE-1^{+} vascular structures, thus identified as lymphatic vessels of the peritoneum. Along with lymphatic vessels, the LYVE-1 antibody stained abundant gap-like structures throughout the peritoneal membrane that were tentatively identified as stomata. Subsequently, PKH26 labelled BMDMs were injected i.p into adult mice, and the parietal tissue isolated 12 hours post injection for staining with primary antibodies to LYVE-1 and CD31 and microscopic imaging (Fig 4-9). The red macrophages can be seen interacting with these identified lymphatic stomata that are distinct from the abundant CD31 positive blood vessels, thus providing preliminary evidence that macrophages may be exiting from the peritoneum via stomata draining into lymphatics

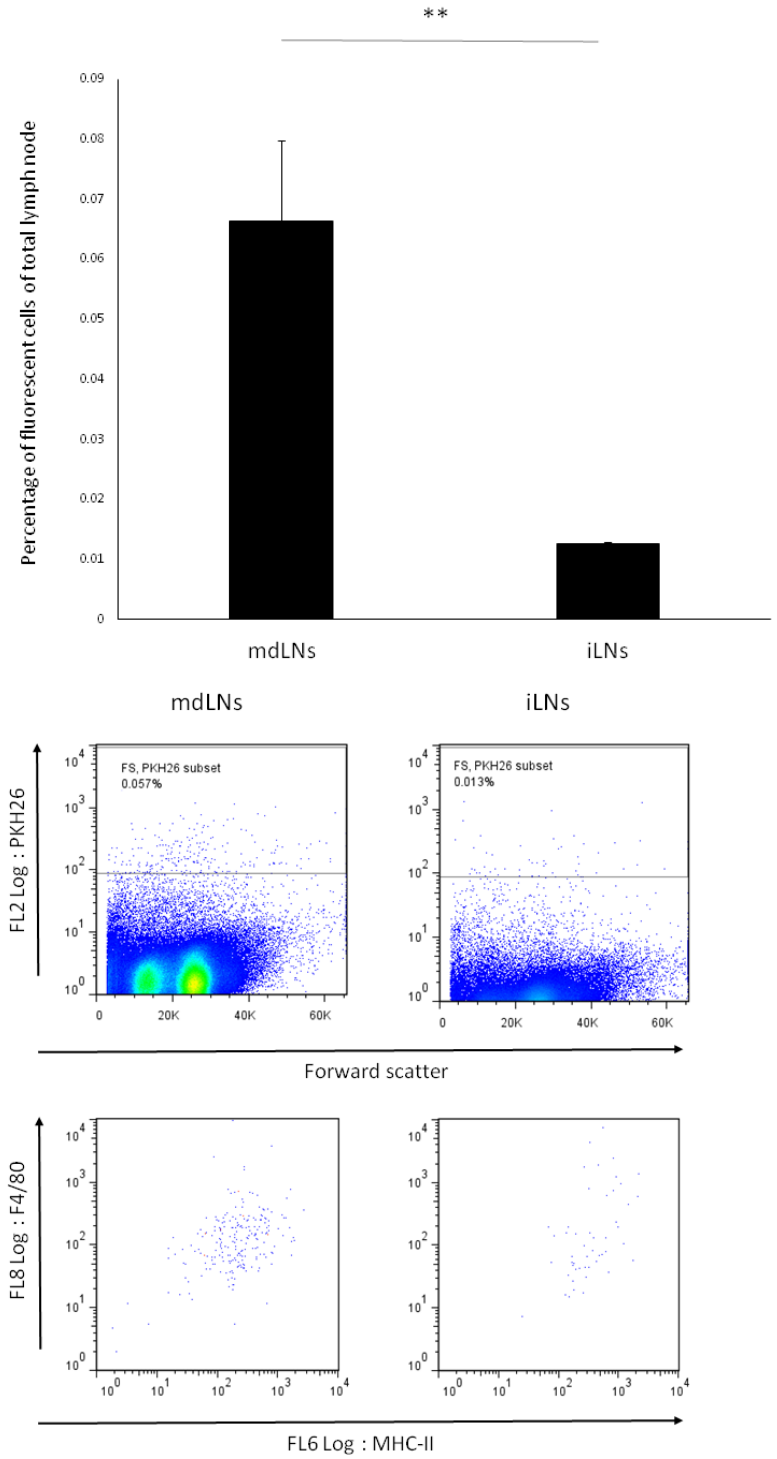


Figure 4-7: Comparative recoveries for dye labeled macrophages in draining and non-draining mediastinal nodes Differentiated BMDMs were injected into the peritoneum of untreated adult female WT mice (aged 8-12 weeks). Draining mediastinal lymph nodes (mdLNs) and non-draining inguinal lymph nodes (iLNs) were collected 24 hours after injection of macrophages and mechanically disrupted to produce single cell suspensions and cells were immunostained for macrophage specific markers, F4/80 (clone CI:A3-1) and MHC-II (clone M5/114.15.2). The graph above shows quantitative assessment of cells arriving at mdLNs and iLNs in WT mice with representative dot plots below the graph. Fluorescent PKH26^{+} cells are gated on for analysis of F4/80 and MHC-II. The graph shown is representative of 3 independent experiments. Data are the mean ± SD of quadruplicate technical replicates. A two-tailed, unpaired Student's t-test was performed on this figure and p values below 0.05 were considered statistically significant (** $p < 0.01$; mdLNs vs iLNs). The appropriate statistical test to analyse this data would be a two way analysis of variance (ANOVA).

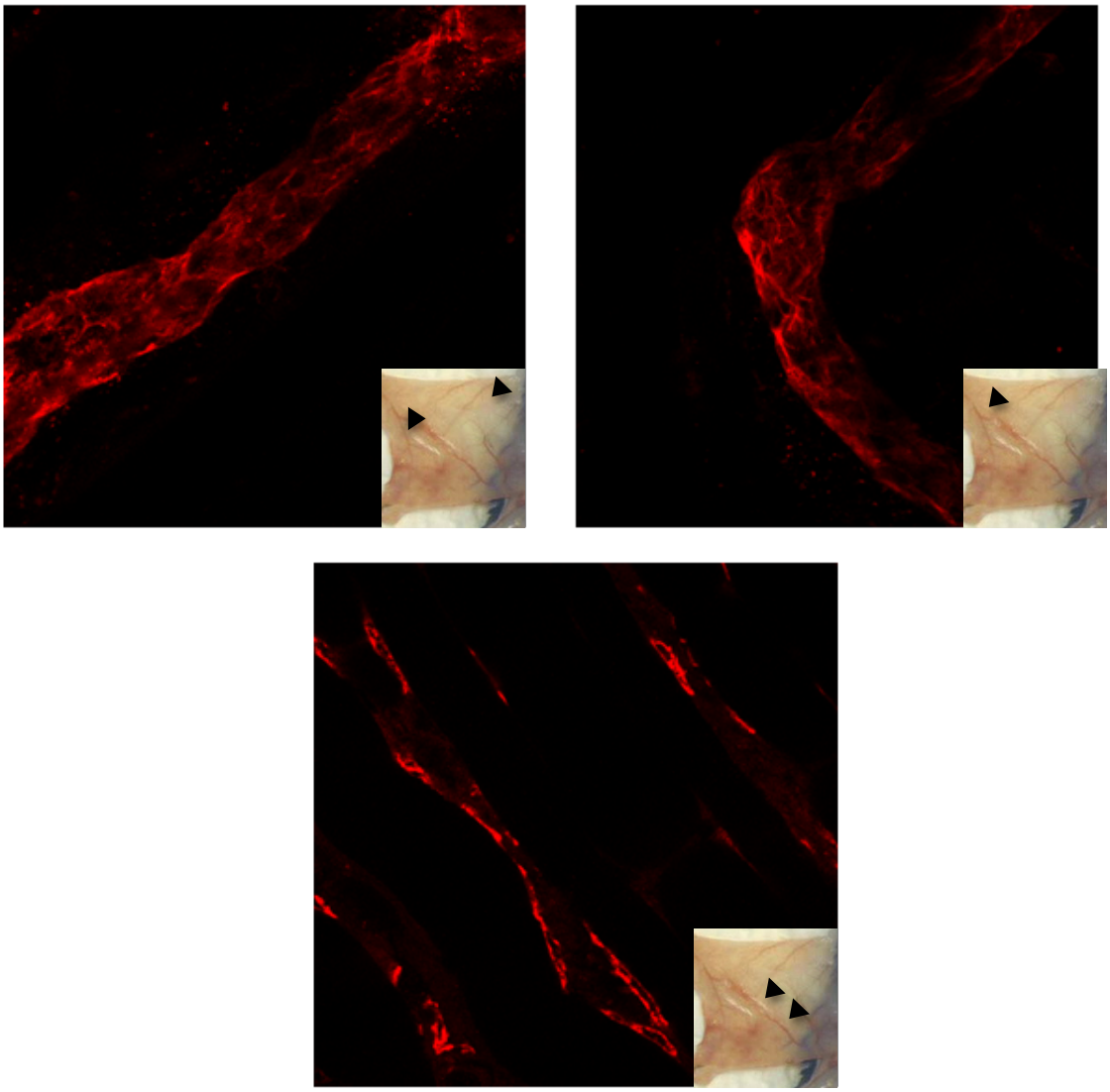


Figure 4-8: Characterisation of LYVE-1 expression on the peritoneal membrane of untreated mice. Untreated female C57BL/6 mice (aged 8-12 weeks) were sacrificed and peritoneal parietal membranes retrieved and processed as wholemount tissue for immunostaining with the lymphatic endothelial surface marker, LYVE-1 (red) using monoclonal antibody C1/8. Tissues were mounted with Vectorshield® (upper and lower panels). The figure shows confocal images of three representative fields from what area of the parietal peritoneal membrane from an experiment repeated 3 times. Small insets of a photograph of the membrane with arrow heads indicate region membrane was imaged after staining. Magnification at 25x.

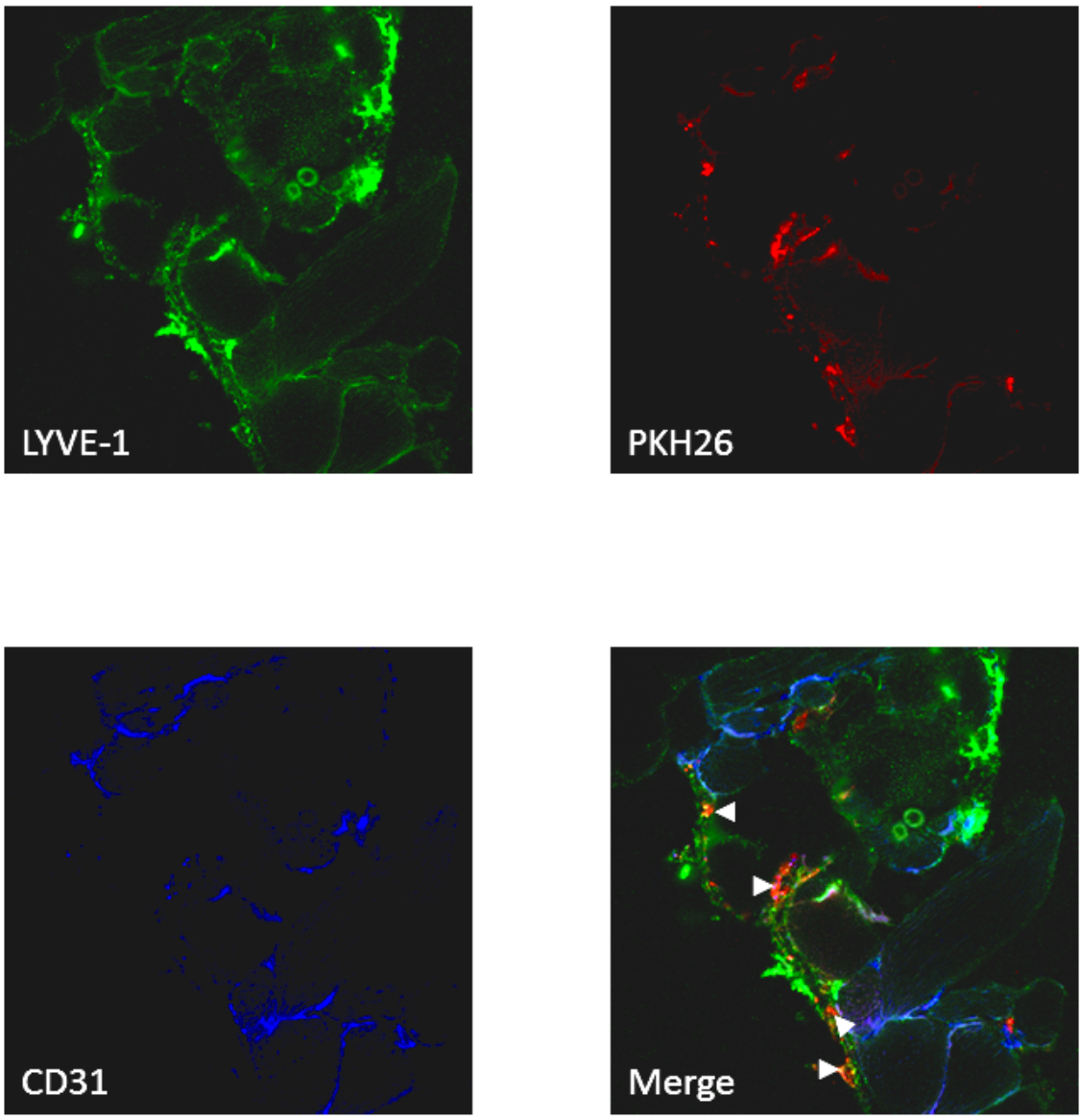


Figure 4-9: Association of BMDMs with structures tentatively identified as stomata in uninflamed mouse peritoneal parietal membrane . Female C57BL/6 mice (aged 8-12 weeks old) were injected with PKH26 labelled macrophages (red) into the peritoneal cavity. After a period of 12 h mice were killed, parietal membranes were processed as wholemount tissue to be immunostained for the lymphatic specific marker, LYVE-1 (green) using polyclonal antibody raised against LYVE-1 and pan-endothelial CD31 (blue) using clone. Membranes were mounted with Vectorshield®. Confocal micrographs are shown of an experiment that was repeated 2 times. White arrowheads indicate to regions of macrophages (red) interacting with LYVE-1^{+} regions (green) tentatively identified as stomata.

4.3.4 The role of LYVE-1 in BMDM trafficking to lymph nodes

One of the major aims set out for this Chapter was to explore the role of LYVE-1 in trafficking of macrophages to draining lymph nodes. As data from Chapter 3 had indicated that LYVE-1-HA interactions contributed to *in vitro* transmigration and the above findings suggested LYVE-1 was expressed on stomata like structures that are putative sites for macrophage exit from the peritoneal cavity, it was reasonable to expect that LYVE-1 disruption might affect BMDM clearance from the peritoneum. The two approaches used to disrupt LYVE-1 function and test its effects on peritoneal trafficking were LYVE-1 gene knock out mice (*LYVE-1*$^{-/-}$) and LYVE-1-specific HA blocking monoclonal antibodies.

Trafficking in *LYVE-1*$^{-/-}$ mice

Since LYVE-1 is abundantly expressed on the lymphatics, it was hypothesised that deleting the gene would have significant consequences on the development of lymphatic architecture from an embryo or normal lymphatic function; the *LYVE-1*$^{-/-}$ mice was subsequently generated in the laboratory of Professor David Jackson. Surprisingly, these mice had normal vessel morphology and patterning as well as non defective dendritic cell trafficking (Gale, Prevo et al. 2007). However, comprehensive analysis of this migration within the Jackson laboratory has revealed that there are lesser numbers within draining lymph nodes at early time points, suggesting that these mice may have a phenotype that was not observed and could possibly be seen with macrophage trafficking. BMDMs were stained with CellTracker™ green CMFDA, to compare numbers of fluorescent cells transiting to the dLN following

injection into the peritoneum of age and sex matched untreated, wild-type (WT) or *LYVE-1*$^{-/-}$ mice. After 24 hours mediastinal lymph nodes were isolated and cell suspensions prepared from the disrupted tissue, followed by staining with an antibody to the myeloid cell marker CD11b, to further validate the macrophage phenotype of the migrated cells (Fig 4-10). The result demonstrates a small but statistically insignificant decrease in macrophages trafficking in *LYVE-1*$^{-/-}$ mice and repeats of the experiment show a consistently small but statistically insignificant decrease. One possible explanation is redundancy, such that another gene or genes may compensate for the loss development in these mice.

LYVE-1 blocking mAbs

To overcome such effects and assess the consequences of LYVE-1 disruption by another method, I next determined the effects of administering wild-type mice with LYVE-1-HA blocking monoclonal antibodies (mAbs). Accordingly, CMFDA labelled BMDMs were injected into the peritoneum of adult WT mice given a single intraperitoneal injection of the LYVE-1-HA blocking antibody C1/8, or a matched isotype control. Mediastinal lymph nodes were then retrieved after an earlier time point of 12 hours as the mAb blockade of *in vitro* transmigration from Chapter 3 signified the effects of the antibody to be active earlier in the process. Cells recovered from lymph nodes were stained with antibodies to CD11b, for subsequent analysis by flow cytometry; the data shown in figure 4-11, demonstrating disruption of LYVE-1 function with the HA blocking mAb C1/8 led to an approximately 2.2-fold decrease of trafficking macrophages. To determine if the strength of blockade of the antibody influenced the reduction

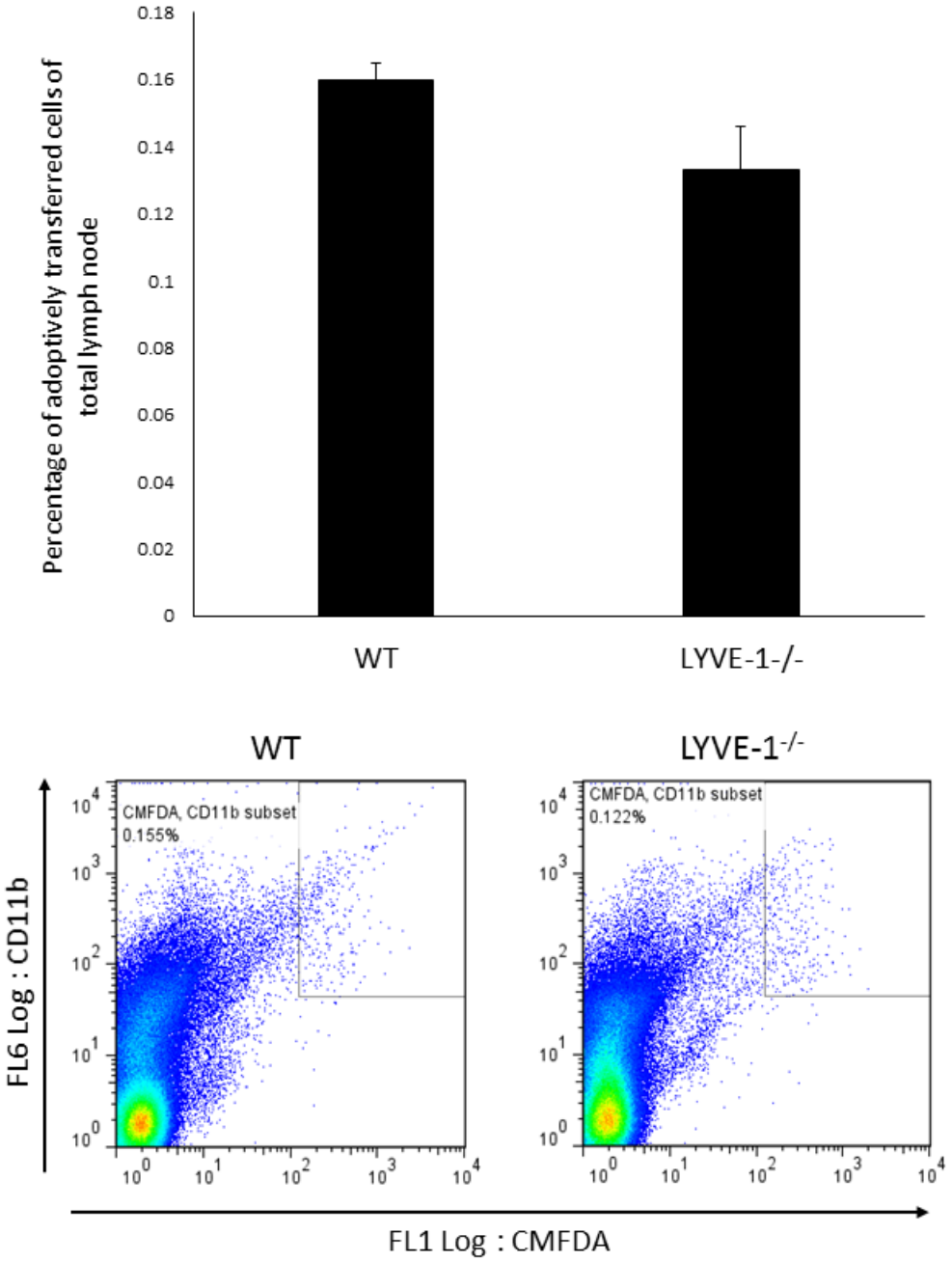


Figure 4-10: Effect of LYVE-1 genetic deletion on macrophage trafficking from uninflamed peritoneal cavity to mediastinal lymph nodes. Adult female mice (8-12 weeks old) of either wild-type (WT) or LYVE-1-/- background were injected with WT BMDMs labelled with fluorescent dye CMFDA. After 24 hours, mice were killed and mediastinal lymph nodes were retrieved, mechanically disrupted to obtain single cell suspensions which were immunostained with myeloid cell marker CD11b (clone M1/70) to further identify macrophages by flow cytometry. The graph above shows quantitative assessment of cells arriving at mdLNs in WT and LYVE-1$^{-/-}$ mice with representative dot plots below the graph. The graph shown is representative of 3 independent experiments. Data are the mean ± SD of quadruplicate technical replicates. A two-tailed, unpaired Student's t-test was performed on this figure and p values below 0.05 were considered statistically significant. The appropriate statistical test to analyse this data would be a two way analysis of variance (ANOVA).

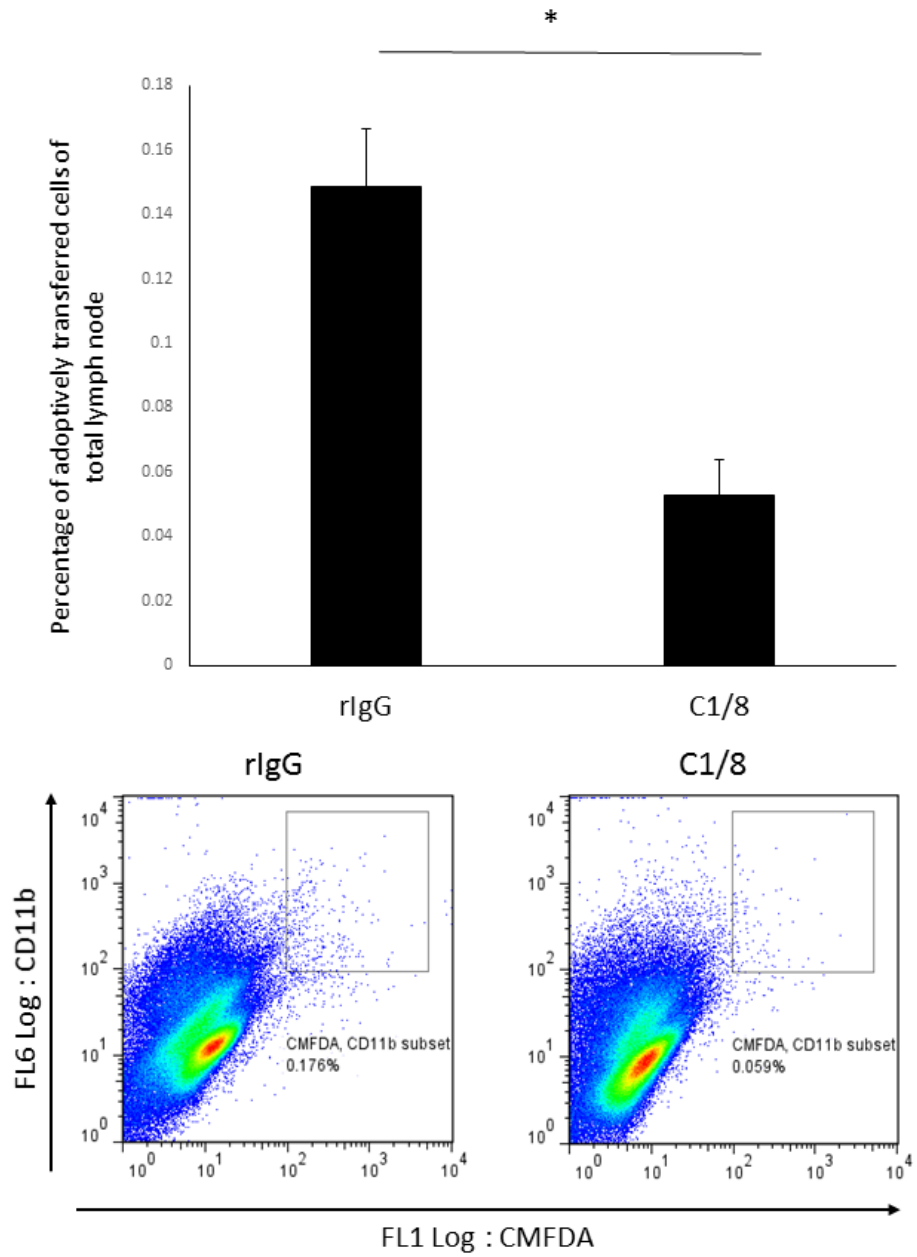


Figure 4-11: Effect of LYVE-1 blocking antibody C1/8 on macrophage trafficking from uninflamed peritoneal cavity to mediastinal lymph nodes. WT adult female mice (8-12 weeks old) were treated with either isotype control, rat IgG, or LYVE-1 blocking antibody C1/8 and 24 hours later injected intraperitoneally (i.p.) with WT BMDMs labelled with fluorescent dye CMFDA. After 12 hours of injection of macrophages, mice were killed and mediastinal lymph nodes were retrieved, mechanically disrupted to obtain single cell suspensions which were immunostained with myeloid cell marker CD11b (clone M1/70) to further identify macrophages by flow cytometry. The graph above shows quantitative assessment of cells arriving at mdLNs in rIgG, or C1/8 treated mice with representative dot plots below the graph. The graph shown is representative of 3 independent experiments. Data are the mean ± SD of quadruplicate technical replicates. A two-tailed, unpaired Student's t-test was performed on this figure and p values below 0.05 were considered statistically significant (* $p < 0.05$; isotype control IgG vs C1/8). The appropriate statistical test to analyse this data would be a two way analysis of variance (ANOVA).

in numbers arriving, the trafficking experiment as above was conducted but with the more potent LYVE-1-HA blocking antibody mAb2125. Figure 4-12 shows that mAb2125 caused a significant 2-fold reduction in BMDMs clearing to draining lymph nodes after 12 hours, indicating that strength of blockade of antibody is not a relevant factor in trafficking.

Taking the data from the LYVE-1 gene knockout and antibody blockade experiments together, these results provide the first tentative evidence that LYVE-1 indeed influences the exit of macrophages from the peritoneal cavity via lymphatics. Judging from the data presented in Chapter 3 (Fig 3-15), it was also possible that the effects of mAb blockade on *in vivo* trafficking would diminish over time and a restoration of numbers within the mediastinal lymph nodes would be observed. To assess this hypothesis, CMFDA labelled BMDMs were injected i.p into WT mice treated with C1/8, or rat IgG; following on from 24 hours, mediastinal lymph nodes were isolated and cells from the tissue were stained with antibodies to CD11b for analysis by flow cytometry (Fig 4-13). As with the result above, blockade by C1/8 promoted an approximate 2.2-fold decrease in trafficking of adoptively transferred BMDMs, with no increased numbers within the LN of C1/8 treated mice at the later time as hypothesised.

4.3.5 Establishment of a suitable mouse peritonitis model to assess macrophage migration from inflamed peritoneum

The combined findings from the previous two subsections yielded preliminary evidence that LYVE-1 mediates exit of macrophages from the normal resting peritoneum to lymph nodes, with a potential exit route via lymphatic stomata on

the peritoneal membrane. The following experiments were designed to test whether LYVE-1 also mediates exit from an inflamed peritoneum. Well established models of studying macrophage trafficking have been with peritonitis induced by the injection of a sterile agent into the cavity; the most common agents of activation being Brewer's thioglyocollate broth or Bio-Gel® polyacrylamide beads. The documented chronological order in which the different leukocyte populations are recruited to the peritoneal cavity in response to thioglycollate is for neutrophils to arrive within the first hour, followed by peripheral blood derived (exudate) monocytes after a further four hours. The monocytes gradually differentiate into macrophages and by 5 days post induction, most neutrophils have undergone apoptosis or have been phagocytosed and a majority of the total cells within an acquired exudate are macrophages. A recent study demonstrated that murine macrophages obtained from thioglycollate stimulated peritoneum do not demonstrate optimal chemotactic movement, in contrast to BMDMs and macrophages from a Bio-Gel® stimulated peritoneum. Also, it was revealed that there is a significant contamination of eosinophils and basophils that were being recognised as macrophages by F4/80 staining, as part of the PEC population from thioglycollate stimulated mice (Prof. DR Greaves, personal communication). Hence, it was concluded that macrophages from thioglycollate induction would not be appropriate to investigate trafficking and it was decided instead to perform the studies using the alternative model of Bio-Gel® polyacrylamide bead (BG bead) induced peritonitis.

To assess the levels of macrophages populating the peritoneum, adult mice were injected i.p. with BG beads which were then allowed to stimulate the

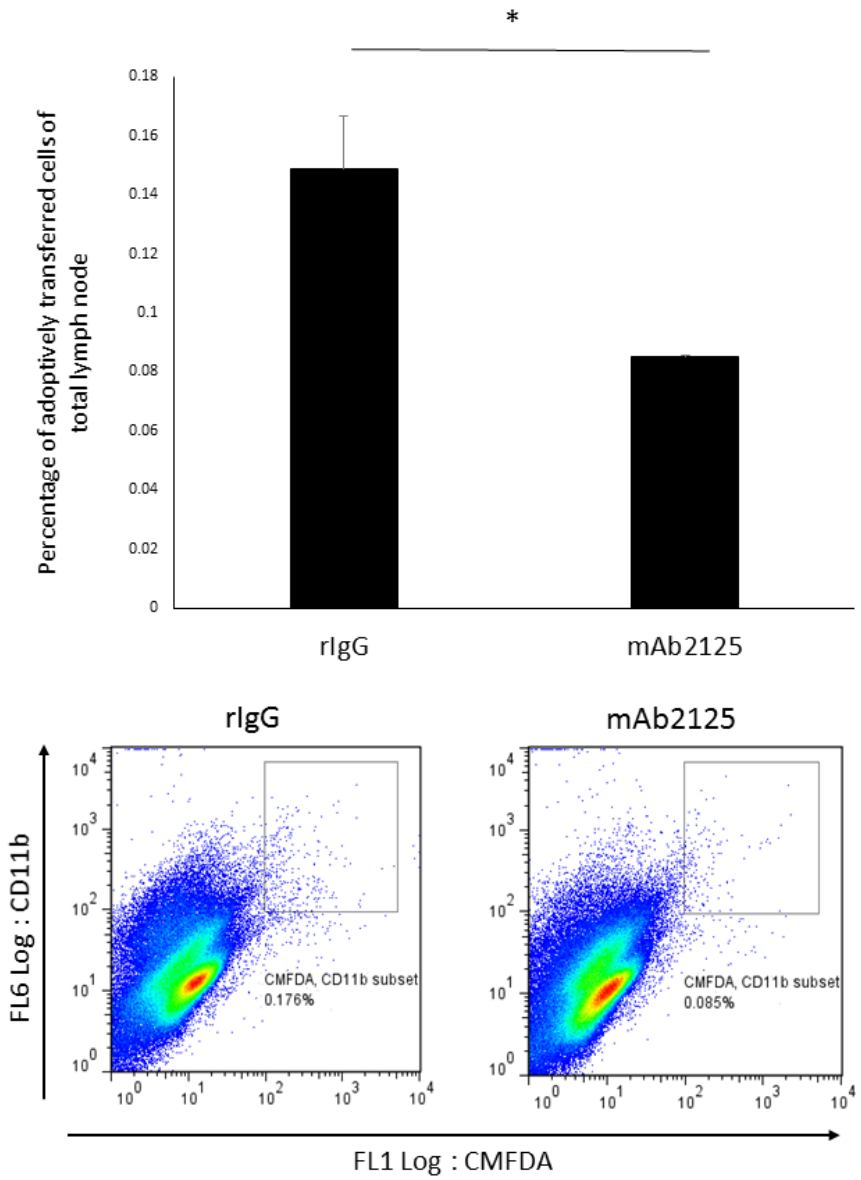


Figure 4-12: Effect of LYVYE-1 blocking antibody 2125 on macrophage trafficking from uninflamed peritoneal cavity to mediastinal lymph nodes. WT adult female mice (8-12 weeks old) were treated with either isotype control, rat IgG, or LYVE-1 blocking antibody mAb2125 and 24 hours later injected intraperitoneally (i.p.) with WT BMDMs labelled with fluorescent dye CMFDA. After 12 hours of injection of macrophages, mice were killed and mediastinal lymph nodes were retrieved, mechanically disrupted to obtain single cell suspensions which were immunostained with myeloid cell marker CD11b (clone M1/70) to further identify macrophages by flow cytometry. The graph above shows quantitative assessment of cells arriving at mdLNs in rIgG, or mAb2125 treated mice with representative dot plots below the graph. The graph shown is representative of 3 independent experiments. Data are the mean ± SD of quadruplicate technical replicates. A two-tailed, unpaired Student's t-test was performed on this figure and p values below 0.05 were considered statistically significant (* $p < 0.05$; isotype control IgG vs mAb2125). The appropriate statistical test to analyse this data would be a two way analysis of variance (ANOVA).

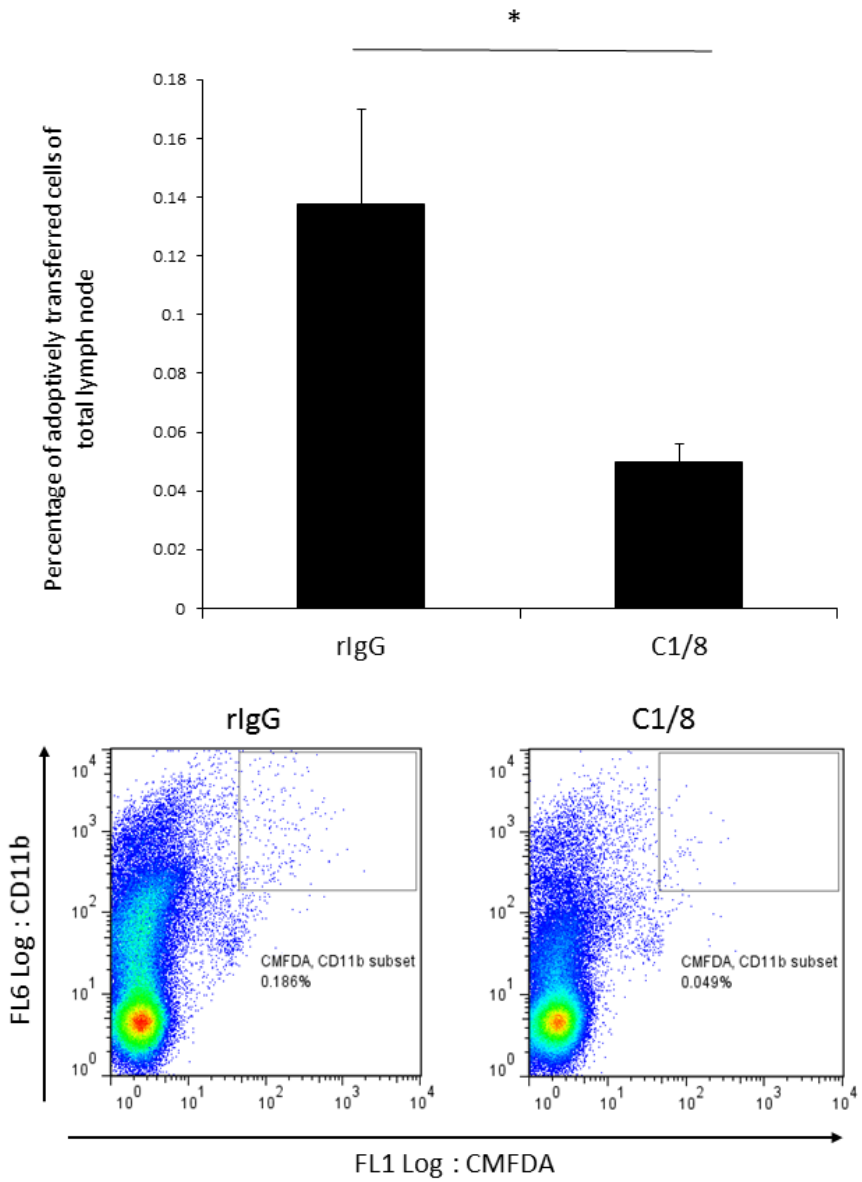


Figure 4-13: Effect of LYVYE-1 blocking antibody C1/8 on macrophage trafficking from uninflamed peritoneal cavity to mediastinal lymph nodes. WT adult female mice (8-12 weeks old) were treated with either isotype control, rat IgG, or LYVE-1 blocking antibody C1/8 and 24 hours later injected intraperitoneally (i.p.) with WT BMDMs labelled with fluorescent dye CMFDA. After 24 hours of injection of macrophages, mice were killed and mediastinal lymph nodes were retrieved, mechanically disrupted to obtain single cell suspensions which were immunostained with myeloid cell marker CD11b (clone M1/70) to further identify macrophages by flow cytometry. The graph above shows quantitative assessment of cells arriving at mdLNs in rIgG, or C1/8 treated mice, with representative dot plots below the graph. The graph shown is representative of 3 independent experiments. Data are the mean ± SD of quadruplicate technical replicates. A two-tailed, unpaired Student's t-test was performed on this figure and p values below 0.05 were considered statistically significant (* $p < 0.05$; isotype control IgG vs C1/8). The appropriate statistical test to analyse this data would be a two way analysis of variance (ANOVA).

peritoneum for 5 days. Afterwards, the cavity was washed and peritoneal exudate cells (PECs) were stained for the macrophage marker F4/80, the neutrophil marker Ly6G and the myeloid cell marker CD11b, for analysis by flow cytometry (Fig 4-14). Myeloid cells make up the majority, and most of these are $F4/80^+$ cells with a minority of $Ly6G^+$ cells. A population of cells could also be distinguished that co-express F4/80 and Ly6G, and which have been reported to be of a monocyte phenotype. The notable population of neutrophils as part of PECs demonstrates the consistent ongoing inflammatory reaction generated by the inability to remove the BG beads from the site of inflammation.

4.3.6 Trafficking of macrophages in a model of Bio-Gel® stimulated peritonitis

The findings with murine BMDMs established that macrophages can traffic to lymph nodes without inflammatory stimuli, a finding that is broadly supported by the data in Chapter 3 demonstrating human monocyte derived macrophages can migrate across monolayers of unstimulated human lymphatic endothelial cells *in vitro*. But those findings also illustrated that macrophages transmigrate across activated LECs in greater numbers.

To determine whether trafficking to draining lymph nodes is enhanced in an inflamed peritoneum, PECs isolated from lavage after 5 days of BG bead stimulation were labelled with PKH26 and injected into either untreated adult mice, or mice at the same stage of inflammation as those from which the PECs were isolated. Mediastinal lymph nodes were retrieved from both sets of mice at intervals of 12, 24 and 36 hours. Isolated cells from the lymph nodes were stained with primary antibodies to markers expressed on the macrophage cell

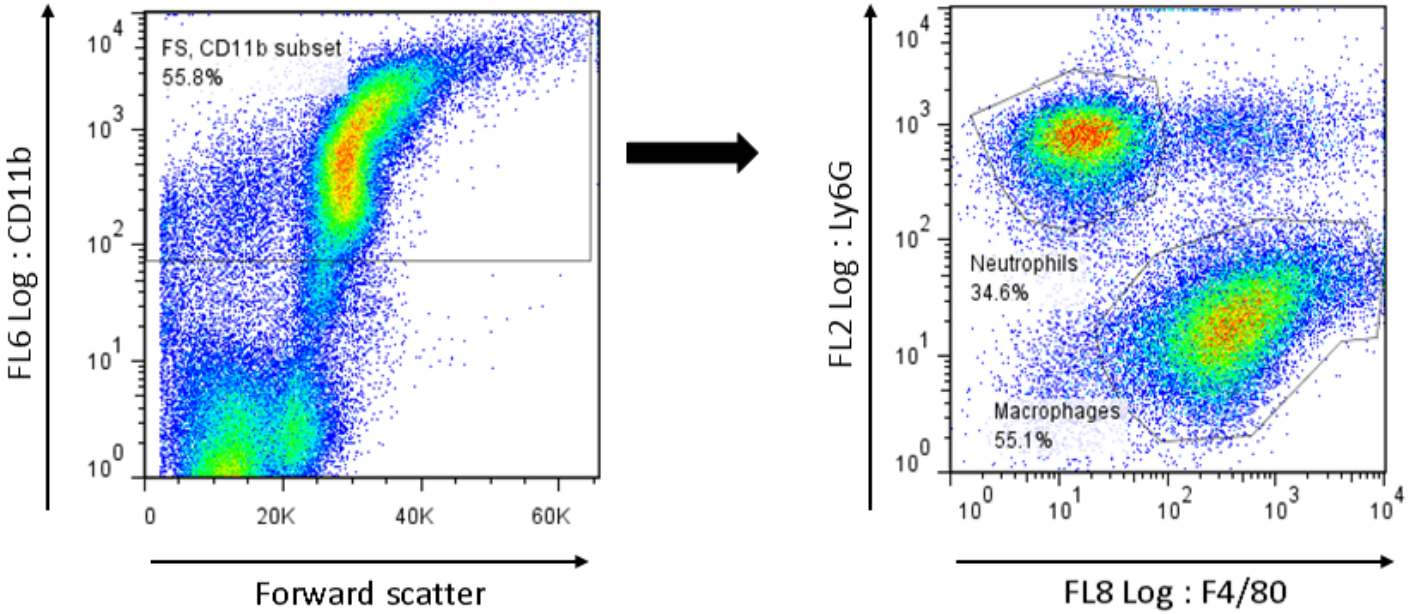


Figure 4-14: Flow cytometric analysis of peritoneal exudate cells (PECs) from inflamed peritoneum of mice. On day 0, adult female C57BL/6 mice (aged 8-12 weeks) were injected with Bio-Gel® polyacrylamide beads. On day 5, the peritoneum of the treated mice was washed with cold PBS and retrieved PECs were immunostained for surface markers, myeloid marker CD11b (clone M1/70), macrophage marker F4/80 (clone BM8) and neutrophil marker Ly6G (clone RB6-8C5), for analysis by flow cytometry. Analysis involves initially gating all CD11b+ cells to further identify Ly6G+ and F4/80+ cells, as indicated by the arrow. Expression levels were quantified by flow cytometry and representative dot plots are shown of an experiment that was repeated > 3 times.

surface, F4/80 and MHC-II, for analysis by flow cytometry (Fig 4-15). Quantification of the PKH26$^+$ population amongst other cells from lymph nodes reveals significantly more adoptively transferred PECs arriving from a BG stimulated peritoneum than an unstimulated one with a difference as great as 8-fold at one point; maximum numbers arrive by 24 hours and little change subsequently at 36 hours. Analysis of the fluorescent cells reveals > 85 % had the phenotype of F4/80$^+$MHC-II$^+$ expected of macrophages.

To distinguish whether the observed migration was proceeding via lymphatics or via the circulation, PKH26$^+$ PECs were introduced into the peritoneum of 5 day BG bead stimulated adult mice and after 24 hours the draining mediastinal and non-draining inguinal lymph nodes were retrieved. Cells isolated from respective lymph nodes were then stained with primary antibodies to F4/80 and MHC-II for investigation by flow cytometry (Fig 4-16). Quantitative comparison reveals significantly more fluorescent macrophages arriving at mdLNs compared to iLNs.

The above result provided persuasive evidence that macrophages migrated to draining nodes almost exclusively via lymphatics. This could be further reinforced by demonstrating whether macrophages enter lymph nodes via afferent lymphatics or via high endothelial venules (HEVs). PKH26 labelled PECs were injected i.p into stimulated adult mice and mediastinal lymph nodes were retrieved after 12 hours. Frozen sections of retrieved lymph nodes were stained with primary antibodies to LYVE-1 as it lined lymphatic sinus endothelia thus indicating of entry via afferent lymphatics, PNAd as it was expressed on HEVs and CD3 to show T cells within lymph node. Stained sections were

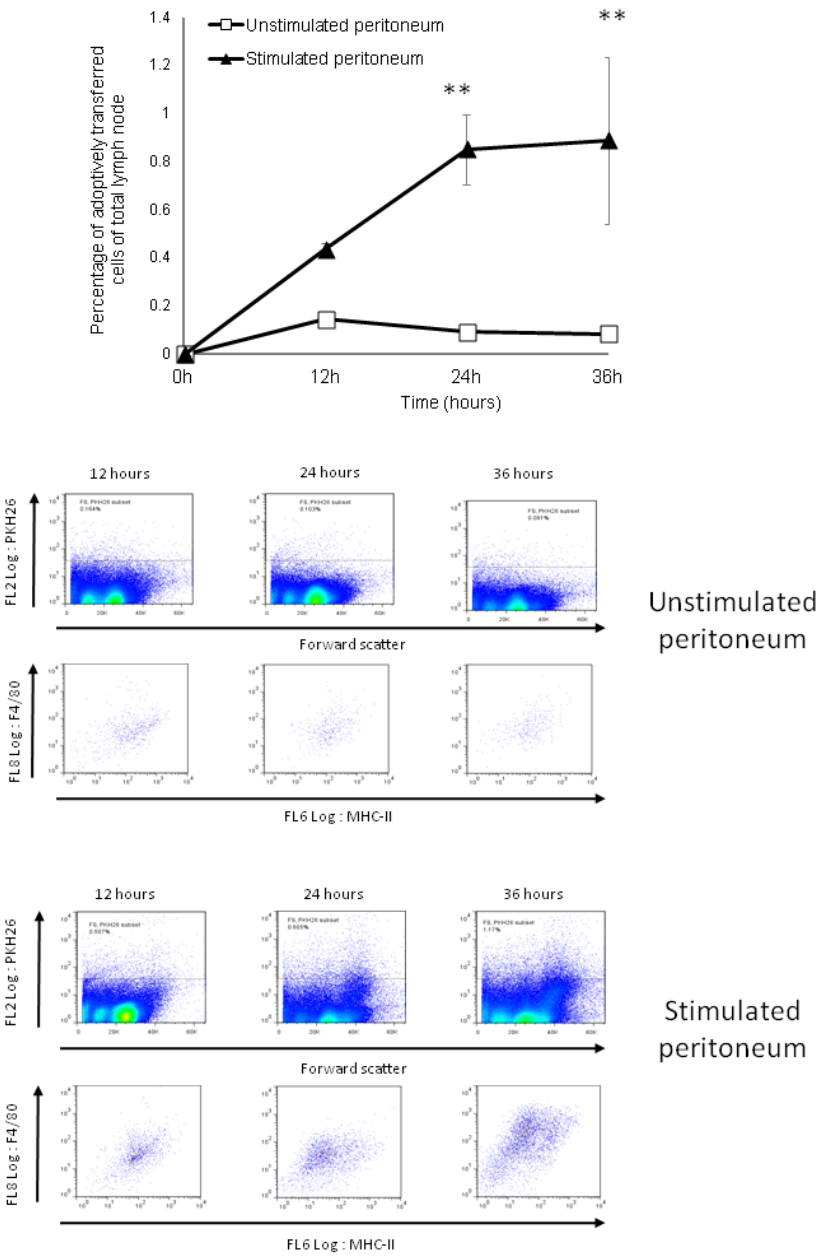


Figure 4-15: Comparison of time courses for macrophage migration to draining mediastinal lymph nodes from normal uninflamed and Biogel® bead stimulated (inflamed) peritoneum. On day 0, adult female C57BL/6 mice (8-12 weeks old) were injected with BG beads. On day 5, the peritoneum of treated mice was washed and retrieved PECs were labelled with PKH26 and injected into the peritoneum of either untreated mice, or 5 day BG bead treated mice. Mediastinal lymph nodes (mdLNs) were collected at time points of 12, 24 and 36 hours after injection of fluorescent cells and mechanically disrupted to produce single cell suspension that were immunostained for the surface markers, F4/80 using clone CI:A3-1, and MHC-II using clone M5/114.15.2 to identify macrophages by flow cytometry. The graph above shows quantitative assessment of cells arriving at mdLNs with representative dot plots below the graph. Fluorescent PKH26$^+$ cells are gated on for analysis of F4/80 and MHC-II. The graph shown is representative of 3 independent experiments. Data are the mean ± SD of quadruplicate technical replicates. A two-tailed, unpaired Student's t-test was performed on this figure and p values below 0.05 were considered statistically significant (** $p < 0.01$; unstimulated peritoneum vs stimulated peritoneum). The appropriate statistical test to analyse this data would be a two way analysis of variance (ANOVA).

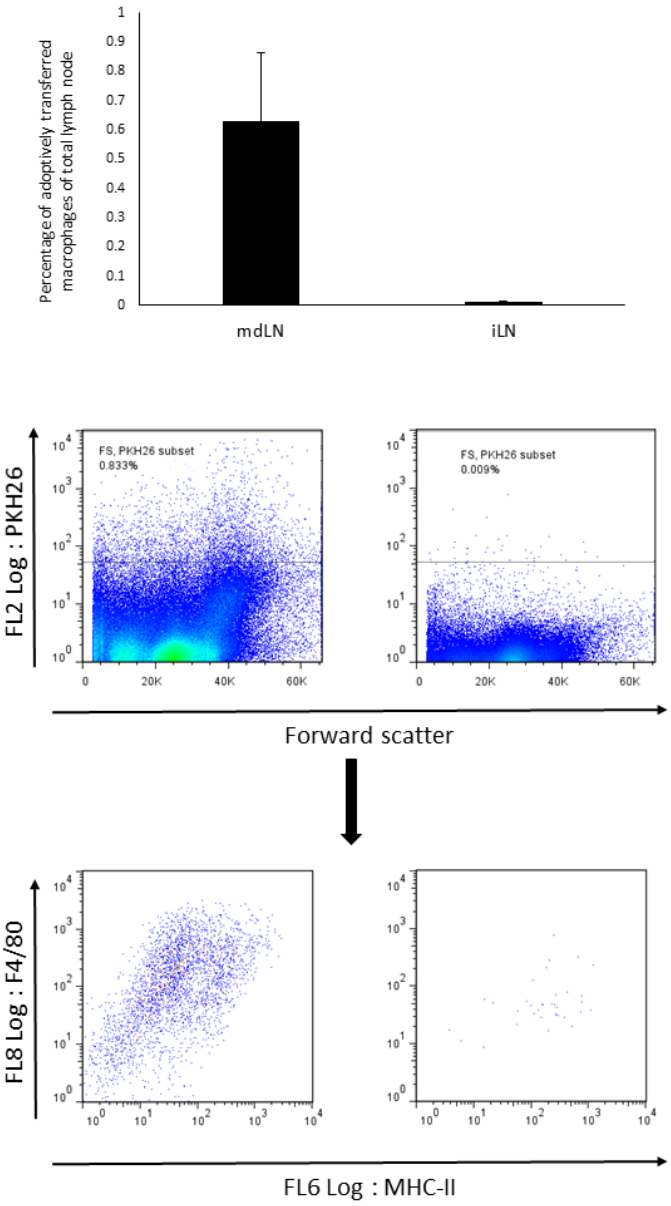


Figure 4-16: Recoveries of macrophages from sterile inflamed peritoneal cavity in draining and non-draining lymph nodes of the preferred route of migration of peritoneal macrophages. On day 0, adult female C57BL/6 mice (8-12 weeks old) were injected with BG beads. On day 5, the peritoneum of treated mice was washed and retrieved PECs were labelled with PKH26 and injected into the peritoneum of 5 day BG bead treated mice. Draining mediastinal lymph nodes (mdLNs) and non-draining inguinal lymph nodes (iLNs) were collected 36 hours after injection of macrophages and mechanically disrupted to produce single cell suspensions and cells were immunostained for cell surface markers, F4/80 (clone CI:A3-1) and MHC-II (clone M5/114.15.2) to identify macrophages by flow cytometry. The graph above shows quantitative assessment of cells arriving at either mdLNs, or iLNs of BG bead treated mice, with representative dot plots below the graph. The graph shown is representative of 3 independent experiments. Data are the mean ± SD of quadruplicate technical replicates. A two-tailed, unpaired Student's t-test was performed on this figure and p values below 0.05 were considered statistically significant. The appropriate statistical test to analyse this data would be a two way analysis of variance (ANOVA).

subsequently examined by confocal microscopy (Fig 4-17 and 4-18). Images taken showed most PKH26^{+} cells within the lymph node in association with LYVE-1^{+} sinus endothelium rather than by PNAd^{+} HEVs. Interestingly, the images also revealed macrophages interacting with CD3+ T cells within the lymph node.

4.3.7 Role of LYVE-1 in exit of macrophages via lymphatics from an inflamed peritoneal cavity

LYVE-1 has been implicated throughout various findings in this Thesis in contributing to migration of macrophages to draining lymph nodes. The results of the *in vitro* adhesion/transmigration experiments in Chapter 3 suggested LYVE-1 might play a role in the early stages of macrophage exit from tissue, specifically transmigration across activated lymphatic endothelium and as such it was likely that disruption of LYVE-1 function would give rise to impaired lymph node trafficking in the BG induced peritonitis model.

As with experimenting trafficking of BMDMs, the same two approaches of studying LYVE-1 function were used i.e. with *LYVE-1*$^{-/-}$ mice and LYVE-1-HA blocking monoclonal antibodies. Although migration of BMDMs from an uninflamed peritoneum appeared to be unaffected in *LYVE-1*$^{-/-}$ mice, it was considered possible that a blocking effect might be manifested in a BG bead inflamed peritoneum due to the greater numbers of macrophages that traffic in response to such inflammation (Fig 4-15). Accordingly, assessment of macrophages recovered in draining lymph nodes involved injecting PKH26 labelled PECs from 5 day BG bead stimulated peritoneum into the inflamed peritoneum of either wild-type (WT) mice, or *LYVE-1*$^{-/-}$ mice. Mediastinal lymph

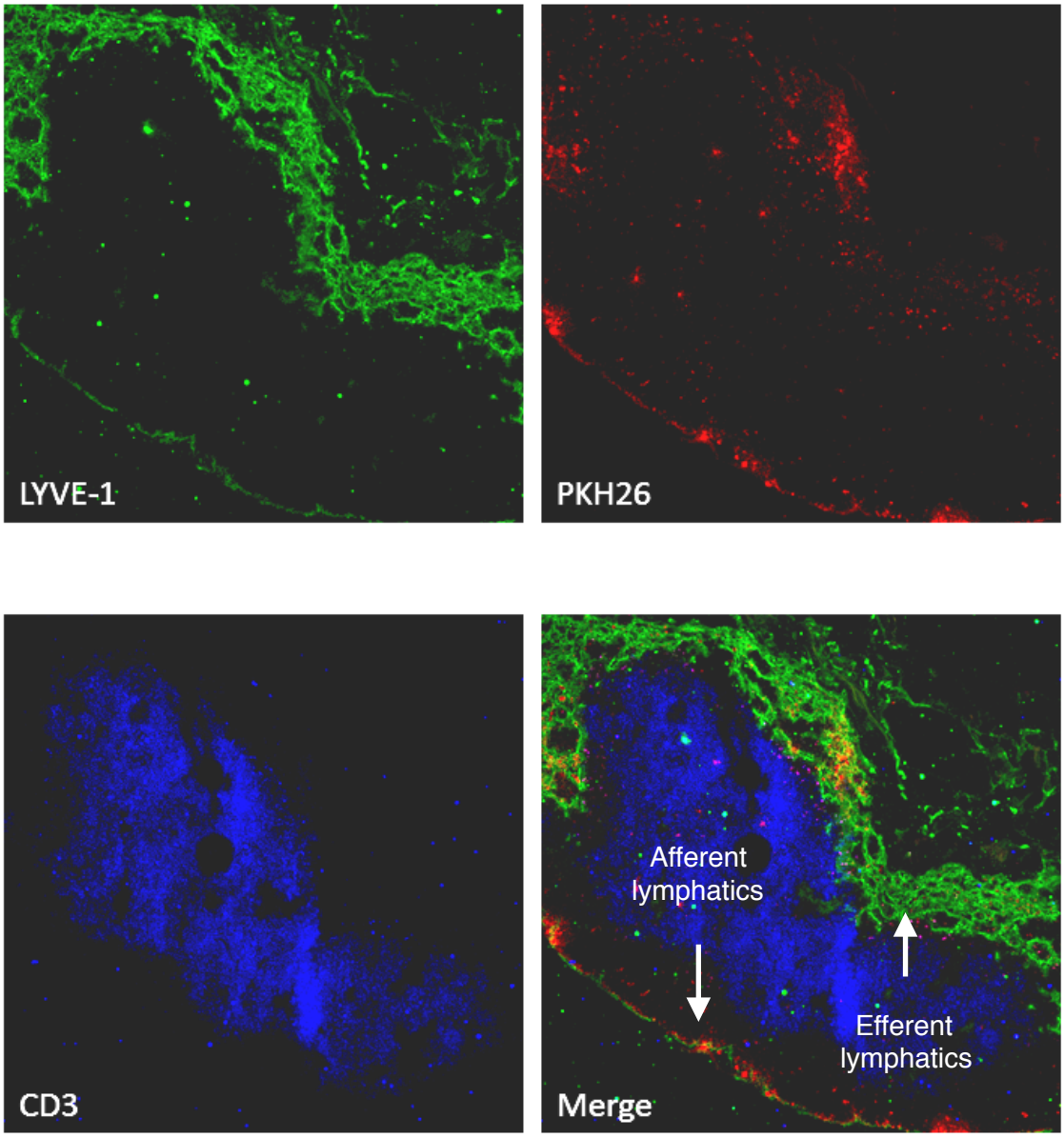


Figure 4-17: Characterisation of peritoneal macrophages in draining mediastinal lymph nodes. On day 0, adult female C57BL/6 mice (8-12 weeks old) were injected with BG beads. On day 5, the peritoneum of treated mice was washed and retrieved PECs were labelled with PKH26 (red) and injected into the peritoneum of 5 day BG bead treated mice. 12 hours after injection of cells, mice were killed and mediastinal lymph nodes were retrieved and embedded in Ornithine carbamoyltransferase (OCT)™ medium. Subsequently, 8 μm serial sections were cut by cryostat and immunostained for LN sinus endothelia marker LYVE-1 (green) using polyclonal antibody raised against LYVE-1 and T cell marker CD3 (blue) with monoclonal antibody 17A2. Sections were mounted in Vectorshield®. Confocal micrographs are shown at magnification of 10x, of an experiment that was repeated two times. White arrows indicate to afferent and efferent lymphatics.

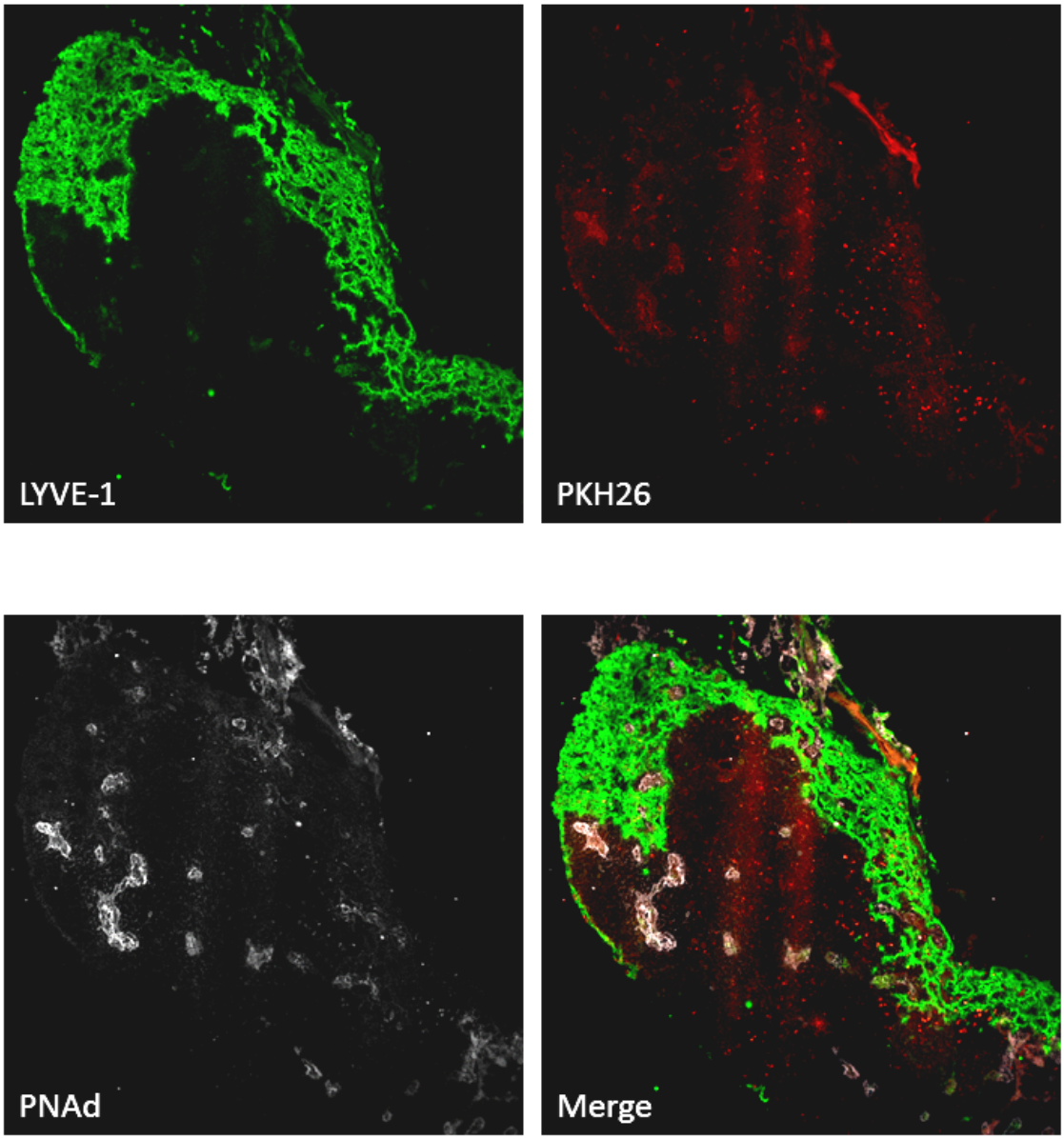


Figure 4-18: Characterisation of lymphatic route of entry of peritoneal macrophages into draining mediastinal lymph nodes. On day 0, adult female C57BL/6 mice (8-12 weeks old) were injected with BG beads. On day 5, the peritoneum of treated mice was washed and retrieved PECs were labelled with PKH26 (red) and injected into the peritoneum of 5 day BG bead treated mice. 12 hours after injection of cells, mice were killed and mediastinal lymph nodes were retrieved and embedded in Ornithine carbamoyltransferase (OCT) ™ medium. Subsequently, 8 μm serial sections were cut by cryostat and immunostained for LN sinus endothelia marker LYVE-1 (green) using polyclonal antibody raised against LYVE-1 and high endothelial venule marker PNAd (grey) with monoclonal antibody MECA79. Sections were mounted in Vectorshield®. Confocal micrographs are shown at magnification of 10x, of an experiment that was repeated two times.

nodes were retrieved from both sets of mice after 12 hours post-injection of PECs and isolated cells from disrupted tissue were stained with primary antibodies to F4/80 and MHC-II for analysis by flow cytometry (Fig 4-19). Quantitative comparison reveals a significant 5-fold reduction in fluorescent cells, of which the majority are F4/80^{+}MHC-II^{+} arriving to mdLNs of *LYVE-1*$^{-/-}$ mice.

As expected, the *LYVE-1*$^{-/-}$ mice displayed defective trafficking in inflamed conditions. The effect of LYVE-1 function blockade on trafficking of macrophages was previously demonstrated with blocking antibodies C1/8 and mAb2125, as shown with BMDMs. PKH26^{+} PECs were injected into BG inflamed peritoneums of adult WT mice that had been treated with either C1/8, or mAb2125 twenty four hours previously. Again, 12 hours post-injection of PECs, draining mdLNs were retrieved and single cell suspensions of the tissues were stained with F4/80 and MHC-II for identification by flow cytometry (Fig 4-20 and 4-21). With both of these blocking antibodies, an approximately > 2-fold reduction in arrival of adoptively transferred macrophages was observed. Taken together with the findings from *LYVE-1*$^{-/-}$ mice, the data suggests the HA receptor has a physiologically relevant role in clearance of macrophages from inflamed tissue.

Since fewer macrophages were trafficking in both experiments where the mice had LYVE-1 function disrupted, it was expected that greater numbers of the adoptively transferred cells would be recovered from the site of introduction, i.e. the peritoneal cavity. To validate this interpretation, PKH26^{+} PECs were injected into the inflamed peritoneum of either WT, or *LYVE-1*$^{-/-}$ mice; cells were washed out from the cavities of these mice 12 hours post-injection of fluorescent cells

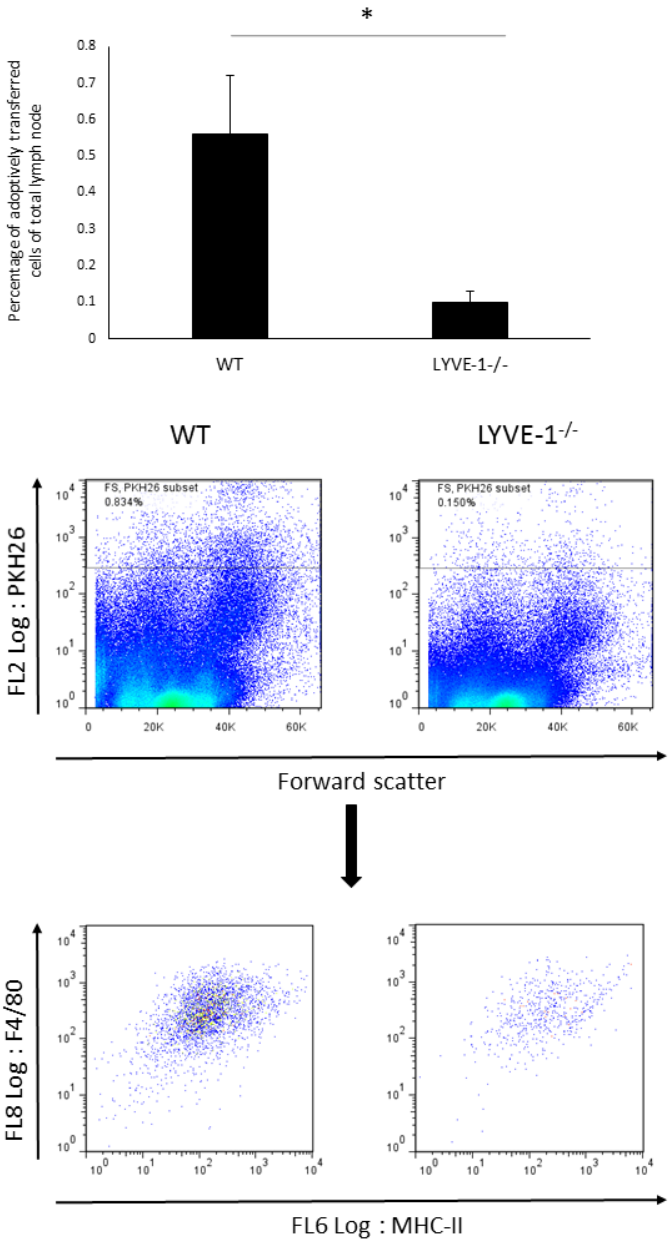


Figure 4-19: Effect of potent LYVE-1 genetic deletion on macrophage exit to draining lymph nodes from inflamed peritoneum in Biogel bead treated mice. On day 0, adult female C57BL/6 mice (8-12 weeks old) were injected with BG beads. On day 5, the peritoneum of treated mice was washed and retrieved PECs were labelled with PKH26 (red) and injected into the peritoneum of 5 day BG bead treated mice of either WT, or LYVE-1$^{-/-}$ background. 12 hours after injection of cells, mice were killed and mediastinal lymph nodes were retrieved and mechanically disrupted to produce single cell suspensions. Cells were immunostained for cell surface markers, F4/80 (clone CI:A3-1) and MHC-II (clone M5/114.15.2) to identify macrophages by flow cytometry. The graph above shows quantitative assessment of cells arriving at mdLNs in rIgG, or C1/8 treated mice, with representative dot plots below the graph. Fluorescent PKH26^{+} cells are gated on for analysis of F4/80 and MHC-II. The graph shown is representative of 2 independent experiments. Data are the mean ± SD of quadruplicate technical replicates. A two-tailed, unpaired Student's t-test was performed on this figure and p values below 0.05 were considered statistically significant (* $p < 0.05$; WT vs *LYVE-1*$^{-/-}$). The appropriate statistical test to analyse this data would be a two way analysis of variance (ANOVA).

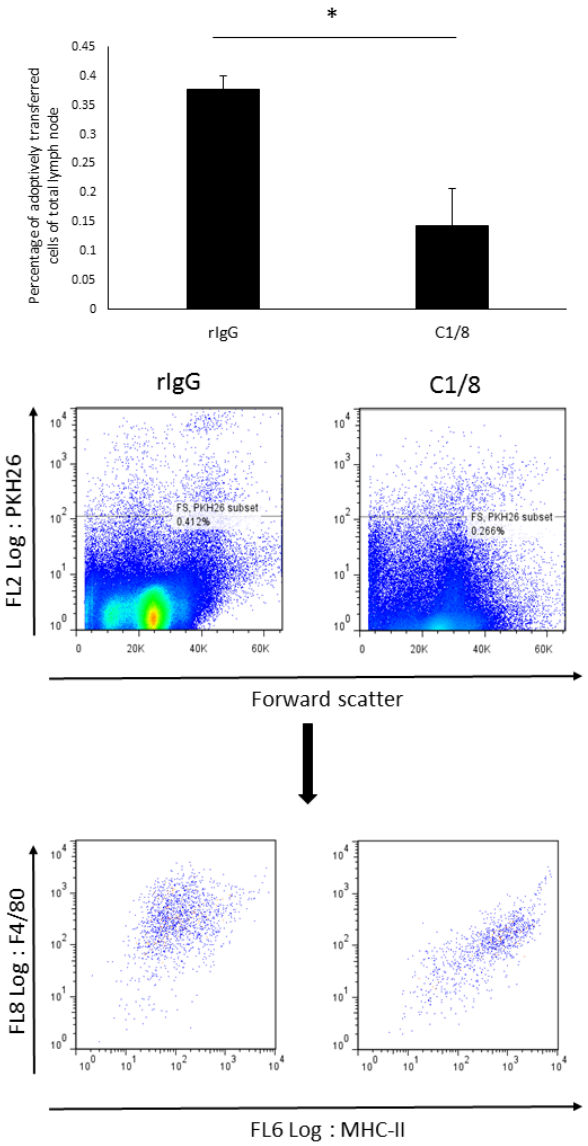


Figure 4-20: Effect of LYVE-1 antibody blockade on macrophage exit to draining lymph nodes from inflamed peritoneum in Biogel® bead treated mice. On day 0, adult female C57BL/6 mice (8-12 weeks old) were injected with BG beads and on day 4, a group of mice are treated with either isotype control rat IgG (rIgG), or LYVE-1 blocking antibody, C1/8. On day 5, the peritoneum of mice, not treated with antibodies, was washed and retrieved PECs were labelled with PKH26 (red) and injected into the peritoneum of antibody treated mice. 12 hours after injection of cells, mice were killed and mediastinal lymph nodes were retrieved and mechanically disrupted to produce single cell suspensions. Cells were immunostained for cell surface markers, F4/80 (clone CI:A3-1) and MHC-II (clone M5/114.15.2) to identify macrophages by flow cytometry. The graph above shows quantitative assessment of cells arriving at mdLNs in rIgG, or C1/8 treated mice, with representative dot plots below the graph. Fluorescent PKH26^{+} cells are gated on for analysis of F4/80 and MHC-II. The graph shown is representative of 3 independent experiments. Data are the mean ± SD of quadruplicate technical replicates. A two-tailed, unpaired Student's t-test was performed on this figure and p values below 0.05 were considered statistically significant (* $p < 0.05$; rIgG vs C1/8). The appropriate statistical test to analyse this data would be a two way analysis of variance (ANOVA).

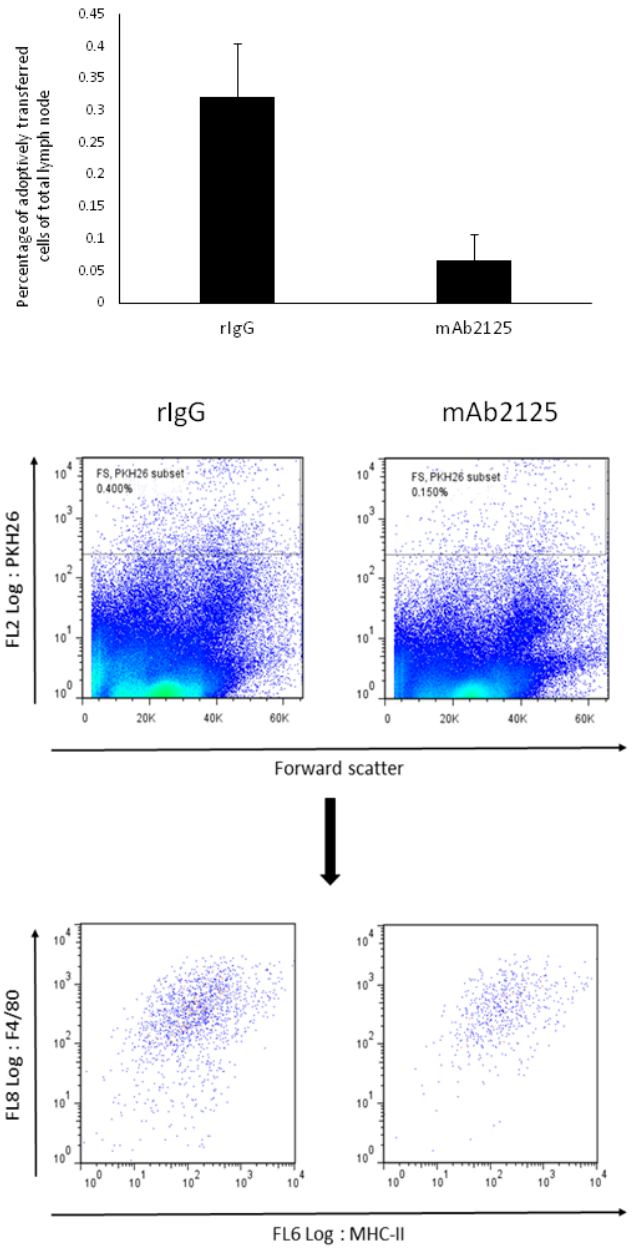


Figure 4-21: Effect of potent LYVE-1 antibody blockade on macrophage exit to draining lymph nodes from inflamed peritoneum in Biogel bead treated mice. On day 0, adult female C57BL/6 mice (8-12 weeks old) were injected with BG beads and on day 4, a group of mice are treated with either isotype control rat IgG (rIgG), or LYVE-1 blocking antibody, mAb2125. On day 5, the peritoneum of mice, not treated with antibodies, was washed and retrieved PECs were labelled with PKH26 (red) and injected into the peritoneum of antibody treated mice. 12 hours after injection of cells, mice were killed and mediastinal lymph nodes were retrieved and mechanically disrupted to produce single cell suspensions. Cells were immunostained for cell surface markers, F4/80 (clone CI:A3-1) and MHC-II (clone M5/114.15.2) to identify macrophages by flow cytometry. The graph above shows quantitative assessment of cells arriving at mdLNs in rIgG, or C1/8 treated mice, with representative dot plots below the graph. Fluorescent PKH26^{+} cells are gated on for analysis of F4/80 and MHC-II. The graph shown is representative of 2 independent experiments. Data are the mean ± SD of quadruplicate technical replicates. A two-tailed, unpaired Student's t-test was performed on this figure and p values below 0.05 were considered statistically significant. The appropriate statistical test to analyse this data would be a two way analysis of variance (ANOVA).

and stained with F4/80 and MHC-II, for subsequent analysis by flow cytometry. The data shown in figure 4-22 supports the hypothesis, demonstrating a > 2.5-fold level of fluorescent macrophages amongst the acquired peritoneal exudate cells from *LYVE-1*$^{-/-}$ mice. As the LYVE-1-HA mAb blockade experiments regarding recovery within the draining LN displayed similar results to the knock out mice, I anticipated a similar result regarding accumulation within the peritoneal exudate. Accordingly, PKH26+ PECs were injected into the inflamed peritoneum of adult WT mice given a single intraperiteoneal injection of the LYVE-1-HA blocking mAbs C1/8, or mAb2125, or a matched isotype control. Draining mdLNs were then retrieved after 12 hours and cells recovered from LNs were stained with antibodies to F4/80 and MHC-II, for subsequent analysis by flow cytometry; the data shown in figures 4-23 and 4-24, surprisingly, demonstrating disruption of LYVE-1 function with C1/8 and mAb2125 led to a significant decrease of fluorescent cells within the peritoneal exudate compared to isotype treated mice. Analysis of the phenotype of the fluorescent cells reveal that the adoptively transferred cells remaining behind were majorly of F4/80^{+}MHC-II^{low} phenotype, i.e. the non-inflammatory population. It is possible that the antibody blockade effects were only effective on lymphatic drainage route and hence the cells could be within another compartment within the peritoneum whereas the knock out mice effects are further widespread.

Overall, the results obtained in the above experiments provide preliminary evidence that LYVE-1 plays a role in guiding macrophage entry to peritoneal lymphatics and their migration to draining lymph nodes. Interestingly, contrasting results were obtained regarding the levels of adoptively transferred macrophages recovered within the peritoneal exudate depending on the

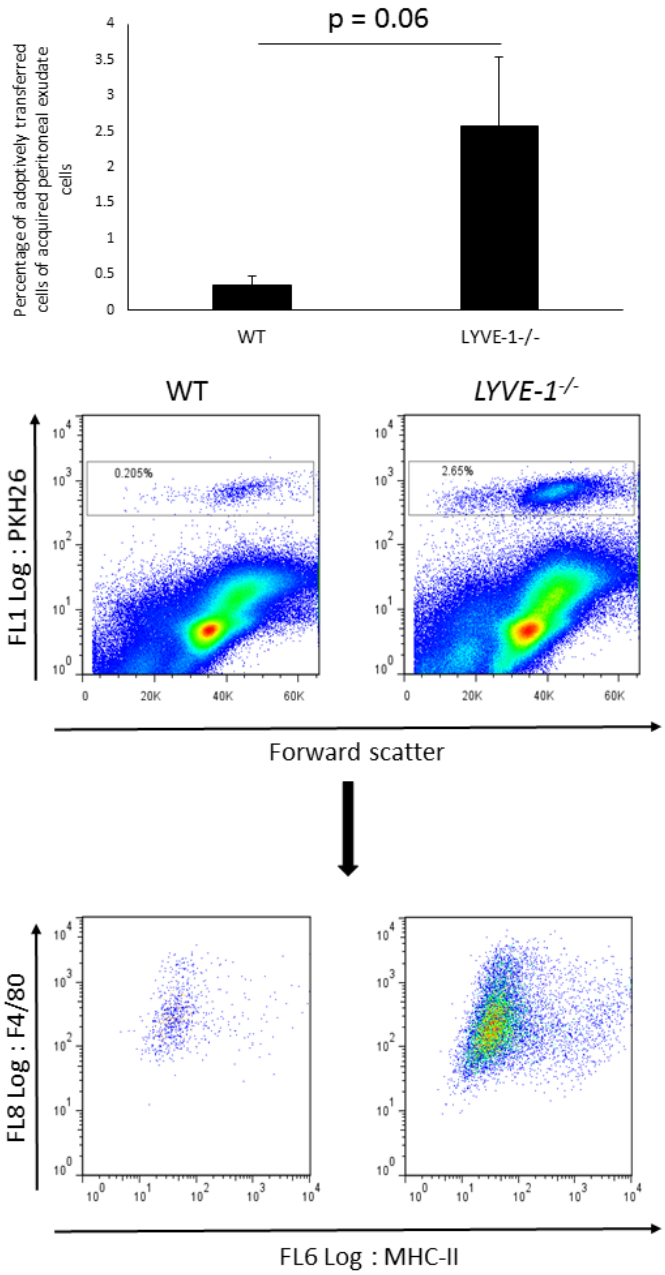


Figure 4-22: Effect of LYVE-1 genetic deletion on macrophage retention within inflamed peritoneal cavity of Biogel® treated mice. On day 0, adult female C57BL/6 mice (8-12 weeks old) were injected with BG beads. On day 5, the peritoneum of treated mice was washed and retrieved PECs were labelled with PKH26 (red) and injected into the peritoneum of 5 day BG bead treated mice of either WT, or LYVE-1$^{-/-}$ background. 12 hours after injection of cells, mice were killed, PECs were retrieved and immunostained for cell surface markers, F4/80 (clone CI:A3-1) and MHC-II (clone M5/114.15.2) to identify adoptively transferred macrophages by flow cytometry. The graph above shows quantitative assessment of cells retrieved by peritoneal lavage in WT, or *LYVE-1*$^{-/-}$ treated mice, with representative dot plots below the graph. Fluorescent PKH26^{+} cells are gated on for analysis of F4/80 and MHC-II. The graph shown is representative of 3 independent experiments. Data are the mean ± SD of quadruplicate technical replicates. A two-tailed, unpaired Student's t-test was performed on this figure and p values below 0.05 were considered statistically significant (p = 0.06; WT vs *LYVE-1*$^{-/-}$). The appropriate statistical test to analyse this data would be a two way analysis of variance (ANOVA).

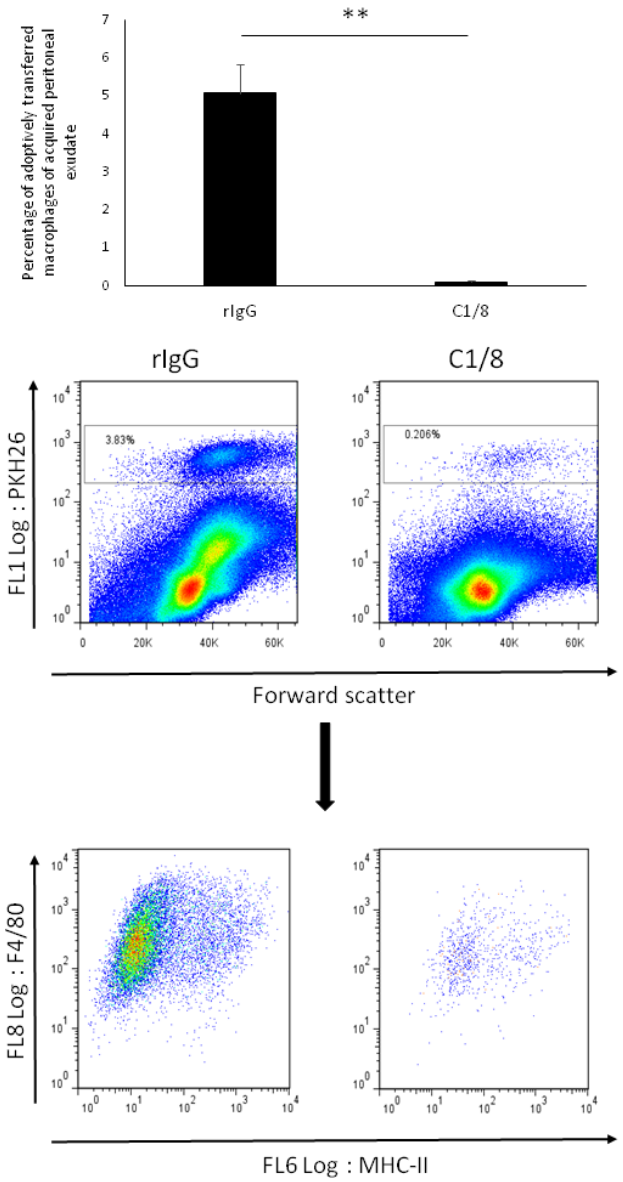


Figure 4-22: Effect of LYVE-1 antibody blockade on macrophage retention within inflamed peritoneal cavity of Biogel® treated mice. On day 0, adult female C57BL/6 mice (8-12 weeks old) were injected with BG beads and on day 4, a group of mice are treated with either isotype control rat IgG (rIgG), or LYVE-1 blocking antibody, C1/8. On day 5, the peritoneum of mice, not treated with antibodies, was washed and retrieved PECs were labelled with PKH26 (red) and injected into the peritoneum of antibody treated mice. 12 hours after injection of cells, mice were killed, PECs were retrieved and immunostained for cell surface markers, F4/80 (clone CI:A3-1) and MHC-II (clone M5/114.15.2) to identify adoptively transferred macrophages by flow cytometry. The graph above shows quantitative assessment of cells retrieved by peritoneal lavage in rIgG, or C1/8 treated mice, with representative dot plots below the graph. Fluorescent $PKH26^{+}$ cells are gated on for analysis of F4/80 and MHC-II. The graph shown is representative of 3 independent experiments. Data are the mean ± SD of quadruplicate technical replicates. A two-tailed, unpaired Student's t-test was performed on this figure and p values below 0.05 were considered statistically significant (** $p < 0.01$; rIgG vs C1/8). The appropriate statistical test to analyse this data would be a two way analysis of variance (ANOVA).

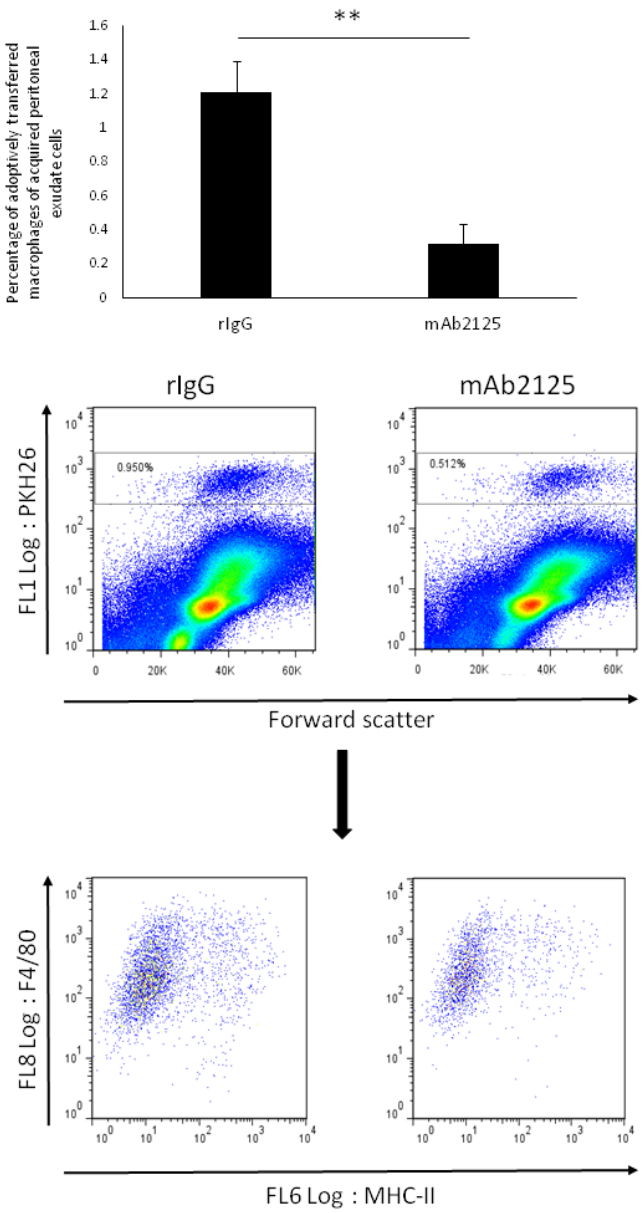


Figure 4-23: Effect of potent LYVE-1 antibody blockade on macrophage retention within inflamed peritoneal cavity. On day 0, adult female C57BL/6 mice (8-12 weeks old) were injected with BG beads and on day 4, a group of mice are treated with either isotype control rat IgG (rIgG), or LYVE-1 blocking antibody, mAb2125. On day 5, the peritoneum of mice, not treated with antibodies, was washed and retrieved PECs were labelled with PKH26 (red) and injected into the peritoneum of antibody treated mice. 12 hours after injection of cells, mice were killed, PECs were retrieved and immunostained for cell surface markers, F4/80 (clone CI:A3-1) and MHC-II (clone M5/114.15.2) to identify adoptively transferred macrophages by flow cytometry. The graph above shows quantitative assessment of cells retrieved by peritoneal lavage in rIgG, or mAb2125 treated mice, with representative dot plots below the graph. Fluorescent PKH26^{+} cells are gated on for analysis of F4/80 and MHC-II. The graph shown is representative of 3 independent experiments. Data are the mean ± SD of quadruplicate technical replicates. A two-tailed, unpaired Student's t-test was performed on this figure and p values below 0.05 were considered statistically significant (** $p < 0.01$; rIgG vs mAb2125). The appropriate statistical test to analyse this data would be a two way analysis of variance (ANOVA).

manner of LYVE-1 function disruption, with mAb blockade not leading to the expected accumulation but instead to a depletion in their numbers, suggesting that such blockade of the lymphatic exit route either leads to redirection via other exit route, accumulation within a compartment that is not available for lavage, or loss via apoptosis.

4.3.8 Redirection of macrophages to other sites with LYVE-1 function blockade by monoclonal antibodies

The reduction in numbers of adoptively transferred cells within the peritoneal cavity of mice injected with LYVE-1-HA blocking antibodies compared to isotype control injected mice might have occurred for several possibilities in particular. Firstly, blockade of the lymphatic route might have redirected clearance via an alternative route (e.g via blood circulation), secondly, blockade may indeed have have led to their accumulation in the peritoneum but in a compartment that was not accessible for lavage (e.g through firm adhesion to the peritoneal membrane) and thirdly blockade may have induced death by antibody toxicity or apoptosis. Initial experiments investigated the first of these possibilities by means of whole body imaging of adoptively transferred macrophages within the peritoneum and associated organs. .

To achieve this, PECs were isolated from 5 day BG bead stimulated mice and labelled with CellVue® NIR-815, a dye structurally similar to PKH26 but which fluoresces at near infra-red fluorescence wavelength, allowing visualisation of their fate after adoptively transfer by means of a LiCOR Odyssey imager which avoided the interference from background autofluorescence normally encountered with animal tissues. Accordingly, BG bead treated mice were

injected with CellVue® NIR-815 labelled macrophages together with either, LYVE-1 mAb2125, or isotype control treated mice, and whole body imaged 12 hours later. As shown by the results in Fig 4-24, in control mice, labeled macrophages (shown as green) were detected within the omentum (folds of visceral peritoneum extending from the curvatures of the stomach), parietal peritoneal membrane and adrenal glands atop kidneys (Fig 4-24b). In contrast in mice treated with mAb 2125, fluorescent macrophages were detected in the spleen and two distinct locations within the thoracic cavity tentatively identified as the lungs. Figure 4-25 shows a quantitative analysis of the fluorescence recovered from the different organs of control and mAb 2125 treated mice. Interestingly, the greatest difference in fluorescence is observed in the spleen where an approximately 50-fold greater level of CellVue NIR-815 labelled cells were present after mAb 2125 blockade compared to isotype control treated mice.

These results suggested that antibody blockade of LYVE-1 had indeed redirected the adoptively transferred cells, preferentially to the spleen. However, the images acquired above provided information in only two-dimensional space. To validate the findings using a different method, PKH26 labelled PECs were injected into the peritoneum of BG bead treated mice co-administered with mAb2125, or an isotype matched control IgG, and after 12 hours, spleens were removed for disruption and staining with the macrophage marker F4/80 for analysis by flow cytometry. The results (Fig 4-26A) reveal a > 3-fold increase in the proportion of $F4/80^{+}PKH26^{+}$ cells in the spleens of LYVE-1 mAb 2125 treated mice compared with controls. Moreover, in line with this increase there was a noticeable increase in the size of the spleens (Figure 4-26B).

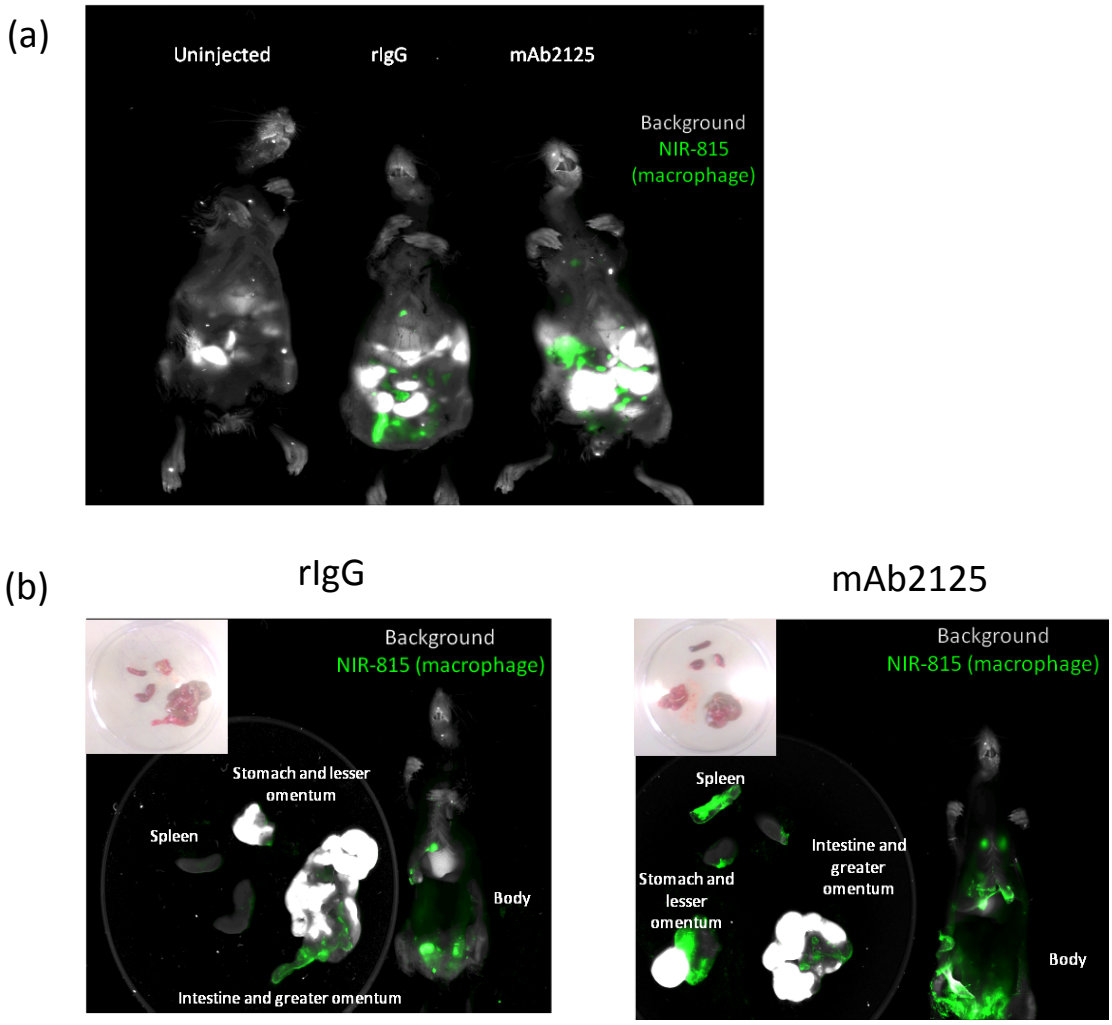


Figure 4-24: Characterisation of adoptively transferred macrophages within whole body of mice treated with LYVE-1 blocking antibodies. On day 0, adult female C57BL/6 mice (8-12 weeks old) were injected with BG beads and on day 4, a group of mice are treated with either isotype control rat IgG (rIgG), or LYVE-1 blocking antibody, mAb2125. On day 5, the peritoneum of mice, not treated with antibodies, was washed and retrieved PECs were labelled with NIR-815 (green) and injected into the peritoneum of antibody treated mice. 12 hours after injection of cells, mice were killed, undergone chemical depilation and imaged with a LI-COR™ near infra-red scanner with background from the starch emitting fluorescence at 700nm (white). (a) Whole body scans are shown of the two antibody treated mice next to an untreated control mouse; no fluorescence is detected in the control apart from the starch background. (b) Organs within the abdominal cavity of the mice illustrated above are retrieved and scanned along with the open body of the mice. Insets show photographs of organs placed on petri dish that were scanned. Images shown are representative of an experiment repeated two times.

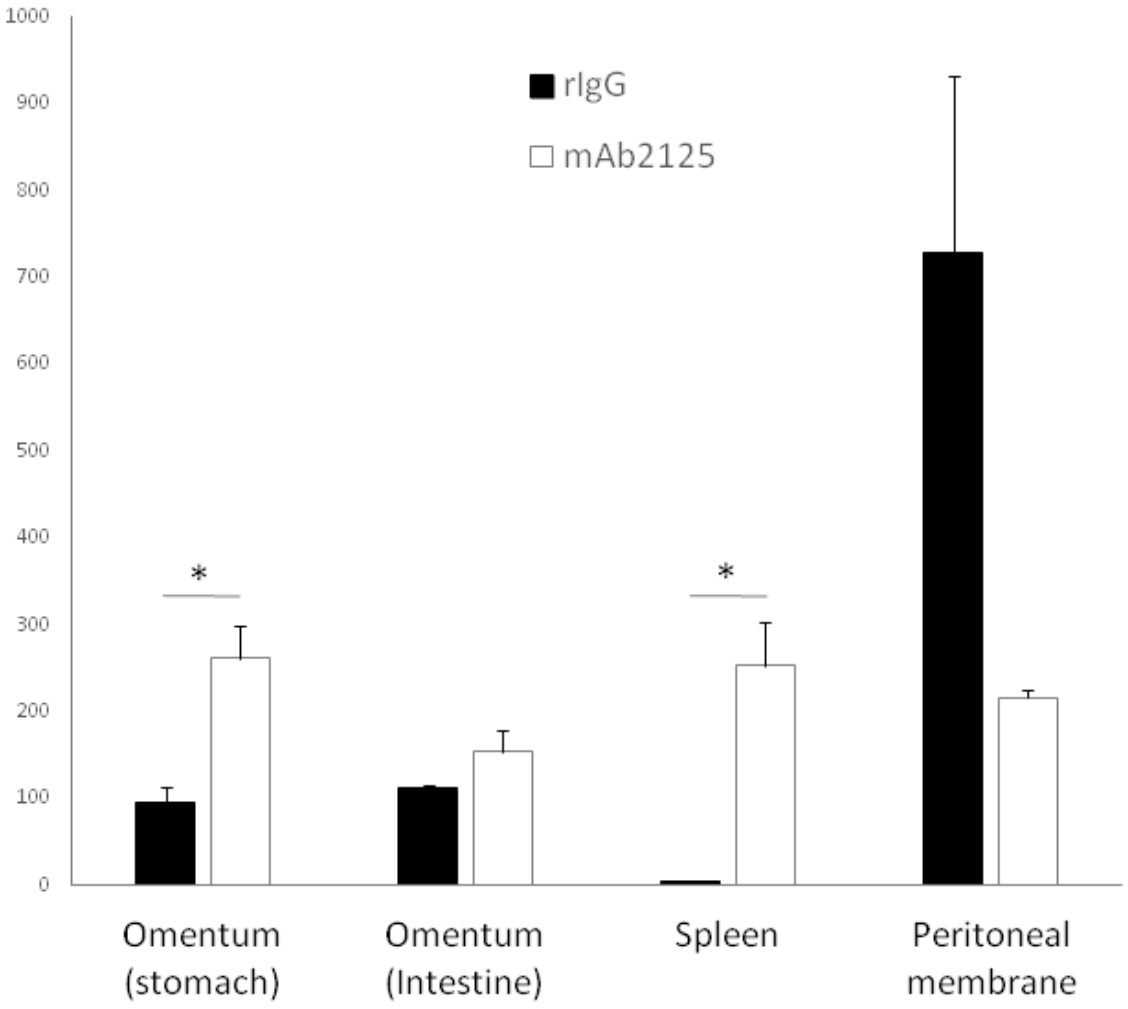


Figure 4-25: Effect of LYVE-1 blocking antibody on macrophage accumulation within other tissues of inflamed peritoneal cavity. On day 0, adult female C57BL/6 mice (8-12 weeks old) were injected with BG beads and on day 4, a group of mice are treated with either isotype control rat IgG (rIgG), or LYVE-1 blocking antibody, mAb2125. On day 5, the peritoneum of mice, not treated with antibodies, was washed and retrieved PECs were labelled with NIR-815 and injected into the peritoneum of antibody treated mice. 12 hours after injection of cells, mice were killed and organs within the peritoneal cavity i.e. stomach (with omentum), small intestine (with omentum), spleen and peritoneal parietal membrane were retrieved and imaged with a LI-COR™ near infra-red scanner and fluorescence quantified over area. Three mice were used per treatment group and data shown are representative of an experiment repeated 2 times. Data are mean ± SEM. A two-tailed, unpaired Student's t-test was performed on this figure and p values below 0.05 were considered statistically significant (* $p < 0.05$; rIgG vs mAb2125).

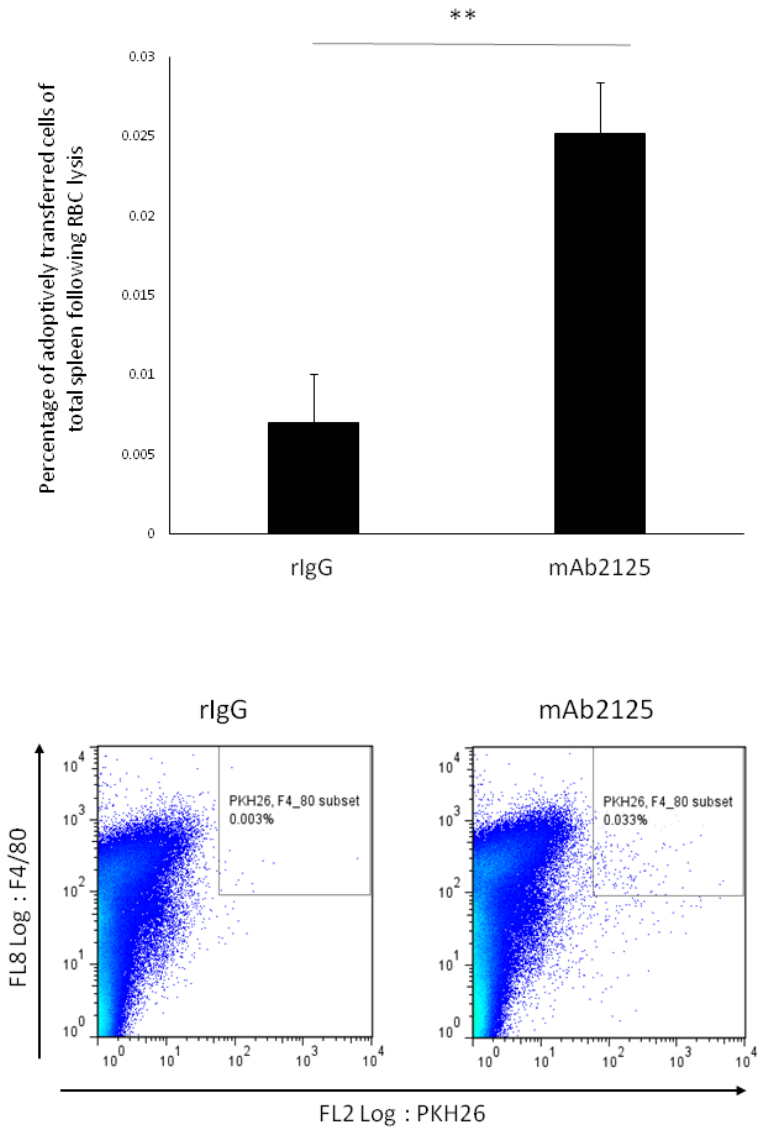


Figure 4-26A: Evidence that LYVE-1 mAb treatment re-directs macrophage exit route from inflamed peritoneum to spleen in Biogel bead treated mice. On day 0, adult female C57BL/6 mice (8-12 weeks old) were injected with BG beads and on day 4, a group of mice are treated with either isotype control rat IgG (rIgG), or LYVE-1 blocking antibody, mAb2125. On day 5, the peritoneum of mice, not treated with antibodies, was washed and retrieved PECs were labelled with PKH26 and injected into the peritoneum of antibody treated mice. 12 hours after injection of cells, mice were killed, spleens were retrieved and immunostained for cell surface markers, F4/80 (clone CI:A3-1) to identify adoptively transferred macrophages by flow cytometry. The graph above shows quantitative assessment of cells arriving at spleens in rIgG, or mAb2125 treated mice, with representative dot plots below the graph. The graph shown is representative of 2 independent experiments. Data are the mean ± SD of quadruplicate technical replicates. A two-tailed, unpaired Student's t-test was performed on this figure and p values below 0.05 were considered statistically significant (** $p < 0.01$; rIgG vs mAb2125). The appropriate statistical test to analyse this data would be a two way analysis of variance (ANOVA).

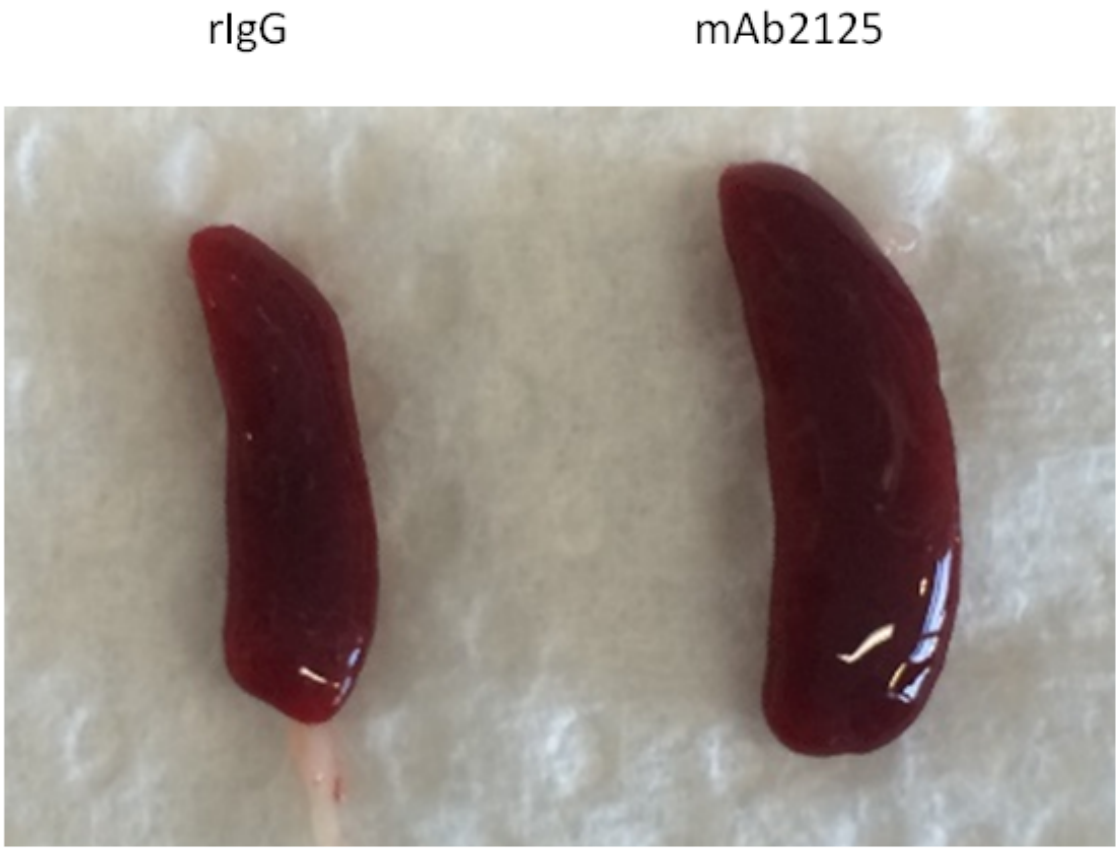


Figure 4-26B: Effect of LYVE-1 antibody blockade on macrophage trafficking to spleen from inflamed peritoneal cavity. Representative photograph of retrieved spleens of treated mice illustrated in 4-26A showing gross enlargement of the organ from mice treated with LYVE-1 blocking mAb2125.

Overall, these data suggest that blockade of LYVE-1-HA binding function in peritoneum redirects exit of macrophages towards several additional organs, with the spleen being the most predominant destination. However, a quick estimation of the numbers and overall size increase of the organ suggests that cell re-direction may be part of the overall effect of the antibody blockade; the other possibility being apoptosis, that I intended to investigate, but unfortunately, due to time constraints could not commence the necessary experiments.

4.4 Discussion

The findings in this chapter have demonstrated that macrophages can exit an inflamed peritoneal cavity, and migrate, albeit in relatively small numbers, via a LYVE-1:HA mediated route to draining lymph nodes. Although exit via lymph has been previously reported by independent studies, my studies have uncovered evidence of a novel mechanism that may involve use of openings resembling peritoneal stomata. Additionally, they identified a role for LYVE-1, expressed abundantly on the lymphatic endothelial cells that are present in these structures, through a combination of studies using genetic knock out mice and blockade of function with monoclonal antibodies.

The notion of macrophage migration via lymph has been somewhat controversial, and most models have studied the phenomenon using a model of inflammatory peritonitis (Gautier, Ivanov et al. 2013). A key set of experiments have provided robust confirmation that macrophages of myeloid origin (i.e. BMDMs) migrate to draining lymph nodes without requiring inflammatory activation of the tissue. The results of experiments in this chapter of my thesis revealed that trafficking of adoptively transferred cells from peritoneum to mediastinal nodes in normal resting mice reached maximal levels within 24 hours and was maintained with only a slight decrease after 36 hours. In addition, these experiments revealed that the state of activation of the macrophage is also important, as LPS activated macrophages arrived in greater numbers at the mdLNs. A calculation of the numbers of cells arriving at the lymph nodes, however, indicates that the lymphatics are a quantitatively minor route for exit from peritoneum, with less than 1 % of 5 x 10^5 input cells trafficking, a conclusion consistent with the findings of Gautier et al. (2013) that

macrophages migrating to lymph nodes are a minor subpopulation. One cannot rule out however that they may nevertheless play important roles in immune surveillance or immune modulation, given that their phagocytic cargoes could conceivably provide information about tissue integrity. The trend towards a decrease in macrophage numbers recovered in peritoneum after 36 hours may indicate that the cells either undergo apoptosis, or move further into blood circulation as suggested by Cao et al. (2005) before restoration of homeostasis. My comparisons with clearance of myeloid origin macrophages from inflamed peritoneal cavity yielded similar kinetics to uninflamed controls, with maximal numbers of inflammatory macrophages being recovered within 24 hours of adoptive transfer but with little change at subsequent time points. Interestingly, much greater numbers were shown to migrate to mediastinal nodes from an inflamed peritoneum, with up to 10 % of input macrophages of total adoptively transferred PECs being recovered after 24 hours, compared to 1 % in the normal resting peritoneum. Nevertheless, despite the greater percentage of input macrophages trafficking in peritonitis, this still represents a quantitatively minor number and again suggests exit via lymphatics is not a significant route for reduction in numbers during resolution of inflammation. Analysis of the macrophages recovered within the lymph node revealed them to express MHC-II, a key molecule involved in antigen presentation and indeed the migratory population may play role in antigen presentation similar to dendritic cells (DCs), whose primary function is to present antigen to naive T cells and initiate adaptive immunity. Macrophages and DCs are closely related, sharing common progenitors, so, it is reasonable for both cells to share similar functions. Delamarre et al. (2005) identified DCs to have limited lysosomal degradation of antigen after phagocytosis compared to macrophages thus retaining antigen

within lymphoid organs for extended periods and promoting an expansive adaptive immune activation unlike macrophages whose interactions were more brief. Perhaps macrophages migrating to lymph nodes are responsible for providing transient information of the environment rather than prolonged activation of T cells. This property is also consistent with differences in the kinetics of trafficking to draining lymph nodes for the two cell populations with the macrophages, as shown above, detected as early as 12 hours (Fig 4-15A) whereas DCs have been reported to take 1-3 days to arrive to lymph nodes (Martin, Ruiz et al. 2002, Mempel, Henrickson et al. 2004, Johnson, Clasper et al. 2006).

Although the process of macrophage exit from the peritoneum has been been described in outline to be via lymphatics, the work presented in this chapter provided novel evidence of how this is achieved *in vivo*. As outlined in the Introduction to this chapter, drainage had been proposed to proceed via the peritoneal membrane that involves exit via lymphatic stomata. Images from confocal microscopy in this chapter show macrophages within stomata like gaps expressing LYVE-1. Migration through gaps is vaguely reminiscent of DCs locating gaps within basement membrane of lymphatic vessels to gain access into vascular lumen via button junctions (Pflicke and Sixt 2009). Interestingly, stomata are strategically located to lead into lacunae which drain to lymphatic vessels and do not appear to be found randomly across the parietal membrane, a similarity seen with the portals on basement membrane which are only found near initial lymphatic capillaries (Abu-Hijleh, Habbal et al. 1995). Pflicke and Sixt (2009) also showed that these pre-existing portals increase in size as DCs begin to associate with them. Further in-depth imaging studies will be required

to determine if such dynamism is also associated with lymphatic stomata and the possible changes these gaps go through in peritonitis.

The mechanisms directing cells towards the stomata from the peritoneal cavity are still a mystery although is reasonable to speculate that it maybe mediated by chemokines. Indeed inhibition of G-protein coupled receptor function by Pertussis toxin (PTX) was reported to prevent macrophage emigration to LNs (Gautier, Ivanov et al. 2013). Peritoneal mesothelial cells surrounding the stomata secrete numerous chemokines, such as CCL2 and CCL5, that would attract Bio-Gel® bead elicited macrophages, although whether these stomata can secrete CCL21, a chemokine primarily associated with trafficking via lymphatics, is yet to be shown (Li, Davenport et al. 1998). However, whether any possible secretion of CCL21 is relevant to macrophage trafficking is another question since it seems CCR7 deficient macrophages are able to migrate to dLNs as readily as WT macrophages. The atypical chemokine receptor 2 (ACKR2) is also believed to regulate macrophage recruitment to lymphatic vessels and coordinates its actions with CCL2 attraction of macrophages to lymphatic vessels (Lee, Danuser et al. 2014). Insight into the roles of chemokines also came from preliminary *in vitro* studies throughout the course of this D.Phil. where I observed supernatant from activated HDLEC monolayers was able to induce rapid migration of human monocyte derived macrophages across bare inserts in transwell chemotaxis assays. Future investigations into chemokine roles in attracting macrophages to lymphatics will uncover further levels to mechanisms driving macrophage trafficking to draining lymph nodes.

Images of lymph node sections shown in this chapter (Fig 4-17 and 4-18) point to macrophages entering via afferent lymphatics rather than through high endothelial venules (HEVs) thus providing further evidence of the afferent lymphatic route macrophages take on clearance from the peritoneal cavity. Interestingly, the images also revealed PKH26 colocalising with $CD3^+$ T-cells in the medulla of the lymph node. Leukocytes arriving via afferent lymphatics are believed to pass antigen to subcapsular sinus macrophages which then activate B cells or via resident DCs which in turn activate T cells (Carrasco and Batista 2007, Gerner, Torabi-Parizi et al. 2015). However, phenotyping of all the fluorescent cells by flow cytometry arrving at dLNs performed throughout this Chapter consistently suggests that the majority co-express F4/80 and MHC-II implying that it is the macrophages interacting with T cells seen in figure 4-17, previously not shown in independent reports with the peritonitis model. Yet, macrophages are well known along with B cells to present antigen to $CD8^+$ T cells whereas indirect presentation by B cells primes $CD4^+$ T cells and hence it will be necessary to phenotype the $CD3^+$ cells to understand which class of T cells the macrophages are interacting with (Constant 1999, Pozzi, Maciaszek et al. 2005). Another insight from this observation, brings to scrutiny the level of activation of the lymphocytes with which macrophages are seen to interact with in draining lymph nodes. Priming of T cells takes place in 3 distinct phases which extends beyond the time frame of lymph nodes isolated 12 hours post transfer of cells as seen here (Mempel, Henrickson et al. 2004). Gautier et al. (2013) identified that the macrophages entering the mediastinal lymph node from inflamed peritoneum expressed the scavenger receptor CD36. B class scavenger receptors, such as CD36, are prominently expressed on the surface of M2 macrophages thus presenting the complexity of the ‘inflammatory’

macrophage phenotype within lymph nodes and complicates the scenario further in terms of subsets within the peritoneal macrophage population that are able to migrate (Canton, Neculai et al. 2013). Also, due to possibly having a partial M2 phenotype, they may function to suppress T cell activation (Huber, Hoffmann et al. 2010). Figures 4-17 and 4-18 also show adoptively transferred macrophages present in efferent lymphatics indicating that mediastinal lymph nodes were not the final destination and that these macrophages travel further up the lymphatic trunk and possibly enter circulation, an observation that has previously been reported (Cao, Lawrence et al. 2005). Further phenotyping with other markers will be required to understand the subset of macrophages arriving and whether a subset within those adoptively transferred macrophages are prone to exit via the efferent lymphatics. Such a scenario does present the question of what the final fate of the macrophages may be? One possibility is that macrophages re-enter the circulation and traffic to other tissues. However, it should be noted that such trafficking may be a a specific property of adoptively transferred cells and may not reflect the functions of native resident inflammatory ones. Further studies employing longer time-courses and sampling other tissues would help to answer these questions.

One of the key findings in this chapter was that exit from peritoneum involved interactions with LYVE-1. The two ways in which this was shown *LYVE-1*$^{-/-}$ mice and function blocking monoclonal antibodies.

The impact of LYVE-1 was initially debated as there was no apparent defect of BMDM migration to mediastinal lymph nodes in *LYVE-1*$^{-/-}$ mice under conditions of normal homeostasis but blocking antibodies C1/8 and mAb2125 were able to cause a reduction in accumulation. It should be noted that *LYVE-1*$^{-/-}$ mice have

been reported to have a normal lymphatic architecture and it is likely that there are compensatory mechanisms which make up for any defects in trafficking in these animals, unlike in wild-type mice that had sudden functional defects in LYVE-1 due to administration of LYVE-1 antibodies. In contrast, *LYVE-1*$^{-/-}$ mice displayed defective trafficking of macrophages to lymph nodes under inflammatory conditions. This suggested LYVE-1 maybe mediating structural alterations in lymphatic vessels during inflammation. The effect of inflammation on initial lymphatic capillaries has been extensively investigated by the laboratory of Donald McDonald; independent publications reporting a change from button to zipper junctions in persistent inflammatory conditions (Yao, Baluk et al. 2012). The appearance of zipper junctions at initial lymphatic capillaries was gradual and was fully apparent after two weeks of mycobacterial inflammation. However, the trafficking experiments were conducted over a much shorter time-frame, so, such changes would seem to be unlikely to cause the defect in migration. Nonetheless, it would be interesting to assess if the kinetics behind the conversion to zipper junctions is altered in *LYVE-1*$^{-/-}$ mice. Zipper junctions are associated with impaired fluid clearance and diminishing health and is unlikely to bolster entry of cells into vessels. Indeed the retention of the adoptively transferred cells within the peritoneal exudate of the knock-out mice indicates failed access of the lymphatics and that LYVE-1 was involved in regulating entry within the initial capillaries.

As mentioned above, both C1/8 and mAb2125 reduced the number of macrophages trafficking to lymph nodes, in both homeostatic and inflammatory conditions. The results establish the importance of LYVE-1-HA interactions in mediating macrophage migration. Interestingly, rather than promoting an

accumulation of macrophages in the peritoneal cavity, as expected and observed with the *LYVE-1*$^{-/-}$ mice, treatment with these antibodies led to a reduction in their numbers, suggesting the cells had either undergone apoptosis or accelerated migration via another route. Analysis of the lavage also revealed that of the fluorescent F4/80 cells amongst the acquired peritoneal exudate cells, most were MHC-II$^{-/low}$, unlike the MHC-II^{+} macrophages within the draining LNs, indicating that trafficking specifically of the latter subset was influenced by LYVE-1 disruption. MHC-II$^{-/low}$ macrophages have been associated with the resident peritoneal macrophage population (Davies, Jenkins et al. 2013), which derive from the yolk sac and which are not considered to be migratory whereas the MHC-II^{+} population are derived from monocytes, which have the greater migratory capacity. Remarkably, the full body imaging of near infra-red (NIR) fluorescence revealed that cells were indeed migrating to different locations across the body with a notable redirection to the spleen. The omentum is another prominent location of migration in homeostasis with increases in fluorescence upon LYVE-1 blockade. It is well established that the omentum is a component of mesentery tissue (i.e. made of from a double fold of visceral peritoneum) and hence would contain lymphatic draining structures along with blood vessels and nerves. It is likely that the omentum functions as an accessory site or a depot since it has large surface area, until increased cell numbers from inflammation are gradually reduced to return homeostasis by undergoing apoptosis or migrating to lymph nodes. In the advent of LYVE-1 function blockade, it is imaginable for it to become a favourable site through which re-entry into the circulation might occur. The mechanism of entry into omentum was not explored as there was insufficient time. Nonetheless, it could be gathered from a superficial consideration of the anatomy that as an

extension of the peritoneum, it would behave similarly to the parietal peritoneal membrane and interactions would be mediated in the same manner. Chemotaxis is one plausible mechanism with omental tissue known to attract B cells expressing CCR5 through production of CXCL13 (Ansel, Harris et al. 2002). Since BG bead induced macrophages respond to CCL5, it is likely they express CCR5 too and would be able to migrate in response to gradients of CXCL13 (Iqbal, Regan-Komito et al. 2013). Adhesion is also an important step in access to the tissue, with lymphocyte entry into omentum dependent upon β1 and β2 integrins, both expressed by macrophages (Carlow, Gold et al. 2009). Although not categorised as secondary lymphoid tissue, the omentum is gradually becoming accepted as a site of adaptive immune activation due to lymphocyte homing and activation within and it is possible that macrophages migrate to the omentum to aid in such a process.

A striking finding was that LYVE-1-HA blocking antibodies induced redirection to the spleen. The reason for migration to spleen is yet to be understood and raises many interesting questions into how LYVE-1 function blockade resulted in such a scenario. One such possible route would be through blood vessels found in peritoneal membrane but transmigrating across endothelium that have zipper junctions and then travelling through circulation to enter the spleen presents an arduous and complex journey. Closer inspection of the anatomy of the abdominal cavity reveals more plausible routes; the greater omentum is in physical contact with the spleen as well as having a network of blood vessels that tie in with the vessels supplying the spleen from the coeliac trunk thus behaving as the likely link for cells migrating across towards the spleen. The involvement of the spleen in recruiting macrophages upon LYVE-1 blockade is yet to be solved but is likely to involve chemokines and adhesion molecules.

Prominent chemokines involved in recruiting T and B cells to the spleen are CCL19/21 and CXCL13, respectively, could also potentially recruit macrophages as they express chemokine receptors to the following chemokines (Ansel, Harris et al. 2002, Luther, Bidgol et al. 2002). The purpose of arriving at the spleen is an interesting one and could possibly be the final location of the cells for further degradation. It is possible that cells migrate to the spleen without LYVE-1 blockade but at later time points, since it appears that LNs are not the final destination with macrophages exiting via efferent lymphatics; by possibly entering circulation via the subclavian vein they could then travel for eventual death in the spleen, similar to other cells including red blood cells (Mebius and Kraal 2005). If so, LYVE-1 blockade would appear to cause macrophages to bypass the long journey and enter the spleen quickly. Examination of the impact of LYVE-1 blockade on the spleen also brought to attention the splenomegaly the treatment caused. Although a measurement was not taken of the increase in size, it seems unlikely that small increase in numbers of macrophages into the spleen would have been the primary cause, thus suggesting the comprehensive impact of LYVE-1 blockade is beyond macrophage trafficking.

Overall, the data in this chapter establish macrophage migration to lymph nodes as a rapid process with LYVE-1 contributing to the overall process. The following chapter will address other components to LYVE-1-HA axis in trafficking and the effect of inflammation on HA presentation for transmigration and trafficking.

Chapter 5.

The role of CD44 in trafficking of macrophages to draining lymph nodes and characterisation of hyaluronan production by macrophages

5.1 Introduction

The work presented in the previous chapters of this thesis has identified the LYVE-1-hyaluronan axis as a new and previously unrecognised component of the machinery that mediates transmigration of lymphatic endothelium by macrophages and that regulates their exit from inflamed peritoneum via afferent lymphatics in mice. In many ways this parallels the utilisation of the CD44-HA axis for exit of leucocytes from the blood circulation via inflamed post-capillary venules, although in that case the orientation is reversed with HA being presented by endothelium and CD44 being present on the transmigrating leucocyte (Clark, Alon et al. 1996, DeGrendele, Estess et al. 1997). As CD44 is not normally expressed in lymphatic endothelium, one can assume that its closest homologue, LYVE-1, fulfills a similar but nevertheless distinct role (Banerji, Ni et al. 1999, Prevo, Banerji et al. 2001). Indeed the current model for the role of the CD44-HA axis in transmigration of blood vascular endothelium proposes a 'sandwich' whereby leucocyte CD44 engages HA that is in turn displayed by CD44 in endothelium. By extension, a similar sandwich has been proposed to operate in the lymphatics, with LYVE-1 substituting for CD44 in lymphatic endothelium (Fig 5-1) (Jackson, Prevo et al. 2001).

CD44, like LYVE-1, is a member of the Link protein superfamily and is regarded as the primary receptor for hyaluronan on haematopoietic and epithelial cells (Aruffo, Stamenkovic et al. 1990, Stamenkovic, Aruffo et al. 1991). Unlike LYVE-1, the CD44 gene undergoes alternative splicing to generate multiple different splice variants with variable extracellular domain inserts that have tissue specific expression patterns (Jackson, Buckley et al. 1992). The range of

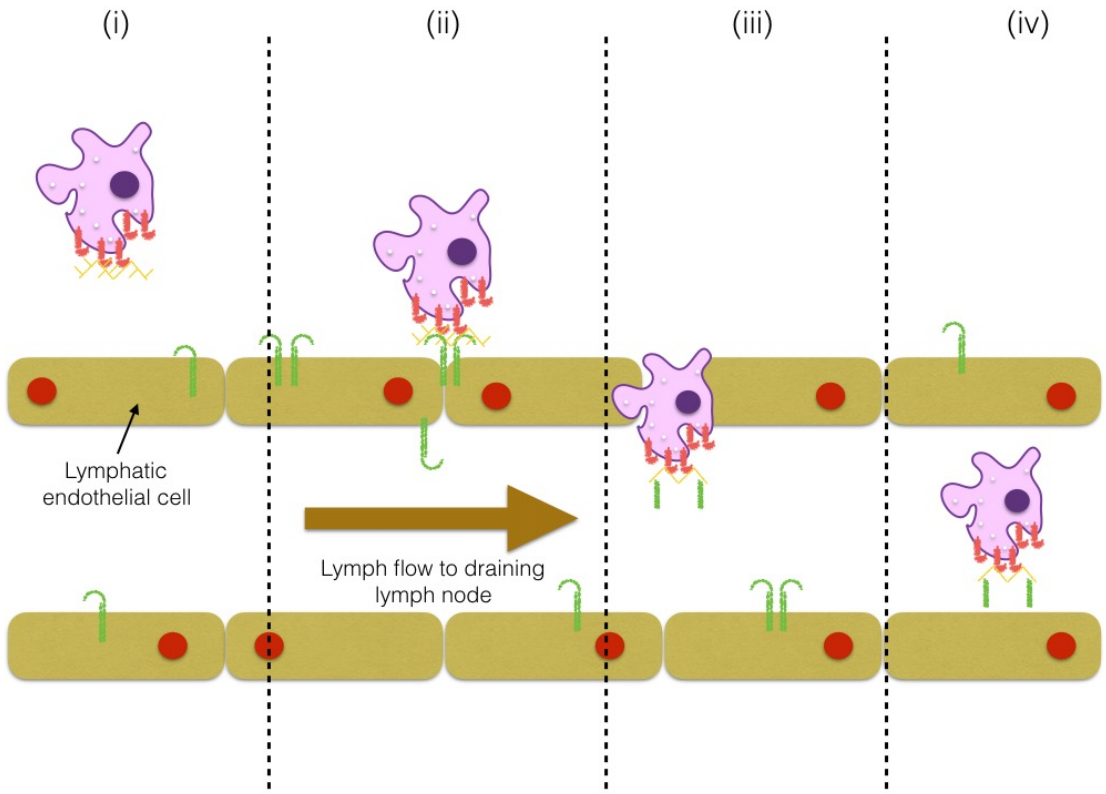


Figure 5-1. Schematic representation of hypothetical mechanism of macrophage transmigration of lymphatic endothelium in transit to draining lymph node during acute inflammation. (i) Macrophages expressing hyaluronan (HA), which is bound to surface CD44, arrive to lymphatic vessel. (ii) Macrophage expressed HA, bound to CD44, engages with clustered LYVE-1 on basolateral surface. (iii) Macrophages transmigrate into the lumen of the vessel, now carrying LYVE-1, acquired from the surface of LECs. (iv) The transmigrated cells migrate to draining lymph nodes.

cell types that express CD44 and its splice variants is large, and includes both monocytes and macrophages which express predominantly the lower molecular weight haemopoietic form, in contrast to epithelial cells and keratinocytes, which express predominantly larger molecular weight (splice Va) (Jackson, Buckley et al. 1992). However, all variants contain the N-terminal HA-binding Link domain, and CD44 on monocytes/macrophages is known to bind HA efficiently, particularly after maturation and exposure to inflammatory cytokines (Levesque and Haynes 1996, Levesque and Haynes 1997, Ponta, Sherman et al. 2003). Numerous functions attributed to CD44 are mediated by its capacity to bind HA, such as, T cell differentiation, pro-apoptosis signalling, axon deterrent, to name a few along with the important role of mediating leucocyte rolling interactions on inflamed blood endothelium for subsequent transmigration (Ponta, Sherman et al. 2003). Both Clark et al. (1996) and DeGrendele et al. (1996) have shown independently that lymphocytes utilise CD44-HA interactions in mediating rolling adhesion during extravasation from the blood circulation in inflamed tissues, with further work extending to similar findings with neutrophils (Khan, Kerfoot et al. 2004, McDonald, McAvoy et al. 2008). The involvement of CD44 in different physiological aspects has been uncovered through the use of function blocking antibodies and CD44 homozygous gene knockout mice (*CD44*$^{-/-}$). Initial observations suggested that *CD44*$^{-/-}$ mice enjoyed a normal healthy phenotype without overt physiological defects, a feature they appear to share with *LYVE-1*$^{-/-}$ mice, although subsequent detailed studies revealed that defects are in fact manifest after exposure to inflammatory conditions (Protin, Schweighoffer et al. 1999, Ponta, Sherman et al. 2003). Notably, Teder et al. (2002) demonstrated that *CD44*$^{-/-}$ mice are unable to resolve acute pulmonary inflammation and edema following bleomycin induced lung injury, due to

accumulation of HA fragments, impaired activation of TGFβ1 and reduced clearance of apoptotic neutrophils, all of which were attributed to the loss of CD44 from recruited inflammatory macrophages. The HA binding properties of CD44 and their regulation are rather complex. The receptor is expressed on quiescent leucocytes in a low affinity or 'off state' with only a low HA binding capacity. However, upon "activation", by exposure to inflammatory cytokines, receptor surface clustering, or encounter with HA complexed with inflammation-associated HA protein adducts, the receptor becomes competent to bind its ligand efficiently (Jackson 2009). As a consequence, particular attention will be paid to such aspects in this present Chapter that is dedicated to understanding the role of CD44 in exit of macrophages from inflamed peritoneum in the sterile peritonitis model presented in Chapter 4.

The contribution of hyaluronan to the overall mechanism of macrophage clearance has been considered widely in this thesis and although the biosynthesis of extracellular matrix molecules by macrophages has been well established, with previous reports providing some insight into production of glycosaminoglycans as well as proteoglycans that can bind HA, particular attention on HA synthesis has been not as broadly investigated (Uhlin-Hansen, Wik et al. 1993, Chang, Olin et al. 1998, Chang, Chan et al. 2012). Since the work on this thesis has dealt with migration of inflammatory macrophages, a component of this chapter will focus on the influence of such an environment on HA production by macrophages. The impact of cytokines and signalling molecules on HA biosynthesis by various cells and cell-lines can be noted in a wide body of literature. Prominently, the influence of inflammatory signals can be seen with microvascular blood and lymph node endothelial cells; TNF-α,

IL-1β and lipopolysaccharide (LPS) are able to up-regulate production although IFN-γ fails to have any effect (Mohamadzadeh, DeGrendele et al. 1998). Another cytokine associated with inflammatory diseases, TGF-β, has been reported to increase levels of HA synthesis and is involved in secretion of a high molecular weight form by human synovial lining cells (Haubeck, Kock et al. 1995). These molecules promote production levels by regulating the protein levels of key family of enzymes involved in biosynthesis, HA synthases, which forms part of my investigations into characterising macrophage HA production. Inflammatory cytokines, such as IL-1β , have also been demonstrated to affect the activity of UDP glucose dehydrogenase which is involved in the synthesis of HA precursor substrate UDP-GlcUA (Wen, Li et al. 2014).

Hyaluronan is a large glycosaminoglycan linear polymer of D-glucuronic acid and N-acetyl-D-glucosamine, secreted by a wide variety of cells including leucocytes. Its synthesis is facilitated by HA synthases, of which three isoforms are presently known about HAS1, HAS2 and HAS3, and are located on the inner surface of the plasma membrane, where they generate HA polymers that are extruded co-synthetically (Jackson 2009). Camenisch et al. (2000) reported that HAS2, unlike either HAS1 or HAS3, is crucial for normal embryonic development. Indeed the *HAS2*$^{-/-}$ phenotype is embryonic lethal, as a result of severe defects in vasculature development and production of a highly compacted extracellular matrix, lacking the hydrating and expanding properties of normal HA-containing matrix. Although the literature has evidence of leucocytes producing hyaluronan and expressing HAS's, it is unclear if a certain HAS dominates the production within these cells. Chang et al. (2012) presented evidence that in the monocyte cell line, THP-1, differentiation into macrophages

is accompanied by a significant up-regulation of HAS2 rather than HAS1 expression, implying that HAS2 may play a particularly important role in HA production in macrophages. As mentioned above, HA is immediately extruded from the surface of cells during biosynthesis, thus contributing to the composition of the extracellular matrix. However, attachment of HA to the cell surface has been demonstrated through binding of the glycosaminoglycan to an active form of its cognate receptor CD44 on most cells, including macrophages, and may be involved in producing a glycocalyx/pericellular coat (Culty, Nguyen et al. 1992, Kennel, Lankford et al. 1993). Interestingly, hyaluronan, released through the pores of the plasma membrane, can remain tethered to the cell surface not only by binding to receptors such as CD44 but also through sustained transmembrane interactions with the synthases (Spicer and McDonald 1998, Ibrahim, Joddar et al. 2007). Lesley et al. (2000) identified that the capacity for binding increases with increasing sizes of HA and it may be that a high molecular weight HA (HMW-HA) produced by macrophages binds to CD44 to present to LYVE-1 for migration via lymphatic vessels; indeed Yang et al. (2012) demonstrated that native HMW-HA is able to induce CD44 receptor clustering that aids in binding to HA whereas smaller weight oligosaccharides of HA inhibited this binding. One important question considered in my work is whether CD44 would indeed be required to anchor newly synthesised HA on the cell surface of macrophages, an event that is likely to be dependent on the size of HA produced. Investigating the role of CD44 in sequestering HA on the surface of macrophages for engagement with LYVE-1 and the impact of CD44 gene deletion or functional disruption forms a relevant component of the studies presented in this current chapter. The critical importance of HA in cell migration is further exemplified by processes such as wound healing and inflammation

(Chen and Abatangelo 1999). Furthermore, HA synthesis during embryogenesis maintains pluripotent progenitor cells in an undifferentiated state by inhibiting their interactions with neighbouring cells and the critically timed reduction in HA synthesis permits cell contact and differentiation during events such as epithelial mesenchymal transition in limb bud formation (Li, Toole et al. 2007). In another context, increased aggressiveness of tumours is associated with an increase in the amount of pericellular HA in the tumour associated matrix (TAM) (Toole 2004). With such diversity in the production of HA and a possibility for this to influence the migratory potential of macrophages, investigations into the levels of production, with a focus on inflammation affecting biosynthesis, are undertaken within this Chapter.

5.2 Aims

The focus of this thesis has been on the LYVE-1-HA axis in mediating transmigration and trafficking of macrophages to draining lymph nodes. The most obvious unifying link between hyaluronan on the surface of macrophages and LYVE-1 on lymphatic endothelium is the cognate receptor CD44 although there is currently little knowledge of the role played by CD44 in the lymphatics. The major aim of the work presented in this chapter was to investigate such roles as well as characterise HA production by the myeloid cells. In particular the following three issues were addressed:

- Does macrophage migration from peritoneum to draining lymph nodes involve CD44?
- Does CD44 disruption affect macrophage transmigration across activated LECs in vitro?
- Does inflammatory activation of macrophages impact their biosynthesis of hyaluronan?

5.3.1 CD44 in trafficking of macrophages to draining lymph nodes

Previous studies have shown that leucocytes, including monocytes, utilise CD44 to mediate rolling adhesion interactions with blood endothelium during transit across blood vessels in inflammatory tissue (Siegelman, DeGrendele et al. 1999). However, the contribution if any of this hyaluronan receptor to leucocyte exit from inflammatory sites via the lymphatics has yet to be determined. One of the main aims of this chapter was to investigate a possible role of CD44 in macrophage trafficking to draining lymph nodes.

Chapter 4 established that adoptively transferred macrophages can migrate from both the normal and inflamed peritoneal cavity to draining lymph nodes and indicated involvement of LYVE-1 in the process, particularly in exit from inflamed sites. In this current chapter I employed the same Bio-Gel® bead sterile peritonitis model to examine the possible role played by CD44. Receptor function regarding lymphatic trafficking *in vivo* was determined with the use of *CD44*$^{-/-}$ mice, first developed by Boehringer Ingelheim, which abolished expression of all isoforms of CD44. As stated above, these mice survive without any developmental defects and show no overt abnormalities as an adult (Protin, Schweighoffer et al. 1999).

Before considering trafficking during inflammation, a preliminary study was undertaken to determine whether there was a contribution from CD44 in exit from an uninflamed peritoneal cavity. Accordingly, differentiated bone-marrow derived macrophages (BMDMs) of either wild-type (WT), or *CD44*$^{-/-}$ genetic

background were labelled with the red fluorescent dye, PKH26, and injected into the peritoneum of age and sex matched untreated adult WT mice. 12 hours after injection of BMDMs (established as the earliest time point in my studies at which macrophages are detected in peritoneal draining lymph nodes in the previous chapter), mdLNs were excised, and after disruption, single cell suspensions were stained with primary antibodies to the macrophage marker F4/80 and analysed by flow cytometry . As shown in Figure 5-2, similar numbers of fluorescent macrophages were detected within the lymph node of mice injected with either WT or *CD44*$^{-/-}$ mice, suggesting no significant impact of receptor loss on macrophage trafficking to these sites.

Although this initial experiment suggested no significant contribution of the receptor, the findings were similar to those obtained for trafficking of BMDMs from the unstimulated peritoneum of *LYVE-1*$^{-/-}$ mice (Fig 4-10). However, since effects became manifest in trafficking of with those mice using the Biogel® bead induced sterile peritonitis model, it was likely that events from the loss of expression of CD44 would also be noticed in such conditions and as such similar studies were clearly warranted with macrophages from *CD44*$^{-/-}$ mice.

To carry out such studies, PECs isolated from the lavage of either wild-type or *CD44*$^{-/-}$ mice that had previously been stimulated with BG beads for 5 days, were loaded with PKH26 and adoptively transferred into the peritoneum of WT mice preconditioned to the same stage of BG Bead induced peritonitis. mdLNs were isolated 12 hours after injection of PECs and subjected to mechanical disruption, followed by preparation of single cell suspensions and staining with primary antibodies to the macrophage markers F4/80 and MHC-II for analysis

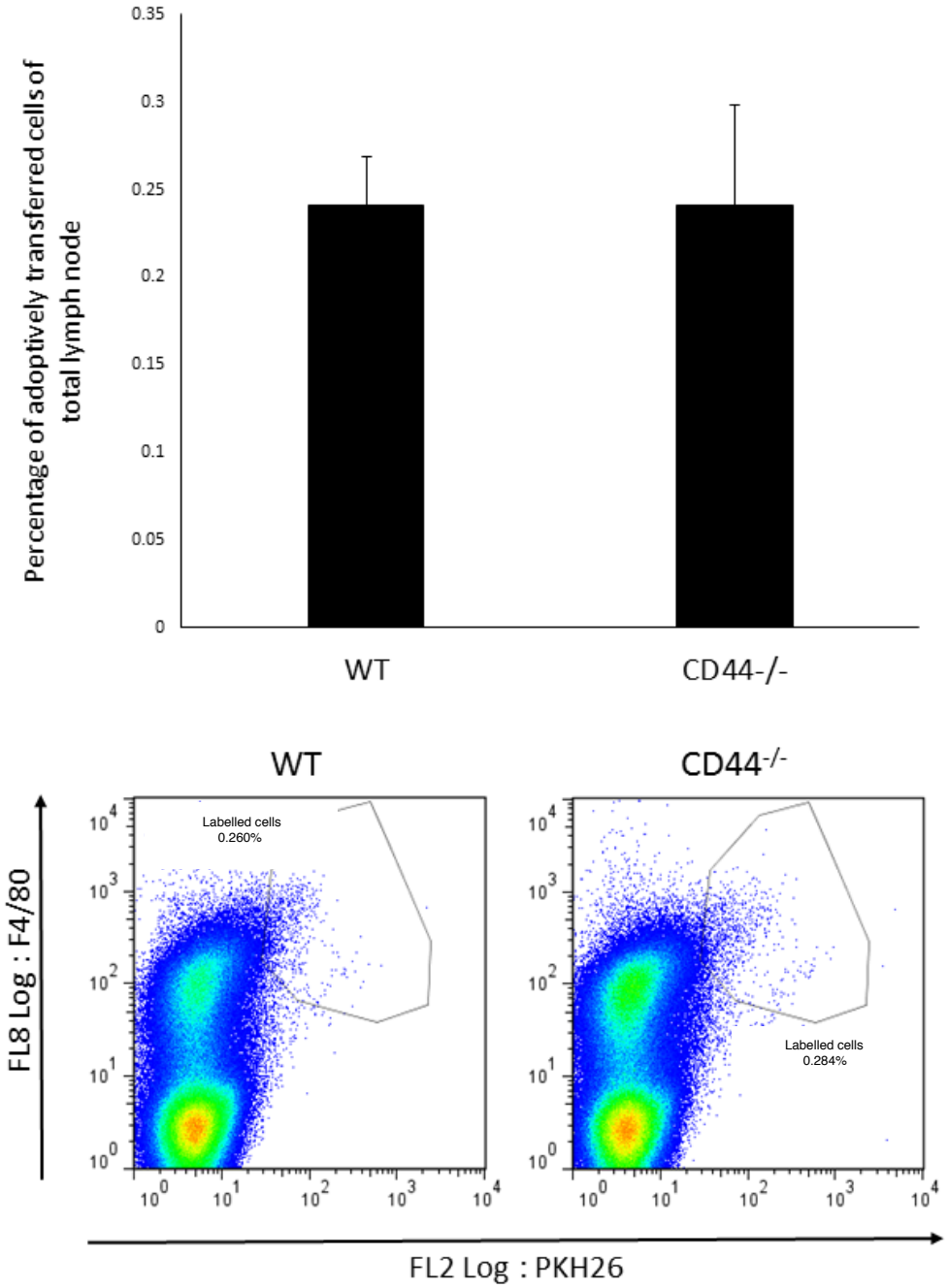


Figure 5-2: Effect of CD44 gene deletion on macrophage trafficking from normal uninflamed peritoneum to draining lymph nodes. Adult female mice (8-12 weeks old) of wild-type (WT) background were injected with WT, or CD44$^{-/-}$ BMDMs labelled with fluorescent dye PKH26. After 24 hours, mice were killed and mediastinal lymph nodes were retrieved and mechanically disrupted to obtain single cell suspensions which were immunostained with macrophage cell marker F4/80 (clone CI:A3-1) to quantify migrating macrophage numbers by flow cytometry. The graph above shows quantitative assessment of cells arriving at mdLNs in WT injected mice with representative dot plots below the graph. The graph shown is representative of 31independent experiments. Data are the mean ± SD of quadruplicate technical replicates. A two-tailed, unpaired Student's t-test was performed on this figure and p values below 0.05 were considered statistically significant. The appropriate statistical test to analyse this data would be a two way analysis of variance (ANOVA).

by flow cytometry. Remarkably, as shown by the results in Figure 5-3, approximately 4-fold fewer *CD44*$^{-/-}$ macrophages were recovered in the draining lymph nodes compared to their WT counterparts.

These data provide the first evidence that CD44 is important for macrophage clearance from inflamed peritoneum via the lymphatics, similar to my findings for LYVE-1. As mentioned in the Introduction to this Chapter, the role of CD44 in exit of leucocytes across blood vessels was specific to developing rolling interactions with endothelium and so seemed to have a redundant role in latter stages of TEM. It was possible that CD44 would also function similarly in trafficking via lymphatics and hence the effect of functional blockade would gradually diminish over time. A preliminary investigation into such a possible effect was carried out; PECs isolated from BG bead stimulated peritoneums of WT and *CD44*$^{-/-}$ mice were labelled with lipophilic dyes PKH26 and CellVue® Lavender (which is structurally similar to PKH26 but fluoresces at a separate wavelength without spectral overlap), respectively, mixed in a 1:1 ratio and re-injected into stimulated peritoneal cavities of WT mice. mdLNs were retrieved from the recipient mice at time points of 12, 24 and 36 hours after adoptive transfer, and appropriate cell suspensions stained with the macrophage marker F4/80 for subsequent analysis by flow cytometry. As can be seen in figure 5-4, there was a greater than 5-fold accumulation of WT macrophages relative to *CD44*$^{-/-}$ counterparts at 12 hours. Although this difference diminished at later time points there was still a significant difference even after 36h. The *CD44*$^{-/-}$ macrophages showed similar kinetics to the WT macrophage with an overall decrease in the numbers within the lymph node from 24 to 36 hours. Hence, the effect of CD44 is consistent across the time course and is likely to be involved in entry into the lymphatics.

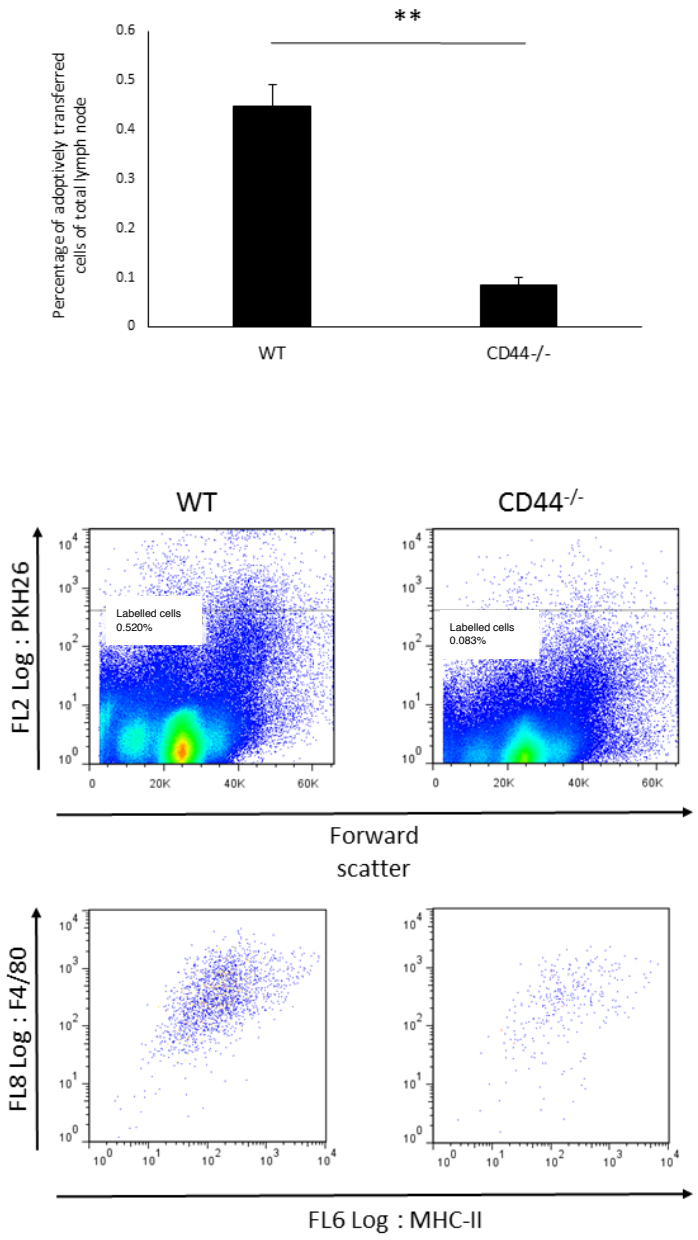


Figure 5-3: Effect of CD44 gene deletion on macrophage exit to draining lymph nodes from inflamed peritoneum. On day 0, adult female C57BL/6 mice (8-12 weeks old) of WT or, *CD44*$^{-/-}$ background were injected with BG beads. On day 5, the peritoneum of treated mice was washed and PECs within the lavage fluid were labelled with PKH26 (red) and injected into the peritoneum of 5 day BG bead treated mice of WT background. 12 hours after injection of cells, mice were killed and mediastinal lymph nodes were retrieved and mechanically disrupted to produce single cell suspensions. Cells were immunostained for cell surface markers, F4/80 (clone CI:A3-1) and MHC-II (clone M5/114.15.2) to identify macrophages by flow cytometry. The graph above shows quantitative assessment of cells arriving at mdLNs in WT injected mice, with representative dot plots below the graph. The graph shown is representative of 3 independent experiments. Data are the mean ± SD of quadruplicate technical replicates. A two-tailed, unpaired Student's t-test was performed on this figure and p values below 0.05 were considered statistically significant (** $p < 0.01$; WT macrophages vs *CD44*$^{-/-}$ macrophages). The appropriate statistical test to analyse this data would be a two way analysis of variance (ANOVA).

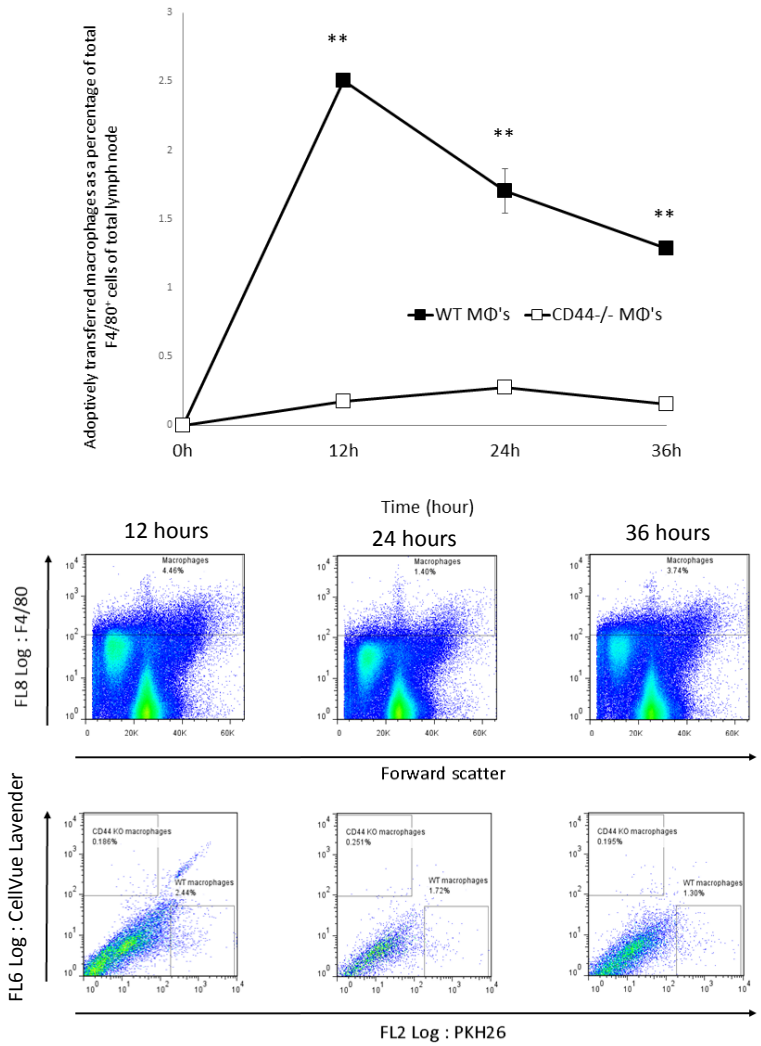


Figure 5-4: Effect of CD44 gene deletion on macrophage exit to draining lymph nodes from inflamed peritoneum over time. On day 0, adult female C57BL/6 mice (8-12 weeks old) of WT or, *CD44*$^{-/-}$ background were injected with BG beads. On day 5, the peritoneal cavities of treated mice were washed and retrieved PECs were labelled with PKH26 (WT macrophages) or, CellVue® Lavender (*CD44*$^{-/-}$ macrophages) and co-injected as a 1:1 ratio into the peritoneum of 5 day BG bead treated mice of WT background. Mice were killed at time points of 12, 24 and 36 hours after injection of cells and mediastinal lymph nodes were retrieved and mechanically disrupted to produce single cell suspensions. Cells were immunostained for cell surface markers, F4/80 (clone CI:A3-1) to identify macrophages which were quantitated by flow cytometry. As part of the analysis, all macrophages (identified as F4/80^{+}) were gated and assessed for the percentage of these cells that had either fluorescent dye. The graph above shows quantitative assessment of fluorescent cells amongst the total macrophage population within the mdLNs of WT injected mice, with representative dot plots below the graph. The graph shown is representative of 1 independent experiments. Data are the mean ± SD of quadruplicate technical replicates. A two-tailed, unpaired Student's t-test was performed on this figure and p values below 0.05 were considered statistically significant (** $p < 0.01$; WT macrophages vs *CD44*$^{-/-}$ macrophages). The appropriate statistical test to analyse this data would be a two way analysis of variance (ANOVA).

5.3.2 The role of CD44 in retention of cells at sites of inflammation

The preceding studies provide foundational evidence for the involvement of CD44 in clearance of macrophages to draining lymph nodes from an inflamed peritoneum,. Next it was investigated whether the reduction in lymph node trafficking was matched by a similar accumulation of macrophages in the peritoneal cavity. Before progressing to answer this question, I investigated whether loss of CD44 expression would impact retention within an uninflamed cavity, expecting there would be no difference as there was equal levels of trafficking of macrophages of both backgrounds to mediastinal lymph nodes, as shown in figure 5-1. Accordingly, PKH26 labelled BMDMs from either WT, or *CD44*$^{-/-}$ mice were injected i.p. into unstimulated WT mice, and after 12 hours, cells acquired from peritoneal lavage were stained with primary antibodies to F4/80 for analysis by flow cytometry (Fig 5-5). Surprisingly, there were approximately 2.5-fold more adoptively transferred cells recovered from mice injected with *CD44*$^{-/-}$ BMDMs compared to WT ones, suggesting that loss of the receptor had diminished their exit from the peritoneum, or enhanced their survival therein.

Next, to determine whether deletion of CD44 affected the recovery of macrophages from the peritoneal cavity of BG bead stimulated mice, PECs from both WT and *CD44*$^{-/-}$ mice were labelled with PKH26 and injected into the peritoneal space of WT BG bead stimulated mice followed by collection of peritoneal lavage fluid at 12 hours and staining with primary antibodies to F4/80 and MHC-II for analysis by flow cytometry. Surprisingly, as shown in Figure 5-6,

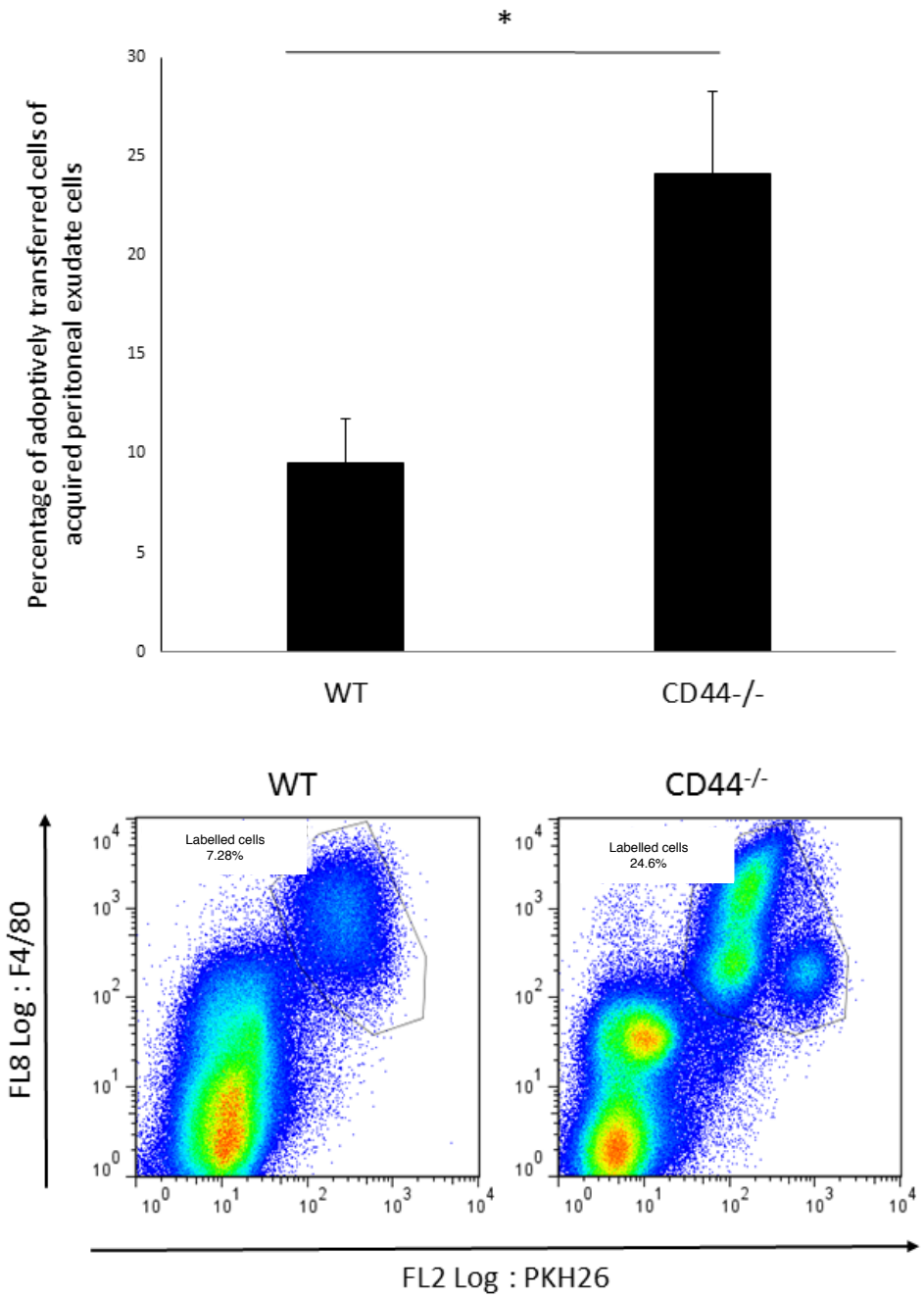


Figure 5-5: Effect of CD44 gene deletion on macrophage retention within normal uninflamed peritoneal cavity. Adult female mice (8-12 weeks old) of wild-type (WT) background were injected with WT, or *CD44*$^{-/-}$ BMDMs labelled with fluorescent dye PKH26. After 12 hours, mice were killed and peritoneal exudate cells were recovered which were immunostained with macrophage cell marker F4/80 (clone CI:A3-1) to further identify macrophages by flow cytometry. The graph above shows quantitative assessment of PECs recovered from peritoneal lavage of mice injected with WT and *CD44*$^{-/-}$ BMDMs with representative dot plots below the graph. The graph shown is representative of 1 independent experiments. Data are the mean ± SD of quadruplicate technical replicates. A two-tailed, unpaired Student's t-test was performed on this figure and p values below 0.05 were considered statistically significant (* $p < 0.05$; WT macrophages vs *CD44*$^{-/-}$ macrophages). The appropriate statistical test to analyse this data would be a two way analysis of variance (ANOVA).

there were more than three-fold fewer *CD44*$^{-/-}$ macrophages present in the peritoneal lavage compared to WT macrophages. Interestingly, this was the reverse of the situation observed when *CD44*$^{-/-}$ and wild-type macrophage recoveries were compared in the lavage fluids of uninflamed peritoneum (Fig 5-5). These data suggest that loss of CD44 does not hinder exit of macrophages from the peritoneal cavity, but may in fact cause their re-direction via other alternative routes – a result reminiscent of the findings with LYVE-1 blockade in chapter 4 that saw numerous other sites across the murine body populated with the adoptively transferred cells, most notably the speen (Fig 4-24).

The time-course for recovery of adoptively transferred macrophages from lymph nodes in Biogel® bead treated mice indicated a transient drop at 36 hours in both WT and *CD44*$^{-/-}$ macrophages. Whether there were substantial changes over time of either WT or *CD44*$^{-/-}$ macrophages within the retrievable cells of the peritoneal cavity was yet to be identified. To explore these kinetics and to confirm the findings from the previous experiment, I co-injected WT and *CD44*$^{-/-}$ PECs isolated from BG stimulated mice, after separate labelling with PKH26 and CellVue Lavender, respectively, in a 1:1 mixture into the peritoneum of BG stimulated WT mice. Lavages of the peritoneal cavity were collected after 12, 24 and 36 hours of injection of the fluorescent cells with the retrieved cells stained with primary antibodies to F4/80 for analysis by flow cytometry (Fig 5-7). Consistent with the data obtained previously, there was a four-fold greater level of WT macrophages than *CD44*$^{-/-}$ macrophages, of the total F4/80^{+} cell population recovered. Also, it can be observed that with WT fluorescent macrophages, there is a significant 75 % drop in numbers from 12 to 24 hours with little change afterwards. However, with *CD44*$^{-/-}$ macrophages, there were

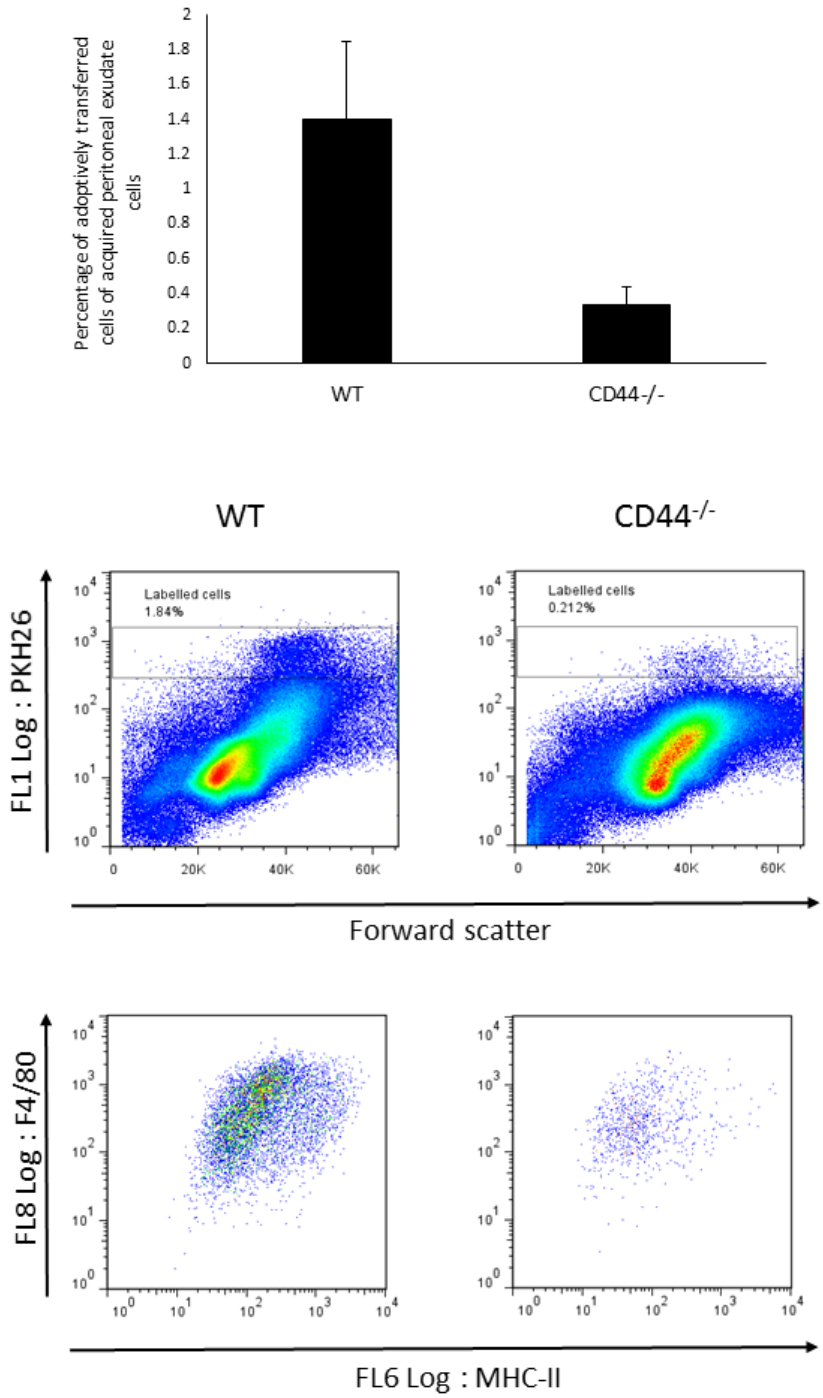


Figure 5-6: Effect of CD44 gene deletion on macrophage recovery from inflamed peritoneal cavity. On day 0, adult female C57BL/6 mice (8-12 weeks old) of WT or, CD44$^{-/-}$ background were injected with BG beads. On day 5, the peritoneum of treated mice was washed and retrieved PECs were labelled with PKH26 (red) and injected into the peritoneum of 5 day BG bead treated mice of either WT background. 12 hours after injection of cells, mice were killed and PECs were isolated and immunostained for cell surface markers, F4/80 (clone CI:A3-1) and MHC-II (clone M5/114.15.2) to identify macrophages by flow cytometry. The graph shown is representative of 3 independent experiments. Data are the mean ± SD of quadruplicate technical replicates. A two-tailed, unpaired Student's t-test was performed on this figure and p values below 0.05 were considered statistically significant. The appropriate statistical test to analyse this data would be a two way analysis of variance (ANOVA).

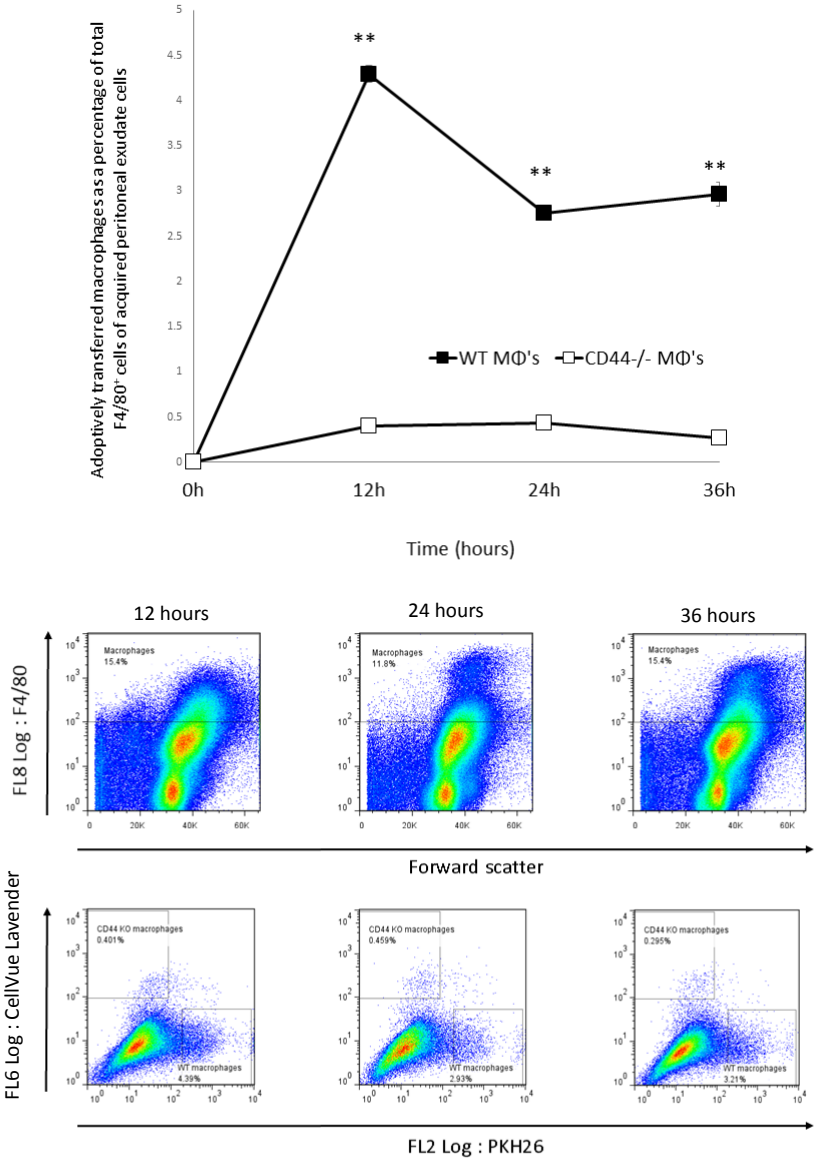


Figure 5-7: Effect of CD44 gene deletion on macrophage retention within an inflamed peritoneal cavity over time. On day 0, adult female C57BL/6 mice (8-12 weeks old) of WT or, *CD44*$^{-/-}$ background were injected with BG beads. On day 5, the peritoneum of treated mice was washed and retrieved PECs were labelled with PKH26 (WT macrophages) or, CellVue® Lavender (*CD44*$^{-/-}$ macrophages) and injected into the peritoneum of 5 day BG bead treated mice of WT background. Mice were killed at time points of 12, 24 and 36 hours after injection of cells and PECs were recovered and immunostained for cell surface markers, F4/80 (clone CI:A3-1) to identify macrophages by flow cytometry. As part of the analysis, all macrophages (identified as F4/80^{+}) were gated and assessed for the percentage of these cells that had either fluorescent dye (identified as adoptively transferred macrophages). The graph above shows quantitative assessment of fluorescent cells amongst the total macrophage population within the peritoneal lavage of WT injected mice, with representative dot plots below the graph. The graph shown is representative of 1 independent experiments. Data are the mean ± SD of quadruplicate technical replicates. A two-tailed, unpaired Student's t-test was performed on this figure and p values below 0.05 were considered statistically significant (** $p < 0.01$; WT macrophages vs *CD44*$^{-/-}$ macrophages). The appropriate statistical test to analyse this data would be a two way analysis of variance (ANOVA).

almost no changes in levels within the retrieved cells between each time point thus suggesting the effects of CD44 occur early in the trafficking process and that the CD44:HA axis is similarly involved, as hypothesised with LYVE-1, in either mediating cell redirection, apoptosis, or retention in a compartment within the peritoneum inaccessible to the EDTA lavage of the cavity.

5.3.3 Redirection of adoptively transferred cells away from lymphatic route with loss of CD44 function

The unexpected finding of fewer *CD44*$^{-/-}$ macrophages than WT macrophages within the peritoneal lavage samples from Biogel® bead treated mice, despite the lower recoveries found in lymph nodes, bore a marked similarity to the findings obtained during the earlier trafficking studies with LYVE-1 function blocking mAbs in Chapter 4. With such similarity in trafficking observations to lymph node and with lack of retention within the peritoneal lavage, it was likely that the *CD44*$^{-/-}$ macrophages were being redirected to other sites within the body as well.

To affirm whether this was the case, both WT and *CD44*$^{-/-}$ PECs were labelled with CellVue® NIR-815 and injected into the inflamed peritoneal cavity of age and sex matched WT mice for whole body imaging using the LiCOR Odyssey imager, essentially as had been done for the LYVE-1 studies in chapter 4. As shown in figure 5-8, labelled macrophages appeared to be present in several organs including, the omentum, as established in the previous Chapter. These control macrophages are predominantly found within omentum in association with the stomach, and so can be concluded to be mainly within the lesser omentum rather than the greater omentum, which was dissected out with the

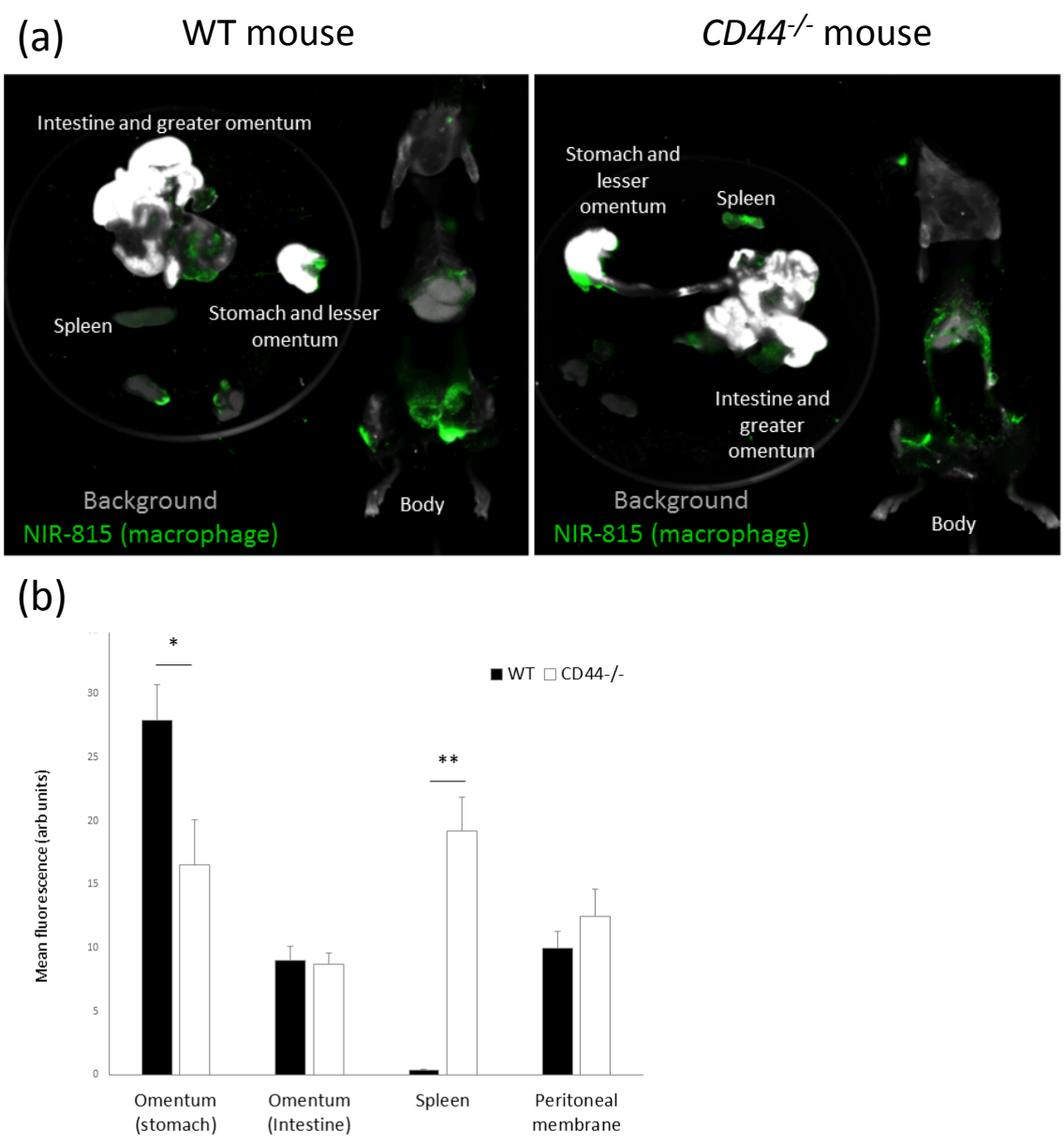


Figure 5-8: Whole body imaging of WT, or *CD44*$^{-/-}$ PECs in visceral organs after adoptive transfer into mice with Biogel® induced peritonitis. On day 0, adult female C57BL/6 mice (8-12 weeks old) of WT or, CD44$^{-/-}$ background were injected with BG beads. On day 5, the peritoneum of treated mice was washed and retrieved PECs were labelled with NIR-815 (green) and injected into the peritoneum of 5 day BG bead treated mice of WT background. 12 hours after injection of cells, mice were killed, subjected to chemical depilation, with peritoneal organs placed on a petri dish and imaged with a LI-COR™ near infra-red scanner with background from the starch emitting fluorescence at 700nm (white). (a) Whole body scans are shown of an experiment repeated two times. (b) The graph below shows semi-quantitative assessment of fluorescence emitted by adoptively transferred NIR-815 dye labelled cells from the visceral organs. The graph shown is representative of 2 independent experiments. Data are the mean ± SD of triplicate technical replicates. A two-tailed, unpaired Student's t-test was performed on this figure and p values below 0.05 were considered statistically significant (* $p < 0.05$; ** $p < 0.01$; WT vs *CD44*$^{-/-}$). The appropriate statistical test to analyse this data would be a two way analysis of variance (ANOVA).

intestines. As expected, the *CD44*$^{-/-}$ macrophages were markedly redirected to the spleen with a greater than 20-fold increase in fluorescence of the organ. There were other changes observed with an increase in fluorescence levels observed for the parietal peritoneal membrane although there was a 65 % decrease in fluorescence associated with the lesser omentum in trafficking of *CD44*$^{-/-}$ macrophages.

Overall, these results provide persuasive evidence that macrophages require CD44 expression for exit from peritoneum via lymph, but that loss of the receptor prompts their exit via alternative routes to organs such as the spleen, much as observed after functional disruption of LYVE-1 .

5.3.4 The effect of CD44 functional blockade on macrophage in vitro transmigration

To seek corroborating evidence for the involvement of CD44 in mediating migration via the lymphatics that was apparent from the above mouse studies, I next investigated the requirements for CD44 expression and function using *in vitro* transmigration assays with human lymphatic endothelial cell monolayers. Because of technical difficulties in isolating and culturing lymphatic endothelium from mouse for these studies, it was decided to carry out the experiments using human cells, in line with the earlier transmigration assays in chapter 3.

Accordingly, CMFDA labelled human macrophages, which were polarised to an M1 phenotype by treatment with LPS and IFN-γ (as detailed in Chapter 3), were incubated with either confluent unstimulated or, TNF-α stimulated HDLEC monolayers after treatment with either the CD44-HA blocking monoclonal antibody (clone BRIC235), or its isotype matched relevant IgG control.

Transmigration was subsequently measured using the UV opaque transwell insert assay system with fluorescence detected in the bottom chamber of the transwell with a plate reader. To ensure effective blockade throughout the period of the assay, the inserts with cultured HDLEC monolayers were maintained in antibody-containing media for the duration of the assays. As shown in Figure 5-9, blockade of CD44-HA binding by antibody had no statistically significant effect on the transmigration of human monocyte derived macrophages across basal condition LECs although there is slight decrease in the levels with increasing difference towards the latter time points.

However, this functional blockade significantly reduces transmigration across activated HDLECs by 45 % with a difference seen at the early stages, unlike with the non-activated LECs.

These results substantiate the findings seen *in vivo* and illustrate that binding of HA by CD44 is an important interaction for exit via lymphatic vessels.

5.3.6 Characterisation of HA production by macrophages

The principle mechanism uncovered throughout this D.Phil. thesis and presented across the various chapters allude to macrophage derived surface hyaluronan as a key component for the transmigration of leucocytes across lymphatic endothelium during inflammation. Blocking the binding of the glycosaminoglycan to either of its two receptors in the systems employed (LYVE-1 and CD44) reduce the number of transmigrating macrophages. HA production is driven by hyaluronan synthases (HASs) of which there are three

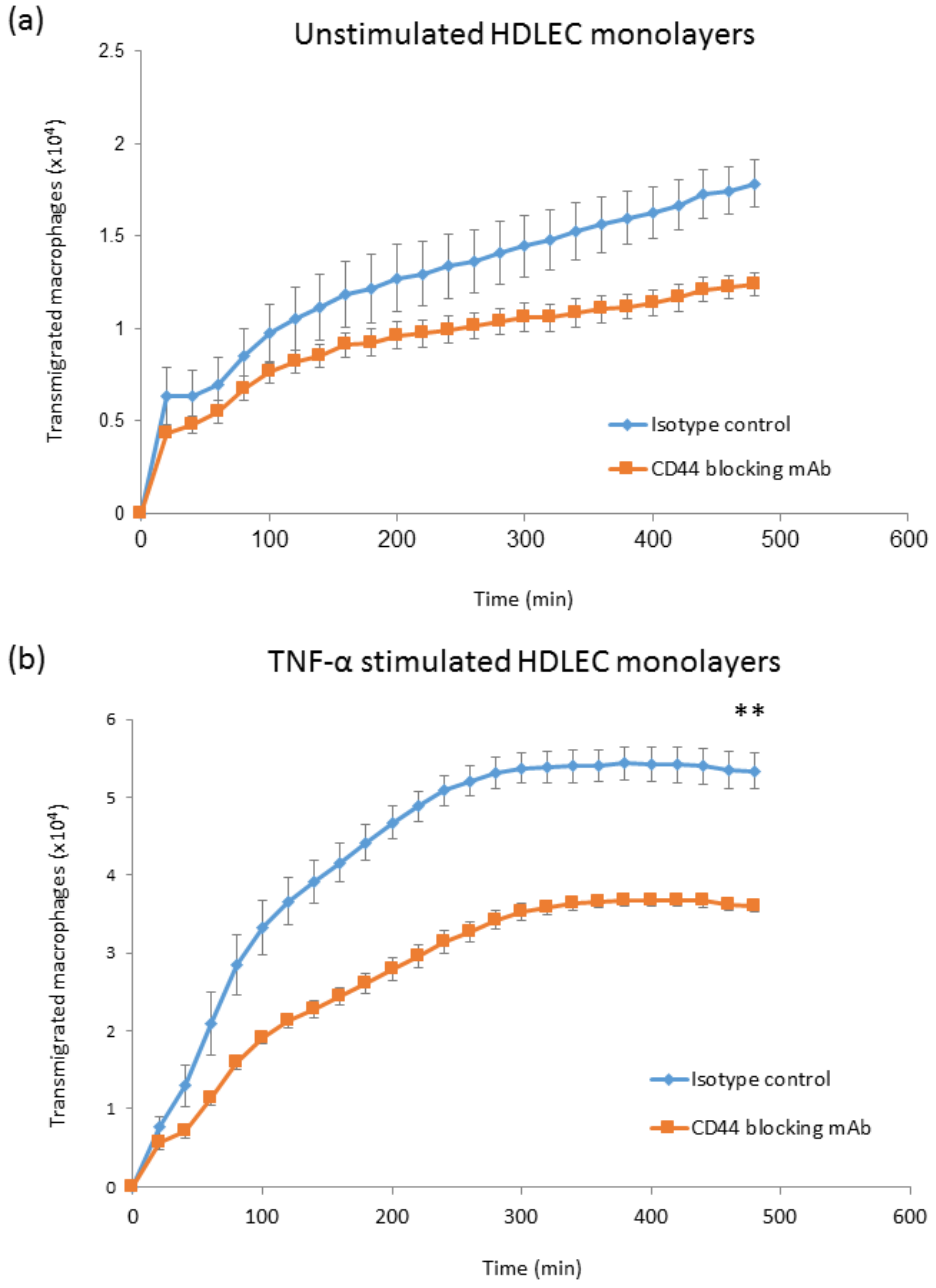


Figure 5-9: Effect of CD44 antibody blockade on macrophage transmigration across primary HDLECs. Primary HDLEC monolayers plated on the lower surface of cell culture inserts of 24 well plates were either activated with TNF-α for 0-24 h, or left unstimulated. Monolayers were subsequently incubated in media containing either 50 μg/ml isotype control IgG (blue), or BRIC235, CD44 function blocking antibodies (orange). CMFDA labelled M1 macrophages (5 x 10^5) were applied to treated HDLEC monolayers, as appropriate and numbers of transmigrating macrophages were measured using a fluorescent plate reader at 20 minute intervals for >10 hours. Time courses are showm for transmigration across (a) unstimulated monolayers, or (b) activated monolayers. The graph shown is representative of 2 independent experiments. Data are the mean ± SD of triplicate technical replicates. A two-tailed, unpaired Student's t-test was performed on this figure and p values below 0.05 were considered statistically significant (** $p < 0.01$; Isotype control IgG vs BRIC235 at 480 mins of transmigration). The appropriate statistical test to analyse this data would be a two way analysis of variance (ANOVA).

known isoforms HAS1, HAS2 and HAS3, and the expression of these enzymes by dendritic cells and lymphocytes has been previously reported (Mummert, Mummert et al. 2002, Mahaffey and Mummert 2007). Inflammatory macrophages, sharing a similar progenitor to blood derived DCs (i.e. monocytes), have the capacity to produce hyaluronan although this is yet to be conclusively shown with primary human monocyte derived populations, similar to those that were utilised throughout for *in vitro* transmigration experiments, despite insights into production by immortalised cell lines and murine cells (Chang, Chan et al. 2012, Chang, Tanino et al. 2014).

To assess the level of expression of two key HAS genes, *HAS1* and *HAS2*, preliminary reverse transcriptase PCR (RT-PCR) assays were carried out on extracted mRNA of cultured human monocyte derived macrophages at different levels of M1 polarisation (i.e. cultured either in GM-CSF alone, or with additional LPS, or with additional LPS and IFN-γ) (Fig 5-10). Basal condition macrophages (i.e. monocytes differentiated in GM-CSF alone) expressed both *HAS1* and *HAS2*. The expression of *HAS2* appeared to be more prominent than *HAS1*. Comparison of the expression of *HAS1* in steady state macrophages to the activated phenotypes (i.e. stimulated with LPS only, or with LPS and IFN-γ) revealed a 2-fold increase in expression upon stimulation with LPS only. But interestingly, this increase in expression is not observed if the cells were stimulated with both LPS and IFN-γ, simultaneously. This result is subsequently reversed on analysis of *HAS2* expression, which displays no significant difference of cells stimulated with LPS alone, but an approximate doubling in expression levels in cells stimulated with both LPS and IFN-γ. With semi-quantitative analysis providing initial clues of the effect of M1 inflammatory cues

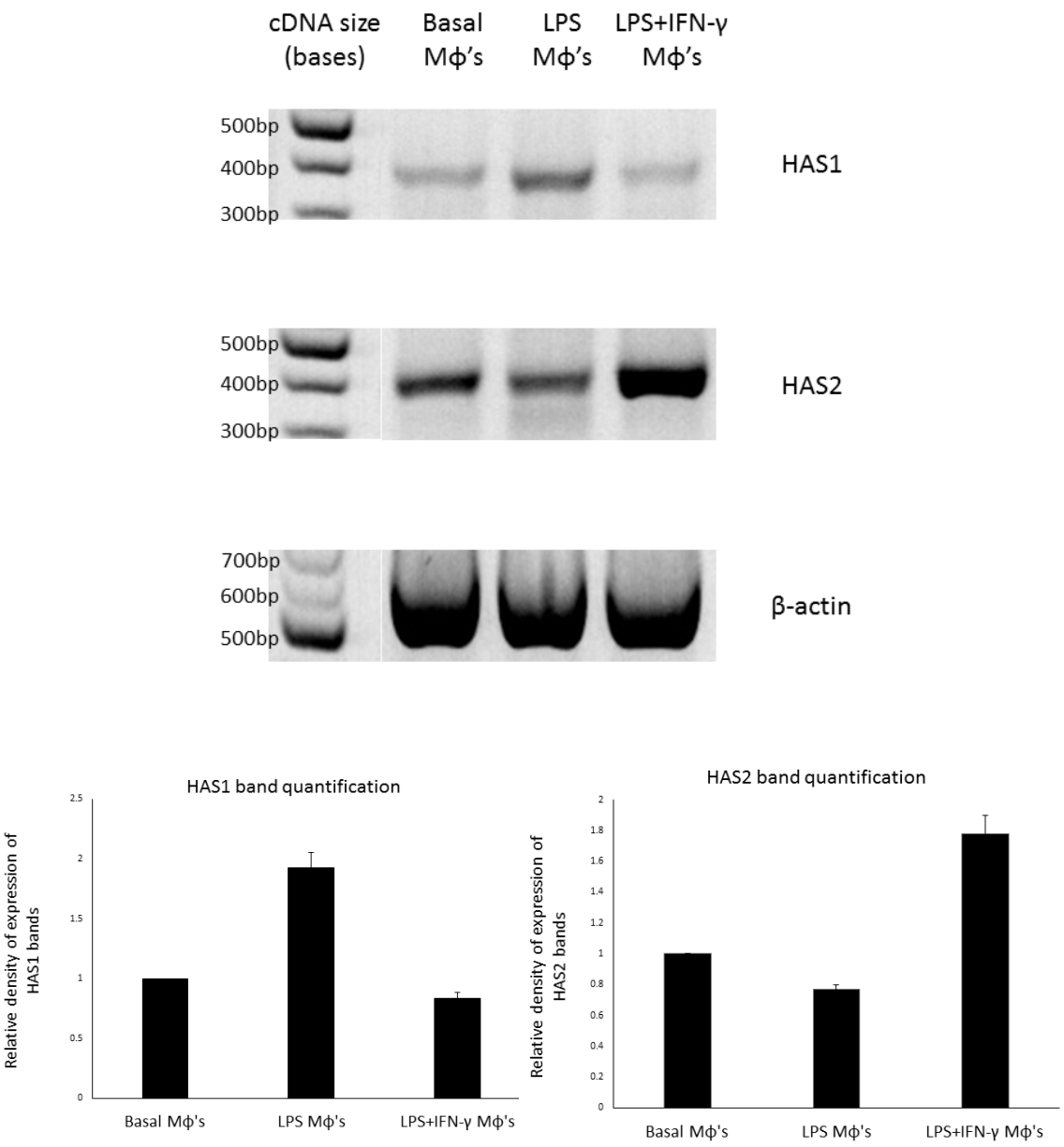


Figure 5-10: Effect of M1 activating agents on HAS1 and HAS2 mRNA expression levels in primary monocyte derived macrophages. Primary macrophages differentiated from monocytes cultured in GM-CSF were stimulated with either LPS alone or, with LPS and IFN-γ for 24 hours. After activation, cells were lysed and mRNA was extracted, which was converted to cDNA. Subsequently, cDNA samples were subjected to RT-PCR using HAS1, HAS2 and control β-actin primers for 39 cycles prior to gel electrophoresis and visualisation with Bio-Rad Molecular Imager® (see methods, Chapter 2). Graphs show semi-quantification of the density of the bands shown in figure relative to the expression density of basal macrophages. Quantification was achieved with ImageJ as described in the methods in Chapter 2. Data are the mean ± SD of the values obtained from 3 independent PCRs.

on HAS expression, the result would be consolidated with quantitative PCR. Unfortunately, due to time constraints this could not be explored but would be an important future experiment to perform.

The above results provide indicatory evidence of the capacity of human monocyte derived macrophage populations to produce their own hyaluronan. However, such data alone would not be sufficient to establish that the macrophages were indeed presenting self-hyaluronan in the in vitro transmigration assays and whether at differing levels depending on level of polarisation to M1 phenotype. To investigate expression of HA and amounts produced by the myeloid cells, homogenous *in vitro* differentiated macrophages had their media supernatants collected along with lysates of the cell populations that were assayed for HA using an assay system, as described in Chapter 2 (Fig 5-11). Presence of HA within the lysates indicated that the cells were producing it within and detection in the supernatants illustrate that the cells were releasing the glycosaminoglycan after production. However, there appears to be no significant differences in the levels of HA detected between unpolarised macrophages and those activated with M1 stimulants (i.e. LPS and IFN-γ) thus suggesting that variable HAS expression did not influence levels of HA production by the macrophages.

Despite no differences found in HA production between basal and M1 macrophages, the antibody blockade of LYVE-1-HA binding for *in vitro* transmigration assays was suggestive of a preference for LYVE-1 to mediate interactions with M1 macrophages rather than non-activated ones thus implying that HA on the surface of M1 macrophages was either more abundant, or in a

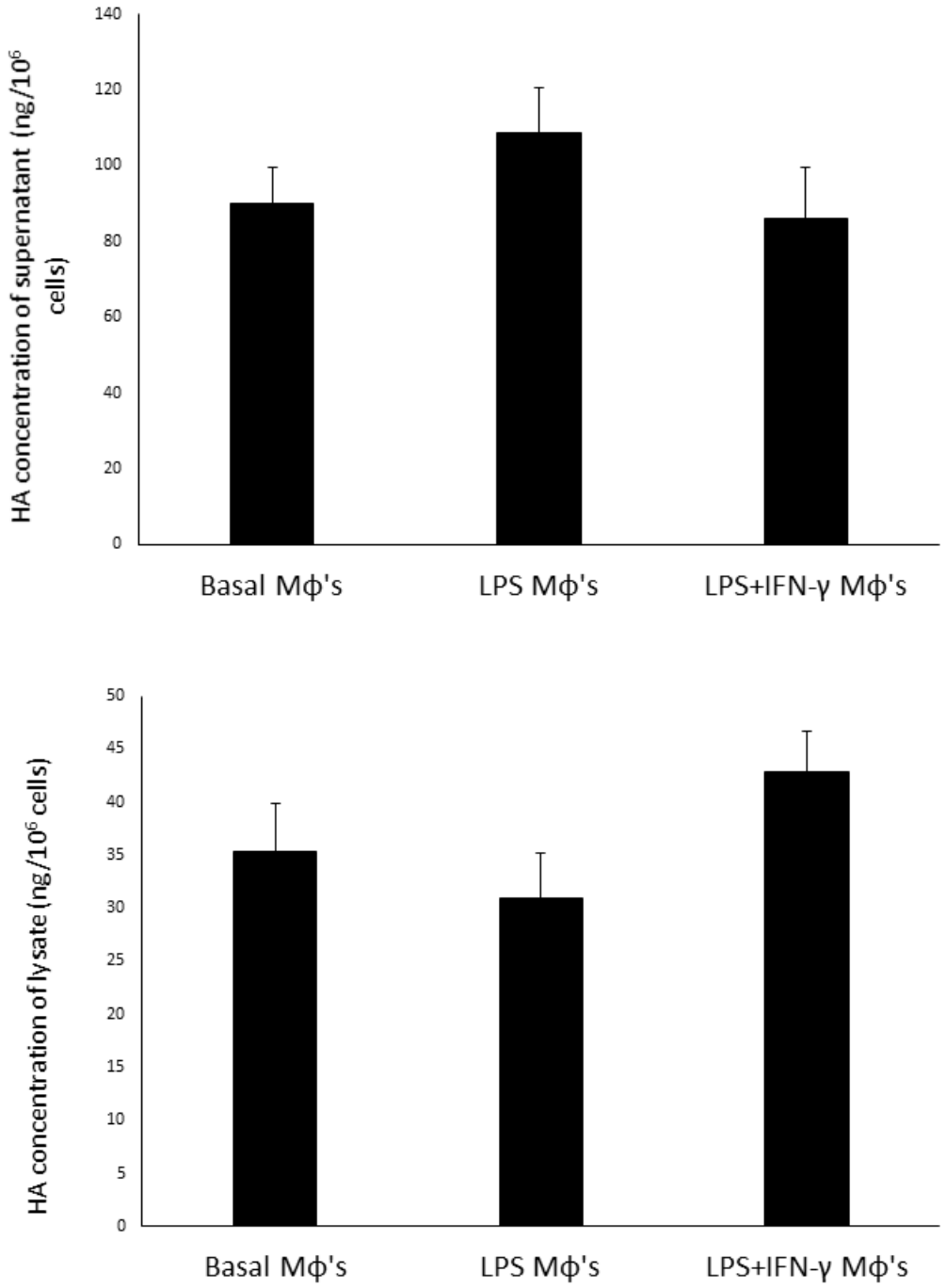


Figure 5-11: Effect of M1 activating agents on hyaluronan production by primary monocyte derived macrophages. Primary macrophages differentiated from monocytes cultured in GM-CSF (50 ng/ml) were stimulated with either LPS alone or, with LPS and IFN-γ for 24 hours. After activation, supernatants of the culture media were prepared along with lysates of the cultured cells. HA levels were quantified with a commercial HA ELISA kit with measurements gathered by a fluorescent microplate reader (see methods, Chapter 2). The graph shown is representative of 2 independent experiments. Data are the mean ± SD of triplicate technical replicates. A two-tailed, unpaired Student's t-test was performed on this figure and p values below 0.05 were considered statistically significant. The appropriate statistical test to analyse this data would be a two way analysis of variance (ANOVA).

conformation to present, or both. It is also worth noting that the assay does not distinguish surface HA from total cell HA acquired from the lysate. Accordingly, to discern any differences in levels of retention of HA on the surface of the cells, macrophages were differentiated *in vitro* on 8 chamber slides and stained with biotinylated HA binding protein (bHABP) and primary antibodies to CD11b for analysis by confocal microscopy (Fig 5-12A). All macrophages demonstrated positive staining for both markers and specificity of bHABP staining to hyaluronan was confirmed by treatment with hyaluronidase which abolished the staining (Fig 5-12B). Also, quantification of the fluorescence of bHABP staining reveals a greater than 2-fold increase in signal from macrophages treated with both LPS and IFN-γ compared to those that were inactivated or treated with LPS only thus assuring greater levels of retention of HA on the surface of M1 macrophages (Fig 5-12C).

The above experiments illustrated human macrophages producing and retaining HA at variable levels depending on level of polarisation. It is plausible that the retention of HA on the surface is dependent on the expression of the key HA binding protein CD44 thus bringing an important aspect of the role of CD44 to trafficking. Preliminary investigations were hence performed to identify whether macrophage derived hyaluronan would be detected at variable levels from murine peritoneal *CD44*$^{-/-}$ macrophages. PECs from BG stimulated peritoneums of both WT and *CD44*$^{-/-}$ mice were immunoselected with F4/80 to separate macrophages from other peritoneal populations, and the cells had their surface HA subsequently quantified with the same kit used to quantify levels of human monocyte derived macrophages. Similarly immunoselected macrophages were also cultured *in vitro* as the human counterparts above and supernatants from these were measured for HA. As shown in figure 5-13, surprisingly, an

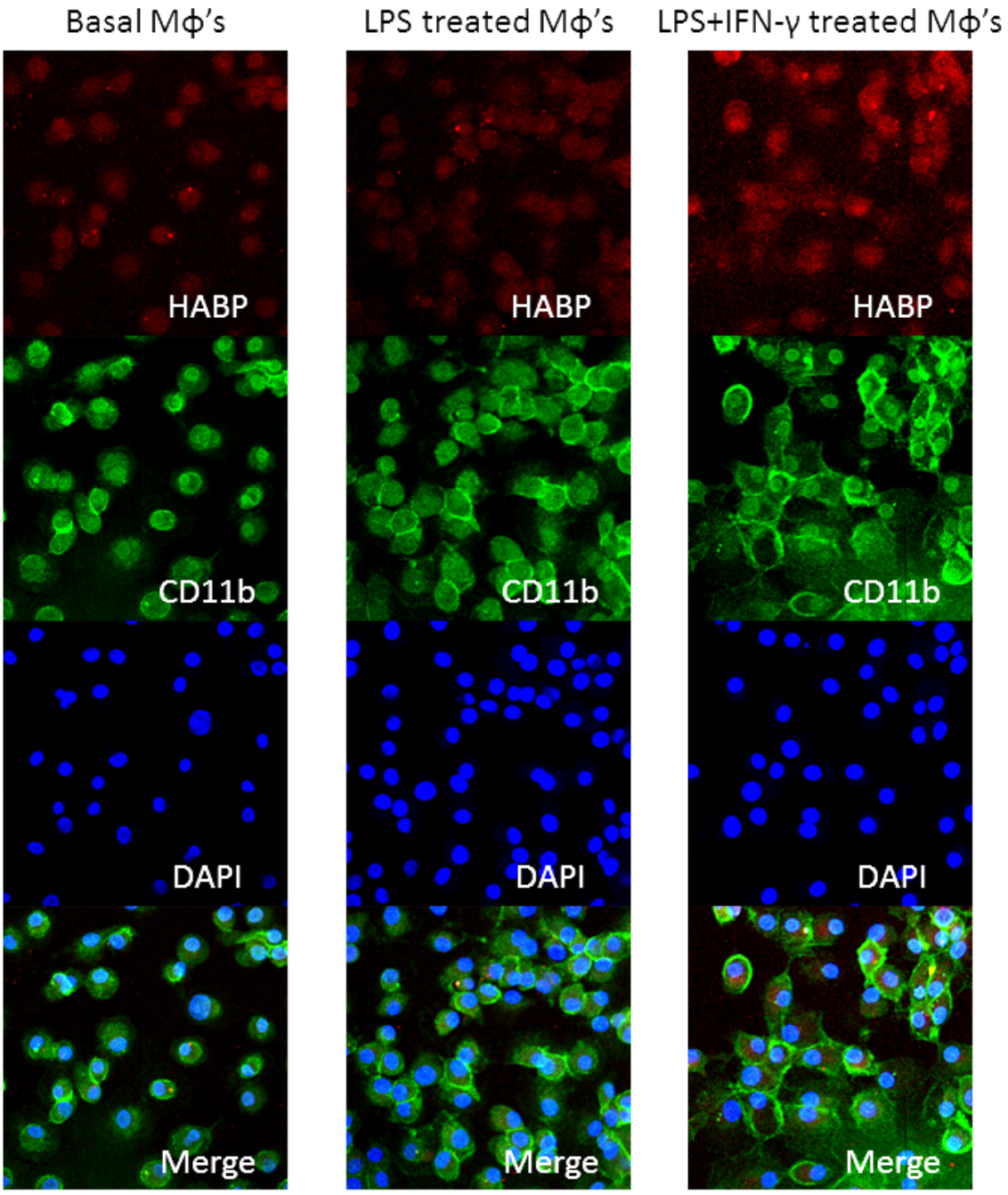


Figure 5-12A: Detection of hyaluronan retention on the surface of primary monocyte derived macrophages. Primary macrophages, on 8 chamber slides, were differentiated from monocytes cultured in GM-CSF and stimulated with either LPS alone or, with LPS and IFN-γ for 24 hours. After activation, cells were stained with primary antibodies to macrophage cell surface marker CD11b (green) using a mouse monoclonal antibody ICRF44 and biotinylated HABP (red). Slides were subsequently mounted in VectaShield™ containing DAPI. Representative images are shown of an experiment repeated three times.

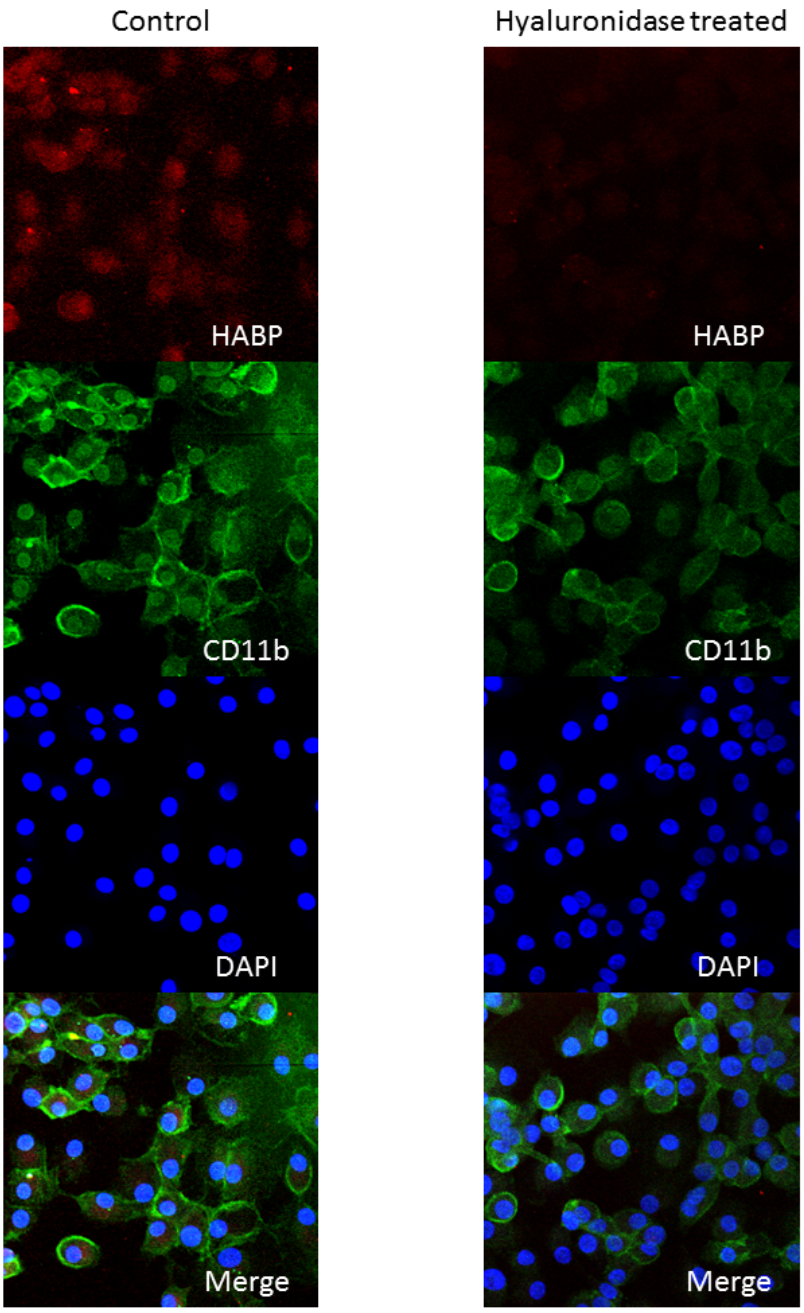


Figure 5-12B: Confirmation of specificity for hyaluronan staining by bHABP on the surface of primary monocyte derived macrophages. Primary macrophages, on 8 chamber slides, were differentiated from monocytes cultured in GM-CSF and stimulated with LPS and IFN-γ for 24 hours. After activation, cells were either treated with hyaluronidase or, left further untreated prior to staining with primary antibodies to macrophage cell surface marker CD11b (green) using a mouse monoclonal antibody ICRF44 and biotinylated HABP (red). Slides were subsequently mounted in VectaShield™ containing DAPI. Representative images are shown of an experiment repeated three times, with images of control cells (left column) from the third column of figure 5-11A and similarly cultured cells were treated with hyaluronidase (right column).

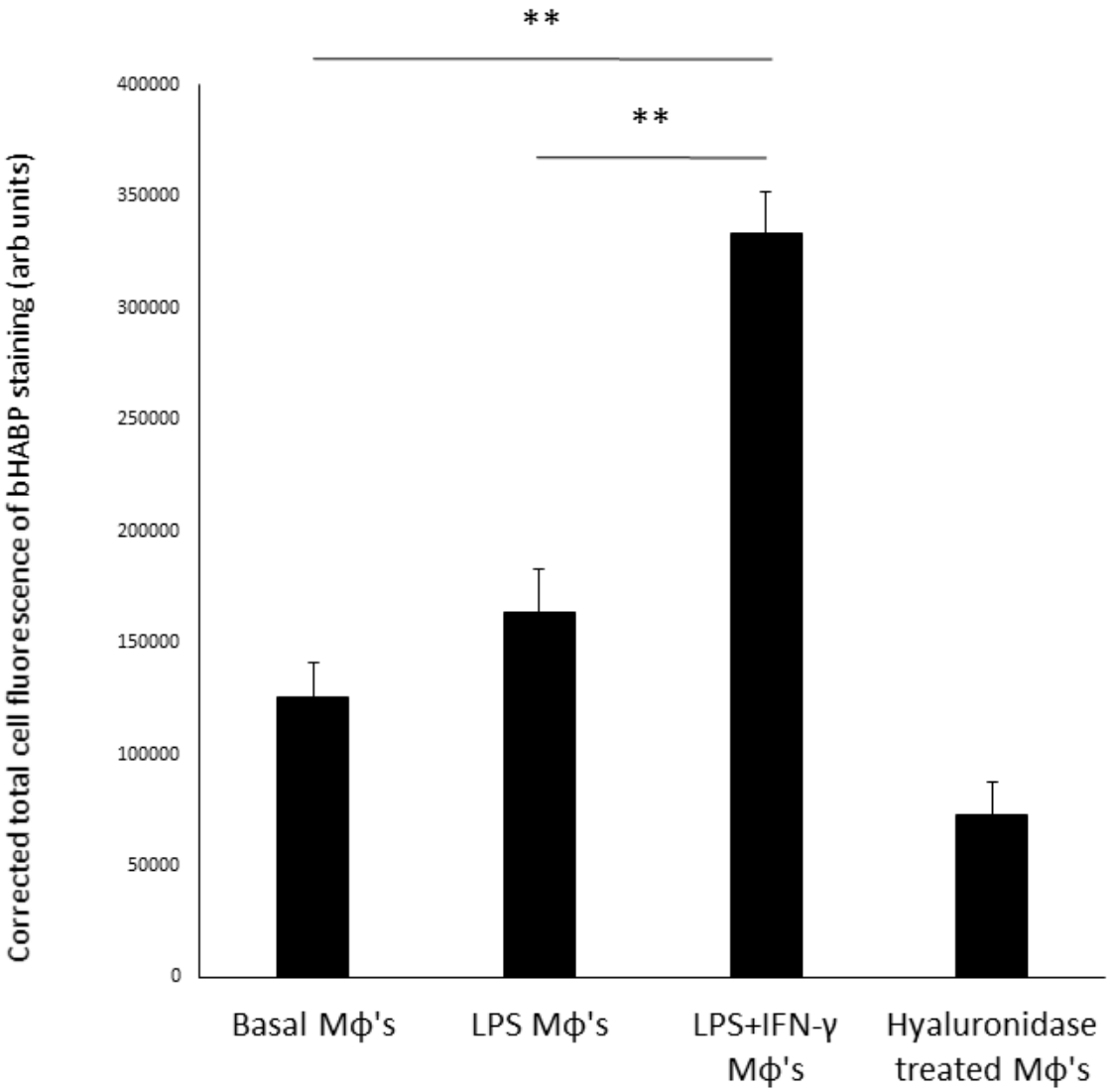


Figure 5-12C: Semi-quantiative measurement of hyaluronan on the surface of primary monocyte derived macrophages. Quantification of the level of fluorescence of bHABP staining from figures 5-11A and 5-11B, as measured using ImageJ software and corrected for area of measurement and background levels. The graph shown is representative of 3 independent experiments. Data are the mean ± SD of sextuplicate technical replicates, with 6 independent cells from the images selected for measurement. A two-tailed, unpaired Student's t-test was performed on this figure and p values below 0.05 were considered statistically significant (** $p < 0.01$; Basal Mϕ's vs LPS+IFN-γ Mϕ's and LPS Mϕ's vs LPS+IFNγ Mϕ's). The appropriate statistical test to analyse this data would be a two way analysis of variance (ANOVA).

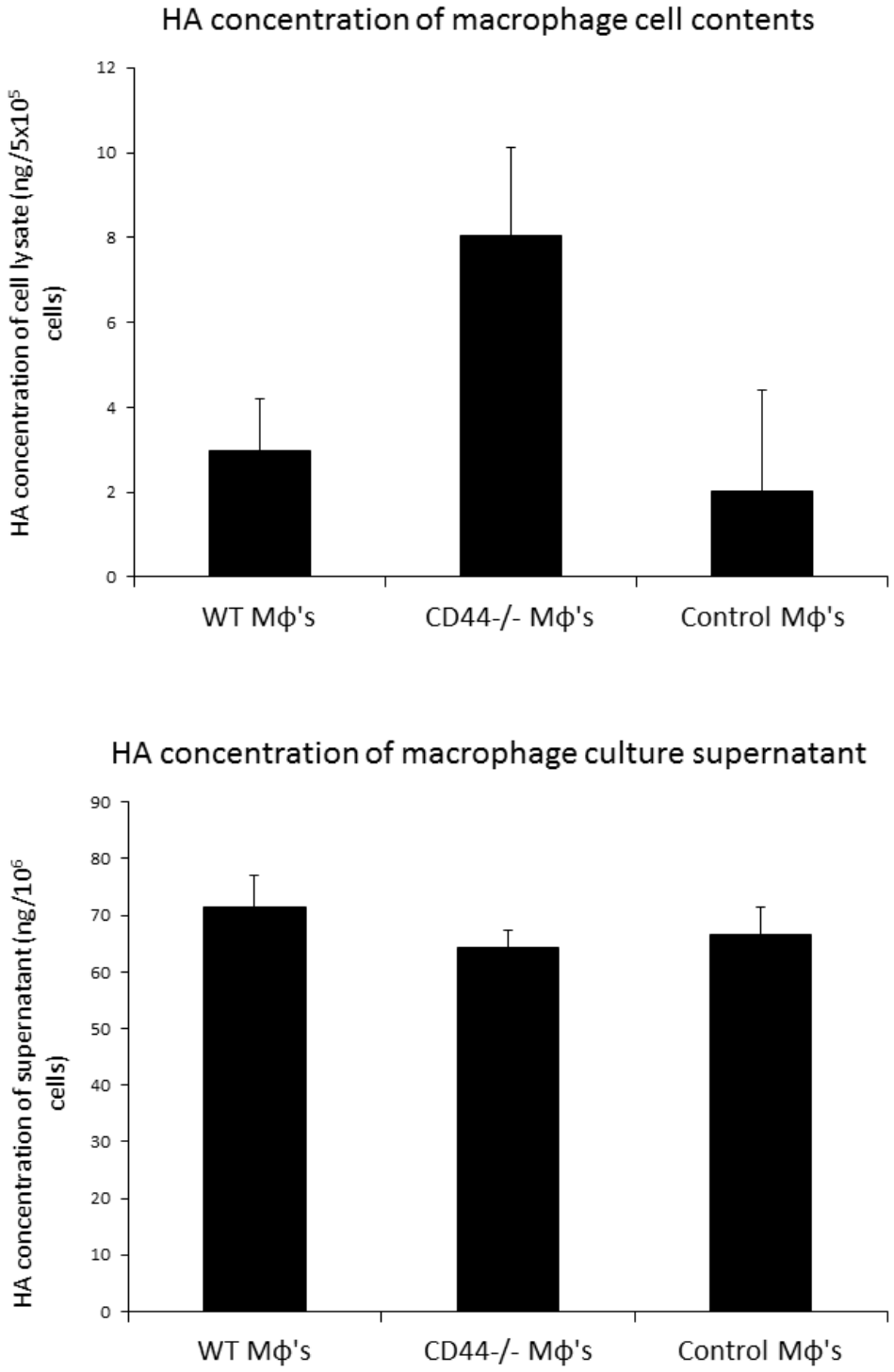


Figure 5-13: Comparison of hyaluronan levels produced by or tethered to the surface of murine peritoneal WT and CD44-/- macrophages. Macrophages isolated from peritoneal exudate cells of BG stimulated mice by MACS selecting F4/80, had their (a) HA levels on the surface quantified using a commercial HA ELISA kit and fluorescence measured with a fluorescence microplate reader. In parallel, such isolated cells were cultured in media for 5 days and (b) culture supernatant was measured for HA using the HA ELISA kit with graphs shown above representative of the experiment performed once. The graph shown is representative of 1 independent experiments. Data are the mean ± SD of quadruplicate technical replicates. A two-tailed, unpaired Student's t-test was performed on this figure and p values below 0.05 were considered statistically significant. The appropriate statistical test to analyse this data would be a two way analysis of variance (ANOVA).

approximately 4-fold greater level of HA was measured on the surface of *CD44*$^{-/-}$ macrophages compared to WT macrophages. However, analysis of the supernatants revealed that HA production was comparable between the two phenotypes thus suggesting that the key difference between the two phenotypes is at the level of retention on the surface. This experiment would require further repeats to establish the result and can be substantiated further with HABP measurement, which could not be done due to time constraints.

Overall, this subsection illustrates macrophages producing hyaluronan and retaining it on the surface which is important for transmigration across lymphatic endothelia.

5.4 Discussion

This results chapter has made the novel observation that macrophages utilise CD44 to traffic to draining lymph nodes and transmigrate lymphatic endothelium on the basis of *in vivo* murine peritonitis models and static *in vitro* assays using primary human lymphatic endothelial monolayers. Additionally, the synthesis of hyaluronan and retention on the surface by macrophages was further established building on the work of previous independent findings with a combination of staining with hyaluronan binding protein (HABP) and commercial HA ELISA kits.

The previous chapters indicated a mechanism by which macrophage derived hyaluronan and binding by its cognate receptor on lymphatic endothelium, LYVE-1, might mediate transmigration of the endothelium and likely subsequent movement towards draining lymph nodes. Besides LYVE-1-HA interactions, the findings of this Chapter provide persuasive evidence of an additional role for the HA receptor, CD44, on macrophages, thus providing a further dimension of regulation in the overall process.

HA-CD44 interactions are critical to numerous physiological processes across the body, with extravasation from blood vessels the one parallel to the observed results above (DeGrendele, Estess et al. 1997). Indeed the involvement of CD44 in lymphatic trafficking has been previously demonstrated with lymphocytes albeit with the receptor interacting with macrophage mannose receptor (MMR) rather than hyaluronan (Salmi, Karikoski et al. 2013). Similarly, *CD44*$^{-/-}$ Langerhans cells have significantly reduced migration to draining lymph

nodes with the primary interaction involved in the process believed to be with osteopontin (Weiss, Renkl et al. 2001). Other independent findings have identified that this migration to draining lymph nodes is mediated by distinct splice form variants of the receptor thus presenting an additional dimension of control to the mechanism (Weiss, Renkl et al. 1998).

My initial investigations focussed on the *in vivo* model of trafficking from the peritoneal cavity in both unstimulated and BioGel® bead stimulated conditions to compare the impact of receptor knock out in steady-state as well as inflammatory migration to draining lymph nodes. Interestingly, *CD44*$^{-/-}$ macrophages fail to migrate in great numbers compared to their wild type counterparts only in inflammatory migration rather than from an uninflamed peritoneal cavity, with the result deriving parallels to the findings with *LYVE-1*$^{-/-}$ mice. The fact that fewer cells migrate from an unstimulated peritoneum may explain why the effects of non-expression of the receptor may not be observed. There is also the issue regarding sensitivity of detection as fewer cells also provide less signal differences to be noticed. With a greater number migrating during inflammation, the receptor function takes effect and the differences become noticeable. Also, other studies have outlined the effects of *CD44*$^{-/-}$ mice are most prominent upon observing disturbances to physiological homeostasis rather than in steady-state conditions. Subsequently, performed *in vitro* transmigration assays also complement the *in vivo* findings where the effects of antibody blockade of CD44-HA binding were on transmigration across activated HDLECs only.

These findings might be interpreted (at face value) as similar to the mechanism used by leucocytes in exiting from blood vessels during inflammation with this interaction most likely supporting rolling interactions within the vessel lumen

(DeGrendele, Estess et al. 1997). However, it is worth noting that transit through the initial lymphatics is unlikely to rely on rolling interactions due to low flow rates and brings to scrutiny the exact role of this interaction in transmigration. It is likely that if not rolling, they may initiate luminal crawling, a manner of movement used by DCs within the lymphatic vessels, and a mechanism that CD44 indeed initiates with bacteria (Tal, Lim et al. 2011). Intraluminal crawling has long been associated with integrins and the influence of this role may come from CD44 since it can function as an accessory molecule to this class of proteins; CD44 has been reported to form a complex with α4β1 integrin which is important to extravasation of T cells from blood vessels (Siegelman, Stanescu et al. 2000). Also, activation of LFA-1 (αLβ2 integrin) was shown to be initiated by cross-linking of surface CD44 (Kelleher, Murphy et al. 1995). An extension on the findings would be to perform *in vitro* adhesion assays with CD44 blocking antibodies to gauge an understanding of the mechanism of action of the receptor in the overall trafficking process.

The contribution of CD44 towards inflammatory transmigration and trafficking also suggests that the polarisation of macrophages is important in expression of the receptor. Proteomic profiles of the different levels of polarisation of monocyte derived macrophages identified increased expression of CD44 in response to M1 stimulating molecules, especially LPS. Interestingly, these signals promote increased binding to hyaluronan by down-modulating chondroitin sulfation of the receptor, indicating further that the functions of the receptor likely arise through ligation with HA (Ruffell, Poon et al. 2011).

As discussed above, hyaluronan binding to CD44 is key to transmigration of lymphatic endothelium by macrophages. The final experiments in this Chapter

addressed the production of hyaluronan by monocyte derived macrophages. Since previous independent publications confirmed that leucocytes, such as DCs and T cells, expressed enzymes for synthesis of hyaluronan (HAS's), it was expected that macrophages would too, as found by my own experiments (Fig 5-9) (Mummert, Mummert et al. 2002, Mahaffey and Mummert 2007). These results correlate with data from publications which have reported macrophages differentiated from other sources, such as human monocyte cell line THP-1 or murine bone marrow derived macrophages, express the hyaluronan synthases 1 and 2. Interestingly, Chang et al. (2014) demonstrated murine BMDMs stimulated with LPS had increased expression of both HAS1 and 2 and that the greatest increase in expression occurred within 2 hours of stimulation with it gradually falling over time. These findings present a possible shortcoming in experimentation with my own data where I had analysed the HAS levels after 24 hours stimulation with LPS and IFN-γ and provides a point for future experiments to analyse the change in levels of HAS expression at different times after stimulation. My data also shows that HAS2 levels are greater than HAS1 levels at basal levels which is in contrast with expression levels in murine DCs and T cells which express lesser, or no HAS2 at all. Cell line monocytes, THP-1, when differentiated into macrophages presented similar findings with minimal detection of HAS1 but upregulated expression of HAS2 (Chang, Chan et al. 2012). This suggests that there might be a preferable HAS for hyaluonan production; yet the variable levels of HAS expression along with differences at M1 polarisation phases did not correlate to contrasting hyaluronan production by the macrophages. The quantified HA production with the ELISA kit has provided a novel method into measuring hyaluronan levels and suitable comparisons are yet to be made, with data in published reports

about HA production by other leucocytes not providing similar manners of quantification. The ELISA results strikes as surprising because numerous reports have identified increased hyaluronan deposition at sites of ongoing inflammation correlating with macrophage accumulation and activation as well (Savani, Hou et al. 2000). However, it is worth considering that such findings were made with staining of tissue sections from *in vivo* experiments with influence from surrounding cells whereas the leucocytes were analysed *in vitro* in isolation. It is also important to note that HA deposition occurs across numerous days whereas observations were made in my experiments 24 hours after activation. Another interesting finding regarding the HA ELISA kit – it produces high variability within replicates of samples as well as repeats of experiments (Haserodt, Aytekin et al. 2011). If the margins are slim, then there may be a loss of significance in the data observed, especially within the cell content where there was a hint of more HA associated with M1 macrophages.

Despite similar levels of hyaluronan production, the striking difference found between M0 and M1 macrophages was the level of retention of the glycosaminoglycan on the cell surface. HABP staining revealed greater levels of binding to macrophages stimulated with LPS and IFN-γ compared to basal or those stimulated with LPS only. The increased polarisation is likely to be linked with CD44 expression as well as increased potential of the molecule to bind to HA (Gee, Lim et al. 2002). As mentioned in the Introduction, CD44 binding to HA is inherently weak due to sialylation of the receptor, a conceivable state on basal state M0 macrophages. However, activation to M1 involves upregulation of pro-inflammatory signatures, such as TNF-α; such molecules are associated with activation of CD44 and promoting the binding of HA that may lead to increased retention on the surface of macrophages (Levesque and Haynes

1997). The impact of improved retention and presentation would plausibly lead to increased interactions with LYVE-1 on lymphatic endothelium and could tie in with increased clearance associated with inflammation (inflammation also connected with M1 macrophage activation). My preliminary investigation into the role of CD44 and HA retention on the surface however, yielded surprising findings, with marginally more HA detected on *CD44*$^{-/-}$ macrophages than WT ones. However, the issues with the experiment performed arise in the way HA would be detected, with one surface of the flattened cell binding with the HA binding protein of the ELISA and another surface remaining undetected thus giving an inaccurate idea of the total amount of HA on the surface of macrophages.

An important aspect of HA function is its size, with smaller sizes associated with pro-inflammatory responses whereas larger sizes are involved in anti-inflammatory functions (McKee, Penno et al. 1996, Matou-Nasri, Gaffney et al. 2009). Whether the size binding to CD44 is small or large is yet to be identified and would be an interesting experiment to conduct as part of future plans.

An interesting finding with the trafficking observed by *CD44*$^{-/-}$ macrophages was the redirection of these myeloid cells to other organs, prominently the spleen, a similar outcome observed with macrophage trafficking from an inflamed peritoneal cavity of *LYVE-1*$^{-/-}$ mice. As discussed in Chapter 4, trafficking to an intraperitoneal lymphoid organ such as the spleen is plausible since exit from the peritoneal cavity is blocked by preventing entry into the lymphatic vessels. Possible mechanisms through which this migration would occur has been discussed in detail in Chapter 4 as well. Despite the demonstration of redirection as one possible effect of the CD44 functional deletion, another

potential mechanism of the effect that was unexplored was apoptosis. Preliminary investigations into trafficking from uninflamed peritoneum of mice showed no significant differences in arrivals of macrophages of either WT, or *CD44*$^{-/-}$ background. However, analysis of the cells from the peritoneal lavage of these injected mice revealed that there were more *CD44*$^{-/-}$ macrophages than WT ones suggesting that the increased accumulation is possibly due to less of these cells undergoing apoptosis with previous reports demonstrating that functional inhibition of the receptor promotes failure of apoptosis in a range of cells, including T cells (Fedorchenko, Stiefelhagen et al. 2013).

Overall, the data in this chapter identify another component to the LYVE-1-HA axis to macrophage trafficking via lymphatics, CD44 on leucocytes being a key receptor in the process, demonstrated both *in vivo* and *in vitro*. It also addresses the capacity of HA production by macrophages and differing levels of surface retention being key to the mechanism as well. With key concepts identified throughout the research of this D.Phil. thesis, the comprehensive impacts of these findings will be examined in the following chapter.

Chapter 6

General discussion

The notion that macrophages might exit sites of inflammation via the lymphatics and migrate to draining lymph nodes was introduced several years ago with the insighful paper by Bellingan et al. (1996), and although persuasive evidence for the process has since been presented in the literature, the phenomenon and its significance remain contentious. Moreover, there is still little knowledge of the precise exit routes that lead from these sites and how they connect to afferent lymphatic vessels, or of the molecular mechanisms that mediate adhesion and transmigration therein. Thus far, the literature implicates both integrins and chemokines as playing roles in macrophage clearance, with peritoneal exit a particularly popular model in the illustrations, although the extent of their involvement in lymphatic entry or migration are poorly defined (Gautier, Ivanov et al. 2013). The main aim of the experiments detailed in this thesis was to investigate these issues and in particular to study the engagement between macrophages and lymphatic endothelium.

6.1 Identification of key adhesion molecules mediating macrophage transmigration across lymphatic endothelium and trafficking

The findings of chapter 3 presented novel demonstration of macrophage transmigration across monolayers of primary human dermal lymphatic endothelial cells (HDLECs) *in vitro*, and revealed that the process is greatly enhanced after activation of HDLEC monolayers with TNF-α. These data also demonstrated that the kinetics of macrophage transmigration are broadly similar to those of monocyte derived dendritic cells, reaching a plateau within 6 hours and continuing over the course of > 10 hours. With adhesion as a preceding step to transendothelial migration, maximal adhesion was observed within

within 2 hours of introduction of the macrophages to the *in vitro* system. Intriguingly, almost all added macrophages to the system adhered to activated LECs although only approximately > 20 % of these cells transmigrated. This suggests that despite being able to adhere to the endothelial cells, certain factors limit the macrophages from crossing over. One such potential molecule is PECAM (CD31); Muller et al. (1993) demonstrated that blockade of homophilic interactions of PECAM on leucocytes with the molecule on vascular endothelial cells was able to prevent transmigration of the cells but did not inhibit adhesion to the endothelium or locomotion along it. The strategic location of CD31 on the tips of the button junctions of lymphatic endothelial cells at initial capillaries suggests an important role in mediating entry into the vessels, feasibly in the manner mentioned above. Another such molecule like PECAM is CD99, with mAb blockade limiting transmigration of neutrophils across blood endothelial cells without affecting previous steps of rolling, adhesion, or locomotion (Schenkel, Mamdouh et al. 2002). With macrophages reported to express CD99 and the molecule present on the surface of LECs, a similar paradigm can be hypothesised. Interestingly, however, in contrast to monocyte derived DC, the endothelial-leucocyte adhesion molecules ICAM-1, VCAM-1 and ALCAM proved to be redundant for transmigration (Johnson, Clasper et al. 2006, Iolyeva, Karaman et al. 2013). Conversely, macrophage-expressed β2 integrin was found to be significantly involved in mediating the process. Hence the question arises as to the identity of the β2 integrin counter-receptor on LEC. It is possible that in macrophages, alternative β2 integrin ligands (the complementary receptor) mediate interactions within lymphatic endothelium. Among such candidates are the junctional adhesion molecules (JAMs), a protein family which includes JAM-1 (also known as JAM-A), JAM-2 and JAM-3,

members of which have been reported to be expressed within the endothelial junctions of lymphatic capillaries, with the integrin ligands for the following JAMs reported to be expressed on the surface of macrophages - αLβ2, αMβ2 and α4β1 (Ammon, Meyer et al. 2000, Baluk, Fuxe et al. 2007, Weber, Fraemohs et al. 2007). Indeed, mice with targeted deletion of the *JAM-1* gene have functional abnormalities in the trafficking of dendritic cells to lymph nodes and it can be hypothesised that macrophages from such mice would not migrate as efficiently either (Cera, Del Prete et al. 2004).

Another leucocyte population which has been demonstrated to mediate adhesion and transmigration via β2 integrin are neutrophils. However, the *in vitro* assays as well as *in vivo* trafficking studies by Rigby et al. (2015) showed a quantitatively greater impact of functional blockade of the integrin on neutrophil migration than I had observed with macrophages, with only a 20 % reduction in macrophage *in vitro* transmigration. A possibly important difference, it highlights that macrophage exit from inflamed sites it likely to be dependent on a wider range of adhesion molecules and could be suggestive of a greater level of regulation. Macrophages are functionally diverse and play an important role in restoring homeostasis by engulfing apoptotic bodies as well as secreting anti-inflammatory cytokines such as IL-4 and IL-10 (Savill, Fadok et al. 1993, Mosser and Edwards 2008). Interestingly, further differences can be seen not only in kinetics of arrival to an inflammatory site but also in the kinetics of *in vitro* transmigration, with neutrophils arriving first as well as transmigrating activated HDLECs much faster than macrophages. Neutrophils promote inflammation (through secretions such as TNF-α, IL-1β and reactive oxygen species) and subsequent tissue destruction and hence their rapid clearance is essential,

demonstrated by their faster transmigration unlike macrophages which require longer due to possible reasons mentioned above (Weiss 1989).

Contrasting reports have been published into the involvement of β2 integrin in adhesion of macrophages to the parietal peritoneal membrane (which would contain the draining lymphatics of the peritoneal cavity). My own results, show something in between of the findings from Cao et al. (2005) and Bellingan et al. (2002); the mAb blockade by the β2 integrin blocking TS1/18 failed to fully inhibit transmigration, only causing a 20 % reduction (fig. 3-13), thus implying that other adhesion molecules expressed by activated HDLEC monolayers are likely to be involved. One group of such molecules is the selectins, a family of carbohydrate binding receptors involved in leucocyte homing. Three glycoproteins make up the selectin family - E-, L- and P-selectin. They specifically bind fucosylated and sialylated glycoprotein ligands while maintaining expression on endothelial cells, leucocytes and platelets. E-selectin expression has been confirmed on cultured primary lymphatic endothelial cells (Sawa and Tsuruga 2008). Unfortunately, due to time constraints, I was unable to assess whether E- or P-selectin was involved in adhesion or transmigration of macrophages to human LECs with a majority of focus in this thesis going towards LYVE-1. Nonetheless, the plausible involvement of this family of adhesion molecules comes from evidence within the Jackson laboratory, as reported by a former member, David Rigby, E-selectin mediates an early step during the *in vitro* adhesion of human neutrophils to TNF-α activated HDLEC monolayers (Rigby DA, 2011, D.Phil. Thesis). Given that neutrophils and macrophages display some similarities in function (such as, antigen presentation, phagocytosis of microbes, inflammatory cytokine secretions) and

share similar transcriptional profiles it is therefore possible that E-selectin could also mediate similar adhesion of macrophages (Clarke and Gordon 1998). With respect to adhesion receptors on macrophages as opposed to LECs, it is also possible that additional integrins besides β2 subtypes are involved in mediating the process, such as $\alpha 4\beta 1$ (VLA−4) and $\alpha 5\beta 1$ (VLA-5). Functional blockade of these two integrins has been reported to reduce the numbers of macrophages arriving at mediastinal lymph nodes from an inflamed peritoneum, resulting in increased numbers of the myeloid cells adherent to the parietal mesothelium (Bellingan, Xu et al. 2002). In this, case however, it remained ambiguous as to whether the role of integrins was primarily in association with lymphatic endothelium or with attachment to the mesothelium; the cell layer that must presumably be traversed by migrating macrophages before they reach underlying lymphatic structures. However, as has been introduced in Chapter 4, the entry to the underlying lymphatics from the peritoneal mesothelium is possibly through stomata within this tissue and so this explanation into the role of integrins may only be partly valid.

My results suggest that macrophage adhesion to the omentum and parietal peritoneal membrane (as illustrated in chapter 4) are important steps to their exit from the peritoneal cavity via lymphatics. One of the key observations from Chapter 4 was that macrophages appeared to interact with structures expressing LYVE-1 on the surface of the parietal peritoneum that have been tentatively identified as stomata. Currently, there appear to be no published reports that have identified markers specific for lymphatic stomata and this preliminary identification would require further investigation to validate the observations made in this thesis. Nonetheless, the images imply that these

might represent entry points for migration via afferent lymphatics to draining mediastinal lymph nodes. Since the omentum is a double fold of peritoneal membrane, it would be interesting to investigate if such similar openings expressing LYVE-1, as on the parietal membrane, are present there as well. It would also provide an indication as to why the omentum was a site of retention for adoptively transferred cells (as observed by Li-COR imaging, fig 4-24). It is likely that adhesion of the macrophages at these sites is thus reliant on cell adhesion molecules involving integrins and likely selectins.

Interestingly, cell adhesion can also provide signals for survival, seen with reduced expression of selectins by apoptotic neutrophils (Dransfield, Stocks et al. 1995); integrin dependent survival as first reported by Meredith et al. (1993) and subsequently expanded in a vast literature. Persistent presence of macrophages at inflammatory sites, seen in chronic inflammatory pathologies (Allison, Ferluga et al. 1978), is driven through binding to these adhesion molecules and it is plausible that blockade of adhesion might lead to reduction in viable macrophage counts due to induction of apoptosis – but this is speculation as I did not measure apoptosis with my *in vivo* peritonitis model. However, by blocking adhesion, clearance might also be affected and lead to accumulation of macrophages while also leading to a possible increase in apoptotic bodies within the environment that is important to be engulfed during the resolution of inflammation. Although this work is clearly only at the initial stages, it is possible in the future by understanding the process better, that selective therapies could be directed to target macrophage adhesion to lymphatic endothelium during inflammation in order to reduce their numbers at inflammatory sites and avoid collateral damage.

Amongst the group of effective selective therapies are monoclonal antibodies, which are able to target a single molecule in complex biological processes, with high specificity. Examples of such developed drugs include targeting molecules such as VEGF-A in angiogenesis (bevacizumab) (Chen, Gore-Langton et al. 2001), cytokines in inflammatory signaling such as TNF-α (infliximab) (Siegel, Shealy et al. 1995) as well as receptors in adhesion (natalizumab). Natalizumab was developed as an α4 integrin antagonist for treatment against relapsing, remitting multiple sclerosis (MS) and Crohn's disease, where leucocyte infiltration is an underlying problem (Kappos, Bates et al. 2011). Targeting α4 integrin in this manner has shown to be effective in reducing this influx, although a side-effect of this treatment is reduced systemic immune surveillance and thus an increased risk from otherwise subclinical infections. Indeed, a proportion of patients treated with Natalizumab have developed progressive multifocal leukoencephalopathy (PML) as a result of latent John Cunningham (JC) virus infections (Bloomgren, Richman et al. 2012). Furthermore, targeting such adhesion molecules will also affect clearance of leucocytes through the lymphatics and hence affect retention at inflammatory sites, a key problem in association with macrophages in chronic inflammation.

Apart from adhesion molecules, an important aspect of transmigration is arrival to the endothelium through chemotaxis. Although, the role of chemokines has not been broadly investigated in this Thesis, Gautier et al. (2013) suggested exit from an inflamed peritoneal cavity was mediated by these molecules by blocking the receptors on macrophages with pertussis toxin. My own preliminary investigations also hinted to this - *in vitro* transwell chemotaxis assays with supernatant from cultured activated HDLECs was able to induce greater

macrophage migration to the bottom chamber than media alone (data not shown). Interestingly, these preliminary investigations also identified a redundant role for CCL21 through use of neutralising mAb AF366. Further investigations would be required to understand which chemokine mediates this migration of which a host of possible ones include CCL2, CCL5, CXC_3CL1 (Kawai, Kaidoh et al. 2009, Johnson and Jackson 2013).

In summary, this Thesis has provided novel evidence by means of *in vitro* assays that macrophage adhesion is a critical step to transmigration across inflamed lymphatic endothelium and that the process is markedly different to that previously observed for monocyte derived DC and neutrophils using similar methodologies. Clearly, further work will be required to identify interacting receptors to β2 integrins on lymphatics and quantify the effect of blockade of the integrin for *in vivo* trafficking. Similar *in vitro* assays can also be used to assess the impact of β1 integrin that was unfortunately left unexplored.

6.2 Role for the LYVE-1-hyaluronan axis in macrophage adhesion/transmigration in vitro and migration via lymphatics in vivo

The results presented in chapters 3 and 4 of this D.Phil. thesis identified a new and previously unreported physiological role for the hyaluronan (HA) receptor LYVE-1 in supporting lymphatic adhesion and migration of macrophages, both *in vitro* across activated HDLEC monolayers and *in vivo* in a mouse model of macrophage trafficking from inflamed peritoneum to draining mediastinal lymph nodes. These findings also provide some of the first indications of the true physiological function of LYVE-1, an enigma that has largely remained unresolved since its discovery over a decade ago in the Jackson laboratory. As LYVE-1 is located on the tips of the button-like junctions of individual LECS, it was originally hypothesised that it may mediate cell entry into lymphatics through a presumptive interaction with HA synthesised or sequestered by migrating leucocytes (Baluk, Fuxe et al. 2007, Jackson 2009). However, evidence in support of such a role has accumulated only recently due to the availability of LYVE-1 knockout mice and LYVE-1 function blocking antibodies. Furthermore, the observation that stimulation of lymphatic endothelium with the pro-inflammatory cytokine TNF-α leads to partial downregulation of LYVE-1 both at the level of mRNA and protein initially appeared to confound such notions (Johnson, Prevo et al. 2007). However, the results of experiments presented in chapter 3 revealed that significant levels of LYVE-1 remain after TNF-α stimulation and that the receptor is redistributed on the LEC surface of cytokine stimulated LEC where it appears to have the capacity to support adhesion and transmigration of monocyte derived macrophages.

The apparent activation of HA binding by LYVE-1 in response to inflammatory cytokine has parallels with the closely related receptor CD44 in monocytes, where the activation is thought to involve receptor surface redistribution or “clustering” (Sleeman, Rudy et al. 1996). Indeed, in the case of CD44, the mechanisms that induce clustering have been uncovered and involve engagement of CD44 with the submembranous ezrin/radixin/moesin complex via a consensus binding motif in the cytoplasmic tail (Hirao, Sato et al. 1996). Although no similar ERM binding motifs are present within the cytoplasmic tail of LYVE-1, it is conceivable that analogous receptor clustering proceeds via similar mechanisms. Clustering of CD44 is likely to be an important process for stable interaction with free HA polymers and in the case of LYVE-1 with cell surface associated HA configurations (chapter 3, section 3.3.8) in order to promote transmigration of macrophages, as each receptor binds the glycosaminoglycan only weakly with Kd values in the medium to high micromolar region and is therefore highly dependent on binding avidity (Lesley, Gal et al. 2004, Jackson 2009, Wolny, Banerji et al. 2010). If LYVE-1 can indeed be activated by stimulation with TNF-α, this might also influence physiological effects besides leucocyte transmigration. For example, one can speculate that activation would affect HA-mediated signalling as well as HA uptake and turnover. In inflammatory environments, high molecular weight matrix associated HA is degraded into smaller fragments that have pro-inflammatory properties distinct from the intact molecule which is thought to be anti-inflammatory (Jackson 2009). Activation of LYVE-1 to bind HA in inflammatory tissues might thus promote clearance of partly degraded HA via lymphatics thus restoring homeostasis. Indeed, experiments described by Laurent and Fraser (1992) showed that injection of exogenous radiolabelled HA into the dermis is

taken up rapidly in afferent lymph. However, Armstrong and Bell (2002) demonstrate that in the turnover of HA from skeletal muscle, the tissues were found to contain undegraded high molecular weight hyaluronan and despite low to intermediate molecular weight HA (<0.8 x 10^6 Da) detected within lymph, this was assumed to derive from a small steady state level of mobile low molecular weight HA present within the tissues. Thus, it was concluded that most HA was in fact degraded *in situ* and the lymphatics may be more of a minor route for clearance. However, this could also indicate, that only low molecular weight HA could bind to LYVE-1 to be transported into lymphatics, despite only a small fraction being transported.

Apart from turning the receptor on with TNF-α, binding of HA to CD44 is achieved by engagement of the antigen receptor on T or B cells, interaction with inflammation-associated HA-protein adducts or non-covalent complexes, or receptor clustering (Jackson 2009). Similar parallels can be drawn with LYVE-1, especially in regard to clustering the receptor to bind to HA. As outlined above, native LYVE-1 in lymphatic endothelium binds free high molecular weight HA only weakly, due in part to modification of carbohydrate chains on the stalk of the extracellular domain by sialylation that is thought to antagonise receptor self-association (and hence inhibit avidity-dependent HA binding) through charge repulsion (Jackson 2009, Nightingale, Frayne et al. 2009). However, data in this Thesis demonstrated that antibody-induced clustering of LYVE-1 could promote adhesion of macrophages to lymphatic endothelium and subsequent transmigration even in the absence of TNF-α activation, a novel finding that suggests the inhibitory effects of LYVE-1 sialylation can be overcome by enforced LYVE-1 clustering. Other preliminary findings from

chapter 3 indicated that LYVE-1 on lymphatic endothelium appeared to form annular rings around adherent macrophages, and suggested that ring formation may be associated with macrophage transmigration across activated HDLECs. The redistribution of the receptor in such a manner would also be consistent with a role in supporting hyaluronan-mediated interactions between the adherent macrophages and LYVE-1. Recent findings from Professor Jackson's group has identified a similar structural formation with DCs adhering to HDLEC monolayers *in vitro* (Johnson LA, manuscript submitted) that are important to their transmigration. However, robust analysis also revealed that these rings were actually transmigratory "cups" that could be disrupted with LYVE-1-HA blocking mAbs or hyaluronidase, and were reminiscent of similar structures observed with ICAM-1 during leucocyte exit from blood vessels (Carman and Springer 2004). Preliminary analysis of the rings around macrophages failed to reveal such cup formation but further experimentation will be required to conclusively dismiss this possibility. At present, the physiological mechanisms that lead to LYVE-1 clustering are not clear and time pressures prevented me from investigating these aspects further in my thesis. Nevertheless, it is reasonable to speculate that the particular organisation of HA on the surface of adherent macrophages may itself promote LYVE-1 clustering and annular ring formation. It is hypothesised that either TSG-6, or SHAP can be one of those molecules *in vivo* which can mediate clustering of LYVE-1, similarly to how TSG-6-HA, or SHAP-HA complexes are believed to cluster CD44 (Lesley, Gal et al. 2004, Zhuo, Kanamori et al. 2006). From a physiological perspective, recent published evidence has shown that the HA surface capsule of group A streptococcus (GAS) is able to bind to LYVE-1, apparently by inducing receptor clustering, in transiting to draining lymph nodes, an important mechanism in its

pathogenesis (Lynskey, Banerji et al. 2015). Lastly, it remains a possibility that adhesion of macrophages to LEC results from enzymatic cleavage of the O-glycans and inhibitory sialic acid moieties from LYVE-1, thereby enhancing the capacity of the receptor for HA binding. It is interesting to note that upon differentiation from monocytes, macrophages express neuraminidase 1 (Neu1), an enzyme that cleaves glycosidic/sialic acid moieties, which is activated by complexing of surface cathepsin-1 (Stamatos, Liang et al. 2005, Liang, Seyrantepe et al. 2006). Whether such a process occurs *in vivo* and contributes to LYVE-1 functional regulation has yet to be explored with future experiments to test this hypothesis involving use of neuraminidase inhibitors and comparison of LYVE-1 sialylation before and after macrophage adhesion/transmigration *in vitro*. The multiple levels of regulation of this process indicate an important step in the transmigration of macrophages and likely other leucocytes across lymphatic endothelium, such as DCs (both human monocyte-derived and mouse bone marrow-derived) that behave similarly.

Elegant studies by Baluk et al. (2007) have revealed that MHC-II$^+$ leucocytes (mainly dendritic cells and macrophages) enter afferent lymphatic capillaries in bronchial tissue by passing through the distinctive endothelial flaps located between button junctions that are present in initial vessels. However, the precise molecular mechanisms that regulate this entry process have yet to be uncovered. It is for example unclear whether DCs enter by means of paracellular migration via these junctions or whether they can also enter via, transcellular migration as has been demonstrated in studies with microvascular endothelial cells that comprised mixed populations of both blood and lymphatic cells. The internalisation of endogenous LYVE-1 after LECs are stimulated with

TNF-α suggests a possible scenario in which macrophages interacting with LECs via LYVE-1-HA mediated interactions might be transcytosed through lymphatic endothelium. Microscopic analysis of vessels in inflammatory conditions has demonstrated that LYVE-1 is not fully removed from the surface and is rearranged across the cell surface (as other junctional proteins are in inflammation) (Johnson, Prevo et al. 2007). The changing dynamic of intercellular junctions most likely facilitates increased fluid and cell entry and it is therefore plausible that LYVE-1 operates to accommodate such increases.

Another curious finding from this thesis was that after adherence to HDLECs, the recovered macrophages appeared to have acquired small amounts of LYVE-1 on their surface (section 3.3.6, fig. 3-22b). Unlike certain subsets of tissue resident macrophages thought to be separately derived from yolk sac, the monocyte-derived macrophages used in this thesis which are of myeloid origin do not express endogenous LYVE-1 (data not shown) (Ginhoux, Greter et al. 2010). Hence, it is likely that such LYVE-1 was derived from HDLEC, by plasma membrane transfer or "biting". Such sharing of plasma membrane has not been described before between lymphatic endothelium and leucocytes, although the curious phenomenon of leucocytes 'biting' off receptors from other cells has been reported, for example with cytotoxic lymphocytes (CTLs) and T helper cells acquiring MHC-peptide complexes from antigen presenting cells (APCs) (Cox, McMichael et al. 2007). In the case of the T cells, such actions were to transform T cells into APCs that could be targeted by other CTLs for killing. The exact consequences of macrophages acquiring LYVE-1 and other components from lymphatic endothelium, should the process occur *in vivo* are unclear, but they suggest intriguing possibilities for the receptor's function. For

example, LYVE-1 could regulate the apoptotic fate of the travelling macrophages within the lymph node in a manner similar to CD44, its closely related HA receptor. Through association with HA, CD44 has been reported to promote activation of focal adhesion kinase (FAK) and resist apoptosis (Fujita, Kitagawa et al. 2002). Since LYVE-1-HA interactions were able to partially influence adhesion to lymphatic endothelium, it is plausible that such a mechanism could influence apoptosis. The role of LYVE-1 in lymph nodes has not been established, despite abundant expression in the floor endothelium of the subcapsular sinus which might indicate a regulatory role for further entry into the cortex and medulla (Banerji, Ni et al. 1999). Acquired LYVE-1 from lymphatic endothelium on macrophages could give a signal for entry into the further regions by interacting with the receptor on lymph node endothelium. However, it also worth noting the possible artifact in the observations made with LYVE-1 on the surface of macrophages; a certain decree of LEC fragmentation after Accutase™ recovery could be the reason for LYVE-1 on the surface of the macrophage rather than a transfer of the receptor.

One of the key surprising results attained throughout this D.Phil. was the redirection of the cells to other organs observed with the *in vivo* peritonitis model upon treating mice with LYVE-1 blocking mAbs. The antibody treatment had caused a reduction in the adoptively transferred macrophages arriving at draining mediastinal lymph nodes and it was expected that the cells would be within peritoneal lavage (similar to trafficking in *LYVE-1*$^{-/-}$ mice). However, these cells were not within the lavage and instead numerous other unexpected locations within the murine body contained the fluorescent cells (Figs 4-22 to 4-24). Trafficking experiments with LYVE-1-HA blocking mAbs revealed the

spleen as the major organ for redirection of adoptively transferred macrophages, and demonstrated that redirection also led to a coordinated expansion of the spleen (splenomegaly) itself (Chapter 4, figure 4-25). The expansion in spleen size in response to redirected macrophage trafficking is not such an odd phenomenon. The hypertrophy of draining LNs in response to FCA injection was reported to arise from B cell entry and release of lymphangiogenic GF (VEGF-A) (Angeli, Ginhoux et al. 2006). It is plausible that macrophages may be releasing angiogenic and lymphangiogenic growth factors and this could be part of the reason for the splenic hypertrophy. Apart from its role on macrophage trafficking, other possible effects of antibody blockade could be related to redirection of fluid drainage; blockade of interstitial fluid entry into lymphatics by antibody could promote similar redirection as observed with the macrophages resulting in enlargement of the organ.

In summary, the experiments reported in this Thesis have shown that the LYVE-1-HA axis has an important role in mediating homeostasis by clearing macrophages from inflammatory sites. However, its physiological roles may be much wider than previously considered and the intriguing possibilities discussed above, such as, the impact of the receptor in fluid drainage as well as its role within lymph nodes, would provide interesting focus for future experiments.

6.3 The importance and contribution of CD44 and HA production for macrophage trafficking to lymph nodes

The findings described in the final results chapter of this D.Phil. thesis (Chapter 5) revealed that in addition to LYVE-1 in lymphatic endothelium, the hyaluronan receptor CD44 on macrophages was also important for clearance of this leucocyte subpopulation from tissues via the lymphatics. CD44 was identified as a critical component both for transit of macrophages across human lymphatic endothelium *in vitro* and for migration of macrophages from the inflamed peritoneum to draining lymph nodes in the mouse *in vivo*, where it appeared to function as a receptor for presentation of endogenous macrophage derived HA to LYVE-1. It has been well documented that CD44-HA interactions mediate trans-endothelial migration (TEM) of leucocytes across blood vascular endothelium (DeGrendele, Estess et al. 1997); the data presented in Chapter 5 provide unique evidence of a similar role in transmigration across lymphatic endothelium. Figures 5-3 and 5-4 show that reduced numbers of *CD44*$^{-/-}$ macrophages traffic from inflamed peritoneum to draining lymph nodes compared to their WT counterparts. Also, figure 5-9 shows that blockade of CD44-HA interaction with mAb BRIC235 inhibited inflammatory macrophages transmigrating activated LECs. As with exit from blood vessels, the data suggests that macrophages present HA through CD44 for adhesion to lymphatic endothelium, most likely through HA counter receptor LYVE-1, similarly to the sandwich model in which leucocyte CD44-HA binds to CD44 on blood endothelium.

An interesting finding from these studies on CD44 was that although it was a critical component of *in vitro* transmigration of lymphatic endothelium and

trafficking from peritoneum in inflamed conditions, blocking CD44-HA interactions did not significantly disrupt *in vitro* transmigration of uninflamed LECs or trafficking from uninflamed peritoneum. This closely paralleled my earlier findings with LYVE-1, in chapter 3 and 4, where *in vitro* transmigration and *in vivo* trafficking of macrophages across activated but not resting lymphatics was impaired by LYVE-1 antibody blockade. However, CD44 on macrophages may be equally well able to present HA under resting conditions as inflamed conditions, since the inflammatory cytokine treatment was applied mainly to LECs not macrophages. This presenting capacity will only have an effect when LYVE-1 is receptive to HA binding – which in my experiments appears to occur after TNF-α treatment of LECs. It is also likely that the two receptors become involved in response to the additional changes that occur in LECs upon activation, such as induction of chemokine secretion etc (McKee, Penno et al. 1996).

The exact mechanism by which CD44 contributes to the adhesion and transmigration of macrophages on lymphatic endothelium is not completely clear. It is most likely that CD44 is acting as a receptor to organise and present macrophage HA in an “appropriate configuration” for LYVE-1 binding. One plausible way is that CD44 organises HA produced by the macrophages in an “appropriate manner” for binding to LYVE-1 and this could be through the use of accessory Link proteins such as TSG-6. TSG-6-HA complexes were shown to bind more avidly than free HA to CD44 in transfected lymphocytes and interestingly this was able to cause firm adhesion than ‘rolling’ action previously reported with CD44-HA (Lesley, English et al. 2002). Biophysical techniques showed that immobilised HA monolayers are condensed and rigidified after addition of full-length TSG-6 or TSG-6 mutants that lack the dimerising CUB

domain, but that only the former appear to crosslink HA (Baranova, Nileback et al. 2011). Also, tentative unpublished evidence from the Jackson laboratory demonstrated that TSG-6-HA complexes induce clustering of the close homolog of CD44, LYVE-1. Hence, it is predictable that crosslinked TSG-6-HA complexes would cluster CD44 but this has yet to be demonstrated. Interestingly, Yang et al. (2012) demonstrate that CD44 clustering on immortalised cell lines is promoted by self production of native high molecular weight HA which can be disrupted by smaller weight oligosaccharides of HA, the evidence implying that the size of native HA produced by cells would play a role in clustering of CD44 and likely tethering of the GAG. The characterisation of HA production in this Thesis suggests that M1 polarisation of the macrophages increases HA tethering on the surface (Fig 5-11), and it is likely that such inflammatory activation is related to clustering of CD44. Indeed the differentiation of monocytes to macrophages with phorbol 12-myristate 13-acetate (PMA) has been shown to coincide with clustering of the receptor and further polarisation could accompany greater levels of clustering and HA binding (Zhang, Zhang et al. 2014). Similar to the TSG-6-HA complexes, it is plausible that CD44-HA complexes on macrophages is able to cluster LYVE-1 and contribute to the LYVE-1 ring formation around adherent macrophages on lymphatic endothelium. Recently published data from the Jackson group demonstrate that group A streptococcus (GAS) bind to clusters of LYVE-1 on the surface of LECs and present HA but it is unknown if these pre-exist or are they induced (Lynskey, Banerji et al. 2015). It also indicates a further step of regulation in the closely controlled process of receptor activation and macrophage trafficking from inflamed tissue.

A second potential yet speculative mechanism of CD44 to contributing adhesion/transmigration of macrophages could be by promoting activation of integrins on the surface of macrophages by sequestering chemokines. CD44 is decorated with heparan sulphate, which can bind to chemokines and in turn initiate signalling events (Tanaka 2000). Such an example of chemokines promoting adhesion is the activation of αMβ2 integrin on the surface of monocytes by CCL2 (Weber, Klickstein et al. 1999). Subsequent activation of integrins clusters the alpha and beta chains of integrins promoting binding to adhesion molecules.

Despite the discussion of mechanisms of CD44-HA complexes binding to LYVE-1 on LECs, a key observation between LYVE-1 and HA interactions was that it did not strongly mediate macrophage adhesion to activated HDLEC monolayers as shown by marginal reduction in adherent macrophages after hyaluronidase treatment of the myeloid cells (fig 3-28) and competitive blockade of LYVE-1-HA with mAb893 (fig 3-23b). Thus, it is likely that even though CD44 is involved in transmigration, it may too not strongly induce adhesion of macrophages to activated LECs. Unfortunately, due to time constraints the impact of mAb blockade of CD44-HA on adhesion of macrophages was not demonstrated but would be an important experiment to pursue in the future.

Another interesting hypothesis to take into consideration is if CD44 bound HA could induce intra-luminal crawling of the macrophages. Indeed, HA binding to CD44 is known to induce lamellipodia outgrowth used by cells for movement towards a stimulus and this might be another method of regulating macrophage migration towards lymphatic endothelium (Oliferenko, Kaverina et al. 2000). Another feature of these CD44 lamellipodia is the presence of matrix metalloproteinases (MMPs) (Abecassis, Olofsson et al. 2003); Rigby et al.

(2015) demonstrated that neutrophil-derived MMPs retracted HDLECs in monolayer culture and created ‘hotspots’ for diapedesis. It would be interesting to explore if lamellipodia from macrophages could interact in such a manner with lymphatic endothelium too, noted by the shared biological similarity with neutrophils.

With numerous possible mechanisms taken into consideration, macrophage CD44-HA interactions provide another level of regulation to a complex process that can be open to manipulation for therapies aiming to contract macrophage burden in chronic inflammation.

Along with CD44 and LYVE-1, the critical component to transmigration was macrophage-derived HA. Macrophages were demonstrated to express key HA producing genes HAS1 and HAS2 and indeed produced HA in culture (Chapter 5). Furthermore, enzymatic cleavage of the HA tethered on the surface, reduced numbers of macrophages transmigrating across activated HDLEC monolayers. HA-mediated interactions are not just limited to the endothelium (which have been noted above) but have also been reported in other cells mediating adhesion of smooth muscle cells and epithelial cells (Ramamurthi and Vesely 2002). The role of HA in macrophage transmigration of the lymphatic endothelium has yet to be confirmed *in vivo*. However, it is likely that interceding the parietal mesothelium and lymphatic stomata associated with draining from the peritoneum (introduced in section 4.1), would involve interactions with the GAG similar to the initial contact with lymphatic endothelium where the requirement of HA to transmigration of lymphatic endothelium was demonstrated. By treating macrophages with hyaluronidase prior to injection into the peritoneum to reduce surface HA, imaging of the parietal peritoneal

membrane would reveal the involvement of the GAG in mediating adhesion to the tissue. These potential interactions with mesothelial cells and tentatively identified stomata would probably be dependent on the expression of counter receptors (mesothelial cells have been reported to have high density of CD44 and the structures identified as stomata in this thesis which were LYVE-1^{+}) (Ross, Ansell et al. 1998). Indeed, cancer cells have been shown to adhere to peritoneal mesothelial cells *in vitro* in a CD44 dependent manner (Lessan, Aguiar et al. 1999). Previous electron microscopy work identified that the openings within the peritoneal membrane, that were termed stomata, had cytoplasmic processes of lymphatic endothelial cells protruding into the submesothelial connective tissue (Wang, Li et al. 2010). It is likely that my LYVE-1 staining identified these structures. Further microscopy experiments would however, be required to explore other markers of these structures. Since, the LECs are protruding, podoplanin would be expected to be observed. Additional marker investigation can involve culture of peritoneal mesothelial and endothelial cells with the methodology established and reproducible from the work by Stylianou et al. (1990) and Yung et al. (1995). Their work has also demonstrated the expression of vimentin, P-selectin, E-selectin, endoglin and PECAM (CD31) amongst others by the endothelial cells. With a range of markers to aid in identification, intravital microscopy can be used to follow macrophage exit from an inflamed peritoneum and discern the involvement of the stomata.

Semi-quantitative measurement of HA on the surface of macrophages using biotinylated HA binding protein (bHABP) in chapter 5 (Fig 5-11C) indicated that the levels increased with increasing polarity to an M1 phenotype even though

the total cellular levels of the glycosaminoglycan as measured by a competitive ELISA remained essentially the same, suggesting that the levels of HA on the surface are a very small proportion of the total cellular HA. From an *in vivo* perspective, within an inflammatory environment such as that in peritonitis, the macrophages population would be expected to comprise mostly M1 types, and their increased levels of surface HA may therefore facilitate interactions with lymphatic endothelium during the exit process. As discussed above, HA mediated interactions were shown to make only a quantitatively minor contribution towards adhesion of macrophages to lymphatic endothelium based on *in vitro* assays; however, similar to CD44-HA interactions on blood endothelium mediating initial weak "rolling" interactions prior to stronger adhesion by integrins and cell adhesion molecules (CAMs), CD44-HA-LYVE-1 interactions may also be as important initially before other more stable interactions occur with other receptor-ligand pairs. A second potential mechanism of HA action on transmigration is through signalling events via binding to LYVE-1. Unpublished evidence from the Jackson group uncovered HA binding to LYVE-1 promoting phosphorylation of VE-cadherin that in turn prevented it from forming homophilic interactions with neighbouring cell VE-cadherin and hence a relaxation of the tight junctions that led to retraction of *in vitro* cultured LECs. With M1 macrophages having more HA to present to LYVE-1, increased levels of signalling could be achieved thus resulting in greater rates of transmigration.

The production of HA could also affect exit of macrophages in an indirect manner by influencing the surrounding environment. Depending on the size of HA released, this could contribute to pro- or anti-inflammatory reactions within the microenvironment (Jackson 2009). Hence, the exit of macrophages and

potentially molecular changes to lymphatics could be affected, as well as secretion of chemokines and cytokines that mediate transmigration of lymphatic endothelium. The demonstration through my own ELISA analysis of HA quantity higher within the supernatant than total cell content of *in vitro* cultured monocyte derived macrophages suggest a capacity of inflammatory macrophages to secrete HA (Fig 5-10). However, to understand the effects of such secretions and analyse the speculations made above, further identification of size of HA molecules by agarose gel electrophoresis methodology proposed by Lee & Cowman et al. (1994) would be required.

Increased HA deposition is a key feature of chronic inflammation and is believed to contribute to increased macrophage retention, an observation found in bleomycin induced lung injuries(Savani, Hou et al. 2000). In contrast, increased HA on the surface of the myeloid cells is beneficial for exit out of inflammatory sites. These conflicting findings can be reconciled by suggesting that increased HA production is only useful at the early stages of acute inflammation, when greater numbers of macrophages must exit peripheral tissue. However, in the progression to chronic inflammation, with increased expulsion of HA into the surrounding environment, cells are restricted in movement and thus prevented from exiting inflammatory sites.

Taken together, it can be seen that CD44 and HA on macrophages can impact the trafficking of macrophages to draining lymph nodes directly as well as by indirect mechanisms.

6.4 Conclusions

Data presented in this thesis represents novel and robust investigation into the mechanisms by which macrophages transmigrate across lymphatic endothelium in their journey from an inflamed tissue site – in this particular case the peritoneal cavity - to draining lymph nodes. The *in vitro* models of transmigration and adhesion provide preliminary evidence for involvement of macrophage β2 integrins in supporting adhesion to lymphatic endothelium as well as a key role for macrophage surface anchored HA via a novel LYVE-1-HA axis. The further finding that CD44 plays an important role in presenting this macrophage derived HA to LYVE-1 is consistent with a sandwich model facilitating transmigration of lymphatic endothelium (Fig 6-1). These roles of LYVE-1 and CD44 identified from *in vitro* studies were further corroborated by experiments with *LYVE-1*$^{-/-}$ animals and *CD44*$^{-/-}$ macrophages in an *in vivo* model of macrophage clearance from the peritoneal cavity in a mouse sterile peritonitis model and the resulting findings, although in many cases preliminary, provide a foundation for future investigations that will identify the molecular mechanisms in more detail and hence advance our understanding of the complex role of HA and its receptors in regulating leucocyte trafficking to draining lymph nodes.

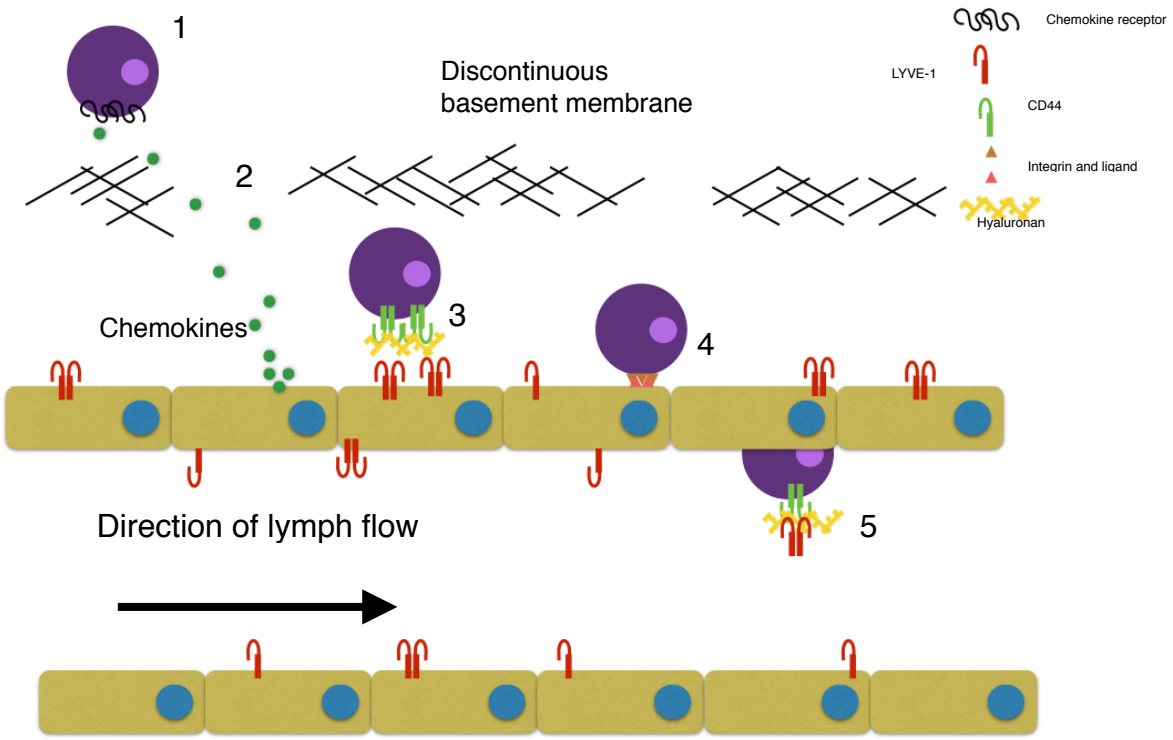


Figure 6-1. Proposed model of macrophage exit during the resolution phase of inflammation via lymphatics. (1) Inflammatory activation of lymphatic endothelial cells at the initial lymphatic capillaries causes secretion of chemokines which guides macrophages towards the vessel. (2) Macrophages encounter the discontinuous basement membrane in association with initial lymphatics and find portals to then face the basolateral suface of lymphatic endothelium. (3) Via self expressed hyaluronan, tethered on to the surface by CD44, the myeloid cells interact with likely clustered LYVE-1 (from activation by inflammatory mediators, such as TNF-α. (4) Upon mediating weak adhesion contacts via CD44-HA-LYVE-1 axis, integrins expressed by macrophages (e.g. β2 integrin) then bind to cognate receptors on LECs, which are yet to be identified (plausibly JAM-A), mediating firm adhesion to the lymphatic endothelial surface. (5) Subsequently, macrophages enter the vessel via either paracellular, or transcellular mode of transmigration, although the dominant mode is yet to be uncovered.

Bibliography

Abecassis, I., B. Olofsson, M. Schmid, G. Zalcman and A. Karniguian (2003). "RhoA induces MMP-9 expression at CD44 lamellipodial focal complexes and promotes HMEC-1 cell invasion." Exp Cell Res **291**(2): 363-376.

Abu-Hijleh, M. F., O. A. Habbal and S. T. Moqattash (1995). "The role of the diaphragm in lymphatic absorption from the peritoneal cavity." J Anat **186 (Pt 3)**: 453-467.

Addison, W. (1842). "Experimental Researches on the Blood Corpuscle." Prov Med J Retrosp Med Sci **4**(99): 403-407.

Aits, S. and M. Jaattela (2013). "Lysosomal cell death at a glance." J Cell Sci **126**(Pt 9): 1905-1912.

Allison, A. C., J. Ferluga, H. Prydz and H. U. Schorlemmer (1978). "The role of macrophage activation in chronic inflammation." Agents Actions **8**(1-2): 27-35.

Amerini, S., M. Ziche, S. T. Greiner and D. C. Zawieja (2004). "Effects of substance P on mesenteric lymphatic contractility in the rat." Lymphat Res Biol **2**(1): 2-10.

Ammon, C., S. P. Meyer, L. Schwarzfischer, S. W. Krause, R. Andreesen and M. Kreutz (2000). "Comparative analysis of integrin expression on monocyte-derived macrophages and monocyte-derived dendritic cells." Immunology **100**(3): 364-369.

Anderson, C. F. and D. M. Mosser (2002). "A novel phenotype for an activated macrophage: the type 2 activated macrophage." J Leukoc Biol **72**(1): 101-106.

Angeli, V., F. Ginhoux, J. Llodra, L. Quemeneur, P. S. Frenette, M. Skobe, R. Jessberger, M. Merad and G. J. Randolph (2006). "B cell-driven

lymphangiogenesis in inflamed lymph nodes enhances dendritic cell mobilization." Immunity **24**(2): 203-215.

Ansel, K. M., R. B. Harris and J. G. Cyster (2002). "CXCL13 is required for B1 cell homing, natural antibody production, and body cavity immunity." Immunity **16**(1): 67-76.

Aruffo, A., I. Stamenkovic, M. Melnick, C. B. Underhill and B. Seed (1990). "CD44 is the principal cell surface receptor for hyaluronate." Cell **61**(7): 1303-1313.

Austyn, J. M. and S. Gordon (1981). "F4/80, a monoclonal antibody directed specifically against the mouse macrophage." Eur J Immunol **11**(10): 805-815.

Avellino, A. M., A. T. Dailey, J. M. Harlan, S. R. Sharar, R. K. Winn, L. D. McNutt and M. Kliot (2004). "Blocking of up-regulated ICAM-1 does not prevent macrophage infiltration during Wallerian degeneration of peripheral nerve." Exp Neurol **187**(2): 430-444.

Badylak, S. F., J. E. Valentin, A. K. Ravindra, G. P. McCabe and A. M. Stewart-Akers (2008). "Macrophage phenotype as a determinant of biologic scaffold remodeling." Tissue Eng Part A **14**(11): 1835-1842.

Baluk, P., J. Fuxe, H. Hashizume, T. Romano, E. Lashnits, S. Butz, D. Vestweber, M. Corada, C. Molendini, E. Dejana and D. M. McDonald (2007). "Functionally specialized junctions between endothelial cells of lymphatic vessels." J Exp Med **204**(10): 2349-2362.

Baluk, P., L. C. Yao, J. Feng, T. Romano, S. S. Jung, J. L. Schreiter, L. Yan, D. J. Shealy and D. M. McDonald (2009). "TNF-alpha drives remodeling of blood vessels and lymphatics in sustained airway inflammation in mice." J Clin Invest **119**(10): 2954-2964.

Banerji, S., J. Ni, S. X. Wang, S. Clasper, J. Su, R. Tammi, M. Jones and D. G. Jackson (1999). "LYVE-1, a new homologue of the CD44 glycoprotein, is a lymph-specific receptor for hyaluronan." J Cell Biol **144**(4): 789-801.

Banerji, S., A. J. Wright, M. Noble, D. J. Mahoney, I. D. Campbell, A. J. Day and D. G. Jackson (2007). "Structures of the Cd44-hyaluronan complex provide insight into a fundamental carbohydrate-protein interaction." Nat Struct Mol Biol **14**(3): 234-239.

Baradi, A. F. and S. N. Rao (1976). "A scanning electron microscope study of mouse peritoneal mesothelium." Tissue Cell **8**(1): 159-162.

Baranova, N. S., E. Nileback, F. M. Haller, D. C. Briggs, S. Svedhem, A. J. Day and R. P. Richter (2011). "The inflammation-associated protein TSG-6 cross-links hyaluronan via hyaluronan-induced TSG-6 oligomers." J Biol Chem **286**(29): 25675-25686.

Barczyk, M., S. Carracedo and D. Gullberg (2010). "Integrins." Cell Tissue Res **339**(1): 269-280.

Barreiro, O., M. Yanez-Mo, J. M. Serrador, M. C. Montoya, M. Vicente-Manzanares, R. Tejedor, H. Furthmayr and F. Sanchez-Madrid (2002). "Dynamic interaction of VCAM-1 and ICAM-1 with moesin and ezrin in a novel endothelial docking structure for adherent leukocytes." J Cell Biol **157**(7): 1233-1245.

Barreiro, O., M. Zamai, M. Yanez-Mo, E. Tejera, P. Lopez-Romero, P. N. Monk, E. Gratton, V. R. Caiolfa and F. Sanchez-Madrid (2008). "Endothelial adhesion receptors are recruited to adherent leukocytes by inclusion in preformed tetraspanin nanoplatforms." J Cell Biol **183**(3): 527-542.

Baumgart, M., V. Moos, D. Schuhbauer and B. Muller (1998). "Differential expression of major histocompatibility complex class II genes on murine

macrophages associated with T cell cytokine profile and protective/suppressive effects." Proc Natl Acad Sci U S A **95**(12): 6936-6940.

Bazigou, E., S. Xie, C. Chen, A. Weston, N. Miura, L. Sorokin, R. Adams, A. F. Muro, D. Sheppard and T. Makinen (2009). "Integrin-alpha9 is required for fibronectin matrix assembly during lymphatic valve morphogenesis." Dev Cell **17**(2): 175-186.

Bellingan, G. J., H. Caldwell, S. E. Howie, I. Dransfield and C. Haslett (1996). "In vivo fate of the inflammatory macrophage during the resolution of inflammation: inflammatory macrophages do not die locally, but emigrate to the draining lymph nodes." J Immunol **157**(6): 2577-2585.

Bellingan, G. J., P. Xu, H. Cooksley, H. Cauldwell, A. Shock, S. Bottoms, C. Haslett, S. E. Mutsaers and G. J. Laurent (2002). "Adhesion molecule-dependent mechanisms regulate the rate of macrophage clearance during the resolution of peritoneal inflammation." J Exp Med **196**(11): 1515-1521.

Bevilacqua, M. P., J. S. Pober, D. L. Mendrick, R. S. Cotran and M. A. Gimbrone, Jr. (1987). "Identification of an inducible endothelial-leukocyte adhesion molecule." Proc Natl Acad Sci U S A **84**(24): 9238-9242.

Bloomgren, G., S. Richman, C. Hotermans, M. Subramanyam, S. Goelz, A. Natarajan, S. Lee, T. Plavina, J. V. Scanlon, A. Sandrock and C. Bozic (2012). "Risk of natalizumab-associated progressive multifocal leukoencephalopathy." N Engl J Med **366**(20): 1870-1880.

Boensch, C., S. S. Huang, D. T. Connolly and J. S. Huang (1999). "Cell surface retention sequence binding protein-1 interacts with the v-sis gene product and platelet-derived growth factor beta-type receptor in simian sarcoma virus-transformed cells." J Biol Chem **274**(15): 10582-10589.

Bouyain, S., S. Rushton and K. Drickamer (2001). "Minimal requirements for the binding of selectin ligands to a C-type carbohydrate-recognition domain." Glycobiology **11**(11): 989-996.

Bradfield, P. F., C. Scheiermann, S. Nourshargh, C. Ody, F. W. Luscinskas, G. E. Rainger, G. B. Nash, M. Miljkovic-Licina, M. Aurrand-Lions and B. A. Imhof (2007). "JAM-C regulates unidirectional monocyte transendothelial migration in inflammation." Blood **110**(7): 2545-2555.

Brown, S., I. Heinisch, E. Ross, K. Shaw, C. D. Buckley and J. Savill (2002). "Apoptosis disables CD31-mediated cell detachment from phagocytes promoting binding and engulfment." Nature **418**(6894): 200-203.

Bystrom, J., I. Evans, J. Newson, M. Stables, I. Toor, N. van Rooijen, M. Crawford, P. Colville-Nash, S. Farrow and D. W. Gilroy (2008). "Resolution-phase macrophages possess a unique inflammatory phenotype that is controlled by cAMP." Blood **112**(10): 4117-4127.

Callahan, M. K., P. Williamson and R. A. Schlegel (2000). "Surface expression of phosphatidylserine on macrophages is required for phagocytosis of apoptotic thymocytes." Cell Death Differ **7**(7): 645-653.

Canton, J., D. Neculai and S. Grinstein (2013). "Scavenger receptors in homeostasis and immunity." Nat Rev Immunol **13**(9): 621-634.

Cao, C., D. A. Lawrence, D. K. Strickland and L. Zhang (2005). "A specific role of integrin Mac-1 in accelerated macrophage efflux to the lymphatics." Blood **106**(9): 3234-3241.

Cao, Y. (2005). "Opinion: emerging mechanisms of tumour lymphangiogenesis and lymphatic metastasis." Nat Rev Cancer **5**(9): 735-743.

Carlow, D. A., M. R. Gold and H. J. Ziltener (2009). "Lymphocytes in the peritoneum home to the omentum and are activated by resident dendritic cells." J Immunol **183**(2): 1155-1165.

Carman, C. V. and T. A. Springer (2004). "A transmigratory cup in leukocyte diapedesis both through individual vascular endothelial cells and between them." J Cell Biol **167**(2): 377-388.

Carrasco, Y. R. and F. D. Batista (2007). "B cells acquire particulate antigen in a macrophage-rich area at the boundary between the follicle and the subcapsular sinus of the lymph node." Immunity **27**(1): 160-171.

Cayrol, R., K. Wosik, J. L. Berard, A. Dodelet-Devillers, I. Ifergan, H. Kebir, A. S. Haqqani, K. Kreymborg, S. Krug, R. Moumdjian, A. Bouthillier, B. Becher, N. Arbour, S. David, D. Stanimirovic and A. Prat (2008). "Activated leukocyte cell adhesion molecule promotes leukocyte trafficking into the central nervous system." Nat Immunol **9**(2): 137-145.

Cera, M. R., A. Del Prete, A. Vecchi, M. Corada, I. Martin-Padura, T. Motoike, P. Tonetti, G. Bazzoni, W. Vermi, F. Gentili, S. Bernasconi, T. N. Sato, A. Mantovani and E. Dejana (2004). "Increased DC trafficking to lymph nodes and contact hypersensitivity in junctional adhesion molecule-A-deficient mice." J Clin Invest **114**(5): 729-738.

Chang, M. Y., C. K. Chan, K. R. Braun, P. S. Green, K. D. O'Brien, A. Chait, A. J. Day and T. N. Wight (2012). "Monocyte-to-macrophage differentiation: synthesis and secretion of a complex extracellular matrix." J Biol Chem **287**(17): 14122-14135.

Chang, M. Y., K. L. Olin, C. Tsoi, T. N. Wight and A. Chait (1998). "Human monocyte-derived macrophages secrete two forms of proteoglycan-

macrophage colony-stimulating factor that differ in their ability to bind low density lipoproteins." J Biol Chem **273**(26): 15985-15992.

Chang, M. Y., Y. Tanino, V. Vidova, M. G. Kinsella, C. K. Chan, P. Y. Johnson, T. N. Wight and C. W. Frevert (2014). "A rapid increase in macrophage-derived versican and hyaluronan in infectious lung disease." Matrix Biol **34**: 1-12.

Chen, H. X., R. E. Gore-Langton and B. D. Cheson (2001). "Clinical trials referral resource: Current clinical trials of the anti-VEGF monoclonal antibody bevacizumab." Oncology (Williston Park) **15**(8): 1017, 1020, 1023-1016.

Chen, W. Y. and G. Abatangelo (1999). "Functions of hyaluronan in wound repair." Wound Repair Regen **7**(2): 79-89.

Choi, I., S. Lee and Y. K. Hong (2012). "The new era of the lymphatic system: no longer secondary to the blood vascular system." Cold Spring Harb Perspect Med **2**(4): a006445.

Christensen, M. S., C. E. Hoy, C. C. Becker and T. G. Redgrave (1995). "Intestinal absorption and lymphatic transport of eicosapentaenoic (EPA), docosahexaenoic (DHA), and decanoic acids: dependence on intramolecular triacylglycerol structure." Am J Clin Nutr **61**(1): 56-61.

Clark, R. A., R. Alon and T. A. Springer (1996). "CD44 and hyaluronan-dependent rolling interactions of lymphocytes on tonsillar stroma." J Cell Biol **134**(4): 1075-1087.

Clarke, S. and S. Gordon (1998). "Myeloid-specific gene expression." J Leukoc Biol **63**(2): 153-168.

Constant, S. L. (1999). "B lymphocytes as antigen-presenting cells for CD4+ T cell priming in vivo." J Immunol **162**(10): 5695-5703.

Cowman, M. K., H. G. Lee, K. L. Schwertfeger, J. B. McCarthy and E. A. Turley (2015). "The Content and Size of Hyaluronan in Biological Fluids and Tissues." Front Immunol **6**: 261.

Cox, J. H., A. J. McMichael, G. R. Screaton and X. N. Xu (2007). "CTLs target Th cells that acquire bystander MHC class I-peptide complex from APCs." J Immunol **179**(2): 830-836.

Culty, M., H. A. Nguyen and C. B. Underhill (1992). "The hyaluronan receptor (CD44) participates in the uptake and degradation of hyaluronan." J Cell Biol **116**(4): 1055-1062.

Czeloth, N., G. Bernhardt, F. Hofmann, H. Genth and R. Forster (2005). "Sphingosine-1-phosphate mediates migration of mature dendritic cells." J Immunol **175**(5): 2960-2967.

Davies, L. C., S. J. Jenkins, J. E. Allen and P. R. Taylor (2013). "Tissue-resident macrophages." Nat Immunol **14**(10): 986-995.

Davis, M. J., M. M. Lane, A. M. Davis, D. Durtschi, D. C. Zawieja, M. Muthuchamy and A. A. Gashev (2008). "Modulation of lymphatic muscle contractility by the neuropeptide substance P." Am J Physiol Heart Circ Physiol **295**(2): H587-597.

Day, A. J. and G. D. Prestwich (2002). "Hyaluronan-binding proteins: tying up the giant." J Biol Chem **277**(7): 4585-4588.

de la Motte, C. A., V. C. Hascall, J. Drazba, S. K. Bandyopadhyay and S. A. Strong (2003). "Mononuclear leukocytes bind to specific hyaluronan structures on colon mucosal smooth muscle cells treated with polyinosinic acid:polycytidylic acid: inter-alpha-trypsin inhibitor is crucial to structure and function." Am J Pathol **163**(1): 121-133.

Deanfield, J. E., J. P. Halcox and T. J. Rabelink (2007). "Endothelial function and dysfunction: testing and clinical relevance." Circulation **115**(10): 1285-1295.

DeGrendele, H. C., P. Estess and M. H. Siegelman (1997). "Requirement for CD44 in activated T cell extravasation into an inflammatory site." Science **278**(5338): 672-675.

Desmouliere, A., A. Geinoz, F. Gabbiani and G. Gabbiani (1993). "Transforming growth factor-beta 1 induces alpha-smooth muscle actin expression in granulation tissue myofibroblasts and in quiescent and growing cultured fibroblasts." J Cell Biol **122**(1): 103-111.

Dransfield, I., S. C. Stocks and C. Haslett (1995). "Regulation of cell adhesion molecule expression and function associated with neutrophil apoptosis." Blood **85**(11): 3264-3273.

Elmore, S. (2007). "Apoptosis: a review of programmed cell death." Toxicol Pathol **35**(4): 495-516.

Esser, S., M. G. Lampugnani, M. Corada, E. Dejana and W. Risau (1998). "Vascular endothelial growth factor induces VE-cadherin tyrosine phosphorylation in endothelial cells." J Cell Sci **111 (Pt 13)**: 1853-1865.

Evanko, S. P., J. C. Angello and T. N. Wight (1999). "Formation of hyaluronan- and versican-rich pericellular matrix is required for proliferation and migration of vascular smooth muscle cells." Arterioscler Thromb Vasc Biol **19**(4): 1004-1013.

Evanko, S. P., S. Potter-Perigo, P. L. Bollyky, G. T. Nepom and T. N. Wight (2012). "Hyaluronan and versican in the control of human T-lymphocyte adhesion and migration." Matrix Biol **31**(2): 90-100.

Fedorchenko, O., M. Stiefelhagen, A. A. Peer-Zada, R. Barthel, P. Mayer, L. Eckei, A. Breuer, G. Crispatzu, N. Rosen, T. Landwehr, N. Lilienthal, M. Mollmann, M. Montesinos-Rongen, L. Heukamp, J. Durig, M. Hallek, G.

Fingerle-Rowson and M. Herling (2013). "CD44 regulates the apoptotic response and promotes disease development in chronic lymphocytic leukemia." Blood **121**(20): 4126-4136.

Ferreira, A. M., C. J. McNeil, K. M. Stallaert, K. A. Rogers and M. Sandig (2005). "Interleukin-1beta reduces transcellular monocyte diapedesis and compromises endothelial adherens junction integrity." Microcirculation **12**(7): 563-579.

Flister, M. J., A. Wilber, K. L. Hall, C. Iwata, K. Miyazono, R. E. Nisato, M. S. Pepper, D. C. Zawieja and S. Ran (2010). "Inflammation induces lymphangiogenesis through up-regulation of VEGFR-3 mediated by NF-kappaB and Prox1." Blood **115**(2): 418-429.

Fuentes, M. E., S. K. Durham, M. R. Swerdel, A. C. Lewin, D. S. Barton, J. R. Megill, R. Bravo and S. A. Lira (1995). "Controlled recruitment of monocytes and macrophages to specific organs through transgenic expression of monocyte chemoattractant protein-1." J Immunol **155**(12): 5769-5776.

Fujita, Y., M. Kitagawa, S. Nakamura, K. Azuma, G. Ishii, M. Higashi, H. Kishi, T. Hiwasa, K. Koda, N. Nakajima and K. Harigaya (2002). "CD44 signaling through focal adhesion kinase and its anti-apoptotic effect." FEBS Lett **528**(1-3): 101-108.

Gale, N. W., R. Prevo, J. Espinosa, D. J. Ferguson, M. G. Dominguez, G. D. Yancopoulos, G. Thurston and D. G. Jackson (2007). "Normal lymphatic development and function in mice deficient for the lymphatic hyaluronan receptor LYVE-1." Mol Cell Biol **27**(2): 595-604.

Gardai, S. J., K. A. McPhillips, S. C. Frasch, W. J. Janssen, A. Starefeldt, J. E. Murphy-Ullrich, D. L. Bratton, P. A. Oldenborg, M. Michalak and P. M. Henson

(2005). "Cell-surface calreticulin initiates clearance of viable or apoptotic cells through trans-activation of LRP on the phagocyte." Cell **123**(2): 321-334.

Gautier, E. L., S. Ivanov, P. Lesnik and G. J. Randolph (2013). "Local apoptosis mediates clearance of macrophages from resolving inflammation in mice." Blood **122**(15): 2714-2722.

Gee, K., W. Lim, W. Ma, D. Nandan, F. Diaz-Mitoma, M. Kozlowski and A. Kumar (2002). "Differential regulation of CD44 expression by lipopolysaccharide (LPS) and TNF-alpha in human monocytic cells: distinct involvement of c-Jun N-terminal kinase in LPS-induced CD44 expression." J Immunol **169**(10): 5660-5672.

Geissmann, F., M. G. Manz, S. Jung, M. H. Sieweke, M. Merad and K. Ley (2010). "Development of monocytes, macrophages, and dendritic cells." Science **327**(5966): 656-661.

Gerner, M. Y., P. Torabi-Parizi and R. N. Germain (2015). "Strategically localized dendritic cells promote rapid T cell responses to lymph-borne particulate antigens." Immunity **42**(1): 172-185.

Gharaee-Kermani, M., R. E. McCullumsmith, I. F. Charo, S. L. Kunkel and S. H. Phan (2003). "CC-chemokine receptor 2 required for bleomycin-induced pulmonary fibrosis." Cytokine **24**(6): 266-276.

Ginhoux, F., M. Greter, M. Leboeuf, S. Nandi, P. See, S. Gokhan, M. F. Mehler, S. J. Conway, L. G. Ng, E. R. Stanley, I. M. Samokhvalov and M. Merad (2010). "Fate mapping analysis reveals that adult microglia derive from primitive macrophages." Science **330**(6005): 841-845.

Ginhoux, F. and S. Jung (2014). "Monocytes and macrophages: developmental pathways and tissue homeostasis." Nat Rev Immunol **14**(6): 392-404.

Girard, J. P., C. Moussion and R. Forster (2012). "HEVs, lymphatics and homeostatic immune cell trafficking in lymph nodes." Nat Rev Immunol **12**(11): 762-773.

Gomez Perdiguero, E., K. Klapproth, C. Schulz, K. Busch, E. Azzoni, L. Crozet, H. Garner, C. Trouillet, M. F. de Bruijn, F. Geissmann and H. R. Rodewald (2015). "Tissue-resident macrophages originate from yolk-sac-derived erythro-myeloid progenitors." Nature **518**(7540): 547-551.

Gordon, S. (2008). "Elie Metchnikoff: father of natural immunity." Eur J Immunol **38**(12): 3257-3264.

Goueffic, Y., C. Guilluy, P. Guerin, P. Patra, P. Pacaud and G. Loirand (2006). "Hyaluronan induces vascular smooth muscle cell migration through RHAMM-mediated PI3K-dependent Rac activation." Cardiovasc Res **72**(2): 339-348.

Graves, D. T. and Y. Jiang (1995). "Chemokines, a family of chemotactic cytokines." Crit Rev Oral Biol Med **6**(2): 109-118.

Gretz, J. E., A. O. Anderson and S. Shaw (1997). "Cords, channels, corridors and conduits: critical architectural elements facilitating cell interactions in the lymph node cortex." Immunol Rev **156**: 11-24.

Gretz, J. E., C. C. Norbury, A. O. Anderson, A. E. Proudfoot and S. Shaw (2000). "Lymph-borne chemokines and other low molecular weight molecules reach high endothelial venules via specialized conduits while a functional barrier limits access to the lymphocyte microenvironments in lymph node cortex." J Exp Med **192**(10): 1425-1440.

Grivennikov, S. I., F. R. Greten and M. Karin (2010). "Immunity, inflammation, and cancer." Cell **140**(6): 883-899.

Gunn, M. D., N. A. Nelken, X. Liao and L. T. Williams (1997). "Monocyte chemoattractant protein-1 is sufficient for the chemotaxis of monocytes and

lymphocytes in transgenic mice but requires an additional stimulus for inflammatory activation." J Immunol **158**(1): 376-383.

Hamann, J., N. Koning, W. Pouwels, L. H. Ulfman, M. van Eijk, M. Stacey, H. H. Lin, S. Gordon and M. J. Kwakkenbos (2007). "EMR1, the human homolog of F4/80, is an eosinophil-specific receptor." Eur J Immunol **37**(10): 2797-2802.

Hampton, H. R., J. Bailey, M. Tomura, R. Brink and T. Chtanova (2015). "Microbe-dependent lymphatic migration of neutrophils modulates lymphocyte proliferation in lymph nodes." Nat Commun **6**: 7139.

Hart, P. D. and M. R. Young (1975). "Interference with normal phagosome-lysosome fusion in macrophages, using ingested yeast cells and suramin." Nature **256**(5512): 47-49.

Haserodt, S., M. Aytekin and R. A. Dweik (2011). "A comparison of the sensitivity, specificity, and molecular weight accuracy of three different commercially available Hyaluronan ELISA-like assays." Glycobiology **21**(2): 175-183.

Hashimoto, D., A. Chow, C. Noizat, P. Teo, M. B. Beasley, M. Leboeuf, C. D. Becker, P. See, J. Price, D. Lucas, M. Greter, A. Mortha, S. W. Boyer, E. C. Forsberg, M. Tanaka, N. van Rooijen, A. Garcia-Sastre, E. R. Stanley, F. Ginhoux, P. S. Frenette and M. Merad (2013). "Tissue-resident macrophages self-maintain locally throughout adult life with minimal contribution from circulating monocytes." Immunity **38**(4): 792-804.

Haubeck, H. D., R. Kock, D. C. Fischer, E. Van de Leur, K. Hoffmeister and H. Greiling (1995). "Transforming growth factor beta 1, a major stimulator of hyaluronan synthesis in human synovial lining cells." Arthritis Rheum **38**(5): 669-677.

Heck, L. W., W. D. Blackburn, M. H. Irwin and D. R. Abrahamson (1990). "Degradation of basement membrane laminin by human neutrophil elastase and cathepsin G." Am J Pathol **136**(6): 1267-1274.

Helske, S., S. Syvaranta, K. A. Lindstedt, J. Lappalainen, K. Oorni, M. I. Mayranpaa, J. Lommi, H. Turto, K. Werkkala, M. Kupari and P. T. Kovanen (2006). "Increased expression of elastolytic cathepsins S, K, and V and their inhibitor cystatin C in stenotic aortic valves." Arterioscler Thromb Vasc Biol **26**(8): 1791-1798.

Heymann, F., C. Trautwein and F. Tacke (2009). "Monocytes and macrophages as cellular targets in liver fibrosis." Inflamm Allergy Drug Targets **8**(4): 307-318.

Hirakawa, S., Y. K. Hong, N. Harvey, V. Schacht, K. Matsuda, T. Libermann and M. Detmar (2003). "Identification of vascular lineage-specific genes by transcriptional profiling of isolated blood vascular and lymphatic endothelial cells." Am J Pathol **162**(2): 575-586.

Hirao, M., N. Sato, T. Kondo, S. Yonemura, M. Monden, T. Sasaki, Y. Takai, S. Tsukita and S. Tsukita (1996). "Regulation mechanism of ERM (ezrin/radixin/moesin) protein/plasma membrane association: possible involvement of phosphatidylinositol turnover and Rho-dependent signaling pathway." J Cell Biol **135**(1): 37-51.

Holness, C. L. and D. L. Simmons (1993). "Molecular cloning of CD68, a human macrophage marker related to lysosomal glycoproteins." Blood **81**(6): 1607-1613.

Hou, W. H., I. H. Liu, C. C. Tsai, F. E. Johnson, S. S. Huang and J. S. Huang (2011). "CRSBP-1/LYVE-1 ligands disrupt lymphatic intercellular adhesion by inducing tyrosine phosphorylation and internalization of VE-cadherin." J Cell Sci **124**(Pt 8): 1231-1244.

Huang, L., M. Yoneda and K. Kimata (1993). "A serum-derived hyaluronan-associated protein (SHAP) is the heavy chain of the inter alpha-trypsin inhibitor." J Biol Chem **268**(35): 26725-26730.

Huang, S. S., F. M. Tang, Y. H. Huang, I. H. Liu, S. C. Hsu, S. T. Chen and J. S. Huang (2003). "Cloning, expression, characterization, and role in autocrine cell growth of cell surface retention sequence binding protein-1." J Biol Chem **278**(44): 43855-43869.

Huber, S., R. Hoffmann, F. Muskens and D. Voehringer (2010). "Alternatively activated macrophages inhibit T-cell proliferation by Stat6-dependent expression of PD-L2." Blood **116**(17): 3311-3320.

Huh, H. Y., S. F. Pearce, L. M. Yesner, J. L. Schindler and R. L. Silverstein (1996). "Regulated expression of CD36 during monocyte-to-macrophage differentiation: potential role of CD36 in foam cell formation." Blood **87**(5): 2020-2028.

Ibrahim, S., B. Joddar, M. Craps and A. Ramamurthi (2007). "A surface-tethered model to assess size-specific effects of hyaluronan (HA) on endothelial cells." Biomaterials **28**(5): 825-835.

Iolyeva, M., S. Karaman, A. H. Willrodt, S. Weingartner, B. Vigl and C. Halin (2013). "Novel role for ALCAM in lymphatic network formation and function." FASEB J **27**(3): 978-990.

Iqbal, A. J., D. Regan-Komito, I. Christou, G. E. White, E. McNeill, A. Kenyon, L. Taylor, T. S. Kapellos, E. A. Fisher, K. M. Channon and D. R. Greaves (2013). "A real time chemotaxis assay unveils unique migratory profiles amongst different primary murine macrophages." PLoS One **8**(3): e58744.

Jackson, D. G. (2009). "Immunological functions of hyaluronan and its receptors in the lymphatics." Immunol Rev **230**(1): 216-231.

Jackson, D. G., J. Buckley and J. I. Bell (1992). "Multiple variants of the human lymphocyte homing receptor CD44 generated by insertions at a single site in the extracellular domain." J Biol Chem **267**(7): 4732-4739.

Jackson, D. G., R. Prevo, S. Clasper and S. Banerji (2001). "LYVE-1, the lymphatic system and tumor lymphangiogenesis." Trends Immunol **22**(6): 317-321.

Jarcho, S. (1972). "Cohnheim on inflammation. I." Am J Cardiol **29**(2): 247-249.

Ji, R. C. (2006). "Lymphatic endothelial cells, lymphangiogenesis, and extracellular matrix." Lymphat Res Biol **4**(2): 83-100.

Johnson, L. A., S. Clasper, A. P. Holt, P. F. Lalor, D. Baban and D. G. Jackson (2006). "An inflammation-induced mechanism for leukocyte transmigration across lymphatic vessel endothelium." J Exp Med **203**(12): 2763-2777.

Johnson, L. A. and D. G. Jackson (2010). "Inflammation-induced secretion of CCL21 in lymphatic endothelium is a key regulator of integrin-mediated dendritic cell transmigration." Int Immunol **22**(10): 839-849.

Johnson, L. A. and D. G. Jackson (2013). "The chemokine CX3CL1 promotes trafficking of dendritic cells through inflamed lymphatics." J Cell Sci **126**(Pt 22): 5259-5270.

Johnson, L. A. and D. G. Jackson (2014). "Control of dendritic cell trafficking in lymphatics by chemokines." Angiogenesis **17**(2): 335-345.

Johnson, L. A., R. Prevo, S. Clasper and D. G. Jackson (2007). "Inflammation-induced uptake and degradation of the lymphatic endothelial hyaluronan receptor LYVE-1." J Biol Chem **282**(46): 33671-33680.

Jokela, T. A., A. Lindgren, K. Rilla, E. Maytin, V. C. Hascall, R. H. Tammi and M. I. Tammi (2008). "Induction of hyaluronan cables and monocyte adherence in epidermal keratinocytes." Connect Tissue Res **49**(3): 115-119.

Joukov, V., K. Pajusola, A. Kaipainen, D. Chilov, I. Lahtinen, E. Kukk, O. Saksela, N. Kalkkinen and K. Alitalo (1996). "A novel vascular endothelial growth factor, VEGF-C, is a ligand for the Flt4 (VEGFR-3) and KDR (VEGFR-2) receptor tyrosine kinases." EMBO J **15**(2): 290-298.

Kakei, Y., M. Akashi, T. Shigeta, T. Hasegawa and T. Komori (2014). "Alteration of cell-cell junctions in cultured human lymphatic endothelial cells with inflammatory cytokine stimulation." Lymphat Res Biol **12**(3): 136-143.

Kalluri, R. (2003). "Basement membranes: structure, assembly and role in tumour angiogenesis." Nat Rev Cancer **3**(6): 422-433.

Kamada, N., T. Hisamatsu, S. Okamoto, H. Chinen, T. Kobayashi, T. Sato, A. Sakuraba, M. T. Kitazume, A. Sugita, K. Koganei, K. S. Akagawa and T. Hibi (2008). "Unique CD14 intestinal macrophages contribute to the pathogenesis of Crohn disease via IL-23/IFN-gamma axis." J Clin Invest **118**(6): 2269-2280.

Kappos, L., D. Bates, G. Edan, M. Eraksoy, A. Garcia-Merino, N. Grigoriadis, H. P. Hartung, E. Havrdova, J. Hillert, R. Hohlfeld, M. Kremenchutzky, O. Lyon-Caen, A. Miller, C. Pozzilli, M. Ravnborg, T. Saida, C. Sindic, K. Vass, D. B. Clifford, S. Hauser, E. O. Major, P. W. O'Connor, H. L. Weiner, M. Clanet, R. Gold, H. H. Hirsch, E. W. Radu, P. S. Sorensen and J. King (2011). "Natalizumab treatment for multiple sclerosis: updated recommendations for patient selection and monitoring." Lancet Neurol **10**(8): 745-758.

Karaman, S. and M. Detmar (2014). "Mechanisms of lymphatic metastasis." J Clin Invest **124**(3): 922-928.

Karkkainen, M. J., A. Saaristo, L. Jussila, K. A. Karila, E. C. Lawrence, K. Pajusola, H. Bueler, A. Eichmann, R. Kauppinen, M. I. Kettunen, S. Yla-Herttuala, D. N. Finegold, R. E. Ferrell and K. Alitalo (2001). "A model for gene

therapy of human hereditary lymphedema." Proc Natl Acad Sci U S A **98**(22): 12677-12682.

Kataru, R. P., K. Jung, C. Jang, H. Yang, R. A. Schwendener, J. E. Baik, S. H. Han, K. Alitalo and G. Y. Koh (2009). "Critical role of CD11b+ macrophages and VEGF in inflammatory lymphangiogenesis, antigen clearance, and inflammation resolution." Blood **113**(22): 5650-5659.

Kawai, Y., M. Kaidoh, Y. Yokoyama, K. Sano and T. Ohhashi (2009). "Chemokine CCL2 facilitates ICAM-1-mediated interactions of cancer cells and lymphatic endothelial cells in sentinel lymph nodes." Cancer Sci **100**(3): 419-428.

Kelleher, D., A. Murphy, C. Feighery and E. B. Casey (1995). "Leukocyte function-associated antigen 1 (LFA-1) and CD44 are signalling molecules for cytoskeleton-dependent morphological changes in activated T cells." J Leukoc Biol **58**(5): 539-546.

Kennel, S. J., T. K. Lankford, L. J. Foote, S. G. Shinpock and C. Stringer (1993). "CD44 expression on murine tissues." J Cell Sci **104 (Pt 2)**: 373-382.

Kessenbrock, K., V. Plaks and Z. Werb (2010). "Matrix metalloproteinases: regulators of the tumor microenvironment." Cell **141**(1): 52-67.

Khan, A. I., S. M. Kerfoot, B. Heit, L. Liu, G. Andonegui, B. Ruffell, P. Johnson and P. Kubes (2004). "Role of CD44 and hyaluronan in neutrophil recruitment." J Immunol **173**(12): 7594-7601.

Kinne, R. W., R. Brauer, B. Stuhlmuller, E. Palombo-Kinne and G. R. Burmester (2000). "Macrophages in rheumatoid arthritis." Arthritis Res **2**(3): 189-202.

Knapp, P. E. and J. A. Swanson (1990). "Plasticity of the tubular lysosomal compartment in macrophages." J Cell Sci **95 (Pt 3)**: 433-439.

Kohda, D., C. J. Morton, A. A. Parkar, H. Hatanaka, F. M. Inagaki, I. D. Campbell and A. J. Day (1996). "Solution structure of the link module: a hyaluronan-binding domain involved in extracellular matrix stability and cell migration." Cell **86**(5): 767-775.

Laurent, T. C. and J. R. Fraser (1992). "Hyaluronan." FASEB J **6**(7): 2397-2404.

Laurent, U. B., L. B. Dahl and R. K. Reed (1991). "Catabolism of hyaluronan in rabbit skin takes place locally, in lymph nodes and liver." Exp Physiol **76**(5): 695-703.

Leak, L. V. (1976). "The structure of lymphatic capillaries in lymph formation." Fed Proc **35**(8): 1863-1871.

Lee, K. M., R. Danuser, J. V. Stein, D. Graham, R. J. Nibbs and G. J. Graham (2014). "The chemokine receptors ACKR2 and CCR2 reciprocally regulate lymphatic vessel density." EMBO J **33**(21): 2564-2580.

Lesley, J., N. M. English, I. Gal, K. Mikecz, A. J. Day and R. Hyman (2002). "Hyaluronan binding properties of a CD44 chimera containing the link module of TSG-6." J Biol Chem **277**(29): 26600-26608.

Lesley, J., I. Gal, D. J. Mahoney, M. R. Cordell, M. S. Rugg, R. Hyman, A. J. Day and K. Mikecz (2004). "TSG-6 modulates the interaction between hyaluronan and cell surface CD44." J Biol Chem **279**(24): 25745-25754.

Lessan, K., D. J. Aguiar, T. Oegema, L. Siebenson and A. P. Skubitz (1999). "CD44 and beta1 integrin mediate ovarian carcinoma cell adhesion to peritoneal mesothelial cells." Am J Pathol **154**(5): 1525-1537.

Levesque, M. C. and B. F. Haynes (1996). "In vitro culture of human peripheral blood monocytes induces hyaluronan binding and up-regulates monocyte variant CD44 isoform expression." J Immunol **156**(4): 1557-1565.

Levesque, M. C. and B. F. Haynes (1997). "Cytokine induction of the ability of human monocyte CD44 to bind hyaluronan is mediated primarily by TNF-alpha and is inhibited by IL-4 and IL-13." J Immunol **159**(12): 6184-6194.

Ley, K. (2003). "The role of selectins in inflammation and disease." Trends Mol Med **9**(6): 263-268.

Ley, K., C. Laudanna, M. I. Cybulsky and S. Nourshargh (2007). "Getting to the site of inflammation: the leukocyte adhesion cascade updated." Nat Rev Immunol **7**(9): 678-689.

Li, F. K., A. Davenport, R. L. Robson, P. Loetscher, R. Rothlein, J. D. Williams and N. Topley (1998). "Leukocyte migration across human peritoneal mesothelial cells is dependent on directed chemokine secretion and ICAM-1 expression." Kidney Int **54**(6): 2170-2183.

Li, H. and J. Li (2003). "Development of the peritoneal lymphatic stomata and lymphatic vessels of the diaphragm in mice." Ann Anat **185**(5): 411-418.

Li, Y., B. P. Toole, C. N. Dealy and R. A. Kosher (2007). "Hyaluronan in limb morphogenesis." Dev Biol **305**(2): 411-420.

Liang, F., V. Seyrantepe, K. Landry, R. Ahmad, A. Ahmad, N. M. Stamatos and A. V. Pshezhetsky (2006). "Monocyte differentiation up-regulates the expression of the lysosomal sialidase, Neu1, and triggers its targeting to the plasma membrane via major histocompatibility complex class II-positive compartments." J Biol Chem **281**(37): 27526-27538.

Ling, G. S., J. Bennett, K. J. Woollard, M. Szajna, L. Fossati-Jimack, P. R. Taylor, D. Scott, G. Franzoso, H. T. Cook and M. Botto (2014). "Integrin CD11b positively regulates TLR4-induced signalling pathways in dendritic cells but not in macrophages." Nat Commun **5**: 3039.

Louveau, A., I. Smirnov, T. J. Keyes, J. D. Eccles, S. J. Rouhani, J. D. Peske, N. C. Derecki, D. Castle, J. W. Mandell, K. S. Lee, T. H. Harris and J. Kipnis (2015). "Structural and functional features of central nervous system lymphatic vessels." Nature **523**(7560): 337-341.

Luft, J. H. (1966). "Fine structures of capillary and endocapillary layer as revealed by ruthenium red." Fed Proc **25**(6): 1773-1783.

Luther, S. A., A. Bidgol, D. C. Hargreaves, A. Schmidt, Y. Xu, J. Paniyadi, M. Matloubian and J. G. Cyster (2002). "Differing activities of homeostatic chemokines CCL19, CCL21, and CXCL12 in lymphocyte and dendritic cell recruitment and lymphoid neogenesis." J Immunol **169**(1): 424-433.

Lynch, P. M., F. A. Delano and G. W. Schmid-Schonbein (2007). "The primary valves in the initial lymphatics during inflammation." Lymphat Res Biol **5**(1): 3-10.

Lynskey, N. N., S. Banerji, L. A. Johnson, K. A. Holder, M. Reglinski, P. A. Wing, D. Rigby, D. G. Jackson and S. Sriskandan (2015). "Rapid Lymphatic Dissemination of Encapsulated Group A Streptococci via Lymphatic Vessel Endothelial Receptor-1 Interaction." PLoS Pathog **11**(9): e1005137.

Mack, M., J. Cihak, C. Simonis, B. Luckow, A. E. Proudfoot, J. Plachy, H. Bruhl, M. Frink, H. J. Anders, V. Vielhauer, J. Pfirstinger, M. Stangassinger and D. Schlondorff (2001). "Expression and characterization of the chemokine receptors CCR2 and CCR5 in mice." J Immunol **166**(7): 4697-4704.

Mactier, R. A., R. Khanna, Z. J. Twardowski and K. D. Nolph (1987). "Role of peritoneal cavity lymphatic absorption in peritoneal dialysis." Kidney Int **32**(2): 165-172.

Mahaffey, C. L. and M. E. Mummert (2007). "Hyaluronan synthesis is required for IL-2-mediated T cell proliferation." J Immunol **179**(12): 8191-8199.

Mahida, Y. R. (2000). "The key role of macrophages in the immunopathogenesis of inflammatory bowel disease." Inflamm Bowel Dis **6**(1): 21-33.

Mamdouh, Z., G. E. Kreitzer and W. A. Muller (2008). "Leukocyte transmigration requires kinesin-mediated microtubule-dependent membrane trafficking from the lateral border recycling compartment." J Exp Med **205**(4): 951-966.

Mamdouh, Z., A. Mikhailov and W. A. Muller (2009). "Transcellular migration of leukocytes is mediated by the endothelial lateral border recycling compartment." J Exp Med **206**(12): 2795-2808.

Mantovani, A., A. Sica, S. Sozzani, P. Allavena, A. Vecchi and M. Locati (2004). "The chemokine system in diverse forms of macrophage activation and polarization." Trends Immunol **25**(12): 677-686.

Marchesi, V. T. and J. L. Gowans (1964). "The Migration of Lymphocytes through the Endothelium of Venules in Lymph Nodes: An Electron Microscope Study." Proc R Soc Lond B Biol Sci **159**: 283-290.

Martin, P., S. R. Ruiz, G. M. del Hoyo, F. Anjuere, H. H. Vargas, M. Lopez-Bravo and C. Ardavin (2002). "Dramatic increase in lymph node dendritic cell number during infection by the mouse mammary tumor virus occurs by a CD62L-dependent blood-borne DC recruitment." Blood **99**(4): 1282-1288.

Martinez, F. O., L. Helming and S. Gordon (2009). "Alternative activation of macrophages: an immunologic functional perspective." Annu Rev Immunol **27**: 451-483.

Martinez, F. O., A. Sica, A. Mantovani and M. Locati (2008). "Macrophage activation and polarization." Front Biosci **13**: 453-461.

Matou-Nasri, S., J. Gaffney, S. Kumar and M. Slevin (2009). "Oligosaccharides of hyaluronan induce angiogenesis through distinct CD44 and RHAMM-

mediated signalling pathways involving Cdc2 and gamma-adducin." Int J Oncol **35**(4): 761-773.

McDonald, B., E. F. McAvoy, F. Lam, V. Gill, C. de la Motte, R. C. Savani and P. Kubes (2008). "Interaction of CD44 and hyaluronan is the dominant mechanism for neutrophil sequestration in inflamed liver sinusoids." J Exp Med **205**(4): 915-927.

McKee, C. M., M. B. Penno, M. Cowman, M. D. Burdick, R. M. Strieter, C. Bao and P. W. Noble (1996). "Hyaluronan (HA) fragments induce chemokine gene expression in alveolar macrophages. The role of HA size and CD44." J Clin Invest **98**(10): 2403-2413.

McNally, A. K. and J. M. Anderson (2002). "Beta1 and beta2 integrins mediate adhesion during macrophage fusion and multinucleated foreign body giant cell formation." Am J Pathol **160**(2): 621-630.

Mebius, R. E. and G. Kraal (2005). "Structure and function of the spleen." Nat Rev Immunol **5**(8): 606-616.

Melichar, B. and R. S. Freedman (2002). "Immunology of the peritoneal cavity: relevance for host-tumor relation." Int J Gynecol Cancer **12**(1): 3-17.

Mempel, T. R., S. E. Henrickson and U. H. Von Andrian (2004). "T-cell priming by dendritic cells in lymph nodes occurs in three distinct phases." Nature **427**(6970): 154-159.

Michalak, M., E. F. Corbett, N. Mesaeli, K. Nakamura and M. Opas (1999). "Calreticulin: one protein, one gene, many functions." Biochem J **344 Pt 2**: 281-292.

Mills, C. D., K. Kincaid, J. M. Alt, M. J. Heilman and A. M. Hill (2000). "M-1/M-2 macrophages and the Th1/Th2 paradigm." J Immunol **164**(12): 6166-6173.

Milner, C. M. and A. J. Day (2003). "TSG-6: a multifunctional protein associated with inflammation." J Cell Sci **116**(Pt 10): 1863-1873.

Mohamadzadeh, M., H. DeGrendele, H. Arizpe, P. Estess and M. Siegelman (1998). "Proinflammatory stimuli regulate endothelial hyaluronan expression and CD44/HA-dependent primary adhesion." J Clin Invest **101**(1): 97-108.

Moser, B. and P. Loetscher (2001). "Lymphocyte traffic control by chemokines." Nat Immunol **2**(2): 123-128.

Mosser, D. M. and J. P. Edwards (2008). "Exploring the full spectrum of macrophage activation." Nat Rev Immunol **8**(12): 958-969.

Mouta Carreira, C., S. M. Nasser, E. di Tomaso, T. P. Padera, Y. Boucher, S. I. Tomarev and R. K. Jain (2001). "LYVE-1 is not restricted to the lymph vessels: expression in normal liver blood sinusoids and down-regulation in human liver cancer and cirrhosis." Cancer Res **61**(22): 8079-8084.

Mummert, M. E., D. Mummert, D. Edelbaum, F. Hui, H. Matsue and A. Takashima (2002). "Synthesis and surface expression of hyaluronan by dendritic cells and its potential role in antigen presentation." J Immunol **169**(8): 4322-4331.

Nau, G. J., J. F. Richmond, A. Schlesinger, E. G. Jennings, E. S. Lander and R. A. Young (2002). "Human macrophage activation programs induced by bacterial pathogens." Proc Natl Acad Sci U S A **99**(3): 1503-1508.

Nezelof, C. (2003). "Henri Dutrochet (1776-1847): an unheralded discoverer of the cell." Ann Diagn Pathol **7**(4): 264-272.

Nightingale, T. D., M. E. Frayne, S. Clasper, S. Banerji and D. G. Jackson (2009). "A mechanism of sialylation functionally silences the hyaluronan receptor LYVE-1 in lymphatic endothelium." J Biol Chem **284**(6): 3935-3945.

Noble, K. E., P. Panayiotidis, P. W. Collins, A. V. Hoffbrand and K. L. Yong (1996). "Monocytes induce E-selectin gene expression in endothelial cells: role of CD11/CD18 and extracellular matrix proteins." Eur J Immunol **26**(12): 2944-2951.

Oliferenko, S., I. Kaverina, J. V. Small and L. A. Huber (2000). "Hyaluronic acid (HA) binding to CD44 activates Rac1 and induces lamellipodia outgrowth." J Cell Biol **148**(6): 1159-1164.

Oliver, G. and K. Alitalo (2005). "The lymphatic vasculature: recent progress and paradigms." Annu Rev Cell Dev Biol **21**: 457-483.

Oremus, M., I. Dayes, K. Walker and P. Raina (2012). "Systematic review: conservative treatments for secondary lymphedema." BMC Cancer **12**: 6.

Pappu, R., S. R. Schwab, I. Cornelissen, J. P. Pereira, J. B. Regard, Y. Xu, E. Camerer, Y. W. Zheng, Y. Huang, J. G. Cyster and S. R. Coughlin (2007). "Promotion of lymphocyte egress into blood and lymph by distinct sources of sphingosine-1-phosphate." Science **316**(5822): 295-298.

Paszek, M. J., D. Boettiger, V. M. Weaver and D. A. Hammer (2009). "Integrin clustering is driven by mechanical resistance from the glycocalyx and the substrate." PLoS Comput Biol **5**(12): e1000604.

Paszek, M. J., C. C. DuFort, O. Rossier, R. Bainer, J. K. Mouw, K. Godula, J. E. Hudak, J. N. Lakins, A. C. Wijekoon, L. Cassereau, M. G. Rubashkin, M. J. Magbanua, K. S. Thorn, M. W. Davidson, H. S. Rugo, J. W. Park, D. A. Hammer, G. Giannone, C. R. Bertozzi and V. M. Weaver (2014). "The cancer glycocalyx mechanically primes integrin-mediated growth and survival." Nature **511**(7509): 319-325.

Perry, R. D. and J. D. Fetherston (1997). "Yersinia pestis--etiologic agent of plague." Clin Microbiol Rev **10**(1): 35-66.

Pflicke, H. and M. Sixt (2009). "Preformed portals facilitate dendritic cell entry into afferent lymphatic vessels." J Exp Med **206**(13): 2925-2935.

Phan, T. G., J. A. Green, E. E. Gray, Y. Xu and J. G. Cyster (2009). "Immune complex relay by subcapsular sinus macrophages and noncognate B cells drives antibody affinity maturation." Nat Immunol **10**(7): 786-793.

Phillipson, M., B. Heit, S. A. Parsons, B. Petri, S. C. Mullaly, P. Colarusso, R. M. Gower, G. Neely, S. I. Simon and P. Kubes (2009). "Vav1 is essential for mechanotactic crawling and migration of neutrophils out of the inflamed microvasculature." J Immunol **182**(11): 6870-6878.

Pierce, G. F., J. Vande Berg, R. Rudolph, J. Tarpley and T. A. Mustoe (1991). "Platelet-derived growth factor-BB and transforming growth factor beta 1 selectively modulate glycosaminoglycans, collagen, and myofibroblasts in excisional wounds." Am J Pathol **138**(3): 629-646.

Platonova, N., G. Miquel, B. Regenfuss, S. Taouji, C. Cursiefen, E. Chevet and A. Bikfalvi (2013). "Evidence for the interaction of fibroblast growth factor-2 with the lymphatic endothelial cell marker LYVE-1." Blood **121**(7): 1229-1237.

Platt, A. M., C. C. Bain, Y. Bordon, D. P. Sester and A. M. Mowat (2010). "An independent subset of TLR expressing CCR2-dependent macrophages promotes colonic inflammation." J Immunol **184**(12): 6843-6854.

Pollard, J. W. (2004). "Tumour-educated macrophages promote tumour progression and metastasis." Nat Rev Cancer **4**(1): 71-78.

Pollard, J. W., A. Bartocci, R. Arceci, A. Orlofsky, M. B. Ladner and E. R. Stanley (1987). "Apparent role of the macrophage growth factor, CSF-1, in placental development." Nature **330**(6147): 484-486.

Ponta, H., L. Sherman and P. A. Herrlich (2003). "CD44: from adhesion molecules to signalling regulators." Nat Rev Mol Cell Biol **4**(1): 33-45.

Pozzi, L. A., J. W. Maciaszek and K. L. Rock (2005). "Both dendritic cells and macrophages can stimulate naive CD8 T cells in vivo to proliferate, develop effector function, and differentiate into memory cells." J Immunol **175**(4): 2071-2081.

Prevo, R., S. Banerji, D. J. Ferguson, S. Clasper and D. G. Jackson (2001). "Mouse LYVE-1 is an endocytic receptor for hyaluronan in lymphatic endothelium." J Biol Chem **276**(22): 19420-19430.

Protin, U., T. Schweighoffer, W. Jochum and F. Hilberg (1999). "CD44-deficient mice develop normally with changes in subpopulations and recirculation of lymphocyte subsets." J Immunol **163**(9): 4917-4923.

Punnia-Moorthy, A. (1987). "Evaluation of pH changes in inflammation of the subcutaneous air pouch lining in the rat, induced by carrageenan, dextran and Staphylococcus aureus." J Oral Pathol **16**(1): 36-44.

Pure, E. and C. A. Cuff (2001). "A crucial role for CD44 in inflammation." Trends Mol Med **7**(5): 213-221.

Radhakrishnan, K. and S. G. Rockson (2008). "The clinical spectrum of lymphatic disease." Ann N Y Acad Sci **1131**: 155-184.

Ramamurthi, A. and I. Vesely (2002). "Smooth muscle cell adhesion on crosslinked hyaluronan gels." J Biomed Mater Res **60**(1): 195-205.

Reed, R. K. and U. B. Laurent (1992). "Turnover of hyaluronan in the microcirculation." Am Rev Respir Dis **146**(5 Pt 2): S37-39.

Reed, R. K., U. B. Laurent, J. R. Fraser and T. C. Laurent (1990). "Removal rate of [3H]hyaluronan injected subcutaneously in rabbits." Am J Physiol **259**(2 Pt 2): H532-535.

Reed, R. K., K. Lilja and T. C. Laurent (1988). "Hyaluronan in the rat with special reference to the skin." Acta Physiol Scand **134**(3): 405-411.

Reitsma, S., D. W. Slaaf, H. Vink, M. A. van Zandvoort and M. G. oude Egbrink (2007). "The endothelial glycocalyx: composition, functions, and visualization." Pflugers Arch **454**(3): 345-359.

Rigby, D. A., D. J. Ferguson, L. A. Johnson and D. G. Jackson (2015). "Neutrophils rapidly transit inflamed lymphatic vessel endothelium via integrin-dependent proteolysis and lipoxin-induced junctional retraction." J Leukoc Biol.

Rosen, H. and S. Gordon (1987). "Monoclonal antibody to the murine type 3 complement receptor inhibits adhesion of myelomonocytic cells in vitro and inflammatory cell recruitment in vivo." J Exp Med **166**(6): 1685-1701.

Ross, J. A., I. Ansell, J. T. Hjelle, J. D. Anderson, M. A. Miller-Hjelle and J. W. Dobbie (1998). "Phenotypic mapping of human mesothelial cells." Adv Perit Dial **14**: 25-30.

Rovin, B. H., J. A. Dickerson, L. C. Tan and C. A. Hebert (1995). "Activation of nuclear factor-kappa B correlates with MCP-1 expression by human mesangial cells." Kidney Int **48**(4): 1263-1271.

Royston, D. and D. G. Jackson (2009). "Mechanisms of lymphatic metastasis in human colorectal adenocarcinoma." J Pathol **217**(5): 608-619.

Ruffell, B., G. F. Poon, S. S. Lee, K. L. Brown, S. L. Tjew, J. Cooper and P. Johnson (2011). "Differential use of chondroitin sulfate to regulate hyaluronan binding by receptor CD44 in Inflammatory and Interleukin 4-activated Macrophages." J Biol Chem **286**(22): 19179-19190.

Salmi, M., M. Karikoski, K. Elima, P. Rantakari and S. Jalkanen (2013). "CD44 binds to macrophage mannose receptor on lymphatic endothelium and supports lymphocyte migration via afferent lymphatics." Circ Res **112**(12): 1577-1582.

Savani, R. C., G. Hou, P. Liu, C. Wang, E. Simons, P. C. Grimm, R. Stern, A. H. Greenberg, H. M. DeLisser and N. Khalil (2000). "A role for hyaluronan in

macrophage accumulation and collagen deposition after bleomycin-induced lung injury." Am J Respir Cell Mol Biol **23**(4): 475-484.

Savill, J., V. Fadok, P. Henson and C. Haslett (1993). "Phagocyte recognition of cells undergoing apoptosis." Immunol Today **14**(3): 131-136.

Sawa, Y. and E. Tsuruga (2008). "The expression of E-selectin and chemokines in the cultured human lymphatic endothelium with lipopolysaccharides." J Anat **212**(5): 654-663.

Schenkel, A. R., Z. Mamdouh, X. Chen, R. M. Liebman and W. A. Muller (2002). "CD99 plays a major role in the migration of monocytes through endothelial junctions." Nat Immunol **3**(2): 143-150.

Selbi, W., C. A. de la Motte, V. C. Hascall, A. J. Day, T. Bowen and A. O. Phillips (2006). "Characterization of hyaluronan cable structure and function in renal proximal tubular epithelial cells." Kidney Int **70**(7): 1287-1295.

Shi, C. and E. G. Pamer (2011). "Monocyte recruitment during infection and inflammation." Nat Rev Immunol **11**(11): 762-774.

Shi, C., P. Velazquez, T. M. Hohl, I. Leiner, M. L. Dustin and E. G. Pamer (2010). "Monocyte trafficking to hepatic sites of bacterial infection is chemokine independent and directed by focal intercellular adhesion molecule-1 expression." J Immunol **184**(11): 6266-6274.

Sica, A. and A. Mantovani (2012). "Macrophage plasticity and polarization: in vivo veritas." J Clin Invest **122**(3): 787-795.

Siegel, S. A., D. J. Shealy, M. T. Nakada, J. Le, D. S. Woulfe, L. Probert, G. Kollias, J. Ghrayeb, J. Vilcek and P. E. Daddona (1995). "The mouse/human chimeric monoclonal antibody cA2 neutralizes TNF in vitro and protects transgenic mice from cachexia and TNF lethality in vivo." Cytokine **7**(1): 15-25.

Siegelman, M. H., H. C. DeGrendele and P. Estess (1999). "Activation and interaction of CD44 and hyaluronan in immunological systems." J Leukoc Biol **66**(2): 315-321.

Siegelman, M. H., D. Stanescu and P. Estess (2000). "The CD44-initiated pathway of T-cell extravasation uses VLA-4 but not LFA-1 for firm adhesion." J Clin Invest **105**(5): 683-691.

Sisto, K. and A. Khachemoune (2008). "Elephantiasis nostras verrucosa: a review." Am J Clin Dermatol **9**(3): 141-146.

Sleeman, J., W. Rudy, M. Hofmann, J. Moll, P. Herrlich and H. Ponta (1996). "Regulated clustering of variant CD44 proteins increases their hyaluronate binding capacity." J Cell Biol **135**(4): 1139-1150.

Spicer, A. P. and J. A. McDonald (1998). "Characterization and molecular evolution of a vertebrate hyaluronan synthase gene family." J Biol Chem **273**(4): 1923-1932.

Stacker, S. A., S. P. Williams, T. Karnezis, R. Shayan, S. B. Fox and M. G. Achen (2014). "Lymphangiogenesis and lymphatic vessel remodelling in cancer." Nat Rev Cancer **14**(3): 159-172.

Stamatos, N. M., F. Liang, X. Nan, K. Landry, A. S. Cross, L. X. Wang and A. V. Pshezhetsky (2005). "Differential expression of endogenous sialidases of human monocytes during cellular differentiation into macrophages." FEBS J **272**(10): 2545-2556.

Stamenkovic, I., A. Aruffo, M. Amiot and B. Seed (1991). "The hematopoietic and epithelial forms of CD44 are distinct polypeptides with different adhesion potentials for hyaluronate-bearing cells." EMBO J **10**(2): 343-348.

Stein, M., S. Keshav, N. Harris and S. Gordon (1992). "Interleukin 4 potently enhances murine macrophage mannose receptor activity: a marker of alternative immunologic macrophage activation." J Exp Med **176**(1): 287-292.

Sumagin, R., H. Prizant, E. Lomakina, R. E. Waugh and I. H. Sarelius (2010). "LFA-1 and Mac-1 define characteristically different intralumenal crawling and emigration patterns for monocytes and neutrophils in situ." J Immunol **185**(11): 7057-7066.

Swartz, M. A. (2001). "The physiology of the lymphatic system." Adv Drug Deliv Rev **50**(1-2): 3-20.

Swartz, M. A. and A. W. Lund (2012). "Lymphatic and interstitial flow in the tumour microenvironment: linking mechanobiology with immunity." Nat Rev Cancer **12**(3): 210-219.

Szabo, M. C., E. C. Butcher, B. W. McIntyre, T. J. Schall and K. B. Bacon (1997). "RANTES stimulation of T lymphocyte adhesion and activation: role for LFA-1 and ICAM-3." Eur J Immunol **27**(5): 1061-1068.

Szuba, A. and S. G. Rockson (1998). "Lymphedema: classification, diagnosis and therapy." Vasc Med **3**(2): 145-156.

Tal, O., H. Y. Lim, I. Gurevich, I. Milo, Z. Shipony, L. G. Ng, V. Angeli and G. Shakhar (2011). "DC mobilization from the skin requires docking to immobilized CCL21 on lymphatic endothelium and intralymphatic crawling." J Exp Med **208**(10): 2141-2153.

Tanaka, Y. (2000). "Integrin activation by chemokines: relevance to inflammatory adhesion cascade during T cell migration." Histol Histopathol **15**(4): 1169-1176.

Tchernychev, B., B. Furie and B. C. Furie (2003). "Peritoneal macrophages express both P-selectin and PSGL-1." J Cell Biol **163**(5): 1145-1155.

Tedder, T. F., D. A. Steeber and P. Pizcueta (1995). "L-selectin-deficient mice have impaired leukocyte recruitment into inflammatory sites." J Exp Med **181**(6): 2259-2264.

Teriete, P., S. Banerji, M. Noble, C. D. Blundell, A. J. Wright, A. R. Pickford, E. Lowe, D. J. Mahoney, M. I. Tammi, J. D. Kahmann, I. D. Campbell, A. J. Day and D. G. Jackson (2004). "Structure of the regulatory hyaluronan binding domain in the inflammatory leukocyte homing receptor CD44." Mol Cell **13**(4): 483-496.

Termeer, C. C., J. Hennies, U. Voith, T. Ahrens, J. M. Weiss, P. Prehm and J. C. Simon (2000). "Oligosaccharides of hyaluronan are potent activators of dendritic cells." J Immunol **165**(4): 1863-1870.

Toole, B. P. (2004). "Hyaluronan: from extracellular glue to pericellular cue." Nat Rev Cancer **4**(7): 528-539.

Torgersen, D., N. P. Mullin and K. Drickamer (1998). "Mechanism of ligand binding to E- and P-selectin analyzed using selectin/mannose-binding protein chimeras." J Biol Chem **273**(11): 6254-6261.

Torzicky, M., P. Viznerova, S. Richter, H. Strobl, C. Scheinecker, D. Foedinger and E. Riedl (2012). "Platelet endothelial cell adhesion molecule-1 (PECAM-1/CD31) and CD99 are critical in lymphatic transmigration of human dendritic cells." J Invest Dermatol **132**(4): 1149-1157.

Tsou, C. L., W. Peters, Y. Si, S. Slaymaker, A. M. Aslanian, S. P. Weisberg, M. Mack and I. F. Charo (2007). "Critical roles for CCR2 and MCP-3 in monocyte mobilization from bone marrow and recruitment to inflammatory sites." J Clin Invest **117**(4): 902-909.

Uhlin-Hansen, L., T. Wik, L. Kjellen, E. Berg, F. Forsdahl and S. O. Kolset (1993). "Proteoglycan metabolism in normal and inflammatory human macrophages." Blood **82**(9): 2880-2889.

van Furth, R. and Z. A. Cohn (1968). "The origin and kinetics of mononuclear phagocytes." J Exp Med **128**(3): 415-435.

Vasiljeva, O., A. Papazoglou, A. Kruger, H. Brodoefel, M. Korovin, J. Deussing, N. Augustin, B. S. Nielsen, K. Almholt, M. Bogyo, C. Peters and T. Reinheckel (2006). "Tumor cell-derived and macrophage-derived cathepsin B promotes progression and lung metastasis of mammary cancer." Cancer Res **66**(10): 5242-5250.

Verreck, F. A., T. de Boer, D. M. Langenberg, M. A. Hoeve, M. Kramer, E. Vaisberg, R. Kastelein, A. Kolk, R. de Waal-Malefyt and T. H. Ottenhoff (2004). "Human IL-23-producing type 1 macrophages promote but IL-10-producing type 2 macrophages subvert immunity to (myco)bacteria." Proc Natl Acad Sci U S A **101**(13): 4560-4565.

Verreck, F. A., T. de Boer, D. M. Langenberg, L. van der Zanden and T. H. Ottenhoff (2006). "Phenotypic and functional profiling of human proinflammatory type-1 and anti-inflammatory type-2 macrophages in response to microbial antigens and IFN-gamma- and CD40L-mediated costimulation." J Leukoc Biol **79**(2): 285-293.

Voisin, M. B., A. Woodfin and S. Nourshargh (2009). "Monocytes and neutrophils exhibit both distinct and common mechanisms in penetrating the vascular basement membrane in vivo." Arterioscler Thromb Vasc Biol **29**(8): 1193-1199.

von Andrian, U. H. and T. R. Mempel (2003). "Homing and cellular traffic in lymph nodes." Nat Rev Immunol **3**(11): 867-878.

von der Weid, P. Y. and D. C. Zawieja (2004). "Lymphatic smooth muscle: the motor unit of lymph drainage." Int J Biochem Cell Biol **36**(7): 1147-1153.

Wagner, D. D. and P. S. Frenette (2008). "The vessel wall and its interactions." Blood **111**(11): 5271-5281.

Wang, S., M. B. Voisin, K. Y. Larbi, J. Dangerfield, C. Scheiermann, M. Tran, P. H. Maxwell, L. Sorokin and S. Nourshargh (2006). "Venular basement membranes contain specific matrix protein low expression regions that act as exit points for emigrating neutrophils." J Exp Med **203**(6): 1519-1532.

Wang, Z. B., M. Li and J. C. Li (2010). "Recent advances in the research of lymphatic stomata." Anat Rec (Hoboken) **293**(5): 754-761.

Weber, C., L. Fraemohs and E. Dejana (2007). "The role of junctional adhesion molecules in vascular inflammation." Nat Rev Immunol **7**(6): 467-477.

Weber, K. S., L. B. Klickstein and C. Weber (1999). "Specific activation of leukocyte beta2 integrins lymphocyte function-associated antigen-1 and Mac-1 by chemokines mediated by distinct pathways via the alpha subunit cytoplasmic domains." Mol Biol Cell **10**(4): 861-873.

Weiss, J. M., A. C. Renkl, C. S. Maier, M. Kimmig, L. Liaw, T. Ahrens, S. Kon, M. Maeda, H. Hotta, T. Uede and J. C. Simon (2001). "Osteopontin is involved in the initiation of cutaneous contact hypersensitivity by inducing Langerhans and dendritic cell migration to lymph nodes." J Exp Med **194**(9): 1219-1229.

Weiss, J. M., A. C. Renkl, J. Sleeman, H. Dittmar, C. C. Termeer, S. Taxis, N. Howells, E. Schopf, H. Ponta, P. Herrlich and J. C. Simon (1998). "CD44 variant isoforms are essential for the function of epidermal Langerhans cells and dendritic cells." Cell Adhes Commun **6**(2-3): 157-160.

Weiss, S. J. (1989). "Tissue destruction by neutrophils." N Engl J Med **320**(6): 365-376.

Wen, Y., J. Li, L. Wang, K. Tie, J. Magdalou, L. Chen and H. Wang (2014). "UDP-glucose dehydrogenase modulates proteoglycan synthesis in articular chondrocytes: its possible involvement and regulation in osteoarthritis." Arthritis Res Ther **16**(6): 484.

Wigle, J. T. and G. Oliver (1999). "Prox1 function is required for the development of the murine lymphatic system." Cell **98**(6): 769-778.

Wilting, J., M. Papoutsi, B. Christ, K. H. Nicolaides, C. S. von Kaisenberg, J. Borges, G. B. Stark, K. Alitalo, S. I. Tomarev, C. Niemeyer and J. Rossler (2002). "The transcription factor Prox1 is a marker for lymphatic endothelial cells in normal and diseased human tissues." FASEB J **16**(10): 1271-1273.

Winger, R. C., J. E. Koblinski, T. Kanda, R. M. Ransohoff and W. A. Muller (2014). "Rapid remodeling of tight junctions during paracellular diapedesis in a human model of the blood-brain barrier." J Immunol **193**(5): 2427-2437.

Wolny, P. M., S. Banerji, C. Gounou, A. R. Brisson, A. J. Day, D. G. Jackson and R. P. Richter (2010). "Analysis of CD44-hyaluronan interactions in an artificial membrane system: insights into the distinct binding properties of high and low molecular weight hyaluronan." J Biol Chem **285**(39): 30170-30180.

Wright, N. B. and H. M. Carty (1994). "The swollen leg and primary lymphoedema." Arch Dis Child **71**(1): 44-49.

Wynn, T. A., A. Chawla and J. W. Pollard (2013). "Macrophage biology in development, homeostasis and disease." Nature **496**(7446): 445-455.

Xu, B., R. M. deWaal, N. Mor-Vaknin, C. Hibbard, D. M. Markovitz and M. L. Kahn (2004). "The endothelial cell-specific antibody PAL-E identifies a secreted form of vimentin in the blood vasculature." Mol Cell Biol **24**(20): 9198-9206.

Yago, T., M. Tsukuda and M. Minami (1999). "P-selectin binding promotes the adhesion of monocytes to VCAM-1 under flow conditions." J Immunol **163**(1): 367-373.

Yao, L. C., P. Baluk, R. S. Srinivasan, G. Oliver and D. M. McDonald (2012). "Plasticity of button-like junctions in the endothelium of airway lymphatics in development and inflammation." Am J Pathol **180**(6): 2561-2575.

Yoshida, R., M. Nagira, T. Imai, M. Baba, S. Takagi, Y. Tabira, J. Akagi, H. Nomiyama and O. Yoshie (1998). "EBI1-ligand chemokine (ELC) attracts a broad spectrum of lymphocytes: activated T cells strongly up-regulate CCR7 and efficiently migrate toward ELC." Int Immunol **10**(7): 901-910.

Yoshimura, T., E. A. Robinson, S. Tanaka, E. Appella and E. J. Leonard (1989). "Purification and amino acid analysis of two human monocyte chemoattractants produced by phytohemagglutinin-stimulated human blood mononuclear leukocytes." J Immunol **142**(6): 1956-1962.

Young, J. W., L. Koulova, S. A. Soergel, E. A. Clark, R. M. Steinman and B. Dupont (1992). "The B7/BB1 antigen provides one of several costimulatory signals for the activation of CD4+ T lymphocytes by human blood dendritic cells in vitro." J Clin Invest **90**(1): 229-237.

Zhang, G., H. Zhang, Y. Liu, Y. He, W. Wang, Y. Du, C. Yang and F. Gao (2014). "CD44 clustering is involved in monocyte differentiation." Acta Biochim Biophys Sin (Shanghai) **46**(7): 540-547.

Zhang, L., T. Yoshimura and D. T. Graves (1997). "Antibody to Mac-1 or monocyte chemoattractant protein-1 inhibits monocyte recruitment and promotes tumor growth." J Immunol **158**(10): 4855-4861.

Zhang, X., R. Goncalves and D. M. Mosser (2008). "The isolation and characterization of murine macrophages." Curr Protoc Immunol **Chapter 14**: Unit 14 11.

Zhuo, L., A. Kanamori, R. Kannagi, N. Itano, J. Wu, M. Hamaguchi, N. Ishiguro and K. Kimata (2006). "SHAP potentiates the CD44-mediated leukocyte adhesion to the hyaluronan substratum." J Biol Chem **281**(29): 20303-20314.

Zohar, R., N. Suzuki, K. Suzuki, P. Arora, M. Glogauer, C. A. McCulloch and J. Sodek (2000). "Intracellular osteopontin is an integral component of the CD44-ERM complex involved in cell migration." J Cell Physiol **184**(1): 118-130.

1.